JOACHIM SCHMID

NATURAL FIRE EXPOSURE OF STRUCTURAL TIMBER

CONTRIBUTION TO DETERMINE THE INFLUENCE IN THE FULLY DEVELOPED AND THE DECAY PHASE

DISS. ETH NO. 27205

Natural Fire Exposure of Structural Timber-Contribution to Determine the Influence in the Fully Developed and the Decay Phase

A thesis submitted to attain the degree of

DOCTOR OF SCIENCES of ETH ZURICH

(Dr. sc. ETH Zurich)

presented by

Joachim Schmid

Dipl. Ing. TU Vienna, Austria

born on 8.1.1979

citizen of Austria

accepted on the recommendation of

Prof. Dr. Andrea Frangi, examiner

Prof. Dr. Stefan Winter, co-examiner

Prof. Dr. Andreas Taras, co-examiner

2020

Natural Fire Exposure of Structural Timber
-
Contribution to Determine the Influence in the Fully Developed and the Decay Phase

Abstract

Natural Fire Exposure of Structural Timber-Contribution to Determine the Influence in the Fully Developed and the Decay Phase

by

Joachim Schmid
DOCTOR OF SCIENCES of ETH ZURICH in Civil Engineering

ETH Zurich

Professor Andrea Frangi, Chair

Structural fire safety is one of the most important design requirements - regardless of the building material. The development of the fire design of timber structures has been adopted to rules developed for non-combustible building materials, which have defined the standard procedure for testing and the common practice for fire resistance design. Recently, the design basics were questioned including the validity of the testing of structural timber components in furnaces and the applicability of the current design framework to structural timber. This thesis developed an understanding of the "fire exposure" to describe the thermal exposure of structural timber members in fire compartments. Further, this thesis reported the investigation of the relevant characteristics of fire-exposed timber in standard fire and under non-standard heating regimes. The focus is given to the thermally modified layer of a fire exposed timber member, the char layer, which has not been considered in many previous research studies in fire safety engineering. An experimental setup was designed to study the behaviour of timber under various fire exposures, the Fire Apparatus for Non-standard Heating and Charring Investigation (FANCI). Analysing the char layer, it was confirmed that a significant amount of energy is stored in this thermally modified part of the structural timber. For fire resistance tests, it was concluded that the contribution of the char layer varies significantly depending on the fire exposure. As a final result, the Timber Charring and Heat Storage (TiCHS)-model, a model was presented to describe the timber charring and the contribution to the compartment fire. The TiCHS-model was proposed to describe the behaviour of tim-ber in laboratory experiments but also for compartment fires when timber surfaces are involved in the fire dynamics. Finally, the TiCHS-model was applied as an add-on to a zone-model. Proposals were suggested for future development to increase the model applicability.

Professor Andrea Frangi
Dissertation Committee Chair

Zusammenfassung

Der bauliche Brandschutz ist eine der wichtigsten Konstruktionsanforderungen - unabhängig vom Baumaterial. Die Entwicklung der entsprechenden Bemessungsregeln für Holzkonstruktionen wurden an jene von nicht brennbare Baustoffen angelehnt welche nahezu zur Gänze auf Normbrandprüfungen basieren. In jüngster Zeit wurde dieses Vorgehen in Frage gestellt, einschliesslich der Gültigkeit der Prüfung von Holzbauteilen in Prüföfen und der Anwendbarkeit des aktuellen Bemessungskonzeptes auf Holzkonstruktionen. In der vorliegenden Arbeit wurde das Verständnis für die *Brandbeanspruchung* erarbeitet um die thermische Beanspruchung von Holzbauteilen in natürlichen Brän-den zu beschreiben. Relevanter Eigenschaften wurden untersucht um das Verhalten von Holzbauteilen im Brand abschätzen zu können. Der Fokus wurde hierbei auf die Kohlessschicht gelegt welche in vielen bisherigen Forschungsarbeiten im Bereich des technischen Brandschutzes nicht ausreichend berücksichtigt wurde. Zur Untersuchung des Verhaltens von Holz unter verschiedenen Brandbeanspruchungen wurde ein Versuchsaufbau entwickelt, der *Fire Apparatus for Non-standard heating and Charring Investigation* (FANCI). Die tiefgehende Analyse der Kohleschicht bestätigte, dass in diesem thermisch modifizierten Teil des Bauholzes eine erhebliche Menge an Energie gespeichert ist. Bei der Analyse von Feuerwiderstandsprüfungen wurde festgestellt, dass der Beitrag der Kohlesschicht in Abhängigkeit von der Brandeinwirkung erheblich variieren kann. Als Endergebnis wurde mit dem *Timber Charring and Heat Storage* (TiCHS)-Modell ein Modell zur Beschreibung der Verkohlung und des Beitrags zur Brandentwicklung vorgestellt. Das TiCHS-Modell wurde verwendet, um das Verhalten von Holz in Laborexperimenten zu beschreiben, aber auch allgemein in Raumbränden, in denen Holzoberflächen an der Branddynamik beteiligt sind. Hierfür wurde das TiCHS-Modell als Aufsatz gemeinsam mit einem vorhande-nen Zonenmodell angewendet. Zuletzt wurden Vorschläge für die zukünftige Entwick-lung gemacht, um die Anwendbarkeit des Modells zu erweitern.

To my parents.

Contents

---

[1]Parts of this Section are content of a publication [168]
[2]Parts of this Section are content of a journal publication [180]
[3]Parts of this Section are content of (journal) publications [162, 167, 176, 174, 173, 179]

---

[4]Parts of this Section are content of (journal) publications [180, 163, 168]
[5]Parts of this Section are content of (journal) publications [178, 166]

List of Figures

List of Tables

List of Acronyms

A-M

AD	Anno Domini
AST	Adiabatic surface temperature
ASTM	American society for testing and maftaterials
BC	Bomb calorimeter
BEC	Model according to Eurocode, Annex B
C	Combustible
CLT	Cross-laminated timber
COST	European cooperation in science and technology
CV	Coefficient of variation
DIN	German industry standard
EC	Eurocode
e.g.	Exempli gratia
EMPA	Swiss federal materials testing institute
EN	European Norm
ETA	European technical assessment
FANCI	Fire and non standard heating charring investigation
FC	Fuel controlled
FEA	Finite element analysis
FSE	Fire safety engineering
HRR	Heat release rate
ID	Identifier
i.e.	id est
ISO	International organisation for standardisation
LC	Load cell
LHV	Lower heating value
MC	Moisture content
MDF	Medium density fibreboard
MPA	Material Testing Institute

N-Z

n.a.	Not available
NA	National Annex
NC	Non combustible
no	Numero
PT	Plate thermometer
PBD	Performance based design
R.H.	Relative humidity
RISE	Research institutes of Sweden
STP	Solid timber panel
STSM	Short term scientific mission
TiCHS	Timber charring and heat storage
TC	Thermocouple
TBC	Thermal boundary condition
US	United States of America
UK	United Kingdom of Great Britain and Norther Ireland
VKF	Swiss association of Cantonal Fire Insurance companies
VC	Ventilation controlled
wt%	Weight Percent
ZSL	Zero strength layer

Notation and Symbols

Symbols and Units

Latin upper case letters

A area, in m^2;

D degree of turbulence; in m/s;

C^K specific heat capacity of the system, in J/ (kg·K);

H heat content, in MJ/kg;

HHV higher heating value, in MJ/kg;

HRR rate of heat release, in kW or MW;

O opening factor, in m$^{1/2}$;

Q fire load, in MJ, or heat of combustion, in J;

Re Reynolds number;

STD Standard deviation;

T temperature, in K or °C.

Latin lower case letters

b thermal absorptivity, in J/ (m$^2 \cdot$ s $^{1/2} \cdot$K);

c specific heat, in J/kg;

d depth;

h height, in mm or m, or heat transfer coefficient, in W/ (m$^2 \cdot$ K);

i counter;

l length, in mm or m;

m mass, in kg, or combustion factor;

n counter;

q heat, in J, or heat density in J/m^2, or fire load density in MJ/m^2;

r fuel-to-air ratio;

s rate of heat release density for a regression rate; in MW/m$^2 \cdot$ mm/min;

t time; in min;

u moisture content; in % by mass;

x location axis; in mm.

Greek upper case letters

Δ difference;

Θ temperature, in K or °C, or equivalency ratio.

Greek lower case letters

α factor;

β regression rate, in mm/min;

ϵ emissivity;

λ heat conductivity, in W/ (m $\cdot$ K);

ρ density, in kg/m^3;

σ Stefan-Boltzmann constant, in W $\cdot$ m $^{-2}\cdot$ K^{-4}.

Subscripts

0	one-dimensional or initial or ambient;
abs	absorbed;
air	air;
ch	char layer;
char	charring;
c	convection;
conv	convection or conversion;
crit	critical;
dec	decay;
design	design;
dry	dry;
ef	effective;
emi	emitted;
eq	eqivalent;
f	floor;
fi	fire situation;
fo	flashover;
hot	hot;
humid	humid;
i	index;
inc	incident;
k	characteristic value;
max	maximum;
min	minimum;

Subscripts (continuation)

g gas;

ig ignition;

lb lower bound;

obs observed;

ox oxidation;

$para$ parametric;

pyr pyrolysis;

pr protection;

r radiation;

rad radiation;

reg regression;

res residual;

s surface;

st structural timber;

w wire;

u moisture content or upper;

ub upper bound;

lb lower bound;

t timber;

tot total;

v vaporisation or ventilation;

$virg$ virgin;

vol volatiles.

Superscripts

$''$ per unit area;

$\cdot$ time derivative.

Preface

The fire design of timber structures was of minor interest due to the limited interest in the building material, which partly resulted from restrictions giving in the building regulations. The reduction of fatalities in building fires and the evolution of the building regulations towards a more performance-based design have opened the market to timber building components in many countries. Other key elements were the advanced industrial production processes with respect to bonding techniques and automated manufacturing processes, which led to the introduction of timber building components in the building market in large scale: cross-laminated timber, a solid, plane timber product that allows the transfer of high loads and fast building erection. With respect to possible effects to the fire safety, limited, pro-active ambitions could be observed when these timber products were launched. Previously, timber components were typically linear members (columns, beams) with a negligible combustible surface in compartments. When solid timber panels with its attractive appearance were introduced and used by architects and designers, the fire safety community started to question the existing design models, which were developed in decades of research studies but, further, the validity of the fire resistance framework for timber structures. To find answers to these questions, studies presented in this thesis made used of several experimental campaigns involving standard fire tests, standard fire furnaces and thereof deviating setups and exposures. The thermal exposure of solid timber panes was investigated by means of furnace tests in fire resistance furnaces with combustible and non-combustible surfaces. The term "thermal exposure" was found insufficient if not, further, the gaseous environment (oxygen concentration and gas movement) would be considered which was defined as "fire exposure". This part of the investigations concluded that the fire resistance testing, currently applied to all types of structural components (combustible and non-combustible ones) is valid as long as the fully developed fire phase is of interest. As an additional result, the development of a potential standard testing methodology for the bond line integrity of cross-laminated timber was proposed. The behaviour of timber in the cooling phase was investigated in a campaign where important properties as charring of the timber and glowing combustion and surface regression of the char layer were investigated. The focus of this part of the investigations was the char layer where limited knowledge is currently available. Understanding of the char layer's behaviour under fire exposure is essential to answer the questions of the fire dynamics when structural timber is left exposed in compartments. The experimental setup, the Fire Apparatus for Non-standard heating and Charring Investigation (FANCI) was developed in this thesis. With the FANCI, the charring of timber up to a heat flux to the virgin wood section of about 320 kW/m^2 was investigated, a maximum charring rate of about 2.4 mm/min and a maximum char layer surface regression rate of 1.8 mm/min was found. The results are highly dependent on the characteristics of the gas flow at the exposed surface. Another experimental part of this thesis focused on the characteristics of the char layer, which protects the virgin wood section and has the ability to store a certain amount of energy. This part of the investigations was launched, as it was not clear if avail-

able knowledge for charcoal is applicable for the char layer structural timber members, which is formed by a fire event. The char layer density was measured and its heat content was determined for various depths. The heat content was found to be similar of charcoal while the density deviated significantly from available prediction models. Results from all three parts were taken to set up an improved charring model able to describe observed effects in the conducted experiments: the TiCHS-model, a model for the timber charring and heat storage was developed which can further be applied for the prediction of the structural timber's contribution to compartment fires. In the TiCHS-model, the following observations were brought together for engineers: (i) the charring of virgin timber, (ii) the endothermic conversion to the char layer in parallel to (iii) the exothermic release of volatiles, (iv) the glowing combustion and (v) the char layer surface regression consuming the remaining, stored energy. Subsequently, the TiCHS-model was validated using data from existing compartment experiments. A good agreement can be reported based on the considered cases implying strict limitations. The TiCHS-model is held open for further improvements in the future when further results from compartment experiments will deliver the required information currently not documented. This thesis reflects a highly exciting phase for the fire design of timber structures and it was an honour to work with this topic in cooperation with many representatives from academia, designers, producers and authority representatives. It comprises knowledge and experience from over 15 years of structural design and research in the field of structural fire engineering, which resulted in an introduction that should also allow non-fire experts to get swiftly in touch with this important topic, identify weaknesses in design approaches and allow for further advances in the future.

Acknowledgments

Chapter 1

Introduction to the thesis

1.1 General

This Chapter provides the motivation for the actual thesis and an overview of the organisation of this thesis document. This Chapter should help to localise quickly the relevant parts for the particular reader. Consequently, it guides the interested reader through the conducted research and it helps the reader with expertise in this field of research to find quickly find relevant Chapters.

1.2 Motivation

The majority of currently available design tools for structural fire design of timber members were developed empirically from tests conducted in fire resistance furnaces. Partly, semi- empirical approaches exist when the field of application was extended for a more practical use. In many countries, buildings with major structural elements made from timber have just recently entered building classes of medium and high-rise buildings. For these buildings, the collapse of main structural elements in the event of fire or the complete loss of the building is considered unacceptable. In previous studies, several research gaps have been identified, which address in general (1) the applicability of furnace tests for timber components and (2) the validity of the current fire resistance framework for timber buildings. The typical framework is widely known to be described with the R (resistance), E (integrity) and I (insulation) characteristics of building components. These characteristics may be associated to buildings depending on their occupancy, importance (e.g. lifeline objects), the neighbourhood and building height. Usually, they are linked to resistance times (in min) to specify a comparison measure. This comparison measure is usually the standard fire testing or models describing the corresponding exposure. However, potentially critical topics were observed with respect to increased use of combustible surfaces or structural timber. The critical topics listed by authorities, researchers and industry representatives are, (a) the external flaming, (b) the behaviour of timber structures in the cooling phase and (c) the burnout of compartments without the intervention of fire services. The questions appeared to be highly relevant for the successful application of products providing combustible surfaces such as timber. It appeared that (1) and (2) cannot be described utilizing sorely results from standard furnace testing. Subsequently, this question leads to the overall contribution of timber to the fire dynamics in all phases but mainly to the fully-developed and the cooling phase with particular effects such as (a), (b) and (c). Consequently, the validity of furnace tests was questioned for timber structures, or more generally, for all building components apart from non-combustible structures. Detailed questions are represented by the radiant flame feedback of surface flaming and the overall contribution of smouldering and flaming combustion in furnace testing and compartment fires. Currently, no common understanding is available to answer these questions. This may be due to limited data, limited research or the limited view by individuals. In this thesis, several of the listed questions are addressed and con-

tributions are provided to solve these questions accordingly. The main objective of this thesis was the description of the structural timber's contribution to design fires. Secondary objectives were the contribution of the smouldering combustion to furnace tests, and the general validity of furnace testing for timber structures.

1.3 Methodology

Based on the identified research gaps or the absence of engineering tools, the research presented in this thesis focused on the behaviour in the decay phase, which may be understood as third phase of a general fire development after the growth phase and the fully developed fire phase. The third phase is further referenced as cooling phase. In this thesis, the third phase should be understood as the phase after, either, point in time when the fire decays or, more relevant for fire exposed structural timber, when the movable fuel is consumed. Besides a comprehensive study of the available literature, experiments were conducted. The core of the experimental campaigns was the design of a novel experimental setup to isolate and study various characteristics and variables relevant for the fire exposure of structural timber in compartment fires. Results were further obtained from experiments conducted in model and large scale fire resistance furnaces. A bomb calorimetry analysis was performed to describe the energy stored in the char layer material after various stages of the fire exposure. A small-scale compartment experiment was performed to verify the findings. To describe the behaviour of structural timber in compartment fires, the definition of "thermal exposure" was extended by the concept of "fire exposure". To study the question of the thermal exposure, furnace experiments were conducted with combustible and incombustible specimens. Under the consideration of the definition "fire exposure", data from the experiments were analysed. Results and derived relationships were utilized to develop a design model for the improved prediction of the heat release of structural timber in compartment fires. Subsequently, the design model was validated using available data from compartment experiments.

1.4 Organisation

1.4.1 General

The thesis is written as monograph with references to journal and conference papers and other published contributions by the author. These references may be allocated at distinct statements within the text or as general references introducing the particular chapter.

1.4.2 Chapters of the thesis

This thesis contains seven Chapters and Appendices.

Chapter 2, "Introduction to the research field", is of a general nature, giving an introduction for the subject of this thesis. This Chapter gives the background to the research field 'fire safety engineering' in general, with important elements of the current framework with focus on structural fire design of timber members. This Chapter comprises a state-of-the art with and is organized in alphabetical order as the preference was given to the reader of selective parts, but the Sections are written in a way that engineers with a limited background in fire safety science should be able to follow the topic.

Chapter 3, "Experiments", presents four experimental campaigns conducted in the framework of this thesis. This Chapter gives an overview of the four experimental campaigns conducted in the framework of this thesis. The reported experiments include experiments designed, performed and analysed by the author of this thesis together with students at ETH Zurich (IBK) and experiments performed as joint-projects. The experimental campaigns were the following:

- eight experiments conducted in standard fire resistance furnaces;

- about 80 experiments conducted in the Fire Apparatus for Non-standard heating and Charring Investigation (FANCI), designed and assembled by the author of the thesis;

- experiments to produce a representative char coal layer that was analysed subsequently with respect to the remaining energy content;

- a compartment experiment in medium scale to investigate the char layer reaction with respect to its yield and location.

For all experimental campaigns, this Chapter includes the description of the particular research question, the material, the equipment, the performance of the experiments and the results obtained. The particular methodologies applied in the experiments are given in the particular Sections. The details of the experiments are included in several reports.

Chapter 4, "Thermal exposure and fire exposure of structural timber", studies the term of thermal exposure with the focus on standard furnace tests and the validity of the tests to describe the thermal exposure of timber components. A secondary aim was to study the contribution of the test specimens to the furnace fuel load. In this Chapter, the unique behaviour of structural timber as fuel load is studied. Apart from a combustion efficiency, it is found that the behaviour is significantly dependent on the creation of a new material, the char layer. The char layer is capable to (temporarily) store energy. Thus, the energy or heat release may be reduced or delayed.

Chapter 5, "Combustion behaviour of structural timber in compartment fires", presents a study about the material properties relevant for the consideration of structural timber as fuel load. Consequently, factors to describe the decay and energy content of the structural timber and the char layer are studied. To describe the structural fuel load provided by fire exposed timber, the char layer yield (density profile and its change over time), the moisture content and the surface area are derived using the corresponding terminology

of the Eurocode [33, 34, 35]. Subsequently, a recently proposed constant fitting factor to reduce the structural fire load is investigated. Here, available fire compartment test are systematically analysed. Utilising data from the experimental campaigns, the background of the fitting factor is investigated. It was found that the energy or heat storing ability of the char layer is the reason for the unique combustion behaviour of structural timber in compartment fires. However, the range of the subsequently introduced modification factor was observed to vary significantly.

Chapter 6, "Development of the Timber Charring and Heat Storage model", describes a framework to describe the behaviour of structural timber in compartment fires, its modification including the creation of the char layer and its decay, and, finally its contribution to the fire dynamics. To do so, the setup of the timber charring and heat storage model, TiCHS, is presented. Consequently, the Chapter addresses the limitation of the inflexibility of a fixed fitting factor investigated. or an alternatively required parameter study. Combining the results from all experimental campaigns, the Timber Charring and Heat Storage-model is developed. The TiCHS-model puts together seven elements. The elements are (1) the energy provided by structural timber, (2) the modification rate of virgin wood to the char layer appearing as progression of the char line, (3) the release of combustible volatiles during the creation of the char layer material, (4) the energy required to modify virgin wood to the char layer material, (5) the energy released during the combustion of the char layer, (6) the energy and (5) the energy release by the char layer during the smouldering combustion. From the experiments it was found that the smouldering reaction needs to be divided in two sub-processes describing the char layer's decay. The sub-processes are the smouldering combustion in the char layer and the final complete decomposition of the char layer at its surface, i.e. the surface regression. The TiCHS-model, set up as framework describing all five listed elements, utilizes a general charring model for the description of progress of the pyrolysis. Currently, the cumulative temperature charring model implemented in the second draft of the fire part of Eurocode 5 [40] is used. This model is based on the empirical charring model developed by Werther [205]. The TiCHS-model is intended for application together with a zone model software to predict the fire dynamics in a compartment. The contribution by the structural fire load is predicted by the TiCHS-model while for the prediction of the movable fire load, typically applied models can be used. Well-known models are available in the corresponding literature [81] in Eurocode 1 [34]. In a final step, the approach using the TiCHS-model is validated using compartment experiments with relevant shares of exposed structural timber surface areas.

Chapter 7, "Summary, conclusions and outlook"' summarizes the content of this thesis, conclusions are given based on this work together with suggested elements of future work.

1.5   Limitations

The main intention of this thesis was contributing to study the fundamentals of fire dynamics when structural timber is involved in compartment fires. Relationships have been found, analysed and derived using data from various sources. As the topic of the fire dynamics is of highly complex nature, no practical application should be performed without a large range of validation. The validation of the TiCHS-model has been performed for compartments with limitations with respect to the movable fuel load, the structural elements and the enclosure geometry. These bounds should be carefully respected. Further, it should be observed that for the development of design fires, vagarious fire scenarios should be investigated. No general valid method is presented to consider the radiative contribution of surface flaming to structural elements other than the origin. Furthermore, it should be highlighted that currently, no combustion model for partly decomposed char layer volumes on the floor is available. These parts of the structural fuel were originally sticking to the ceiling or walls, thermally modified at this location under one-dimensional heat flux and subsequently decomposed by the char layer combustion before falling-off the structural elements due to bond line integrity failure. Subsequently, these elements are exposed to three-dimensional heat flux from multiple sides in an oxygen rich environment.

Conducting the experiments, analysing the data and setting up the model, it was aimed for a transparent approach and a correct determination analysis results. However, the author of this thesis takes no responsibility or warranties of its general application in practice. The model allows experts in the field of fire engineering the prediction of the compartment fire only when all relevant aspects are verified. No general guarantee can be given with respect to a general completeness, accuracy, reliability, suitability or availability with respect to the TiCHS-model or elements hereof. Any general reliance placed on the TiCHS-model or elements hereof are therefore strictly at the individual's risk.

Chapter 2

Introduction to the research field

2.1 General

This Chapter is written as an introduction to the research field of fire safety design for timber structures with the focus on the interaction of the material with the fire compartment during the fully developed fire and the cooling phase. It provides an overview of the state of the art, reflects on current practice and includes recently published research results. Additionally, research results from the experimental campaigns, the simulations and the discussions obtained during this PhD are referenced under the corresponding headings. Initially, in Section 2.2, the history and principles of structural fire safety design are presented, including more recent developments with respect to the fire safety framework. In Section 2.3, the fire behaviour of the building material wood and timber members respectively is presented including relevant influencing factors.

Parts of the introduction are taken from the author's contributions to conference and journal publications [175, 53, 174, 167, 176, 162, 163, 164, 109, 170, 177, 166]. These contributions were a result from the author's collaborations with colleagues from ETH Zurich and external academia. The referenced work was organised and led by the author of this PhD, while valuable contributions were provided by the co-authors and persons acknowledged in the publications.

2.2 The fire safety design of structures

2.2.1 General

Historically, fire safety has been of major concern since the beginning of civilisation. The building material timber is - together with stone - one of the oldest building materials used in human history. Due to its natural given structure, wood provides linear building components used for bending and buckling members. Access to the raw material (e.g. dimension, species) has developed building traditions, which vary from region to region. Aside from this, the access to processing techniques had a great impact on the use of building materials, which resulted in engineered wood products such as glued-laminated timber (available now for more than 100 years), wood based I-joists, and, more recently, in large timber panels such as solid timber panels (STPs) and cross-laminated timber (CLT). The historic use of timber as building material becomes apparent when investigating historic temple buildings of up to five storeys, e.g. see Figure 2.1 (a); The Japanese pagoda exceeding 35 m height, built around the year 600 AD, would today still be an exception according to many building regulations today and would require special permits. Building traditions have always been affected by the practitioner's experience and have been significantly influenced by incidents such as tsunamis (Lisbon 1755; resulting in top stories only in light wood construction) and - with respect to fire safety design - by severe accidents. Relentless conflagrations e.g. in London 1666 or Oslo 1624, see Figure 2.1 (b), resulted in the ban of combustible exterior surfaces similar to fire hazards during wars in

Vienna 1683, which resulted in the requirement for incombustible, reinforced attic floor construction.

Recently, a fatal fire accident in London in a tall concrete building with attached polyurethane based exterior insulation with a classification in disagreement to existing legislation [69] resulted in the introduction of limitations for combustible materials including timber structures. The limitations with respect to the combustibility (reaction to fire classification) were chosen, as they are easier to control as the execution a quality insurance system. A quality insurance system comprises the verification of built practice with respect to applicable rules and a comparison of the foreseen material choice and detailing and the actual execution on the building site. To set distinct rules, the United Kingdom (UK) decided to introduce further requirements. In addition to traditional minimum requirements with respect to the resistance against collapse, the explicit requirement for burnout has been brought up for structures exhibiting a significant share of timber surfaces [18]. Here, it should be noted that no common understanding for burnout exists.

Fire has always been seen as threat for life since the beginning of civilisation and reflected in important sections of the building regulations; the characterisation of the products and materials is done with respect to specific properties. These characteristics are preliminarily based on observations which are (1) the production of sparks, (2) the release of smoke and toxic gases, (3) the flame spread and (4) the contribution to the fire development, which were typical reasons for many disastrous historic fires, see example in Figure 2.1 (b). Not only the varying experience in various countries and regions but, further, the different access to materials (e.g. adobe, stone, timber), the use of other units (e.g. foot and meter) or simply the availability of different dimension of logs created significant differences in building traditions which are described today in the building regulations.

With the European legal framework for fire safety, a common market for products is aimed for - including a common testing and classification philosophy. Moreover, a common understanding has been established. Figure 2.3 shows the interaction of standards with the building regulations: In general, it is up to the national regulations to define the overall level of safety. This means that some parts of design standards (e.g. National appendices of Eurocode [33]; NA in Figure 2.3) or particular factors might be specified individually for a country. Furthermore, the (regional) building regulations define certain building categories, which have to meet certain criteria, e.g. building heights (often limited due to the accessibility of the highest floor elevation by fire services).

2.2.2 Fire resistance framework

While fire accidents were always known to be a potential threat to human settlements and life, the systematic and experimental research of structures in fire began after 1870. Various growing cities saw the need for a better understanding of fires and its effect on buildings and, thus, initiated research in this field. Thus, fire research was started in some

Copyright M. Cartwright
(a)
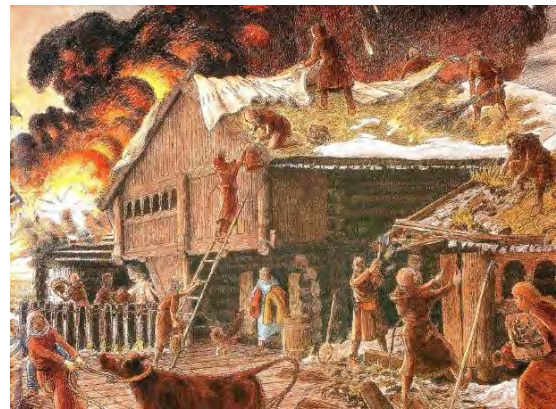
"Middelalderbyen i Oslo", copyright E. Schia
(b)

Figure 2.1: The five-storey pagoda of the Buddhist Horyuji monastery, Nara, Japan (a) and a painting of the great fire of Oslo 1624 (b).

larger cities (e.g. Denver, New York, Chicago, London, Berlin). When fire safety came into focus for several authorities, research institutions started to investigate fire resistance with various ad-hoc procedures [9, 10]. In the very beginning of the 20th Century, some of the first proposals for standardised fire tests were made [155]. The purpose of tests was to address the misuse of the term 'fire proof' for building elements frequently used by building contractors and product providers in the building industry. In the first rules, a constant minimum temperature, duration, fire exposed area and mechanical load was prescribed. It should be noted that the first fire tests could be considered as compartment fire tests or experiments with a fuel load that was topped-up during the fire. Higher fuel flow into the compartment during the test would have not changed the temperature of the fully developed fire within the test compartment, as these tests represented ventilation controlled fires. Originally, it was not obvious that fires could have different temperatures and later, a mean temperature during the test was defined. It was believed that the definition of the steep temperature rise in the beginning of the fire curve was due to the introduction of industrial burners rather than the flashover. About fifteen years later, in 1918, a new standard fire test was introduced by the ASTM, which required temperature control following a prescribed time-temperature curve for the duration of the fire. This time-temperature curve was based on a fit of fire curves used by various laboratories [9]. Today's standard time-temperature curve used in Europe (EN/ISO fire curve) differs only very slightly, see Figure 2.2. Until today, further regulations have been implemented and standards designed to answer the need of our society, e.g. EN 1363-1, ISO 834-1 and ASTM E119, which are slightly different but reproduce the physics of heat transfer in a targeted range [5, 37, 85]. It should be noted that combustible products, more specifically timber columns, were used as reference products, i.e. timber was not excluded from fire testing [83]. This fire testing in huts would be called compartment tests or experiments nowadays. By trend, they provided less repeatability than today's fire resistance tests in furnaces. However, by trend, they allowed allowed analysing the effect of different room usage (occupancy) and furniture distribution in realistic fires [9, 10, 162]. Tests and approvals were often done by means of comparison to a reference building structure, until, in 1928, Ingberg [84] introduced the concept of 'building fire severity' proposing an equivalence between comparative fire ratings obtained from furnace tests and fires in real buildings. A one-hour fire rating obtained in a furnace test following a standardised temperature curve would be equivalent to a fire in a compartment with a fire load density of about 900 MJ/m^2, which for most occupancies (except e.g. libraries) is significantly above the 80% fractile of fire load densities listed today, see e.g. Eurocode 1 [33]. Following the introduction of the fire severity concept, the first comprehensive fire regulations were developed in the United States and Great Britain [50, 136]. These regulations made use of the standard fire testing and expressed fire requirements using the one-dimensional scale, the time that a structure must be able to resist the standard fire. In these standards, buildings were divided into types from 'fireproof', without any combustible materials, to 'wood construction' with prescribed restrictions concerning e.g. building heights, usage or detailing. An important type, 'exterior-protected construction' required incombustible

exterior walls with a fire rating of two hours, while the interior load-bearing structure could be made of timber and required only 45 minutes of fire resistance. A collapse of the interior after this duration was explicitly accepted. This type is comparable to many houses built between the 17th and 20th Century in major cities in Europe with exterior masonry walls and timber based floor and roof structure.

Nowadays, fire resistance ratings in Europe are often not as detailed and differentiated as the aforementioned regulations. Rules aim for being open for product development without specifying particular building solutions to allow for further development of new design in line with the given rules. Nevertheless, the number of fatalities is low or decreasing in developed countries; examples for UK, Sweden and Switzerland are given in Figure 2.4 (a). This is a result of many factors, e.g. the fire load reduced significantly and the heating systems became more reliable at the same time that building quality increased. Additionally, the focus of current fire regulations is broader. Beside the consideration of the structure, it includes further technical and organisational measures, see Figure 2.4 (b), e.g. active measures such as sprinklers to limit fires and fire spread, smoke exhaust systems to move hot gases and over pressurised staircases providing clean air on evacuation and routes also to be used by the fire services. However, it should be noted that the original concept with its limitations was re-evaluated in many national fire regulations. In the re-drafting and reviewing process, the building's and structure's importance (including the building class and occupancy) was incorporated in the required fire resistance rating without deeper investigations (e.g. R15 for staircases or R90 for hospitals). The development, consideration and maintenance of all fire safety measures should be a continuous element from the strategic definition throughout the use of a building. This continuity of fire safety planning is reflected by its inclusion in all phases of a building project, e.g. also implemented in all eight stages of a building project according to the RIBA plan of work [184].

The European framework aims to describe the fire performance of a product or a component in a harmonised way. Yet, it should still allow for a tailor-made implementation of the products in individual national markets where the products have to meet different requirements based on the particular building regulations. The European framework for the products and building components characteristics with respect to fire safety is divided in (I) 'reaction to fire' and (II) 'fire resistance', which both can be qualitatively related to the phases of a fire. This division is used to characterise a material, a product, or a component or a combination to a system with respect to (I) the phase of the fire development from ignition to flashover and (II) the phase of a fully developed fire including the cooling phase, see Figure 2.3 (a).

2.2.3 Fire safety objectives

The main objective of fire safety is the protection of humans, including inhabitants, visitors the fire services. Furthermore, the limitation of property damage may be an objective, especially for multi-compartment or commercial buildings. Specified requirements
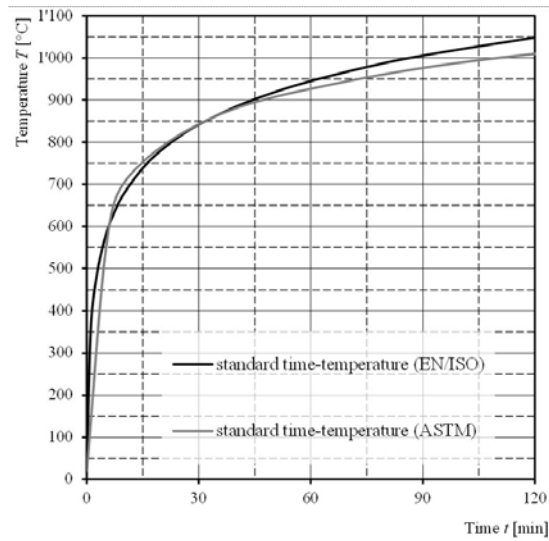
Figure 2.2: Time-temperature curves of EN 1363-1 [37] and ISO 834-1 [85] respectively and ASTM E119 [5]. Source: J. Schmid et al. [162].
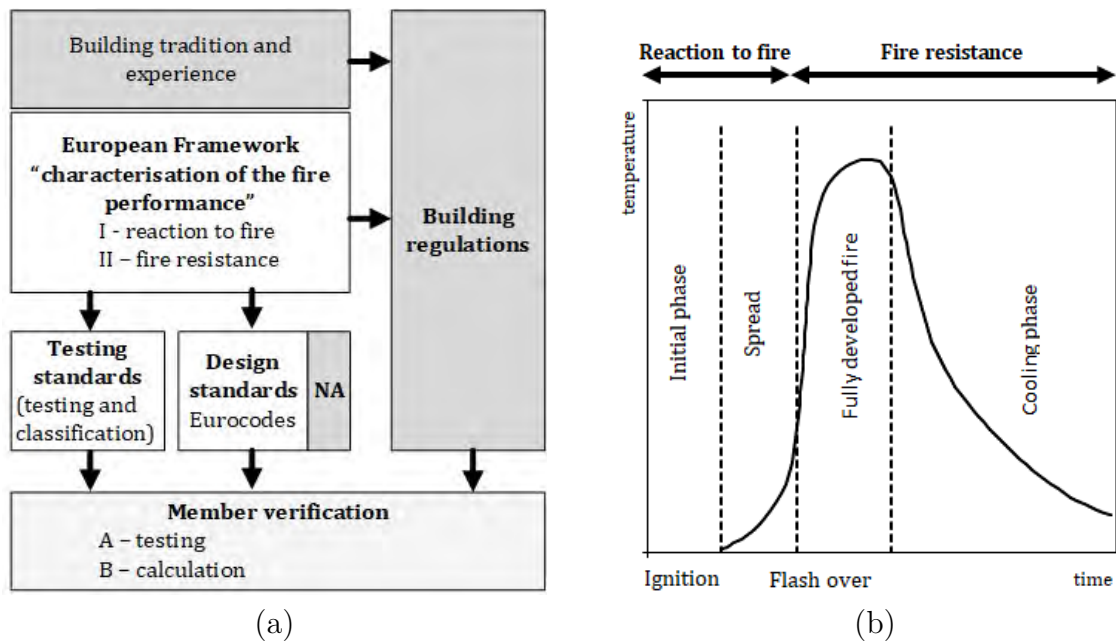
Figure 2.3: Interaction between framework elements relevant for fire safety with the filled elements based on national legislative (a) [164] and the connection of the characteristics "Reaction to fire" and "Fire Resistance" with a qualitatively fire time-temperature curve (b) [164]. Own images.

can be fulfilled by one element of the set of fire safety measures or by a combination and interaction of passive (i.e. structural fire safety), active (e.g. technical), and operational (e.g. fire services) measures, see Figure 2.4 (b). This chapter focuses mainly on passive measures. Generally, the fire safety objectives are project and situation independent and a common understanding exists among most countries. In contrast, the requirements which are set to achieve the fire safety objectives are normally situation dependent (e.g. they are dependent on the occupancy) and vary between countries. For example, the objective 'protection of humans' can be guaranteed by safe means of escape. Related to this objective, building regulations may prescribe two independent staircases. Further examples of prescriptive codes are the specification of various fire resistance ratings (e.g. load-bearing resistance for 60 minutes standard fire, R60). The requirement of preventing a building collapse is currently a major topic in the fire safety science community when timber structures are discussed. It is discussed that the structural component or the structure might pass a given minimum resistance against collapse, but the combustibility of the structure will increase the fire duration and might counteract burnout, which was earlier assumed to occur when the movable fire load is consumed. Fire safety regulations aim for the same level of safety for buildings with combustible products, such as timber, as for buildings with non-combustible products. Discussions increased due to the entry of timber components in the market of medium and high-rise buildings. For small buildings, a collapse is often considered acceptable which does not apply to high-rise buildings especially when people are supposed to remain in adjacent compartments instead of evacuation. Thus, it is not surprising that, additionally to the existing framework, it is intended to introduce a requirement for burnout in Great Britain [18], which might be relevant in addition to further prescriptive requirements.

2.2.4   From 'prescriptive' to 'performance based' fire safety design

Generally, building regulations reflect the state of practice based on positive experience and typically applied standard solutions; partly, catalogues exist with accepted solutions. Thus, innovative design risks to exceed given restrictions. To evaluate new ideas which exceed the regulated scope, or which are not covered by them, methods that are more complex have been developed. Methods using standard solutions, e.g. from catalogues, are often referred to as 'prescriptive' methods and advanced methods are often referred to as 'performance based' with an idealistically clear distinction between the two terms. When it comes to fire safety design, the fire resistance ratings, e.g. R90, may appear as 'prescriptive' as methods are available to calculate the rating and, thus, adopt an assembly's fire rating which is considered in some countries as 'performance based design' (PBD) as a component's performance can be optimised. However, it should be highlighted that the developed fire resistance ratings implied certain boundary conditions. To present the generally smooth transition between 'prescriptive' design and PBD two examples, (1) the design of evacuation routes from a metro station and (2) the design of the structural fire resistance of a beam are presented in the following. Both cases are
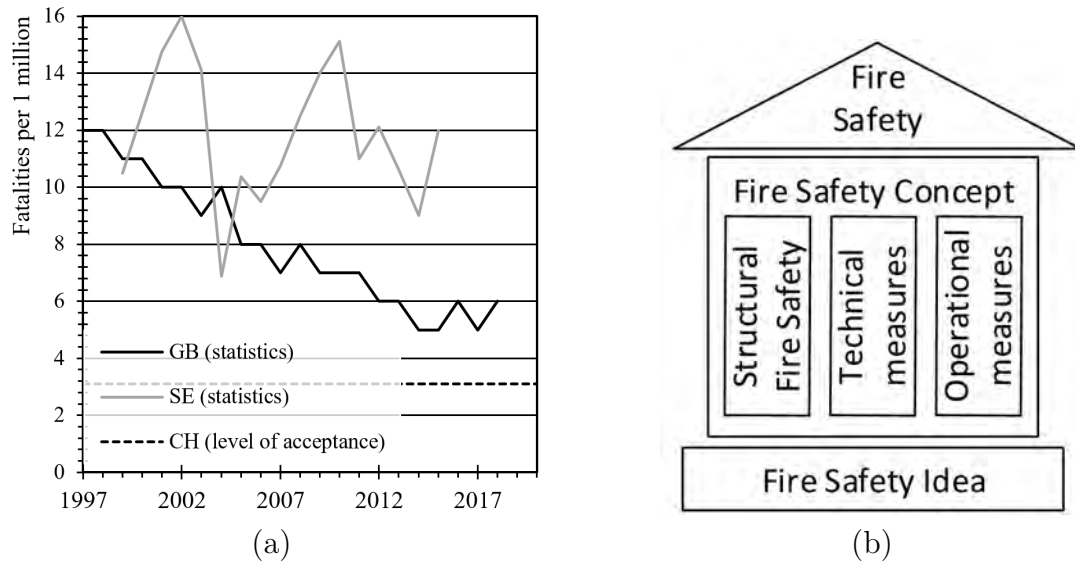
Figure 2.4: Yearly fatalities in building fires in Great Britain (GB) and Sweden (SE) in comparison to the accepted and reached level in Switzerland (CH) (a) [131, 135, 200] and the schematic setup of fire safety engineering measures (b). Figures from Schmid et al. [164].

schematically shown in Figure 2.5. The term 'prescriptive' refers to simplified verification methods, where distinct design rules are available based on tradition and good experience. The corresponding design is are considered to be applicable for typical design answers. Thus, those prescriptive methods are the least flexible as they are limited to solutions where experience is available. On the contrary, complete flexibility is given with probabilistic methods, which are considered to be not limited to specific problems. Contrary, probabilistic methods should be able to provide design justification for any boundary condition. The derived solution is then tailor made for the actual project. By trend, these solutions can not transferred to other situations as minor differences in the input may lead to large differences in the output. However, probabilistic methods should provide the most efficient design. Probabilistic methods are generally time consuming and require sound probabilistic background for a large number of decisions. E.g. large data sets for failure statistics are required for all relevant parameters. Thus, probabilistic methods are applied mainly in academic studies, which might create problems when not all project partners share the same level of knowledge. Typically, the responsibility is shifted to the engineer with increased complexity. In the reverse situation, the authority takes more responsibility for the fire safety with simpler methods, which leads, together with the roughness of the methods, to rather conservatively set requirements. Applying PBD together with prescriptive design rules seems to be reasonable when a building exceeds actual regulations in limited areas. However, special care should be taken combining both

example 1: evacuation of a metro station

Prescriptive	Performance based		Probabilistic
defined exit width per person, max distance to surface, ...	evacuation within 10 minutes	tenable conditions during evacuation in a given fire scenario	expected number of fatalities per time period below target
simple calculation	evacuation simulation for a given scenario	evacuation and fire/CFD simulation for a given scenario	evacuation and fire/CFD simulations for probabilistically derived scenarios

example 2: timber beam in fire

Prescriptive	Performance based		Probabilistic
given minimum dimensions and other requirements	reach of standard fire requirement R30/R90/...	no structural failure in given scenarios (fire load, spread rate, ...)	probability of collaps smaller than a probability target
table values	analytical calculation models	simulations	probabilistic simulations

model simplicity   **consequence of fire**

Figure 2.5: Continuous transition of methods for the fire safety design for two examples from prescriptive- to performance based- to probabilistic design. Figure by R. Fahrni [164].

methods as the overall objective might be different or difficult to define for prescriptive rules applied traditionally.

2.3 Structural timber in fire - characteristics, measurement techniques and typical values

2.3.1 General

The following Sections 2.3.2 to 2.3.48 provide an alphabetical list of characteristics, which influence fire dynamics. General characteristics are given aside from characteristics that are only valid for timber. The consideration of the listed characteristics may be relevant for testing, experimenting and designing structural elements. In contrast to other traditional building materials such as stone, concrete, masonry and steel, timber members are combustible elements which have significantly different characteristics when exposed to fire (e.g. the creation of a char layer, low heat conduction) and may have significantly different influences on the fire dynamics. Differences are, among others, the contribution to the fire load and the low thermal absorptivity in compartment fires or furnace tests. In the past, several authors, e.g. Leikanger-Friquin [62], collected influencing factors on the charring rate, while the influence of the overall fire performance is of multiple sources and the factors overlap. The following sections provide an introduction into the research topic

of the fire design of timber structures but, in addition, point out research needs and lack of data. Besides the state of the art, recent research results are referenced which have been observed, collected and published by the author complemented with numerous external references. For the successful implementation of design tools, a common understanding is of major importance. For several characteristics listed below, it becomes apparent, that it is currently not possible to deliver generally accepted answers or practical understanding for the engineer.

Since the beginning of civilisation, wood has been used as an energy source and a building material. The combustibility of the material is a naturally given characteristic that offers advantages and limitations. Numerous authors have researched wood as an energy source, i.e. a fuel. The focus was typically the production of energy, or the production of favourable energy sources, e.g. char coal or other basic products such as methanol, pyroligneous acid needed mainly in industrial processes, see e.g. Klar [99]. When it comes to the building material structural timber, its performance and behaviour in fire was of overall interest since the beginning of research of structures fire resistance. In particular, in the first studies to develop the fire resistance framework, timber structural members were explicitly included [50, 136]. Not only the structural behaviour, but the material behaviour has been researched already in early days of fire resistance research, e.g. by Bamford et al. [12]. After the Second World War, detailed research about timber's charring behaviour became available. While it can be noticed that material scientists mainly investigated isolated characteristics, e.g. the heat of pyrolysis (see Section 2.3.33) or the ignition (see Section 2.3.27), structural engineers focused on the performance of isolated timber members. Due to practical reasons and limited funding, studies aim often for finding the all-in-one device suitable for every purpose. This is firstly, generally valid experimental boundary conditions (e.g. the standard fire), and secondly, correlations, derived for this particular boundary condition and subsequently extended to a large range of applications. Thus, for the structural fire design of timber, the content of many investigations was the effects of the standard fire on the remaining virgin cross section (misleadingly named residual cross section, see also Figure 2.7) as it has been used to determine the load-bearing capacity. The available calculation models typically used a (one dimensional) charring rate to assess the corresponding charring depth which describes the remaining virgin cross section at a time of fire exposure.

2.3.2 Adhesives

Adhesives have been used for more than 100 years to create linear timber members such as beams and columns. Typically, these elements utilise adhesives to create joints in the direction of the lamellae (butt or finger joint bonding), and on their wide surfaces (face bonding). Besides linear members, more recently, plane members have been introduced to the market utilising bonding techniques mainly by adhesives. As adhesives might soften when heated, it is apparent that a glued member may be affected in fire situation. The effect of the fire exposure on bonding should be assessed together with the observed tem-

perature gradient in fire exposed timber. When exposed to standard fire, the temperature gradient is very steep for unprotected timber members. Typically, at a distance of about 40 mm beyond the char line, a normal temperature can be measured [171]. The strength reduction of finger joints has been extensively researched in experiments and simulations and it was shown that finger joints do not reduce the load-bearing capacity of glulam beams for most of the cases, see e.g. Klippel et al. [101, 57]. For CLT, effects of the bonding failure can be observed when the charring or charred layers may fail. This may occure when the bond line exhibits temperatures between about 250°C and 500°C [24, 44, 45]. Simplified, the fall-off can be described by the Eurocode 5 [35] charring model, which assumes that the CLT is a multi-layered assembly [104]. Currently, for CLT, only a full-scale fire resistance test are applicable to prove sufficient thermal stability of the bond line [4]. Similar methods in less than full-scale are currently under development, e.g. by Klippel et al. [102].

2.3.3   Air

Air is the mixture of gases on earth, generally understood at ambient condition, i.e. not affected by a combustion process. Air consists of two major constituents, i.e. nitrogen and oxygen, whereby the latter is an essential for combustion and is of major influence on the description of the general conditions in a fire compartment and, in particular, of timber when exposed to fire. The density of air is a function of the gas temperature, the air pressure and the air humidity. The density of dry air at normal condition (20°C) at sea level (101 300 Pa) is about $1.20\,\mathrm{kg/m^3}$ and can be calculated following equation Eq. 2.1, wherein the second term remains unused for dry air.

$$\rho_{air,humid} = \frac{p_{air,dry}}{R_{air,dry} \cdot T} + \frac{p_{vapor}}{R_{vapour} \cdot T} \tag{2.1}$$

where

$\rho_{air,humid}$	is the density of humid air, in $\mathrm{kg/m^3}$;
$p_{air,dry}$	is the pressure of dry air, in Pa;
p_{vapor}	is water vapour pressure, in Pa;
T	is the gas temperature, in K;
$R_{air,dry}$	is the specific gas constant of dry air, 289.06 J/(kg $\cdot$ K);
R_{vapour}	is the specific gas constant of water vapour, 461.49 J/(kg $\cdot$ K).

For simplicity, the air density can be estimated solely on the gas temperature. This becomes especially relevant in the fire situation where the gas temperature is significantly above 100°C and water vapour is neglected:

$$\rho_{air,hot} = \frac{p_{air,0}}{287.1 \cdot T_g} \tag{2.2}$$

where

$\rho_{air,hot}$	is the density of hot air, in kg/m³;
$p_{air,0}$	is the exterior air pressure, e.g. 101 300 Pa at sea level, in Pa;
T_g	is the gas temperature, in K;
T_0	is the ambient gas temperature, in K.

In this work, the air density has been used for the evaluation of gas flow in the experiments performed as well as in the TiCHS-model, see Chapter 6, where the gas velocity and the oxygen concentration together form a measure for the oxygen contact intensity affecting the fire exposure, see also Section 2.3.17.

2.3.4 Anatomy of wood

The anatomy of wood for species typically used for structural timber is well researched and documented in the literature. On the contrary, limited information is available about the anatomy of fire exposed timber, i.e. the virgin wood heated above about 105°C (used for drying processes) or of the thermally modified part of the section, the char layer which represents a completely different material. During fire exposure, both materials, i.e. the char layer and the virgin wood heated above the drying point, experience unsteady heating in addition to the exposure to certain gas compositions.

Lingens [116] analysed samples from various levels (zone 1: char, zone 2: char line, zone 3: heated wood and reference material) of specimens previously exposed to standard fire in a model scale furnace but could not draw clear conclusions from his analysis of the microstructure using light optical microscopy. Interestingly, Lingens, combined the char layer to one zone only which might imply limitations on a more detailed view of the charring behaviour of structural timber and its contribution to the fire dynamics by smouldering.

The porosity of wood is believed to be linked to the different charring rates which vary for some timber species. The diffusivity of wood is apparently linked to the combustion and decay behaviour of wood as the charring rate, typically expressed as rate perpendicular to the grain, is reported to increase significantly when the heat flux is along the grain direction, see Section 2.3.32. It can be assumed that the diffusivity of the char layer affects its combustion behaviour. Probably due to the limitation of studies focusing on exposure using the standard fire where typically low oxygen concentrations are measured in the furnace, the anatomy of the char layer has not been studied adequately in the past.

2.3.5 Arrhenius equation

For advanced calculations of the thermal response of timber including the charring behaviour of structural timber the Arrhenius equations can be used. According to the Arrhenius equation, the temperature dependent reaction of materials is captured empirically by the description of the material's kinetics [11]. In its original form, the Arrhenius

equations defines the reaction rate by means of the activation energy and a constant factor describing the temperature dependent chemical reaction:

$$k_i = A_i \cdot e^{\frac{-E_i}{R \cdot T}} \tag{2.3}$$

wher
k is the reaction rate, in mol/(m$^3 \cdot$ sec);
i is the index for the material number;
A is the pre-exponential factor for the reaction;
E is the activation energy for the reaction, in J/mol;
R is the universal gas constant, 8.314 J/(mol $\cdot$ K);
T is the temperature, in K.

Using one equation for every material, several equations of the type given in Eq. 2.3 can be defined for several main components in wood. Some proposals for the kinetic factors for wood and the char layer only are available and describe the activation energy and the collision factor (pre-exponential factor) for up to seven materials (including water and char) considered as the components of wood [129, 119, 194].

2.3.6   Burnout

Today, burnout is understood as the end of the decay of a previously fully developed fire. However, no common understanding is yet available. The terminology definitions concerns questions if this point in time should be defined with (a) the consumption of the movable fire load, (b) the end of flaming combustion or (c) the end of glowing and smouldering combustion. In early building codes, burnout was understood as the consumption of the fuel by the interior and internal structural collapse was acceptable if limitation to the building and the compartmentation could be expected [136]. Apparently, for large or complex buildings where structural collapse is not acceptable, other measures should be foreseen. The need for an improved description results further from the "stay-put" methodology, where occupants are asked to stay in their compartments and no safe evacuation is provided. Apparently, if a major share of the structure is made from combustible building products such as timber, the fire design could be found insufficient as structural members may continue burning until collapse after the consumption of the energy provided by the interior, i.e. the movable fire load. Establishing the existing framework including the definition of the fire severity, see Section 2.2.2, no combustible building materials where included in the analysis [84, 110]. Recently, scientists investigated conditions (incident heat flux and air flow) with respect to flaming and smouldering extinction of structural timber which are intended for the future design for burnout, see Section 2.3.16.

2.3.7   Burning rate

The burning rate was originally used to describe the consumption of a material when exposed to heat, often described in material and fire science as a mass loss rate (g/s). After the discovery to determine the heat release rate (HRR) based on the oxygen consumption in the exhaust gases by calorimeters, it could be replaced in many cases. In investigations of the combustion behaviour of timber, the term burning rate should be clearly defined to avoid misunderstanding. The burning rate could be misunderstood as the charring rate, which is given in mm/min and used to describe the rate of the thermal modification of the virgin wood into the char layer or as mass loss rate. More recently, the mass loss rate was studied by several authors to describe the end of any combustion within a timber specimen, e.g. [43, 3]. This characteristics may be used to define the point of self-extinguishment in the future. However, from a general point of view, it should be considered that a mass loss unit of a timber specimen could imply the complete consumption of the corresponding mass, i.e. 100% of the virgin wood is converted to volatile fuel, and, finally, released as energy and combusted to heat, or, that a certain, higher amount of wood mass has been converted to char material which has significantly less density but still contains energy. In the latter case, only a certain share of energy would have been released during the conversion process while the remaining energy would still be stored in the specimen. The consequence of the latter is that the heat release rate of structural timber can not be assessed accurately by mass-loss measurements as done in practice [71]. To enable the determination of the HRR based on mass-loss measurements, the density change of the char layer needs to be taken into account.

2.3.8   Char layer

The char layer is the layer of the thermally modified wood remaining attached to virgin timber section at its fire exposed side. The ability of a material to remain attached to another product or material is defined as stickability in the terminology of fire design. The char layer is formed during the pyrolysis of the timber member. In general, limited information is available about the char layer formed on structural timber. In fire resistance engineering, it is assumed that the char layer separates the original wood material from material formed under heat at a certain temperature. In design standards, the charring temperature is specified as the isotherm occurring at 300°C or 550°F. Previous studies indicate that for slower heating rates, the temperature might be lower. By simulating the charring behaviour in a more general way focusing on the kinetics of the material, the char line is typically defined as the zone where the highest rates of decomposition can be observed. While it is noted that the difference of the charring temperature of ±50°C is considered irrelevant for high exposure levels, for slow heating curves and during the cooling phase of a fire, it might be relevant to find an improved definition independent of the reference scenario, currently the EN/ISO fire exposure. After its formation, the char layer undergoes thermal expansion and further decomposition including the regression of

its surface and considerable cracking. Hadvig [72] found that the cracking occurs about 6 mm away from the char line, indicated in Figure 2.7. Besides shrinkage across the fibre direction, significant cracking of the char layer occurs across the grain direction of the original wood fibre direction in a certain pattern, which was studied by e.g. Winter et al. and Li [213, 114]. However, due to the apparent random nature and the related limited available common understanding of this effects, typically effective material properties - sometimes referred to as apparent material properties- are described by lumping various effects to basic thermal material properties, i.e. density, conductivity and specific heat of the charred part of wood, see e.g. Källsner et al. [95]. In handbooks, the char layer is often described as insulation layer, which is also reflected by the common understanding about its main function. While the timber is considered to have a relatively low heat conductivity, i.e. about 0.1 W/(mK) in FSE, corresponding values for the char layer are significantly less, i.e. 0.07 W/(mK) with a large scatter [77]. However, the change of its thickness or the contribution by glowing or smouldering combustion is not considered.

Some authors collected information for the density of the char layer, indicated as char yield. The yield was found to be in a range between 25% and 20% [62, 145, 63, 197] of the original wood density without specifying the reference moisture content nor the decomposition state of the char layer or the level (i.e. the depth) of the referenced material. It should be highlighted that the density is typically referenced as fixed value, e.g. 22% [145]. Spearpoint et al. referenced a maximum yield of 33% of dry wood [186].

Applying the thermal modelling of EN 1995-1-2, Annex B [35], subsequently referred to as the BEC-model [180], the density of this layer would vary between about 75% (intersection at 300°C) and 0% at the at 1200°C. On average, the density of the char layer would exhibit a mean density of 23% over the charring depth. Contrary to this, Law et al. [111] assumed complete decomposition of the char layer already at 600°C, see Figure 2.6.

The char layer surface regression (sometimes referred to as char layer contraction or char layer oxidation) describes the change of the original surface' location and is a measure of the reduction of the total cross section thickness, i.e. virgin wood and char layer thickness [175, 170]. All definitions with respect to a charring timber section used in this work are shown in Figure 2.7.

2.3.9 Charring

The charring of timber in the context of material science is understood as the process of destruction of wood which chars if heated sufficiently. The process occurs in several stages [156]. The process is sometimes also referred to as pyrolysis although pyrolysis comprises several processes. During charring the timber members gets reduced with respect to the virgin wood at the expense of the formation of a thermally modified layer, the char layer. The charring in the context of structural engineering of timber structures is understood as the reduction of an initially defined timber section by a certain charring depth. In the design process, the process is described as a rate, i.e. a charring rate
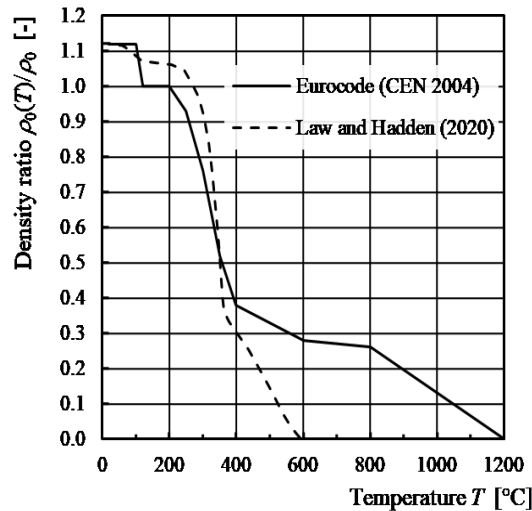
Figure 2.6: Density reduction according to the BEC-model [35] and an alternative by Law et al. [111]. In the area exceeding 300°C, the temperature profile is associated with the char layer. Own figure.

β in mm per min, see Section 2.3.10. During fire exposure, a char layer is formed at the same time as the original section is reduced by the so called charring depth d_{char}. The fire part of Eurocode 5 [35] defines the char line as the border-line between char layer and the residual virgin cross-section using the location of the isotherm in a heated section specifying the temperature to 300°C. The charring depth is typically reported in fire resistance tests with a single value, rarely does photographic documentation exist where the shape of the char layer can be further analysed, see Figure 2.8 (a). For the development of future design models, the consideration of the variation of the charring depth might be useful. Thus, more advanced methods are currently under development, see Figure 2.8 (b).

2.3.10   Charring rate

The charring rate is commonly understood as the progress of charring and is determined using different approaches. The progress is induced by the heating (thermal modification) of wood at the char line. Consequently, it can be described as the reaction due to the heat balance, i.e. the heat to the char line from the side of its fire exposure and and the heat conducted into the uncharred section. Commonly, empirical models base the charring rate prediction on the external heat flux and, eventually on the moisture content and/or the density of the wood.

The measurement approaches can be grouped in (T) temperature based, (M) mass
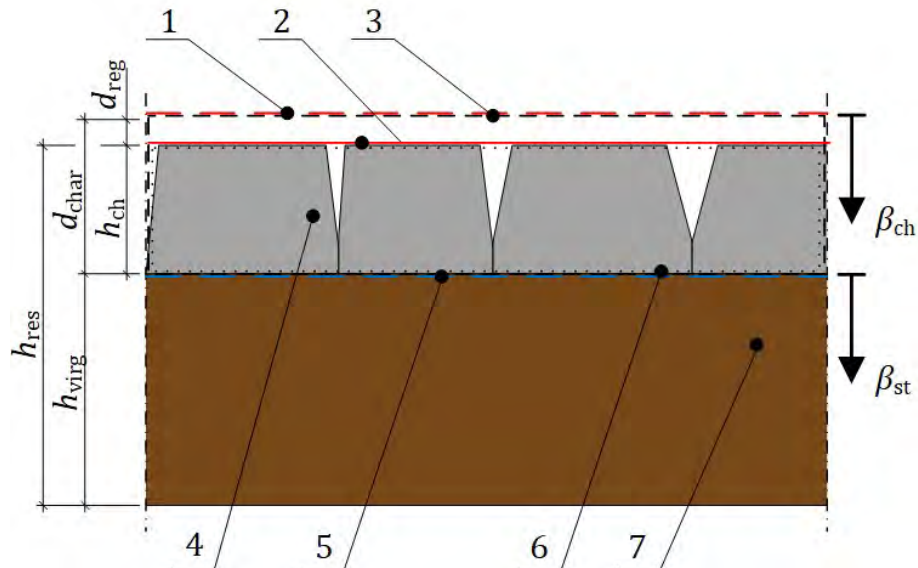
Key:

1	original surface (broken red line)	d_{reg}	char layer surface regression depth
2	char layer surface (red line)	d_{char}	charring depth
3	charring bulk volume (broken black lines)	h_{ch}	char layer thickness
4	char layer including voids and cracks	h_{res}	residual thickness (total section)
5	char line (blue broken line)	h_{virg}	residual thickness (virgin section)
6	char layer bulk volume (dotted black lines)	β_{ch}	char layer surface regression (rate)
7	virgin wood section	β_{st}	charring of the wood section (rate)

Figure 2.7: Definitions of section measurements with respect to the char layer. Own image.

       (a)   (b)
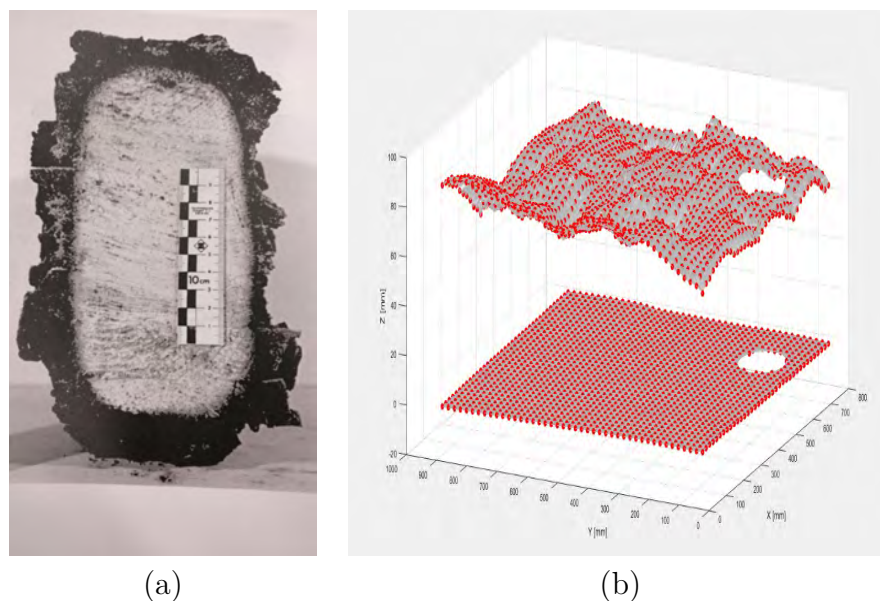
Figure 2.8: Reported cross section after a fire exposure: A representative section reported by Kordina et al. (a) and the 3D-scan of the surface of a residual virgin cross section of a CLT model scale specimen [170] (b).

based, (G) geometry based or (O) other measurement approaches [170]. Typically, all measurements are referred back to a change of the geometry, i.e. the description of a charring depth which is then set in relation to a time which can be the complete duration of the (fire) exposure or parts hereof. In general, a limitation of all methods is, firstly, the assumption of a constant charring rate and, secondly, the uncertainty of the charring between the termination of the fire exposure and the end of the extinguishing work, typically done with water after removal of the specimen from the furnace. In the following, the methods are grouped with respect to their main measurement characteristic.

(T) Temperature measurements within timber specimens have been frequently used to document the progress of charring. Typically, wire type thermocouples (TCs) or sheathed TCs are used to detect the temperature profile (sometimes referred to as heat wave) within the solid. The significant difference between the highly conductive sensor and the insulating material should be considered when installing temperature sensors in timber for fire exposure, see Chapter 4. Generally, the time when temperatures within the solid show 300°C is derived by (linear) interpolation, in combination with the location of the sensor, so that the charring depth at a certain time can be determined. For consecutively arranged sensors, this procedure is appropriate for the determination of the progress of constant charring rates while this procedure should to be discussed for varying charring rates. A limitation of this method is the limited spatial validity, the possible influence of too dense sensor installation and falsified temperature measurement due to the reduced temperature

at the hot junction due to the metallic sensor.

(M) The mass loss of timber specimens exposed to heat may be utilised to detect the progress of charring. In general, the fact that the char layer has a significantly reduced density could be used to correlate the charring depth, and subsequently the charring rate, with the mass loss measured either discretely or continuously throughout a fire experiment. Such a method would address the typical limitation of other methods with respect to the spatial validity as an average value could be expected. However, in a comprehensive study investigating the charring behaviour of CLT elements, Fahrni (IBK report 2021, currently in drafting stage) could not find a correlation suitable for further calculations. The apparent range of results is most likely related to the significant range of char layer density from below 10% to above 20% of the reference dry wood density, see Chapter 3. An example of the utilisation of the mass loss as indicator for the charring rate is given in Figure 2.10.

(G) A common procedure to determine a charring depth is the measurement of the residual virgin section after exposure in comparison to the initial geometry before the fire exposure. Assuming a constant charring rate, the charring rate is typically determined as the ratio of the measured charring depth and the time of fire exposure. In general, the traceability of the reported data in the literature is poor as no figures with a reference measure is given and typically only one value is given without further details such as the location of the measurement and the specification of the value's characteristic, i.e. if it is a minimum, a maximum and a mean or median value. Often, exemplarily selected sections are given and rarely the char layer is reported in these images. In the only standard document dealing with the measurements of the virgin cross section after a furnace test, EN 13381-7 [160, 38], a limited number of measurements is requested for linear timber members, i.e. beams or columns, while the determination of the virgin cross section of timber frame assemblies relies solely on temperature measurements. The advantage of this method is that the spatial validity can be improved by increasing the number of measurements. A draw back of this method is that it represents just one moment at the time of termination of the test or experiment including the risk for uncontrolled charring before the finalisation of extinguishment works.

(O) Lingens reported a continuous determination of the charring depth in model scale furnace experiments using a wolfram needle which was pushed through the fire compartment into the fire exposed specimens with a defined force [116]. A limitation of the method reported is the heat conduction of the needle which is in constant contact with the specimen and allows a burning-in exceeding the char line depending on the density of the specimen. A further draw back of the method is the limited spatial validity of one measurement. Alternatively, the density change at the char line can be detected by micro drilling (resistograph [27]) which is typically used for the evaluation of the density profile in virgin wood. Theoretically, the technique

would be applicable to detect the change of the material's density during fire exposure including the location of the char line and the density of the char layer. A limitation is the limited spacial validity and the highly inhomogeneous local density of the char layer, including voids and cracks reaching from the char line to the fire exposed surface. Using one of the mentioned approaches to detect the residual virgin cross-section, a density difference or a charring temperature, or a combination hereof, the charring rate can be defined.

The definition of the 'basic design charring rate' in the revised Eurocode (EN 1995-1-2) [40] is given as the charring rate of initially unprotected (plane) wood members or wood-based board (panel) without considering effects of size, gaps, joints etc. The particular member's characteristics such as gaps, conductive components (e.g. metal connectors) or fire protection systems may change the 'basic design charring rate'. A typically, well-known value is $\beta_0 = 0.65$ mm/min for spruce exposed to standard fire. Interestingly, the simplified rate of $\beta_0 = 0.65$ mm/min seems to be a constant value although the temperature in standard fire shows a constant increase with proceeding time. This is considered as indicator for the efficient insulation property of the char layer. For exposure in standard fire exceeding 60 min, experimental results show a decrease of the charring rate [100, 116, 107, 161].

Despite comprehensive data for charring under standard fire (e.g. [59, 107]), a large number of investigations in various apparatuses using a radiant heat source are available [197]. Frequently, authors refer to these setups with the application of a constant heat flux which leaves room for interpretation as, in general, only the set-point of the apparatus is left constant while the thermal boundary conditions result in a highly variable absorbed heat flux. When only considering the external heat flux, a correlation of $R^2 = 0.72$ was found for softwood by Tran et al. [197] which could be improved to $R^2 = 0.83$ by further considering the density, see Figure 2.9. It should be noted that the specimens used were often clear wood specimens with very limited dimensions (e.g. $100\,\text{mm} \times 100\,\text{mm}$ for cone-calorimeter tests) without wood features where it was possible to limit the scatter of the material properties. In general, it should be noted that the applied heat flux is of quite low magnitude considering compartment fires or furnace tests where the external heat flux may exceed 180 kW/m^2, see Chapter 4. A general charring model was recently proposed by Werther et al. [205, 206] which has been implemented in the revision of Eurocode 5 [40]. The model proposed by Werther is a cumulative energy model correlating the temperature with charring observed in a large number of tests and experiments. Werther proposed upper and lower bounds, for Eurocode 5 [40] a function representing the mean value is proposed:

$$d_{char,design} = \left(\frac{kT}{2.5 \cdot 10^5}\right)^{\frac{1}{1.47}} \tag{2.4}$$
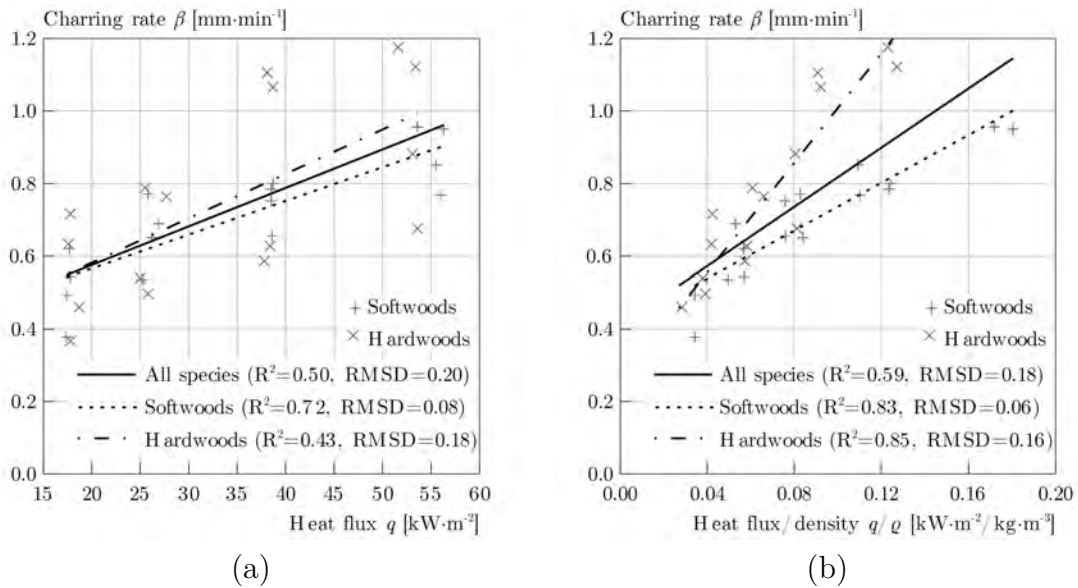
Figure 2.9: Charring rate for soft and hardwood modified from [197]: depending on the external heat flux (a) and the external heat flux and the density (b). Figures provided by P. Palma.

where

$d_{char,design}$ is the charring depth for a design fire; in mm;

kT is the cumulative thermal impact described by the temperature, in $K^2 \cdot min$.

Besides the test setup and the fire exposure, the product choice may influence the charring rates considerably. Figure 2.10 shows an example for charring of exposed CLT in a real fire compared to the corresponding model of Eurocode 5 for standard fire; although the exposure has been reported to be significantly different [47], the charring rates agree well.

2.3.11   Combustibility

The combustibility is a characteristic typical for grown materials, e.g. wood. Materials which have been produced by heating above a certain level are typically not combustible. In Europe, there is a combustibility classification system available to distinguish further between the combustible materials. A non-linear scale from A to E is available whereby classes A are not combustible and timber is typically in class D. The classification follows three tests in total whereby the combustibility test is done to verify class A by determining the material's mass loss at high temperatures, see e.g. Östman et al. [142].
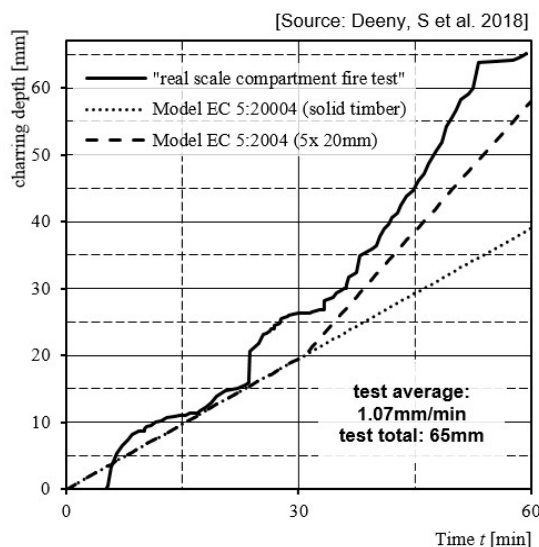
Figure 2.10: Charring rate determined from mass-loss measurements and a comparison to the model provided in Eurocode 5 [35] for solid timber (dotted line) and a product consisting of 20 mm-layers (broken line). Own image, data for the "real scale compartment fire test" taken from Deeny et al. [47].

2.3.12 Density

The density of wood varies with the moisture content. It appears that, by trend, the density of wood correlates with the strength. The dry density, shows a strong correlation with the heat content and an influence on the charring rate [31, 188, 197, 207]. However, the density varies significantly within one timber product (e.g. a glulam beam), see e.g. Steiger [188]. Just [93] found that the density varied along a timber stud between about $500\,\text{kg/m}^3$ and $700\,\text{kg/m}^3$, resulting in a difference of about 11% in the charring rate. Thus, mainly due to the lack of reliable input data for the design process, the density is not used by some design models, e.g. Eurocode 5. In contrast, other design models use representative densities as an input for their charring models [81]. However, as timber is sometimes classed using different representative densities (mean, characteristic or minimum), the procedure and the related model approaches can be questioned. In contrast, in this work, a reference density will be used in various relationships. Consequently, this reference will be used for the design model proposed in Chapter 6. The use of deviating densities should be carefully assessed with respect to the uncertainties of the source material expected in the product and the building project.

2.3.13   Draft

Draft may boost smouldering combustion of a char layer and interfere with the self-extinguishing when superimposed with the accidental loading case fire. The effect on self-extinguishing has been observed by Crielaard et al. [43], whereby an imposed air flow may change the conditions for self-extinguishing. Furthermore, variation of the gas flow may have a significant effect on the expected change of the charring rates [168]. In this work, the draft within a compartment is not further studied, but the effect of air and gas flow respectively is studied.

2.3.14   Emissivity

The emissivity ε_s is a solid's surface property, mathematically an expression between null and unity, describes the share of a radiant heat flux which is emitted. A perfect black body exhibits an emissivity with unity, contrary, in FSE lower values apply. Werther [205] collected results from literature for, virgin wood, char and the char layer, see Table 2.1, which deviates slightly from Eurocode [34] where the use of $\varepsilon_s = 0.8$ is suggested regardless of the material under investigation. Values of Table 2.1 were originally collected by Werther [205] and extended with further literature where it is stated that most organic or oxidized surfaces have an emissivity of values close to 0.95. According to Kirchhoff's law, the absorptivity and the emissivity can be assumed to be equal. However, this does not apply when the source body emitting radiation and the target body receiving radiation have very different temperatures; in this case different values must be used [209].

	min	max
virgin wood (spruce)	0.56	0.76
char layer	0.79	0.95

Table 2.1: Surface emissivity of (blond) virgin wood and the char layer.

2.3.15   External flaming

The external flaming of a compartment fire is an important factor of a fire scenario. The external flaming may be specified as external HRR or as flame geometry, mainly the vertical part of the flame length. The amount of the external flaming may be crucial for the facade material's ability to stay attached to the structure and the vertical fire spread to the next storey. Due to the contribution of structural timber to the total fire load, especially for ventilation controlled fires, in the steady state phase, the combustible volatiles created by the pyrolysis of fire exposed structural timber, can not burn inside but outside the compartment. Further, the horizontal fire spread to adjacent building objects may be boosted for increased external flaming. Multiple observations are available in the

literature [117, 74], quantification show that in some cases only 30% of the structural fire load by the timber surfaces (CLT) combust within the compartment, see Brandon [22]. Another, physically based approach showed that a significant reduction of the HRR in the steady state burning phase can be traced back to the energy stored in the char layer [180], see also Section 3.4 and Chapter 6.

2.3.16 Extinction

Fire extinction can be reached if one of the three requirements is removed from the combustion process. In general, the essentially elements are the availability of (1) fuel, (2) oxygen and (3) energy, well presented in the literature [49, 81, 205]. The balance of the three elements are the focus in combustion science. The science of fire dynamics has the aim to understand and predict the involved processes. The related material sciences distinguish in flaming combustion and smouldering combustion, thus, extinction can be related to the occurrence of flames (flame extinction) or smouldering (smouldering extinction). Both the flaming and smouldering extinction under certain conditions are content of various research studies [15, 51, 212]. It should be noted that smouldering combustion may spontaneously convert to flaming combustion. The extinction occurs due to the reduction of one or more of the three essentially needed elements. Extinction may occur by itself or due to an intervention activity. Corresponding to the elements for combustion, extinction may occur due to the burnout of the fuel or the oxygen or the removal of the energy. These three elements are normally tackled by a fire safety measure, e.g. by e.g. a suppression system or a fire service.

In general, it is unlikely that an active system (e.g. suppression by sprinkler or a fire service) is capable to extinguish a fully developed fire. A simplified energy balance shows the following: Typically, a fire in an apartment (residential occupancy) has a energy release rate (HRR) of $250 \, \text{kW/m}^2$ related to its floor area (assumed to be $100 \, \text{m}^2$ in this example). If the fire size is not limited by window openings, it provides a theoretical maximum total heat release of $25 \, \text{MW}$. Water has a heat of vaporisation of about $2300 \, \text{kJ/g}$ equivalent to $2.3 \, \text{MJ/l}$. A typically used fire hose with a standard mouthpiece discharges 100 l/min equal to 1.7 l/s. Thus, seven water hoses, with a total discharge of 700 l water per minute would deliver water capable to absorb an equivalent energy release to the fire ($25 \, \text{MW}$); however, they would need to be placed perfectly to reach the fire source. Already installed in the compartment, sprinkler heads are a better measure to discharge water close to the fire source, a discharge exceeding 10 l/s per square meter (typical value for a conventional sprinkler system) would just fulfil the simplified energy balance. A factor not included here is the contribution by structural timber surfaces which may contribute up to about $100 \, \text{kW/m}^2$(per surface area of the structural timber; a floor-related area factor exceeding 3.0 may be considered if all surfaces are exposed timber, see Chapter 6. Obviously, the presented comparison neglects detailing (e.g. water pressure, water droplet size, pipe flow rate) and should not be used for design.

2.3.17   Fire exposure

Exceeding the term of thermal exposure, see Section **??**, the fire exposure further describes the compartment environment in terms of the gas characteristics important for combustible materials. Thus, beside the thermal exposure the environment in terms of gas concentrations and movements at the surface of a specimen is described. See also Chapter 4.

2.3.18   Fire protection systems

Passive fire protection system may protect a surface of a structural member initially of for the entire duration of the fire. They may encapsulate the member and prevent the start of charring at the combustible surface or, protect the member partially and reduce the heating of the member behind the attached fire protection system. Contrary, reactive surface treatments (e.g. in intumescent coatings) may be applied to allow for the creation of an isolating layer when exposed to fire.

2.3.19   Flaming combustion

Besides smouldering combustion, flaming combustion is one of the two burning modes of structural timber exposed to heat which require oxygen. Flaming combustion is a field of science studied and documented by numerous authors [12, 137, 204]. Flaming combustion is of interest as characteristic for a material as flames would allow for fast horizontal and vertical fire spread, thus, this characteristics is studied mainly with respect to the reaction to fire characteristics, compare Figure 2.3 (b). The process represents released energy as heat which may contributes to the radiative feedback to the burning surface of the fuel leading to sustained flaming and increased material damage or conversion to combustible volatiles. The specification of a burning rate or mass loss rate might imply considerable uncertainties as stated in Section 2.3.7. The flaming combustion of a surface provides a potential heat source as the flaming would emit energy back to the surface. Tewarson et al. found the heat flux radiated back to be about 25 kW/m^2 [193] while another found a value exceeding a triplicate [146]. Typically, the conditions for flaming combustion are investigated at ambient conditions, i.e. in air, as this field of science considers the early stage of fire, i.e. the field of reaction to fire. It should be considered that the conversion of timber to char produces combustible volatiles, mainly hydrocarbons, carbon monoxide and hydrogen. The condition for sustained burning with flames for timber have been described in the literature using a burning rate, e.g. by Bamford et al. [12] of 9 kg/(m$^2 \cdot$ h) for timber while Bartlet et al. found a significant range between 9 kg/(m$^2 \cdot$ h) and 18 kg/(m$^2 \cdot$ h) [14]. Other authors specify the critical limit for flaming combustion with an exposures of about 45 kW/m^2 [51], described as incident or external heat flux. It is recommended to use the values with care as the limits neglect that behaviour may be governed by the fire exposure of the particular material,

see Section 2.3.17. Thus, further consideration should be given to the gas temperature and the compartment environment including the gas flow characteristics at the material's surface.

2.3.20 Gas characteristics

The gas characteristics are considered in this work as part of the fire exposure, see Section 2.3.17. The variation and distribution of the gas characteristics (concentration of oxygen, velocity) is of significant influence for compartment's behaviour in general and especially for combustible materials.

The gas velocity is of fundamental importance to describe the dynamics between a fire compartment and the exterior where hot and cold gases are exchanged. The gas velocity is typically measured by an anemometer (e.g. vane or hot-wire anemometer) which are not suitable for the fire situation where probes may be used. Using probes (e.g. Pitot-tube or Prandtl probe) to measure a gas pressure difference, a gas velocity can be derived when the gas density (correlating with the gas temperature) is known. Although calibrated measurement devices are available even for high temperature applications [121, 132], their use in compartment experiments is still limited. Thus, essential values for the modelling and the validation of calculation models are rare. Drysdale reports velocities in the range of 5-10 m/s [49]. Experiments with the focus on fire fighting tactics measured velocities out from an apartment into a staircase of up to 6 m/s without any imposed wind and up to 10 m/s with imposed wind, see e.g. Madrzykowski [118].

The gas velocity or the movement of gases in the case of fire is driven by the temperature difference of the ambient air and the combustion products and the resulting differences in density and gas pressure, respectively. The movement of gas occurs in both the horizontal and vertical direction. Vertical flow can be observed within a room but more so where a staircase is present, due to a stack effect occurring. This stack effect, sometimes also referred to as chimney effect, occurs due to the draft between two points caused by the absolute gas pressure difference.

2.3.21 Glowing combustion

The glowing combustion is an oxidative process and is the combustion of a material without the emission of flames but with light [87]. In this thesis, it is understood as relevant part of the decomposition process of the char layer material together with the smouldering combustion, see Sections 2.3.31 and 2.3.36. The onset of the non-sustained glowing combustion is reported for an external heat flux of 8 kW/m^2 [49], most likely for 20°C ambient air.

2.3.22 Heat content

The heat content, also referred to as heating value or the energy content of a substance, is the measure of the quantity of heat stored in a fuel which may appear in solid (s), liquid (l) or gaseous (g) state or a combination hereof. In fire science, typically the net calorific value is used and specified in the literature. Terms as lower heating value (LHV) or gross energy might be used as synonyms. Wood is one of the most frequently studied fuel, its heat content is between 17.1 MJ/kg and 18.1 MJ/kg for dry wood (UHV). Recently, this value has been used to estimate the contribution of structural timber to fires, among others, for the fuel estimation in fire resistance tests [167, 109, 162].Recently, it was proposed to base the calculation of the structural fuel load by timber upon the net calorific value of wood to estimate the heat release rate by structural timber depending on the charring rate [163], see also Chapter 6.

2.3.23 Heat of gasification

The heat of gasification ΔH_g of a solid describes the change of a material to the volatile state, see e.g. Staggs [187]. In combustion science, it is a fundamental property as solids need to change their state to gasiform to combust and release the embedded energy. The energy required to produce the volitales, i.e. the heat of gasification, is considerably greater for solids than for liquids as chemical decomposition is involved [49]. The value is usually linked to the estimation of a burning rate expressed as mass loss rate as a response to heat exposure. The heat of gasification is the sum of the energy required to heat the solid and the latent heat of vapourisation ΔH_v also known as enthalpy of vapourisation of heat of evaporation. The relationship of both values are shown in the following Eq. 2.5. In practice, it is a complex task to estimate a unique heat of gasification property as there is no specific temperature at which volatile gases are produced as the volatile gases are created rather over a temperature range. The method which is commonly used to specify the heat of gasification assumes a constant mass loss rate to allow for a practical simplification resulting in Eq. 2.6.

$$\Delta H_g = \int_{T_a}^{T_P} c_p(T)dT + \Delta H_v \tag{2.5}$$

$$\Delta H_g = c_p \cdot (T_P - T_a) + \Delta H_v \tag{2.6}$$

where

ΔH_g	is the heat of gasification, in J/kg;
ΔH_v	is the heat of evaporation, in J/kg;
c	is the heat capacity, in J/(kg $\cdot$ K);
T	is the specific gas constant of dry air, 289.06 J/(kg $\cdot$ K);
T	is the temperature, in K;
a	index referring to ambient conditions;
p	index referring to pyrolysis conditions.

Tewarson and Pion presented a way to define an effective heat of gasification $\Delta H_{g,ef}$ using a best fit for unsteady mass-loss rates observed in practice [193]. However, this method experiences limitations for char-forming polymers and in the case of the absence of a flame. Both chases are valid for structural timber in compartment fires, typically under-ventilated, which is the topic of this thesis. Generally, it was found that the heat of gasification correlates with the incident radiant heat flux [187]. Sibulkin [182] stated that changes of the incident radiant heat flux would result in changes of the gasification rate but limited changes in the heat of gasification. Sibulkin [182] specified a value for the heat of gasification about 3 MJ/kg for semi-infinite slabs after 1 min exposure. Mikkola [128] collected literature data and found a significant range for the heat of gasification of wood between 1.4 MJ/kg and 7.0 MJ/kg. It is assumed that the large range may be due to the significant differences in the test setup or the sample size. Spearpoint et al. further investigated various species and summarised analysis results perpendicular and along the grain direction. For comparison reasons, Bunbury [30] quantified the released energy during the production process of char coal to 6% of the energy content, equivalent to about 1.1 MJ/kg for reference of 17.5 MJ/kg, thus, in about the same order of magnitude, see Table 2.2. The heat of gasification will be considered as input in the TiCHS-model to describe the formation of the char layer, see Chapter 6.

		min				max
		[30]	[128]	[186]	[182]	[128]
ΔH_g	[MJ/kg]	1.1[*]	1.4	1.6[**]|2.9	3.0	7.0
$\frac{\Delta H_{g,ef}}{HHV}$	[-]	0.06[*]	0.08	0.09[**]| 0.17	0.17	0.40

[*]   not reported as heat of gasification

[**]   along the grain direction

Table 2.2: Heat of gasification reported in the literature.

2.3.24   Heat flux

In fire science, the heat flux is used frequently used as description of flow of thermal energy or heat. For the application in fire science, for further consideration it seems

practical to distinguish between the heat flux within a solid (conduction, i.e. temperature transfer within a material) and the radiant heat flux which describes the heat flux to a solid's surface without a medium, see also Section 2.3.34. Some scientists consider the use of incident heat flux (terms typically used are incident heat flux, imposed heat flux, radiation heat flux) as more accurate compared to temperature and these are essentially needed to define fires at a greater resolution [92]. In general, heat flux may occur within a solid (i.e. conduction) or without a medium (i.e. radiation). The heat flux within a medium is caused by a temperature difference (Newton's Law of Cooling). Contrary, incident radiant heat flux does not require any media and is an electromagnetic energy emitted from solids above the absolute zero point (-273.15°C or 0 K).

In fire science, the incident radiant heat flux is usually measured using heat flux sensors (HFS). Typically, a Schmidt-Boehler type sensor is used which is a water cooled copper body exhibiting a highly conductive material with a black-coloured sensor area at the measurement surface. The HFS measures the absorbed heat flux over the embedded sensor which induces an electrical signal proportional to the (hot) heat flux from the sensor's surface to the (cold) bottom of the body. Thus, a conductive heat flux resulting from a temperature difference is measured. A HFS may be calibrated to either signal an "absorbed heat flux" or an "incident heat flux". While an absorbed heat flux is dependent on the surface temperature and the heat losses at the surface, including the solid's conduction away from the hot surface, an incident radiant heat flux is generally material independent. Measuring an indent radiant heat flux, it should be noted that the measured values are valid only for the actual system, e.g. the HFS. Changing to another solid or material, the surface temperature and the absorbed heat flux are strongly dependent on the actual thermal material properties which are in general not identical and differ significantly for building materials.

The consideration of an incident heat flux may be required to describe e.g. ignition of materials when the gas temperature around a solid is low; as soon that the solid receives a significant radiation from flames of a burning item the estimation of the incident heat flux is of complex nature. Further information about the use of the heat flux is given in Section 2.3.45 and Chapter 4, where the thermal exposure of non-combustible and combustible products is discussed.

2.3.25 Heat release rate

The heat release rate (HRR or $\dot{\rho}$), typically given for a compartment (sum) or per unit area, i.e. the heat release density, has been of interest for material studies to investigate the reaction to fire characteristics. Before the development of the oxygen consumption method, the burning rate was determined based on the mass loss of a specimen, assumed to be equivalent to the heat released. However, for structural timber, the mass loss rate seems to be inappropriate to describe the combustion behaviour as the loss of one mass unit may be the result of one mass unit of structural timber and the corresponding release of energy or the conversion of two mass units of structural timber to one mass unit of char

layer material. The latter corresponds to a significant lower heat release as the energy stored in the char layer material is significantly higher. This fact will be addressed by the TiCHS-model developed in Chapter 6 in this thesis. The current standard setup to measure the heat release rate is the cone calorimeter test according to ISO 5660 [86] where the mass loss (rate) is measured simultaniously to the oxygen reduction in the exhaust to determine the HRR. The HRR and the observed behaviour under certain exposures of cone calorimeter tests are frequently used in calculation models. Due to the undefined thermal boundary conditions, the results including the related observations should be used with care, see Chapter 27 in [81], further literature for FSE [209] and Chapter 4 in this thesis. Another setup to determine the reaction to fire characteristics is the single burning item (SBI) setup. In both setups, further the smoke released is measured, see e.g. Östman et al. [142]. A general model to describe the development of the combustion by the HRR of a single item or even the entire movable load is the t-square-fire model [79]. It should be noted that the HRR of a single burning item would correspond to a fuel controlled fire whereby the burning of a similar item in a compartment fire might be different due to the limitation of the combustion by the available ventilation openings. To address this combustion behaviour the

For FSE purposes, in general, and more recently also used frequently for studies of the fire dynamics of compartments with exposed timber surfaces, industry calorimeters are use. Typically, these indoor calorimeters, described in the literature, e.g. by Dahlberg [46], are used where the total HRR from large burning items (e.g. vehicles) or fire compartments should be estimated. An example of measurements of compartment fires where no timber surfaces were involved (Test 1-1) and with the involvement of CLT is shown in Figure 2.11. It should be noticed that the maximum HRR in this example is above 10 MW which exceeds the measurement capacity of many European laboratories. In the near future, the Centre of Fire Research (ZeBra) in Braunschweig, Germany, will provide facilities with a calorimeter up to 20 MW.

2.3.26 Heat transfer

The heat transfer from one solid to another can be described using their initial temperature and their associated thermal properties, i.e. density, heat conductivity and heat capacity. While this type of heat transfer, the conduction, is a quite simple mathematical problem even in non-steady state conditions, the heat transfer between a (heated) gas and a solid through its surface is of increased complexity. To solve the heat transfer applicable for fire science, the thermal boundary conditions need to be taken into account where in addition the convective heat transfer from the gas (depending on the gas- and surface characteristics), the radiation to the surface and surface heat losses have to be considered [49, 209]. See also Section 2.3.45 and Chapter 4.
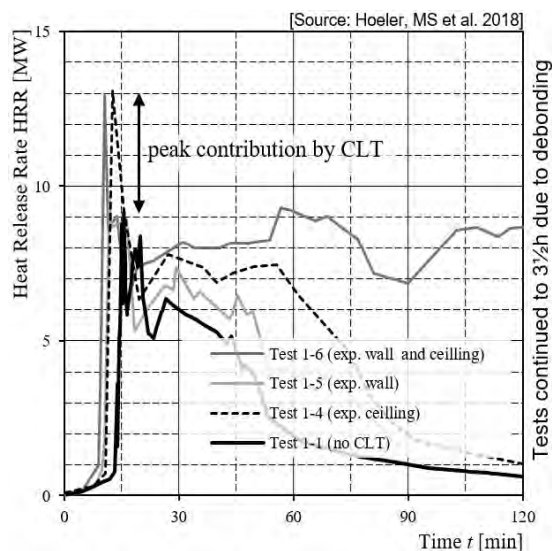
Figure 2.11: Examples of measured HRR of compartment fires with and without exposed timber surfaces (CLT). Image source: Schmid et al. [179], data modified from Hoehler et al. 2018 [80].

2.3.27 Ignition

The ignition of a material is an important characteristic of a material. Typically, it is distinguished whether, besides a radiative heat flux emitting device, an additional external energy source (e.g. electric spark generator) is needed for the ignition or a certain externally applied heat flux is sufficient. Consequently, the ignition is referred to as auto ignition, sometimes referred to as self-ignition, or as piloted ignition. This characteristic relates to the description of the "reaction to fire" phase, compare Figure 2.3. Typically the ignition characteristic is tested in a cone calorimeter setup [86] representing one method to describe the reaction to fire characteristics of a material. The time to ignition of a material can be related to the time to flashover when the material is used as enclosure surface [143].

In the cone calorimeter setup, typically, a horizontally arranged solid sample of macro-scale (surface area 100 mm × 100 mm) is exposed to an electric radiant heater which was previously set to a certain effect to reach a default level of a HFS, i.e. an absorbed heat flux. The ignition characteristic can be understood as the potential start of the fire growth relating to the early stages of a fire. Implicitly, the characteristic is connected to ambient conditions, i.e. a low gas temperature and the availability of oxygen. Looking at the characteristic of ignition from a more physically based approach, ignition of a material is related to the surface temperature of the material which is in balance between the received and dissipated energy. The energy is received by radiation and conduction and dissipated by radiation and conduction. Generally, a heat balance at the material's surface has to be

solved considering the element's characteristics, i.e. the material's surface characteristic and orientation, the heat of conduction of the solid, and the description of the environment which includes the incident radiant heat flux and the gas temperature. After ignition, the test sample is exposed to an external radiant heat flux and the eventually available flames. Typically the gas characteristics are not further described, considered or documented. For a physically correct description of the ignition behaviour and the behaviour after the ignition it is essential to consider the thermal exposure. For detailed information about the thermal exposure, see Section 2.3.45.

For the physically correct description of the ignition characteristics of wood, it is further required to observe (a) that wood is a solid material which has to create combustible gases able to ignite but, further, (b) that wood will form a thermally modified material, the char layer. Babrauskas specified the surface temperature required for ignition of wood between 300°C and 365°C [13] based on a literature study indicating ranges between about 200°C and 500°C for piloted ignition and auto ignition. Babrauskas listed various influencing variables (sample's size, moisture content and orientation, testing method, definition of ignition, piloted/auto ignition). Babrauskas further mentioned a minimum incident radiant heat flux for ignition of about 4.5 kW/m² but highlighted the uncertainties related to this value. Bartlet reportet an ignition criterion with 12 kW/m²± 2 kW/m² [14]. The apparently significant difference shows that the thermal boundary conditions should be clearly specified and considered when discussing this value, see Section 2.3.45 and Chapter 4.

2.3.28   Mass loss

The mass loss or mass loss rate is a basic characteristic used in the field of reaction to fire. The mass loss rate is typically determined by the cone calorimeter setup described in ISO 5660 [86]. Recently, the mass loss rate was used for fire resistance calculations to estimate their contribution to the fire dynamics. In corresponding studies, cone calorimeter test setups were utilised to measure the extinction of wood (see also Section 2.3.16) of timber under various conditions, studied e.g.by Bartlett et al. [15]. Bartlett et al. specified a so-called critical mass loss rate density for auto-extinction of 3.65±1.25 g/s per m² (corresponding to 13.1 kg/h per m²). Klippel et al. [102, 103] used the mass loss of a solid timber panel (STP) in furnaces under standard fire as comparison measure for the mass loss of CLT to detect the falling-off of charring layers, also reported in Chapter 3. Corresponding to the reduction of the virgin wood section by charring, a mass loss of the specimen can be measured. For EN/ISO exposure, for solid timber with a reference density of about 450 kg/m³at 12% MC, a specific mass loss of about 15 kg/m² per hour was derived. Inspired by the use of mass loss for fire resistance design, further authors investigated the influence of the wood sample orientation on the mass loss, i.e. horizontally and vertically. Further, the variability of reported values for the extinction under air flow showed that results more severe than the value determined by Emberly et al. [3]. In Chapter 6 the mass loss of char will be used to determine the contribution of the char

layer to a fire.

2.3.29   Modification

Various wood modification techniques of the surface, the depths closer to the surface and of the complete section are available. Those techniques are well documented in the literature [127, 144]. Some studies show that the ability to create combustible volatiles can be changed significantly by the application of wood modification. However, the effects on the charring rate, and, thus, contributing potentially to the improvement of the load-bearing capacity are reported to be very limited [133].

2.3.30   Moisture content

The moisture content MC of timber relates to the water stored in wood. At its maximum, it can reach up to 20% for sawn timber which increases the risk for mould. Technically dried wood shows typically a MC of 10%, similar to structural timber in buildings [64]. In general, the MC of a member is in balance with the environment with a certain inertia depending on the geometry and the ventilation. In a fire situation, the wood containing more water has a reduced heating value. Effects on the charring behaviour of the MC are significant but within a reasonable range for relevant situations [205, 206]. The charring rates available in the literature are typically related to an equilibrium MC (EMC) in a range of 9% to 12%. The moisture content of structural timber will be considered in this thesis by means of a reduced heat content which accounts for the evaporation energy.

2.3.31   Oxidation of the char layer

The oxidation of the char layer, in the literature referenced as char layer oxidation is the exothermic reaction of the char layer with oxygen, e.g. Morrisset et al. [130]. The oxidation of the char layer should be considered in the context of flaming combustion (combustion with flames and the emission of light), smouldering combustion (combustion without flames and the emission of light) and glowing combustion (combustion without flames but the emission of light) [87]. In this thesis, the oxidation of the char layer is understood as the general decomposition of the char layer which ban be quantified by the mass loss of the char layer. The mass loss of the char layer occurs due to the composition of the char layer material, i.e. the loss of mass, or the loss of volume by surface regression. The characteristic of the oxidative process should be essentially included in the consideration of the fire dynamics when exposed timber surfaces are designed. In Chapter 6, it is shown that this characteristic should further be considered when experiments are done to analyse the behaviour of timber in fire. See also Sections 2.3.36 and 2.3.37.
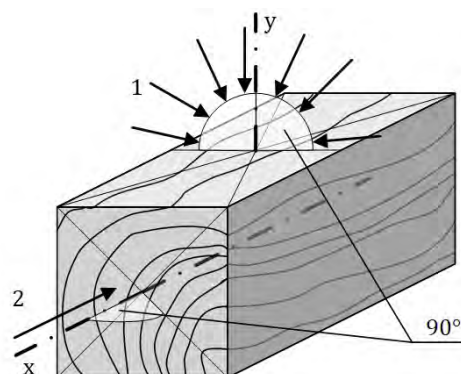
Figure 2.12: Charring directed perpendicular to the grain direction (1) and parallel to the grain (2). Own image.

2.3.32 Permeability

The permeability of timber is reported to have a significant influence on the material's behaviour in fire. In various studies, the charring behaviour is discussed for a large number of species, with differences often traced back to the species rather than the density. Limited knowledge is available about the charring behaviour along the fibre direction due to its limited applicability in practice. Similarities at ambient behaviour (increased moisture transport) let one conclude that the, typically increased charring rates along the fibres, is caused by the increased diffusivity of the material. Design rules of Eurocode address this influence by the increase of the charring rate for heat flux along the grain direction, x-axis in Figure 2.12. The significantly different charring behaviours should be considered when construction details are designed regardless whether exposed to the standard fire or any design fire.

2.3.33 Pyrolysis

Pyrolysis is the decomposition process of a solid by a thermal modification. This may occur in a fire or, generally speaking, by increase of the temperature. In absence of oxygen, it is called anaerobic; consequently pyrolysis can occur in an inert environment but combustible volatiles may be created as side product to the thermal modification of the solid. Conversely, oxidative pyrolysis takes place with oxygen. Pyrolysis is often referred to as thermally neutral although the conversion process is endothermic [63] and releases combustible volatiles [30]. In structural timber engineering, pyrolysis is often understood as the charring behaviour only, i.e the conversion of the timber to a char layer. In this work, the pyrolysis process is considered describing various stages, i.e. the formation of the char layer due to heat (endothermic process in an inert environment), the release of combustible volatiles during this process; the pyrolysis is understood to be responsible for

the creation of a new material, i.e. the char layer material, which has a varying density with a maximum energy yield. Thus, the process of the pyrolysis is considered to consume and release a certain amount of energy, but, most importantly, the created material will be considered as exhibiting a heat storage in the TiCHS-model developed in Chapter 6. The consumption can be described by the conversion of a material to another by the breakage of its molecular structure. Numerous studies on the pyrosis exist including models to describe this complex process [128, 88] whereby literature characterises often the pyrolysis together with the combustion of a material.

2.3.34 Radiation

Radiation is probably the most common source of misunderstanding in the field of fire safety engineering. In general, radiation is understood as the heat transfer by electromagnetic waves. However, it can describe (i) the emitted radiant heat flux, sometimes referred to as the external radiant heat flux or (ii) the incident radiant heat flux to the surface of a solid. The incident radiant heat flux to a surface may originate from a single source or multiple sources. Further, the radiant heat flux could be understood as (iii) the share of this incident radiant heat flux which would be absorbed by a particular surface considering an absorptivity factor. As a part of the absorbed radiant heat flux will be re-emitted by the surface, the radiant heat flux could be understood as (iv) the net heat flux to the surface which is the sum of the reversely oriented absorbed and emitted radiant heat flux. The context is addressed in the relevant literature, see eg. Wickström [209, 81]. The issues of the radiation definition are part of Chapter 4 in this thesis.

2.3.35 Robustness in the fire situation

In general, the structural robustness is an important characteristic of a structure that prevents initial damage to spread disproportionately [1]. Due to the limited common understanding of the structural robustness which might be caused by rather vague requirements in the past, in many projects robustness has been achieved implicitly, often based on engineer's experience and not quantified. It can be assumed that this lack of clarity with respect to the quantification of the structural robustness may have contributed to the relatively undefined means of its verification in normal condition, but, especially in the fire design. The application of the concept of robustness in the fire design is not straight forward, and has been addressed in recent projects by significantly different means ranging from redundant sprinkler feed or continuous beams instead of single-span beams. Generally, it can be stated that, if the robustness in the normal situation is understood as a redundancy measure of structural elements, accordingly, the robustness in the fire situation should be understood redundancy measure of FSE elements. Thus, robustness of a system in the fire situation should be assessed with respect to eventual failure of the considered FSE element. A major challenge is the quantification of the failure risk of the designed system which comprises (a) actual failure probability of one

element, but, further, (b) the conservativeness of the particular verification tool. While (a) might be addressed with appropriate data origin from statistics, (b) should be seen together with the robustness of the calculation model. Rein et al. [150]and Johansson et al. [90] showed previously, that the prediction of the fire development is still a concern for non-combustible structures. When it comes to timber structures, using available tools for the verification of the fire design of timber structures, e.g. FDS, Zone or simplified methods, an increased parameter study is recommended [177]. For timber structures, this parameter study should focus the sensitive parts of the timber structure which are especially the ventilation condition resulting in different contributions to the fire dynamics and fire durations respectively, see also Chapter 6 of this thesis where a framework for considering the structural timber's contribution is developed. It should be highlighted, that there is no general way to define conservativeness for all properties affecting the contribution by structural timber. For example, an apparently unfavourable instantaneous combustion of the charred depth directly after its creation should be discussed. On one hand, the complete combustion of the heat content provided by structural timber, would lead to a high total HRR eventually combined with significant exterior flaming. However, the temperatures in an already under-ventilated fire compartment are not expected to increase. It would be more unfavourable for the design, if the energy would remained stored in the char layer until the movable fire load is consumed, and, the structural load combust afterwards. Thus, design tools describing the heat storage would be needed. Alternatively, an increased parameter study seems to be justified to address the robustness of the verification procedure, until further knowledge about the fluid dynamics in structural timber compartments is available [177].

2.3.36 Smouldering combustion

Smouldering combustion is an oxidative process of a material without the emission of flames or light [87]. Contrary, the glowing combustion is the combustion without flames but with the emission of light. The smouldering and glowing combustion is considered in this thesis as the main reaction of the char layer understood as char oxidation. Both reactions, described as the decomposition of the char layer material. As flaming combustion, smouldering and glowing combustion occur when wood is exposed to sufficient heat under the availability of oxygen. It should be considered, that due to the apparently dense structure of timber (including the presence of water), timber in its original condition can not smoulder or glow while the thermally modified material, the char layer, may undergo smouldering or glowing combustion. The smouldering and glowing combustion of the char layer may self-extinguish or be self-sustaining depending on the (compartment) environment. Currently, the smouldering or glowing combustion is discussed with respect to burnout, see Section 2.3.6. For sustained smouldering a radiant heat flux density of about 10 kW/m^2 was specified by Ohlemiller [139], further, a limiting surface temperature of 200°C was found by White et al. [208]. The smouldering combustion of the char layer seems to be controlled by the availability of oxygen but further its intensity of the

contact. Thus, an imposed air flow is able to enhance the smouldering combustion after ignition [139, 140, 49]. Ohlemiller [139] found forward and reverse smouldering and described it as function of airflow velocity between 0 and 6 m/s. Besides Reverse smoulder was found between 3 cm/s and 5 cm/s and was exceeded by forward smoulder between 3.5 cm/s to 8 cm/s. In general, the smouldering of a char layer sticking to a virgin wood section was not found to be not sustaining, due to the significant variation of the permeability of the char layer over its thickness with a less permeable zone near the virgin wood section [139]. The corresponding effect of char layer smouldering was found to be within a range of 30 kW/m²to 50 kW/m² [138]. Crielaard found that smouldering of wood occurred in a cone calorimeter for an external heat flux above 6 kW/m²while smouldering sustained at higher heat fluxes [43]; an imposed air flow of 0.5 m/s was favourable while a further increase to 1.0 m/s may induce sustained smouldering.

2.3.37   Surface regression

The surface regression of charring timber describes the reduction of the char layer thickness and can be specified as a rate. In the scientific literature, this process may be referred to as surface oxidation, surface shrinkage, char oxidation, char recession or char contraction [62]. With respect to the term char oxidation, it should be considered that the combustion reactions within the char layer are also oxidative, endothermic reactions. Chantani et al. specified a maximum surface regression at exposure levels of 30 kW/m²to 50 kW/m² in a cone calorimeter test setup of about between 0.3 mm/min and 0.4 mm/min, respectively, depending on the exposure level and the direction of the incident heat flux with respect to the fibre direction [214]. In a fire tunnel experiment, Schmid et al. reported surface regression of about 0.15 mm/min for an oxygen rich environment [175]. The char layer surface regression (rate) is discussed further in Chapters 4 and referred to as β_{ch} in this thesis, see Figure 2.7.

2.3.38   Stickability

The stickability describes the ability of a part of a component to stick to other parts. Typically, the stickability is assessed for a fire protection system when attached to a structural member [160, 39]. Generally, solid timber when fire exposed, is not considered as a compound of virgin wood and a thermally modified layer, the char layer. However, for the prediction of the charring behaviour it is essential to determine the ability of the char layer to stick to the virgin layer. The stickability of the char layer is rarely documented in fire test reports as the char layer is typically excluded from the interest of labs and researchers. Lingens [116] documented the stickability of the char layer in model scale tests for solid timber panel type specimens.

Material	$[\,r\,]$	$[\,\phi\,]$
	$[\,\mathrm{mass_{air}/mass_{fuel}}]$	[-]
Wood (pine)	5.14	1.7
Char	10.63	1.3

Table 2.3: Major characteristics of combustion of wood and char.

2.3.39 Stoichiometry

The stoichiometry is the doctrine of the calculation of reactants and products in chemical reactions in chemistry. The stoichiometry is founded on the law of mass conservation. The stoichiometry is basis of the combustion physics where chemical reactions are described by chemical balance equations. The combustion physics based on stoichiometric burning is presented in various sources in the literature, e.g. [49, 63, 81]. A simple example from the combustion of methane gas using oxygen from air is given in the following equation:

$$\mathrm{CH_4 + 2O_2 \rightarrow CO_2 + 2H_2O}$$
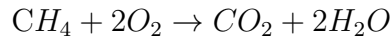
Using the stoichiometric balances, the combustion of various materials can be described. Contrary to the description of the combustion of methane, the description of the reaction of polymers in liquid or solid form is more complex. In the combustion processes described in fire safety engineering, the required oxygen is not supplied as pure oxygen but is supplied as air containing mainly oxygen and nitrogen. Typically, fuel-to-air ratios r are used describing the combustion in air of complex materials such as wood. Werther [205] has collected valuable information about the stoichiometric combustion of wood. Further guidance can be found in the relevant literature, e.g. [49, 63, 81]. Besides the perfect combustion balancing, in practice, a larger amount of air is needed, which is considered using an additional equivalency ratio ϕ where unity corresponds to the perfect combustion according to stoichiometry. The equivalency ratio is defined as given in Eq. 2.7:

$$\phi = \frac{(\mathrm{fuel/air})_{\mathrm{actual}}}{(\mathrm{fuel/air})_{\mathrm{stoichiometric}}} = \frac{r_{\mathrm{actual}}}{r_{\mathrm{stochimetric}}} \tag{2.7}$$

Consequently, for the discussion of the combustion of structural timber, the most important input are the fuel-to-air ratios r and the equivalency ratios ϕ exemplarily given for wood and char are given in Table 2.3.39.

2.3.40 Species

The species may provide a certain variation of the heat of content (per unit mass) and the density which result in differences in the contribution to the (structural) fire load and the charring behaviour respectively. Further, species show a variation of the

main components (cellulose, lignin and hemicellulose) and the wood extract substance, comprising oil, tar and gum which may change product's reaction to fire behaviour and the fire resistance performance [78].

2.3.41 Strength grade

The strength grade has a direct and an indirect influence on the fire design of a timber member. Timber products are typically graded with respect to a reference strength, e.g. the bending strength. The strength grade is decisive for the member's design as it is decisive for its section geometry, i.e. a direct influence. In general, the strength is correlated with the density of the timber [169], while, in charring models (e.g. by Eurocode 5 [35]), the density influence is neglected. Consequently, if a low grade member is foreseen, its dimension would be increased while the charring rate and depth remains unchanged. Thus, the reduction of the load-bearing capacity by the reduction due to a charring depth would be less significant for a low grade member, i.e. the indirect influence.

2.3.42 Test setups

A large number of test setups are available to evaluate characteristics with respect to the reaction to fire or fire resistance or to serve scientific purposes. While test setups are partly understood as standardised methods, experimental setups tend to be more focused on particular research questions. The most important test setups for the investigation of the reaction to fire characteristics and fire safety engineering questions are calorimeters. The methodology of calorimeters is based on the oxygen depletion principle utilising the fact that the heat release per unit mass of oxygen consumed is independent on the type of fuel. The principle replaced the previously documented "burning rate" described as the change of mass with time (mass loss rate), see Section 2.3.7. Calorimeters are used in cone calorimeter, which are considered as a standard setup intended for the investigation of the reaction to fire properties of a sample, with limited test sizes of 100 mm × 100 mm [86]. A further field of the application of calorimeters are industrial calorimeters used for the measurement of HRR of various objects or compartments [46].

2.3.43 Temperature

In fire science, the measurement and estimation of the temperature is essential for the documentation of the environment and the condition of building components. From a structural point of view, the temperature measurements are essential to document the heat transfer within components. The accuracy and reliability of the temperature measurements are of significant importance when they are used for the development of prediction or design models. Typically, thermocouples (TCs) are used to measure the temperature by utilising two dissimilar electrical conductors, which induce a voltage along the wires

dependent on the temperature at the hot junction. Various types exist combining different metal alloys, which differ in the use for different temperature ranges and working environments. In industrial high temperature applications, typically metal sheathed type sensors (sheathed TCs) are used which offer the advantage of re-use during many heating cycles and quick application. In fire science, often wire type sensors (wire TCs) are installed as disposable material. In general, the measurement error of the TC device is very limited (e.g. $\pm 3\,\mathrm{K}$ for type K at 600°C). However, it should be considered that the measured temperature represents the sensor temperature only (i.e. the temperature of the hot junction) rather than the temperature of the solid or the compartment at its location without the consideration of further influencing factors. Depending on the design of the temperature sensor, they might be more or less sensitive to radiation and convection. TCs have been used in many studies investigating fires and the material behaviour in fire. Using a TC within a solid, experience and research led to general agreements with respect to the installation of the sensors [37, 53, 199]. Especially in low-conductive materials, the use of TCs should be turned to one's attention as measurement errors connected to the installation may significantly influence the sensor's temperature at the hot junction.

In compartment fires, the compartment or room temperature used for the verification of the design is a result of a temperature prediction using a model. The time-depending temperature estimation may be the result of a simplified calculation appropriate for (i) the calculation by hand eventually assisted by automated calculations - typically spreadsheet calculations, (ii) zone models or (iii) field models. In tests and experiments, temperature measurements of the compartments are typically done using bare wire TCs, sheathed TCs and plate thermometers (PTs). Bare wires are further used or within a components in interlayers or for temperature measurements within a solid. In room compartments, often TC trees combining TCs of the same type are used to record a temperature profile over the compartment height; examples of TC trees are given in Figure 2.13. Similarly, grouping of TCs in a specimen at a certain position are referred to as TC station. For the determination of material properties, the development of calculation models but also for classification of products the correct temperature measurements are essentially needed. For timber products, the progress of charring is often tracked by temperature readings, see Section 2.3.9. In several research studies, a simple installation has been aimed for neglecting the basics of physics. Thus, the location of the char line and, subsequently, the models based upon the flawed temperature prediction may be incorrect. Corresponding correction models should be used with care as they might be fitted to certain exposure conditions, especially if they are based on calculation models which use material properties determined for certain heating rates or, more generally, for a certain fire exposure.

Typically values of the compartment temperature may exceed 1000°C, for simplified calculations and fundamental model for the prediction of the fire dynamics, compartment temperatures of 1100°C are used [49]. Typically, glass fibre insulated, wire type thermocouples (type K) are classified for the use up to about 550°C (assumed melting temperature of the conductor's insulation material), however, unless moved, experience shows that temperatures up to 1000°C can be measured.

<div style="text-align:center">
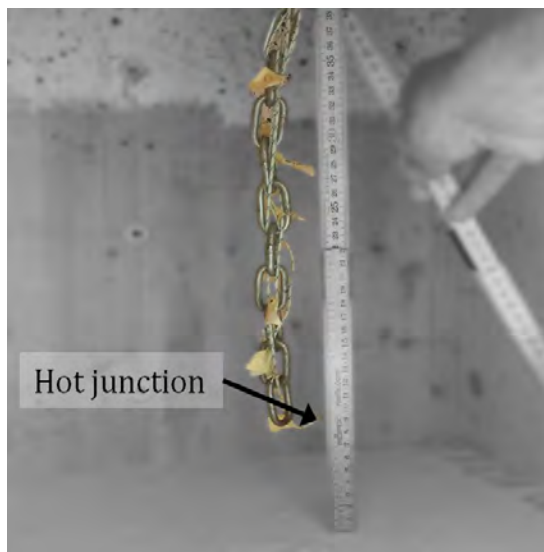
Own image.   Image by Y.Hasemi.

(a)   (b)

</div>

Figure 2.13: Thermocouple trees as horizontal arrangement of numerous TCs to measure the distribution of the temperature in a fire compartment. A simple TC in a small scale compartment (a) and an insulated TC tree installed for a large scale compartment experiment (b).
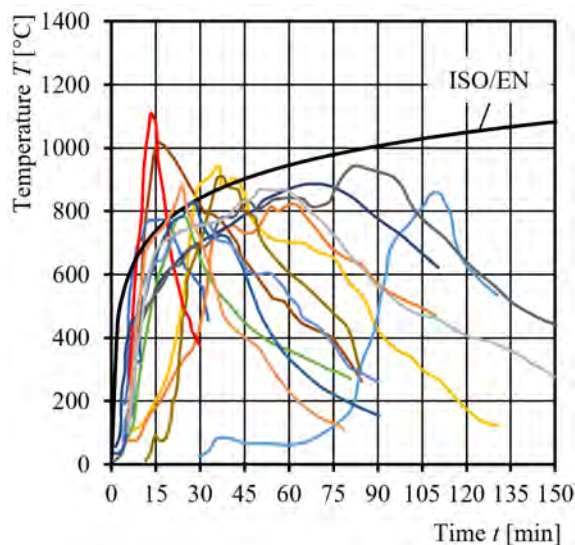
Figure 2.14: Development of room fire temperatures from Kawagoe [96] in comparison to EN/ISO fire. Own figure.

2.3.44 Temperature of the fire compartment - prediction methods

In Section 2.2, the background of the EN/ISO exposure was summarised. It is evident that for using the standard fire time-temperature curve, sometimes referred to as normalised fire or standard fire or EN/ISO fire, neither the growth phase nor the cooling phase is represented. The standard fire should be understood as a measure of comparison, used in the actual fire resistance framework as reference for building components, but also included as requirements in building regulations, see Section 2.2. In the past, many scientists believed that the standard fire is a severe case of a fire for any building material, compare Fornather et al. [55]. Thi which is most likely based on the limited experimental data. Exemplarily, the temperature curves considered by Kagowe in comparison with the EN/ISO fire is given in Figure 2.14. From more recent experiments it is known that the temperatures of the standard fire are likely to be especially by timber construction due to the limited thermal inertia of the enclosure, see e.g. Su et al. [190].

An approach to modify the EN/ISO time-temperature curve to particular compartments with further variables describing the boundaries with further input variables (opening factor, thermal absorptivity, fire development rate) has been developed for the parametric fire design. Following this parametric fire design methodology, depending on the boundaries, the EN/ISO exposure is modified with respect to the time and the theoretical final temperature. While the inexistence of the growth phase may be accepted if the post-flashover phase is of major interest for structural fire resistance design, the simplified description of the cooling phase with a linear decrease may be considered as

oversimplification. In the past, some attempts were done to modify the cooling phase to allow for a better fit with more complex temperature prediction models in the cooling phase [54], however, the modifications have never been considered for implementation in the Eurocode documents. The parametric fire design methodology has been implemented in Eurocode 1 [34]. With respect to its application, large deviations can be observed. E.g. in United Kingdom and Scandinavia the parametric fire design is frequently used if PBD is required while other countries rely on other simplified models (e.g. Germany) or rely on zone or field models. A benefit of the parametric fire design given in Eurocode 1, Annex A, is that it allows to predict corresponding (one-dimensional) charring rates and, thus, the remaining virgin cross-section of structural timber using Eurocode 5, Annex A [35].

An approach to overcoming the limitations with respect to the missing growth phase and the oversimplification of the cooling phase has been presented by Zehfuss et al. [215, 216]. Contrary to the parametric fire design which is based on a modified EN/ISO exposure, the simplified model is derived from an advanced model (zone model CFAST [91]) considering typically available environments and verified heat release rates and fire load densities of various occupancies. Recently, Wade et al. proposed the application of a two-zone model for the prediction of HRR and corresponding compartment temperatures exposed surfaces of structural timber [202]. Wade et al. showed that it is possible to reliably calculate the fire dynamics if a combustion efficiency reducing net heat of combustion and a fuel access factor is known. In Chapter 6, a method is developed to predict the fire dynamics with the TiCHS-model considering the timber charring and heat storage.

2.3.45   Thermal exposure

The term "thermal exposure" is not defined in a commonly agreed manner, although it is often understood as thermal loading and assumed to be the correspondent term to wind load in fire safety engineering. The origin of misunderstandings seems to be the perspective of the engineer's problem. From a product point of view, the thermal exposure might be understood as simply the heating of the product made from a certain material. Thus, the problem could be based on the thermal properties of the material only which requires the resolution of the heat transfer within the solid. However, the problem could be slightly raised to a typical problem of building physics where the difference between an exterior and interior temperature would lead to a certain temperature profile within a component including a certain transition resistance [65]. In the fire situation, the transition resistance would correspond to the convective heat transfer and the radiative losses of the component's surface. From a fire dynamics point of view, the thermal exposure can be understood as the description of (1) the environment including the imposed or incident heat flux and the gas temperature and (2) the interaction of this environment with the solid, comprising of a convective heat transfer for the particular surface and a surface temperature in balance with the solid and the environment. In this case, for a defined product or solid, the thermal exposure could be defined as radiation, convection and gas temperature as the missing elements are results from the exposure. For combust-

ible materials, it seems apparent, that additionally a fire exposure should be defined, see Section 2.3.17. For further information about the thermal and fire exposure, see Chapter 4.

In the fire situation, engineers found it practical to estimate the incident heat flux on the black body radiation temperature only. The applicability of this rough method should be carefully assessed as the error risks to exceed 15% if the emissivity and the convective part are neglected and a difference between radiation and gas temperature is excluded. Exemplarily, the standard time-temperature curve after 120 min gives a fire temperature of about 1050°C; the corresponding, simplified estimation would result in about 175 kW/m^2, considering losses with a factor of 0.8 would result in 140 kW/m^2. Mikkola estimated the convective part of the total heat flux for EN/ISO exposure in furnaces to 14.7 kW/m^2 [128]. Measurements taken in fire resistance furnaces presented in Chapter 4 indicate values for an incident heat flux of 175 kW/m^{2}with an error estimation of ±25 kW/m^2.

2.3.46 Travelling fires

Travelling fires are non-uniform, locally restricted limited fires [149], typically appearing in large spaces. They recognize significantly different zones with far-field and near-field temperatures. Contrary to growing fires , which will engulf the entire compartment (fire volume) at a certain time, the travelling fires have a flame front edge and a flame end edge. Typically, it is assumed that the fire origin at the floor is limited to a certain area that moves in the compartment with a certain fire spread rate, e.g. between 0.1 mm/s (wood cribs in the open space) to about 20 mm/s (maximum in experiments). The available methods are developed for non-combustible compartments. For compartment with structural timber the situation of a limited fire area and limited fire time would represent a favourable situation as the char layer creation is typically less severe in these fires. However, compartment fire accidents with significant shares of combustible surfaces show that the fire growth may exceed the fire spread rate and fully-developed fires can be expected despite the large size and volume of the compartment, see Table 2.3.46. It appears that fully developed fires are more likely for structural timber compartments also in large spaces.

Gas	Formula	[%] per volume	[%] per mass
Nitrogen	N_2	78.08	75.52
Oxygen	O_2	20.94	23.14
Carbon dioxide	CO_2	0.04	0.06
Argon	Ar	0.90	-
Methane	CH_4	<0.001	-

Table 2.5: Major constituents of dry air (ambient condition).

Accident	Area	Fire origin and primary fuel	Time to flashover [min]	fire spread rate [mm/s]
Fukuyama, Japan [94]	980 m^2	mattress and plywood wall boards	9.0	65.0
Nottingham, UK [29]	>1500 m^2	electric fault and structural timber[1)	n.a.	n.a.

n.a. not available
[1) building was not in use yet

Table 2.4: Fire accidents in large compartments.

2.3.47 Oxygen concentration

The oxygen concentration in air or a fire compartment can be specified as a percentage by volume or mass (in dry air: 20.95% by vol. or 23.1% by mass, see Table 2.3.47) or, typically used in modelling, as the total mass in a compartment, i.e. kg. The latter is favourable as the calculation of the expansion of air can be omitted. Besides the gaseous constituents, air contains further solid particles (e.g. dust, pollen) and water vapour whereby the latter may change the expansion of humid air significantly when heated. In severe fires, i.e. ventilation controlled fires, the fire temperature exceeds 1000°C where the appearance of water vapour is neglected in simplified design except for the reduction of the heat content, see Section 2.3.30.

Besides a fuel (fire load) and an energy source (heat), oxygen (air) is required for a combustion. In an experimental study, Schmid et al. [175] observed that about 15% by vol. oxygen concentration is needed for flaming combustion in a fire tunnel which was the main finding of another study by Jervis [89]. In practice, this limit is used by some gas suppression systems which lower the oxygen concentration to about 10%. Typically, in a fire resistance furnace no flaming is visible except the burner flame where a well-defined

fuel mixture is blown into the compartment. Besides flaming combustion, smouldering may occur in a combustible component providing a porous material structure such as the char layer. A lower limit for the minimum oxygen concentration needed for combustion is given as a function of the gas temperature, in general, the hotter the gas, the lower the required oxygen concentration which varies between 2% and 10% used by software packages such as B-RISK [201]. The critical oxygen concentration is given in Eq. 2.8 and plotted for the example of EN/ISO fire exposure and a parametric fire in Figure 2.15. The oxygen concentration (per mass) in the compartment and the critical limit associated with the actual gas temperature will be used in the TiCHS-model, developed in Chapter 6.

$$O_{crit} = \frac{T_{fo} - T_g}{T_{fo} - T_0} \cdot (O_0 - O_{fo}) + O_{fo} \tag{2.8}$$

or further simplified to

$$O_{crit} = \frac{873 - T_g}{580} \cdot 8 + 2 \tag{2.9}$$

where

O_{crit} is the critical oxygen concentration for combustion, in % by vol.;

O_0 is the minimum oxygen concentration for combustion at room temperature, in % by vol.;

O_{fo} is the minimum oxygen concentration for combustion at flashover temperature, in % by vol.;

T_{fo} is the flashover gas temperature, in K (normally assumed to be 600°C);

T_g is the gas temperature, in K;

T_0 is the ambient gas temperature, in K (normally assumed to be 20°C).

The Eq. 2.8 and 2.9, respectively, describe the decreasing dependence of a combustion process on the availability of oxygen when the temperature increases. Hadden performed bench scale tests in standard setups to estimate the effect of oxygen [70]. By exposing peat to low external heat fluxes from up to about 40 kW/m2, he found a decreasing mass loss when samples were exposed in ambient and nitrogen environments. Hadden found a weak influence on the gas flow which will be experimentally followed up in this thesis in Chapter 3.

2.3.48   Zero-strength layer

The zero-strength layer (ZSL), also designated as d_0,is part of a design concept given in Eurocode and designated in the literature as Reduced Cross Section Method (RCSM) or, more correctly, referred to as the Effective Cross Section Method (ECSM) [35, 105]. The model provides a simplified, user-friendly design concept to account for the reduced properties of timber exposed to fire or heat. In addition to the reduction of the original section
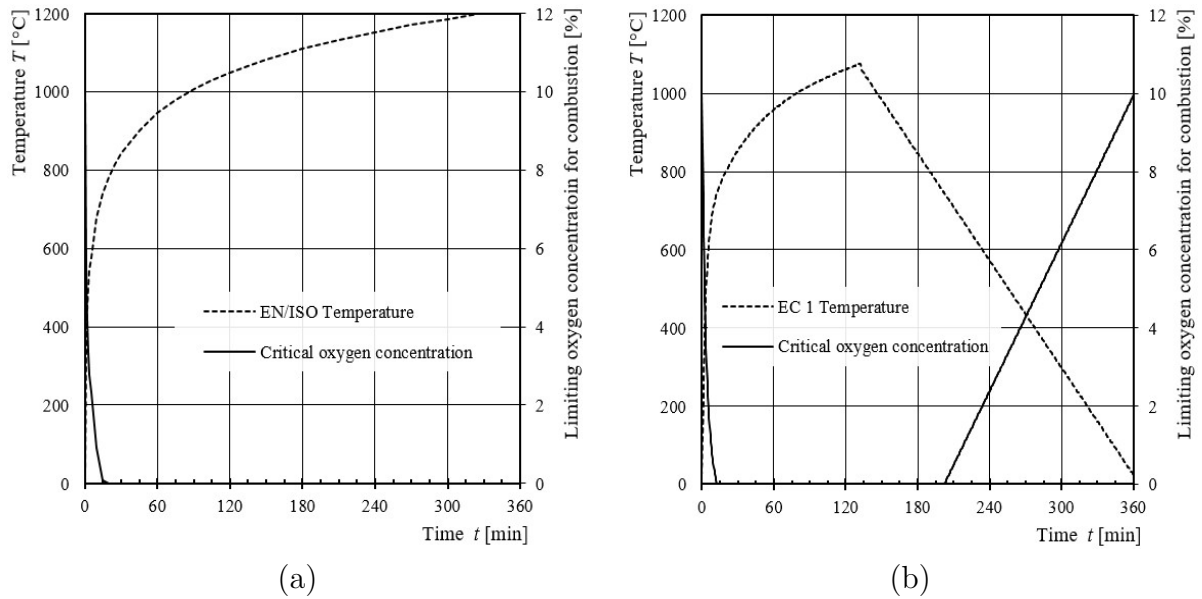
Figure 2.15: Limiting oxygen concentration as function of the temperature. Example of EN/ISO exposure (a) and of a parametric design fire (b). Own figures.

by the charring (step 1), a fictitious thickness, the ZSL, is removed from the remaining virgin cross section obtained after the removal of the char layer (step 2), and the resulting, effective cross section is assumed to have normal strength and stiffness properties [171]. Exemplarily, the reduction of the load-bearing capacity in bending with respect to the two-step design procedure is shown in Figure 2.16. The design concept was originally intended for glulam beams and standard fire up to 60 min [157]. When Eurocode was drafted, it was believed that the concept can be automatically applied to other members (e.g. buckling members) and extended to any fire exposure duration; consequently, no limitations with respect to the state of stress or duration has been implemented. Answering the needs in practice, the application field was further extended to other products (e.g. CLT [172] and I-joists [106]). For non-standard fire, test results indicate significant deviations from the original concept [108]. Recently, an empirical concept for the extension of the ZSL design concept for parametric design fires was proposed based on fire tests [25, 108]. In this work, it is assumed that limited structural timber in a compartment, e.g. single linear members, contribute insignificantly to the total fire load. As shown in Figure 2.16 (b), for larger sections, an increased share of the losses in the relative load-bearing capacity are attributed to the charring of the member. In this thesis, the strength (and stiffness) losses of the heated virgin section are not further studies although considered relevant.
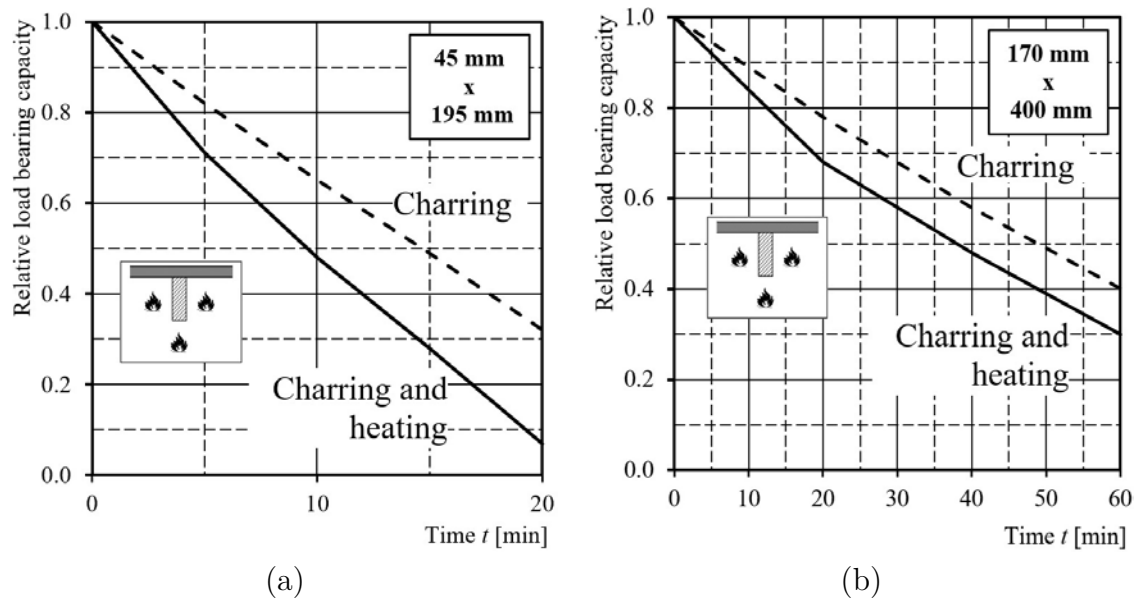
Figure 2.16: Effect of the reduction of the load-bearing capacity of a glulam beam in bending by charring and charring and heating according to Eurocode [35] for a small cross section (a) and large cross section (b). Own figures.

Chapter 3

Experiments

3.1 General

This Chapter presents a summary of experiments and tests performed within this PhD thesis. These experiments aimed at contributing to the knowledge increase with respect to the fire safety design for timber structures with the focus on the interaction of the material with the fire compartment. As stated in earlier work of the author, it is assumed that the behaviour of structural timber in fire in all phases can be understood only if the behaviour of the wood material and the char layer material is properly studied. Thus, many aspects of this thesis investigate the apparently reactive behaviour of the char layer when exposed to fire.

The experiments were performed by the author of this PhD thesis in cooperation with colleagues, students and staff at ETH Zürich and partner universities and institutes. Comments and data provided by D. Brandon, N. Werther and U. Wickström have been considered. The experiments were partly embedded in third-party funded research projects and served multiple purposes. In the particular sub-chapters, the declared purpose is specified with focus on this PhD thesis. The content of all sections is related to the investigation of the timber structures in real fires, aiming for the development of required input for engineering models which describe the interaction of the fire compartment with timber structures in design fires and vice versa. Further details of the experiments presented here are given in the associated IBK report [165].

3.2 Investigation of the behaviour of structural timber in furnace environments

Typically, timber components are tested according to fire resistance standards, e.g. EN 1363 [37], although the material is combustible and it is apparent that testing of such elements will result in the observation of reduced furnace fuel consumption compared to the testing of incombustible components. In this Section, several questions recently raised by the community of fire safety engineers will be studied with respect to the validity of furnace test results for timber structures in general. The discussion of the topic includes the fuel consumption in furnace tests, the surface flaming of exposed timber surfaces in fires and leads to the debate of the term of thermal exposure. As a result, the term "fire exposure" has been defined extending the term "thermal exposure" by the availability of oxygen in terms of concentration and flow characteristic. The investigation of the fire exposure of timber comprised model-scale experiments and a full-scale experiment on a fire testing furnace. Comprehensive data is made available in an IBK report [165], a COST Action FP1404 STSM report [161] and has been published in some journal publications [162, 167]. The applied measurement approach determining a product specific mass loss rate was utilised in an attempt to answer the question of glue line integrity of engineered wood products which use adhesive such as CLT; A testing methodology has been proposed and is currently under further development [102, 103].

3.2.1 Particular research question

The particular research question of this experimental campaign was to answer the applicability and limitations of fire resistance tests performed in furnaces for timber structures. In the fire safety community, some experts share the opinion that surface flaming at unprotected timber surfaces might remain undetected by the control devices of furnaces and, thus, the thermal exposure is not equivalent for combustible and incombustible components. Further questions are the mass loss rate under standard fire, the specimen's contribution to the total energy required to fire the furnace, the conditions in the furnace (gas composition and gas concentration) and the char layer creation (stickability, thickness, surface regression and density).

3.2.2 Experimental approach

To investigate the influence of the combustibility to the thermal exposure, model-scale experiments were performed at the VKF lab in Dübendorf, Switzerland, and one full-scale experiment was performed at the Research institutes of Sweden (RISE) lab in Borås, Sweden. Exceeding the instrumentation of standard fire resistance tests, for the experiments of this campaign, an increased instrumentation was implemented including a gas analysis. Besides plate thermometers (PTs) for controlling the furnace according to the standard fire time-temperature curve in accordance with EN 1363-1 [37], a heat flux sensor (HFS), bi-directional probes [121] and further temperature sensors have been installed in the furnace and the specimens. Furthermore, the change of the specimen mass using load cells. The mass loss during the experiments was compared to the measurements of the residual cross sections (remaining cross section and virgin wood section) after the experiment. All experiments were performed using the standard fire. While the model-scale experiments were conducted in an oil-fired furnace, the full-scale experiment was performed in a gas-fired furnace.

In the model scale furnace experiments, one STP was fire exposed on its lower, unprotected side (combustible surface; C), the second STP was initially protected by an incombustible fire protection system which allowed for the prevention of the start of charring for over 90 min. After the detection of the start of charring, the fire protection system was manually pushed away from the timber surface to study the change of the furnace environment when the timber surface was exposed directly to the fire.

3.2.3 Material and equipment

The specimens of this campaign were designed to allow for one-dimensional charring. In addition, it was aimed for avoidance of any potentially available influence of the glue line to allow drawing conclusions about the charring behaviour of solid timber. In total, three solid timber panels (STPs) were designed to study the thermal exposure of the specimen and the furnace environment when initially unprotected timber and initially

protected timber is fire exposed. Spruce wood was chosen for all specimens STP I, STP II and STP III as it is the most common softwood in construction in Europe.

The STPs of the model-scale experiments at VKF were factory-made dowel-laminated panels with the outer measurements of 800 mm× 960 mm (length × width) and a thickness of 165 mm. They were manually dissembled and re-assembled at ETH Zürich to improve the fit between the individual boards (width 50 mm) and install the TCs in the specimen in instrumented beams, see Figure 3.1 (a). Before re-assembling and after the installation of TCs in five TC stations per specimen, the specimens were stored in a climate room at about 20°C with controlled air humidity with R.H. of 65% to reach an EMC of 12%. The material MC was further verified with 12±2% directly before the installation of the STPs on the furnace on the day of the experiment. The fire protection system of STP II consisted of a double layer system comprising of a gypsum -based board (inner panel) and a mineral fibre based board (outer panel). Thus, the inner panel provided a substantial heat sink (bound water in the gypsum) and could delay the heating of the timber surface as long as water was evaporating and the outer panel provided significant mechanical fixation of the decomposing gypsum board.

The STP III of the full-scale experiment at RISE was directly assembled on the furnace by manually arranging thirteen glulam beams. The beams were brought together with stone wool fitting parts and arranged transversely to prevent horizontal bond lines in parallel to the fire exposed surface; thus, a 145 mm thick STP was created.
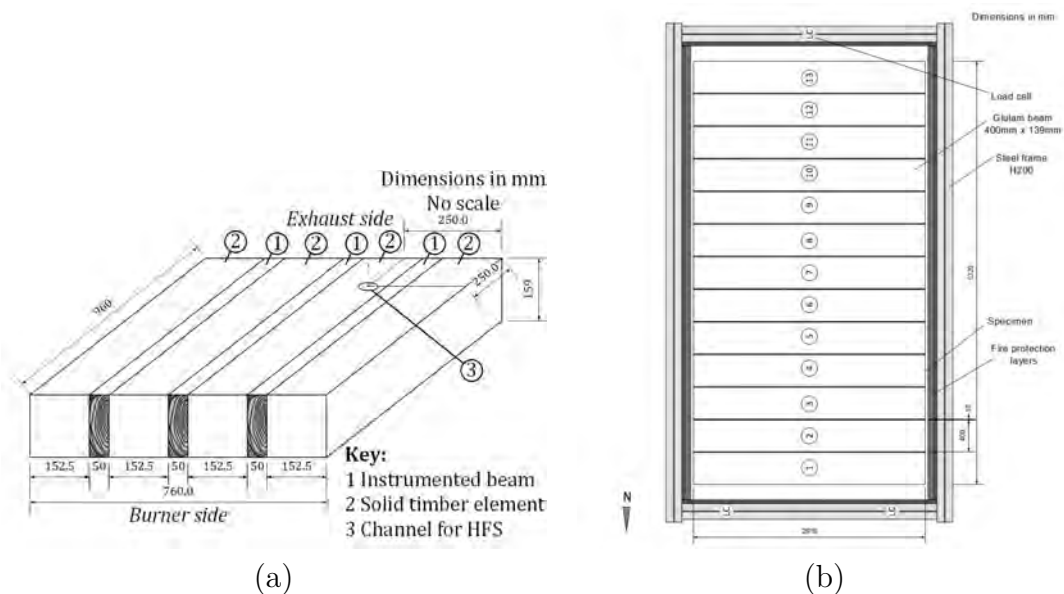
Figure 3.1: Assembly of the wood section of STP I and STP II (a) and of STP III (b) [161]. Own figures.

3.2.4 Installation and Measurements

In the model-scale experiments, i.e. in STP I and STP II, wire TCs (designation of the temperature measurement setup: K-w-t-0.1/1.2/1.65-pe according to Fahrni et al. [53] were installed in five stations with their measurement point at the centre line of the instrumented beams to detect the location of the 300°C isotherm which was considered representative for the char line. The length of the TC parallel to the isotherms directly after the hot junction was at least 50 mm to avoid disturbance of the temperature measurements in low conductive material, as suggested in the literature [19, 37, 53]. In all experiments of the model-scale experimental campaign, a heat flux sensor was used to take measurements at various positions (vertical coordinates) and locations (horizontal coordinates), thus, flush with the exposed surface, behind and at the level of the HFS, above and away from the burner.

To analyse the furnace compartment environment, in the model-scale furnace and in the full-scale furnace, sample gas was extracted at various locations. The locations were directly under the fire exposed surface, centric in the furnace compartment and in the exhaust channel. In the model-scale experiment, only one oxygen analyser was available while the extracted gas was analysed simultaneously in the full-scale experiment [109].

In the full-scale experiment, the instrumentation was mainly installed in the furnace compartment and the furnace wall to investigate and compare the thermal exposure of the STP with an incombustible slab which is not reported in this document but published in [109]. Besides the control PTs, PTs at all internal furnace sides facing the side of its installation and the opposite side were installed. Additionally, a furnace brick about 500 mm above the furnace floor was equipped with internal TCs to study the thermal exposure of the furnace wall.

All specimens were supported by three load cells each to follow the change of the mass and determine the specific mass-loss rates. The model-scale experiments used a wood frame while a steel frame was used for the full-scale experiment.
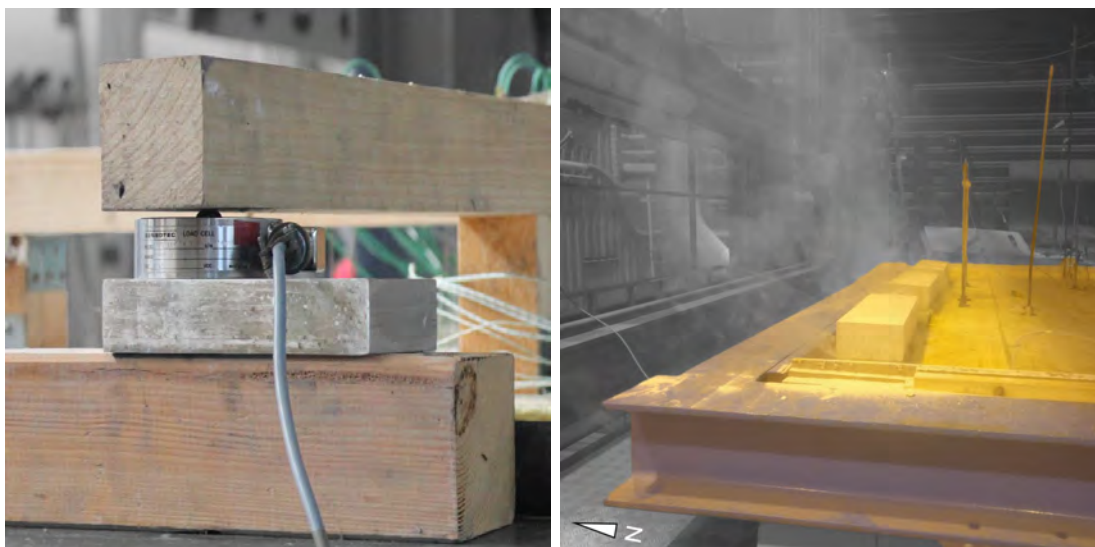
Figure 3.2: Indirect support of the specimens on the furnace walls. Support of STP I (left) and of STP III (right). Own images.

3.2.5 Results

In the following, results are presented with respect to the measurements of the gas velocity in the furnaces and the remaining cross section after fire exposure. Results with respect to the oxygen concentration are used in Chapter 4 to evaluate the fire exposure of non-combustible and combustible specimens in fire resistance furnaces.

Gas characteristics. The oxygen concentration in the furnaces were measured at various locations and positions, for results see Chapter 4. The minimum oxygen concentration required by EN 1363-1 of 4% was fulfilled with an average of about 5%, regardless of the combustibility of the specimen. Besides the oxygen concentration, in the full-scale furnace at RISE, a complete gas analysis was done with the extracted sample gas. The analysis showed a significant amount of CO near the combustible surface indicating smouldering oxidation in the specimen, see Lange et al. [109].

In the furnaces which were used to expose the specimens STP I, STP II and STP III, the gas velocity was measured near the exposed surface of the STPs. The gas velocity was measured with one bi-directional probe (25 mm diameter) in the direction of the burner axis in the oil fired VKF model scale furnace and with four bi-directional probes (12 mm diameter) in the gas fired RISE full scale furnace in the direction of the burner axis and in the transverse direction. The bi-directional devices were similar to those presented by McCaffrey et al. [121].

In Section 3.4, further experiments with two specimens of STP type, fire exposed for 120 min are presented. Both specimens were standard fire exposed at the oil fired model

Location,	VKF	RISE				MPA	
specimen,	STP I	STP III				BC1	BC2
probe no.	I	I	II	III	IV	I	I
n	50	1081				16	22
$v_{abs,mean}$ [m/s]	2.2	0.8	1.1	0.9	0.6	1.7	2.8
(STD) [m/s]	1.5	0.5	0.5	0.9	0.6	0.9	0.8

Table 3.1: Gas velocities close to the exposed sample's surface in three different furnaces.

scale furnace at MPA Stuttgart, Germany. For comparison reasons, both experiments had a bi-directional probe (25 mm diameter) and a commercially available Pitot-tube (producer: Kimo) installed, the results are included in this Section.

The limited data recording possibilities resulted in significantly different data sets for the pressure measurements in the VKF, the RISE and the MPA furnace respectively. In the MPA furnace, minimum and maximum readings were recorded manually at randomly distributed time increments. The weighted average of the derived absolute gas velocity, $v_{abs,mean}$, and the STD of the gas velocity is collected in Table 3.1 with further details. The derived gas velocities in the furnaces and experiments respectively are plotted in Figure 3.3. The significant difference between the furnace control of the two experiments performed at MPA might be traced back to the control approach (i.e. the interaction of the ventilation, the burner effect, the furnace over pressure) by the MPA team which was changed between the first experiment (BC2) and the second experiment (BC1).
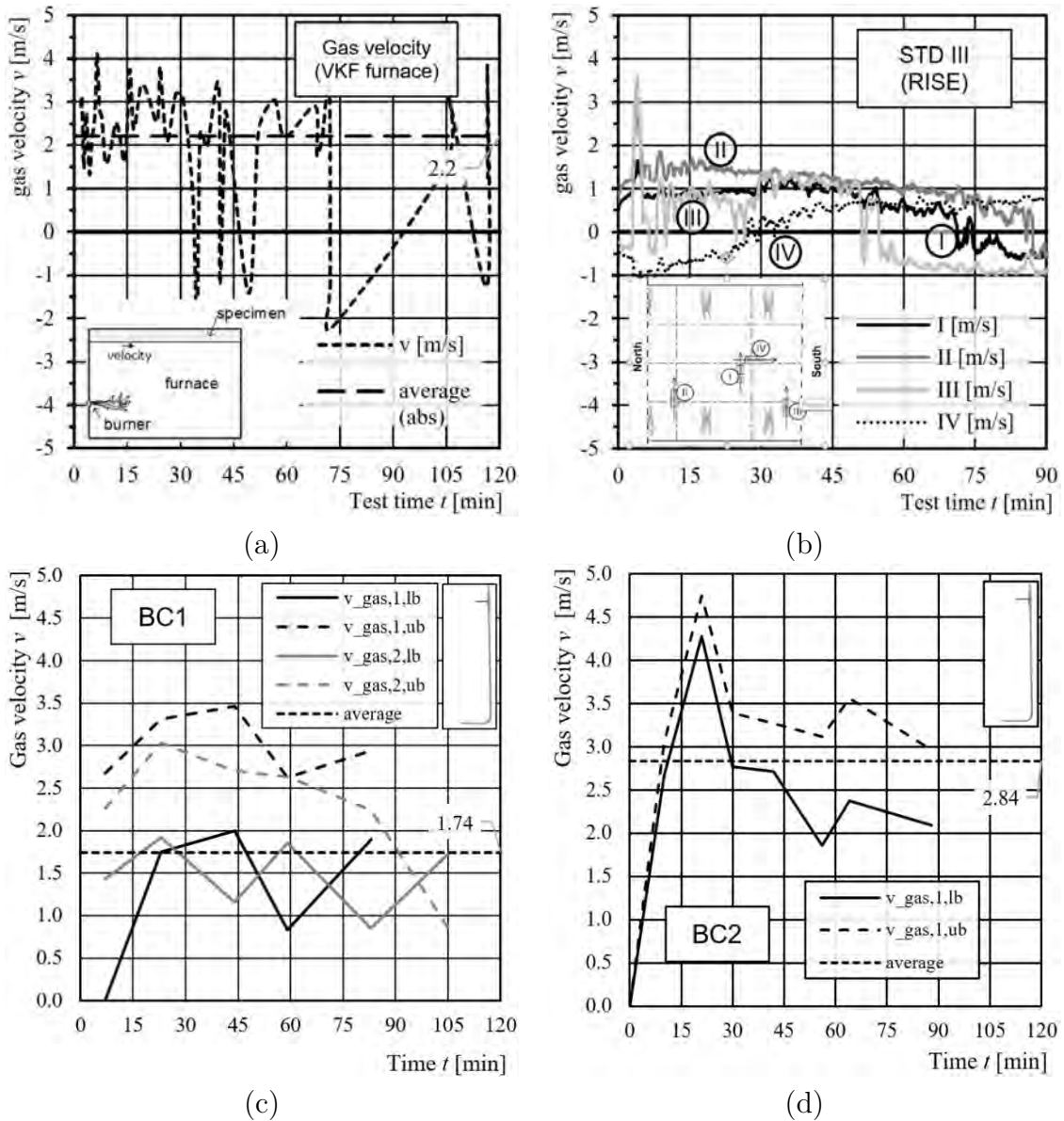
Figure 3.3: Derived gas velocities near the surface in the furnace at VKF (a), RISE (b) and MPA for BC1 (c) and BC2 (d). Own figures.

Temperature measurements. Temperature measurements were taken in the furnace by control PTs as requested by testing standards [37]. Exceeding standard requirements intense instrumentation in the compartment with various types of temperature sensors were made and have been presented in parts in Lange et al. [109] and with respect to internal measurements in the solid (STP I) in Fahrni et al. [53]. In the model scale experiments, the surface temperature was measured with an adjustable U-shaped sheathed thermocouple as previously applied by Werther [205]. Although the temperature meas-

urements might be influenced by disturbances due to its conductive sheathing and the feeding length within the furnace compartment, surprisingly consistent measurements were observed, see Figure 3.4.

(a)

(b)
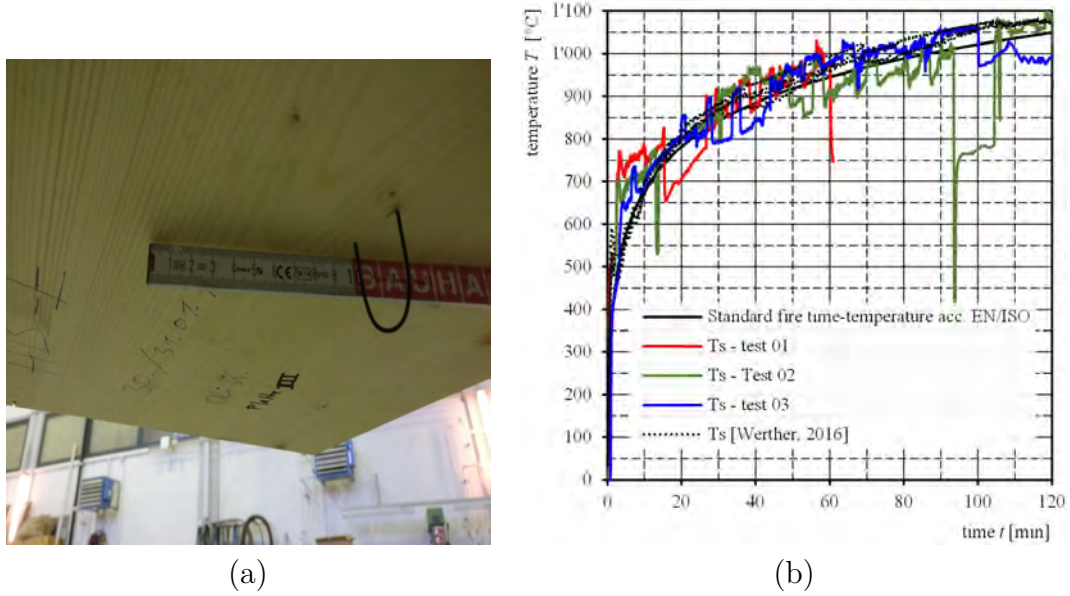
Figure 3.4: Surface TC as used in the compartment test for indicative measurements (a) and measurement results (b). Own image and figure.

Remaining cross section. For all specimens involved in the experimental campaign, the residual virgin cross section h_{virg} was recorded various measurement techniques. The techniques comprised traditional measurements with rulers using various resolutions and novel 3D-scanning techniques [170]. Exemplarily, results are given for the available surface in a 2D-graph and as cumulative distribution in Figure 3.5. The charring rate was estimated assuming a linear charring rate over the time of fire exposure; the estimation follows Eq. 3.1.

$$\beta_i = \frac{d_{char}}{t_{fi}} = \frac{h_0 - h_{virg}}{t_{fi}} \tag{3.1}$$

where:
d_{char} is the charring depth, in mm;
h_0 is the thickness of the original member section, in mm;
h_{virg} is the thickness of the residual virgin wood section, in mm;
t_{fi} is the time of the fire exposure, in min;
β_i is the charring rate at location i, in mm/min.
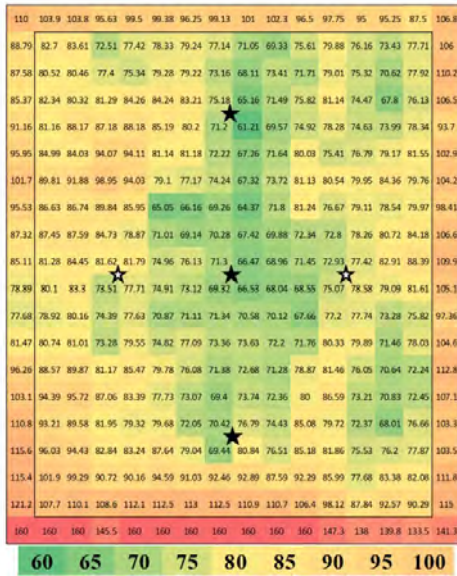
(a)

Mesh size 50 mm x 50 mm.
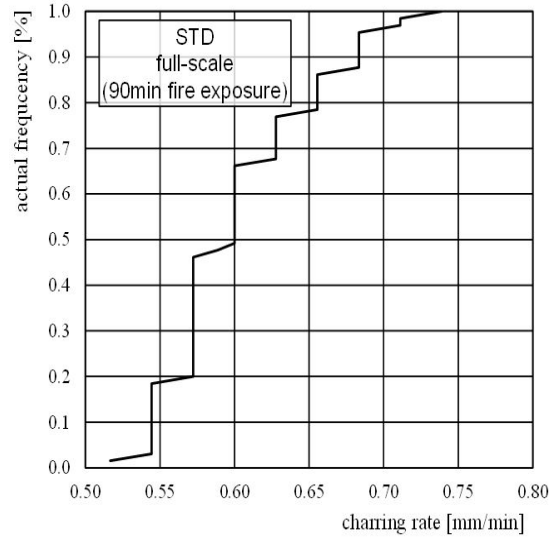
(b)

Figure 3.5: Results of the manual measurements of the residual virgin cross section of the initially unprotected STP specimens. Charring rates of STP I (a) and of STP III (b). Figures by M. Klippel.

Mass loss. Information about the mass loss is typically measured in bench scale tests dealing with the reaction to fire properties, e.g. when using the cone calorimetry. For fire resistance tests, this procedure is typically not applied. Based on the model scale experiment STP I with a reference density of about 450 kg/m³ at about 12% MC, Klippel et al. [102] presented a reference mass loss rate for solid timber in the model scale furnace of 15.4 kg/m²per hour. This value is proposed as comparative value for solid timber to describe no falling off (loss of stickability) of charring parts of the structural timber component. The mass loss of the experiment STP I was further compared to four further experiments performed in the VKF furnace of another series documented by R. Fahrni [52]. In this three experiments, the main objective was the determination of the statistical analysis of the charring rate when the EN/ISO exposure would be stopped at 30, 60, 90 and 120 min, respectively. The results are summarised in Table 3.2.

During the full scale experiment at RISE, STP III, besides LC recordings, manually readings were done. The start of the experiment represents the mass loss given in Figure 3.6 (a). The estimation of the load of the LC at the start of the experiment results in 22.4 kN or 2288.2 kg while the LC showed a slightly higher value of 25.6 kN, see Tables 3.3 and 3.4. The mass loss of the specimen was measured by the LCs to be 235 kg, values are provided in Table 3.4. Considering the exposed area (exposure of 95% of the beam length) of 13.8 m², the specific mass loss would be about 17.0 kg/m² for the fire exposure

	1	2	3	4	5	6	7	8
			STP 30	STP 60	STP 90	STP III	STP 120	STP I
1	ρ_{12}	[kg/m^3]	447.9	448.7	450.0	464.4	450.8	454.0
2	ρ_0	[kg/m^3]	399.9	400.6	401.7	414.5	402.5	405.4
3	Δm	[kg]	5.5	11.0	16.0	306.3	22.0	22.4
4	$\Delta \dot{m}$	[kg/h]	14.9	14.9	14.4	306.3	14.9	15.4
5	β_{st}	[mm/min]	0.67	0.63	0.61	0.61	0.62	0.61
6	$\rho_{ch,0}$	[kg/m^3]	76.5	51.9	53.9	81.2	54.7	35.2
7	$\rho_{ch,0}/\rho_0$	[-]	0.19	0.13	0.13	0.20	0.14	0.09

Table 3.2: Comparison of the experiment STP I (120 min) with other experiments performed in the VKF furnace.

	mass	weight
	[kg]	[kN]
Frame	1255.4	12.32
Instrumentation (1.5 kg each)	51.0	0.50
STP III	981.8	9.63
Sum	2288.2	22.45

Table 3.3: Specimen mass estimation before the start of the experiment.

of 90 min and 11.3 kg/m^{2}per hour assuming a linear relationship. However, a deeper analysis of manually taken recordings of the individual LC channels showed significantly deviating signal and measurements respectively of LC 1, see Figure 3.6 (b). It can be assumed that LC 1 got heated during the experiment. Thus, LC 1 recordings were disregarded and a trend line determined using the recordings of LC 2 and LC 3. A shift of the trend line (see Eq. 3.2) through the origo resulted in a more reasonable estimate of the mass loss per hour of 14.1 kg/m^2. This value is slightly lower than the value estimated in the model scale experiment STP I which was about 15.4 kg/m^{2}h.

$$m(t_{fi}) = 0.235 \cdot t_{fi} - 2.673 \qquad (3.2)$$

where:
m is the mass loss per square meter exposed area, in kg/m^2;
t_{fi} is the time of the fire exposure, in min.

The mass of the residual cross section of the specimen STP III without a char layer of all thirteen the glulam beams was 592.2 kg. The shape of the residual beams showed that they didn't experience fire exposure over their full length due to the support on the angle attached to the frame, see Figure 3.7 (a). The fire exposed effective length was estimated to 2785 mm considering the beam length of 2910 mm, the uncharred support length

event	mass	weight
	by the sum of the load cells	
	[kg]	[kN]
start of experiment	2607.0	25.57
end of experiment	2371.0	23.26
after removal of the char layer	2404.0	23.58

Table 3.4: Specimen mass (including frame and instrumentation) from load cell readings during the experiment and after removal of the char layer.
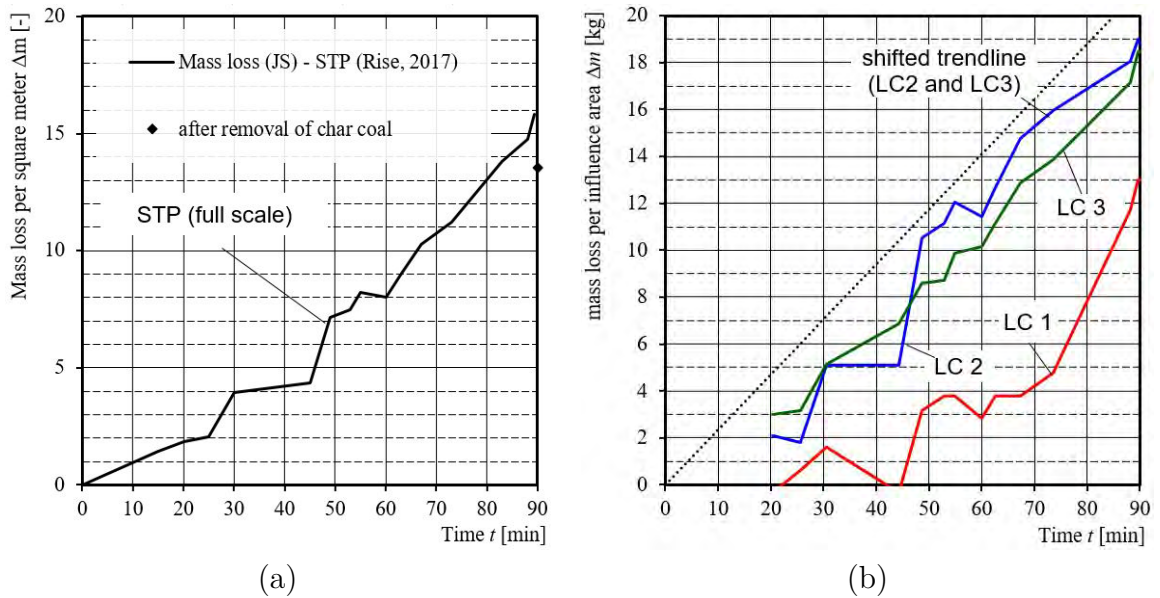
Figure 3.6: Mass loss determined from the load cell readings during the experiment and after removal of the char layer (a) and the derived specific mass loss per unit area for the individual load cells (b). Own figures.
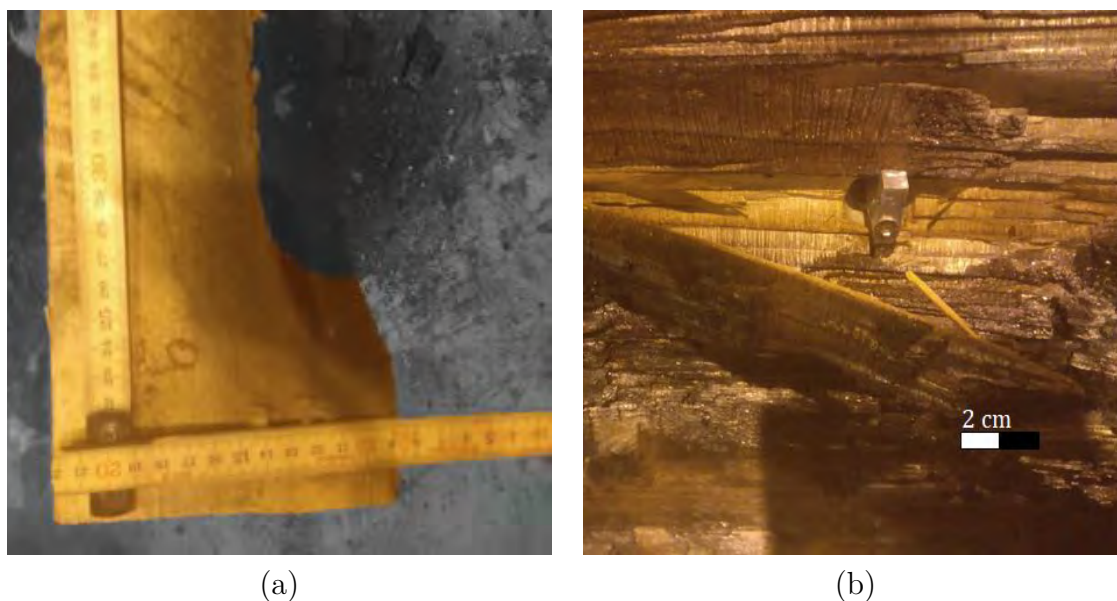
Figure 3.7: Shape of the beam nine after removal of the char layer (a) and orientation of the measurement device perpendicular to the grain direction (b). Own images.

of 35 mm (on both sides) and the rounding (radius assumed to be equal to the charring depth), see Figure 3.7. Using the mean charring rate of 0.61 mm/min, a total char volume of 0.8 m³ can be estimated for 90 min fire exposure. Considering the original beam density of 464 kg/m³, the charred volume corresponds to about 371 kg (in total) wood or a mass loss of 24.6 kg/m²(for the exposed area of about 14.5 m²). Comparing this reference mass with the corrected mass loss estimated by the load-cells, the char layer exhibited a density of about 65 kg/m³. This is about 14% of the source wood material at 12% MC. For the similar model scale experiment (STP I) presented in this document, the density of the char layer was estimated to be as low as 11% of the source material, assumed at 12% MC. To correctly calculate the energy content of the specimen's contribution to the fire it seems to be essential to estimate the remaining char layer mass; it is recommended to measure the mass of the specimen before extinguishing work, and either, of the collected dry char layer or the residual, cleaned specimen for all future experiments and tests with structural timber.

3.2.6 Main findings

The main findings of the presented experiments concern many parameters which can be utilised for the improvement of future experiments and the estimation of a specimen's contribution to the fire:

- The extended setups exceeding standard fire resistance test requirements allowed to describe and isolate relevant characteristics;

- The mass loss in furnaces of solid timber is in a range of 14.1 kg/(m$^2 \cdot$ h) to 15.4 kg/(m$^2 \cdot$ h);

- The char layer surface regression in the furnace experiments was close to zero;

- The oxygen measurements in the furnace compartment indicate a oxygen concentration in the range of 5% away from a combustible specimen's surface and significantly reduced up to 0% near the specimen;

- No surface flaming could be observed in furnaces, neither visually nor by measurements with HFS or PT sensors flush at the surface of a combustible specimen;

- High CO concentration near the combustible specimen's surface indicate smouldering combustion;

- The char layer density seems to be correlated with the standard deviation of the gas velocity rather than the gas velocity itself;

- Various measurement techniques can be applied for the measurement of the residual virgin section; the use of rulers for measurements delivers a good accuracy when a reasonable amount of measurements is used and the location of the measurements is chosen in undisturbed regions.

3.3 Investigation of the behaviour of structural timber in oxygen rich environments [1]

In general, today's assessment of the fire resistance of structural components is based on empirical or semi-empirical models derived mainly from fire resistance tests performed in fire resistance furnaces. The structural fire design of timber members is based on one hand on the prediction of the reduction of the initial cross section by charring and, on the other hand, on the consideration of the losses in strength and stiffness in the virgin wood section which experienced some heating below the char line. This two-step procedure is the most important concept of Eurocode [35], originally developed for linear members and further adopted for novel structural products [171]. The available models rely on basic design charring rates developed for the standard time temperature curve. These are able to reproduce typical effects required in fire resistance design such as the reduced thermal exposure (e.g. through a fire protection system which is not able to encapsulate the member for the entire design duration) and sudden temperature increase at their surfaces (e.g. after the fall-off of a fire protection system). In general, the available models are not validated for other fire exposure deviating from standard fire. While the pre-flashover

---

[1]Parts of this Section are content of a publication [168]

phase is typically short in time, the decay phase may exceed the duration of the post-flashover phase. Recently published research results show, that the total fire duration may increase significantly due to a longer post-flashover phase which might require an adjustment of fire resistance ratings [174, 178]. Reasons the deviation are to be found in the combustibility of structural timber which contributes to the exterior flaming and provide further fuel when the oxygen concentration in the compartment increases towards normal as the movable fire load is consumed. Currently, engineers lack of a common approach to solve the associated questions in general and lack of proper tools to predict the timber member's behaviour in the cooling phase or consider the timber member's contribution to the fire dynamics in the compartment.

3.3.1 Particular research question

The particular research question of this experimental campaign was to create input data for a fire design model for timber structures which is able to consider its behaviour in the cooling phase when the fire decays. Typically, post-flashover fires are ventilation controlled, i.e. the availability of oxygen is limited by the inflow through openings. In contrast, in the cooling phase, the oxygen concentration in the fire compartment increases and change the combustion conditions in the compartment. Besides the charring behaviour of the timber specimens used, the char layer creation and reaction was the focus of this investigation.

3.3.2 Material and equipment (FANCI setup)

Initially, the existing standard test and experimental setups were evaluated for the description of parameters considered relevant in this part of the thesis. The relevant parameters and conditions are (1) the swift variation of the incident radiant heat flux up to 120 kW/m^2, (2) a controlled gas flow with velocities of variable ranges exceeding about 5 m/s, (3) the recording of the mass loss, (4) the achievement of about one-dimensional heat flux within the specimens limitedly affected by any edge disturbance, (5) the measurement of the char layer surface regression and (6) the charring of the virgin section with potential instrumentation to follow the temperature development within the specimen and (7) quick extinguishment after the termination of an experiment. Among others, the standardised cone calorimeter [86], the fire propagation apparatus [6], the (modified) OSU apparatus [197], the recently presented experimental setups H-TRIS [120] and the fire tunnel used by the author of this thesis in a previous study [175] were evaluated but found unsuitable due to the insufficient description of the six parameters and the conditions given above. Thus, the Fire Apparatus for Non-standard Heating and Charring Investigation (FANCI) was designed for the purpose of this study, see schematic drawing in Figure 3.8. Ambient air was used as the gaseous medium in contact with the specimen, the applied variation of the velocity between 1 m/s and 6 m/s (at ambient conditions)
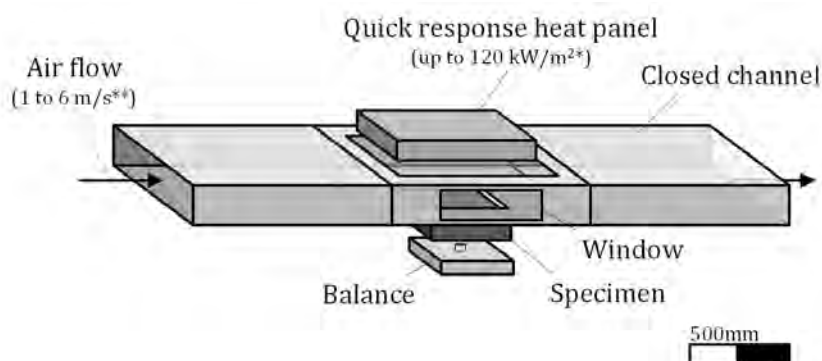
Figure 3.8: Schematic view of the FANCI setup with the combustion unit between the inflow and outflow channels. Image by J. Schmid [166]

was considered to sufficiently describe the typical ranges of oxygen concentration and gas velocities in compartment fires.

During the experimental campaign, the setup was developed to isolate the characteristics of interest. The core of FANCI setup is a combustion chamber with a specimen support and a quick response radiant heat panel attached around an channel that allows cross-flow over the specimen's surface. The channel is fed by a fan whereby two types of setups were created to create an either highly turbulent flow environment (ht) or a moderately turbulent flow environment (mt). Calming units at both the inlet and outflow were arranged to allow for an approximately homogeneous gas flow over the specimen. All units had an individual length of about 950 mm, see Figure 3.9. The gas flow was investigated over the surface of the specimen at ambient condition using an anemometer. A homogeneous flow was observed at lower reference velocities which decreased with increased velocity. However, above the specimens surface, indicated in the flow axis in Figure 3.10, a reasonable homogeneity was found. The degree of turbulence at the ambient stage was evaluated initially using a dynamic pressure sensor (producer: Testo) at the specimen's surface, see comparison of ht and mt in Figure 3.10.

The timber specimens were of laminate spruce specimens with an initial mass of about 3 kg (density about 435 kg/m^2 at 12% MC) with an exposed surface of about 0.25 m × 0.25 m (length × width), Figure 3.11 shows the assembling of a typical specimen. The laminate specimens (STPs) were made from spruce wood beams to represent solid timber made of softwood. Five beams (width 44 mm to 45 mm; depending on the series) were arranged with annual rings parallel to the fire exposed side and were edgewise bonded. Specimens were either equipped with internal TCs to measure the inside temperature
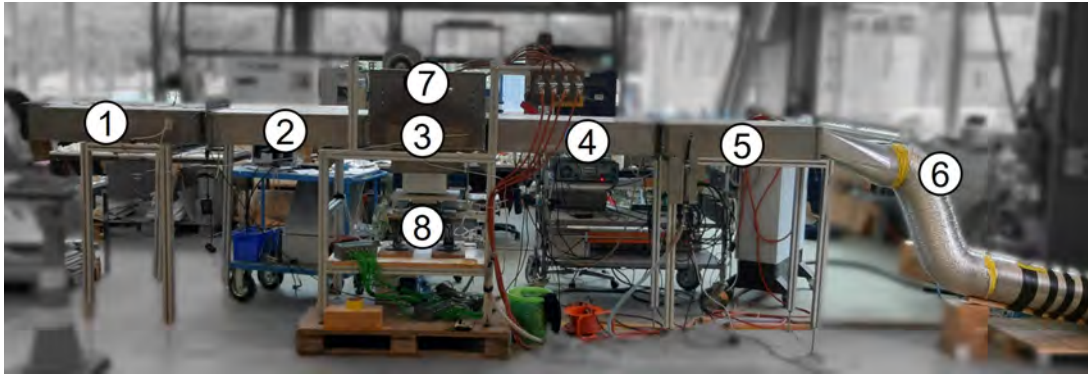
Key:

1	Unit I - Inflow unit	5	Unit V - Outflow unit
2	Unit II - Calming unit	6	Exhaust channel
3	Unit III - Combustion unit	7	Heat panel body
4	Unit IV - Calming unit	8	Specimen support

Figure 3.9: The FANCI setup at ETH Zürich with all units used in series 7 to 10. Image modified from F. Hirzel.

change or left uninstrumented. For the instrumented specimens, the three inner beams, i.e. beams "L" (left), "M" (middle) and "R" (right) were equipped with wire TCs while the side beams "SL" and "SR" were left uninstrumented, since potential edge effects could have resulted in disturbed temperature measurements. In general, the TCs were inserted in selected depths using a default pattern (multiples of 6 mm as used by e.g. Tran et al. and König et al. [197, 107]). By default, TCs were installed at least in triplicates for one depth.

3.3.3 Experiments

During the experimental campaign, between November 2016 and June 2020, in total, ten series of experiments were performed with the FANCI setup. The experiments focused on isolating characteristics and studying them in ranges previously identified as relevant. Furthermore, in the experiments measurements were done which had typically left unconsidered or which were found to have fragmented documentation in the literature. Excluding trial runs to test the setup, 73 experiments were performed whereby 35 specimens were equipped with internal TCs. The experiments lasted up to 55 min, though majority of the experimental duration was 20 min. About two thirds of the experiments were performed under ht conditions (43 experiments). The overview of the experimental series including the investigated parameters are given in Table 3.5.

At the day of the experiment, the specimen was taken from the climate room at ETH Zürich, where the source material and the ready made specimens were stored at 65% RH. The mass of the specimen was recorded using a lab scale directly before the
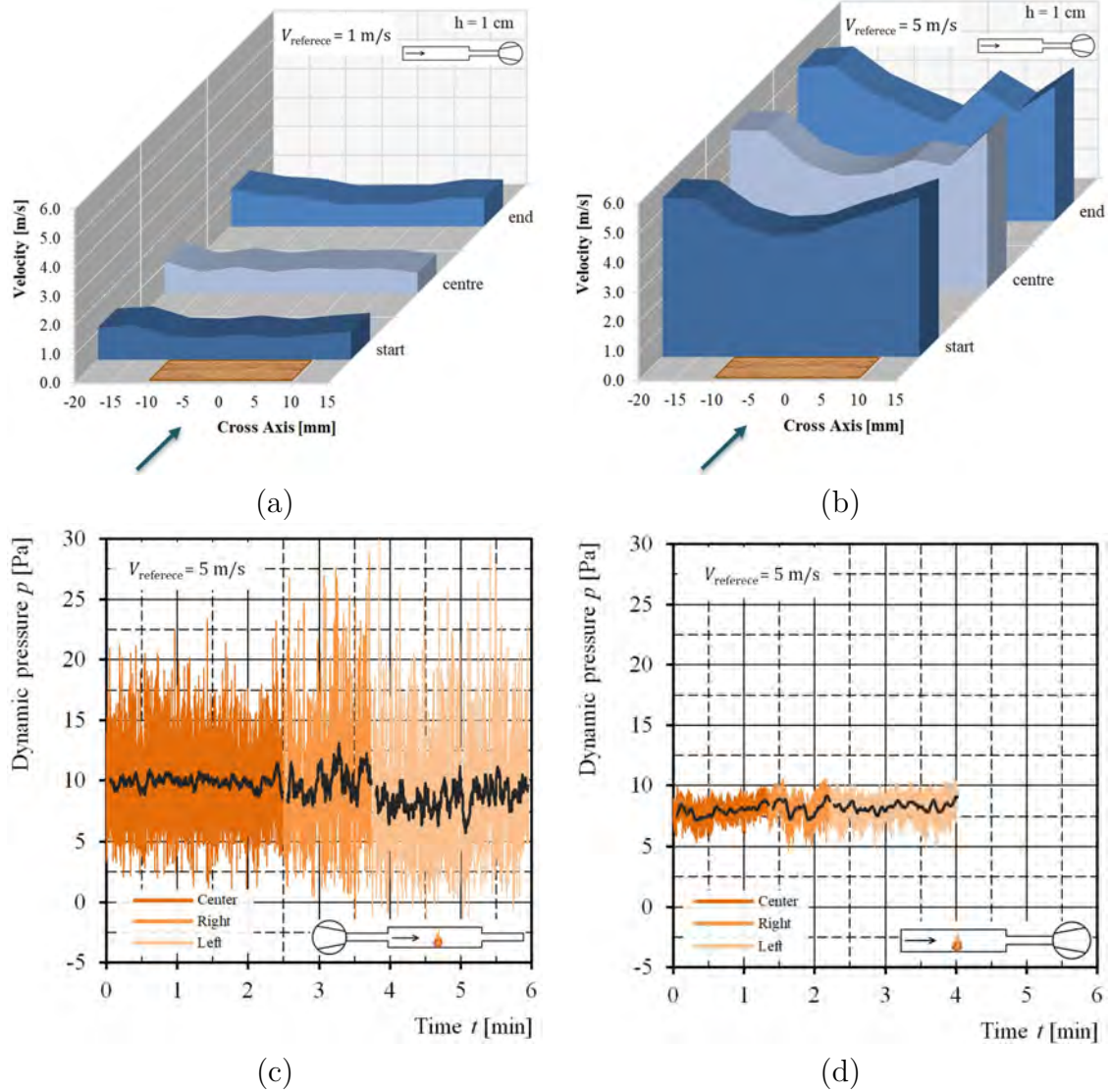
Figure 3.10: Analysis of the gas flow in the FANCI setup. Gas flow over the specimen's surface at velocities of 1 m/s (a) and 5 m/s (b). Dynamic pressure as indicator for the degree of turbulence in highly turbulent conditions (c) and moderately conditions (d). Images modified from J. Felder.
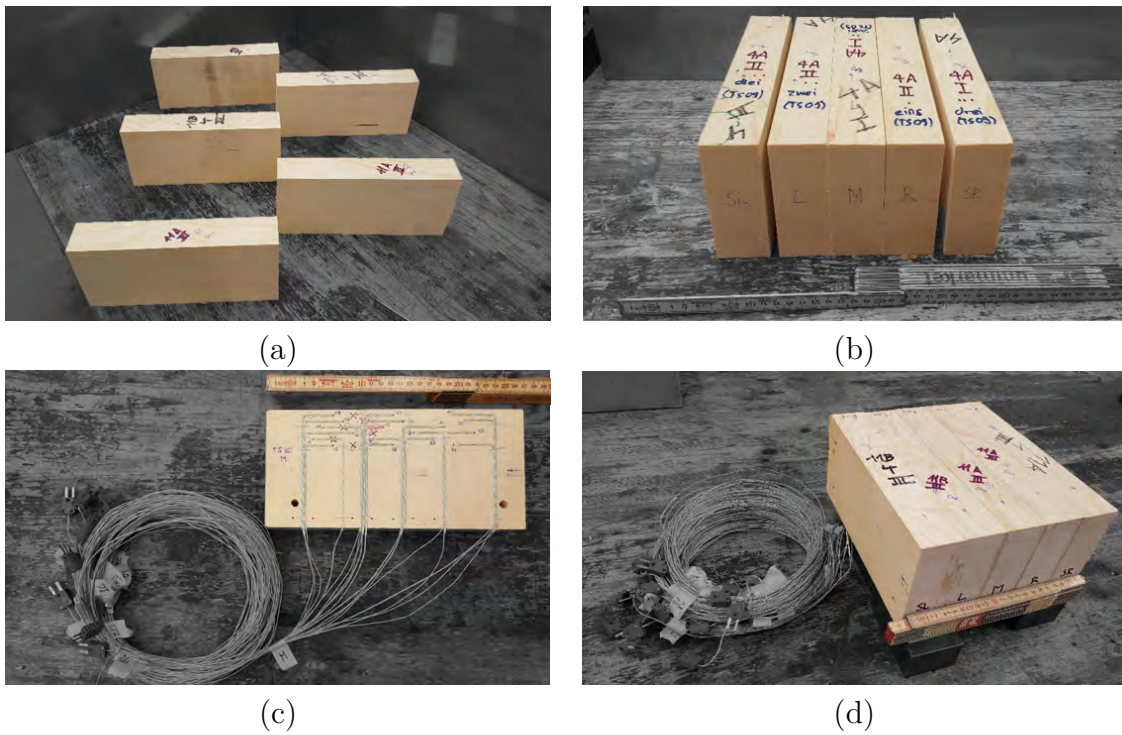
Figure 3.11: Assembling of an instrumented specimen. Beams after planing (a), after selection of clear wood beams (b), after instrumentation (c) and gluing (d). Images by A. Totaro.

	1	2	3	4	5	6	7	8
	Series no.	Series ID	no. of experiments	turbulence [-] ht | mt	$v_{gas,0}$ [1] [m/s] min | max	t_{exp} [min] min | max	$\dot{q}''_{ext}$ [2] [kW/m²] min | max	$\rho_{wood,12}$ [2] [kg/m³] min | max
4	1	CF	6	6|-	1.5|1.5	12|25	25|115	405|500
5	2	MH	7	7|-	2.0|2.5	13|55	35|120	360|630
6	3	TR	5	5|-	2.5|2.5	12|20	50|100	355|465
7	4	DW	4	4|-	1.0|2.5	12|21	75|90	395|445
8	5	AT1	7	7|-	1.0|6.0	20|41	50|100	320|429
9	6	LA	9	9|-	1.0|5.0	12|20	75|120	370|416
10	7	JF	8	1|7	2.5|6.0	20|25	50|100	420|420
11	8	AT2	8	4|2	2.5|5.0	14|20	45|120	420|n.a.
12	9	AH/AS	11	-|11	1.0|5.0	5|20	<5|100	400|485
14	10	FH	8	-|8	1.0|5.0	20|40	<5|100	410|460

n.a.   not available
[1]   rounded (steps 0.5)
[2]   rounded (steps 5)

Table 3.5: Overview of experiments performed in the FANCI setup.

experiment including the distance holders, all cables and sealant tape (if applicable) and installed on the support of the FANCI setup. Various types of support systems were used which allowed to keep the specimen's exposed surface flush in the combustion chamber, see Figure 3.8. Before the start of the experiment, the actual environment (air pressure, room temperature) was recorded. The individual set points are the reference gas velocity above the specimen and the external heat flux controlled by the active current input previously correlated to HFS measurements. Before any experiment, the gas flow at the specimen's surface was re-evaluated by an anemometer and flow modified accordingly. During the experiment, the flow was recorded using differential pressure sensors at the inflow and in the combustion unit, i.e. unites I and III in Figure 3.9. The degree of turbulence during the experiment was recorded using three pressure sensors at the specimen's surface, see Figure 3.12 (a).

For most of the experiments, one to two surface TCs (sheathed TCs) were placed at the surface of the specimens to get an indication of the surface temperature. Although it can be stated that the TCs are obviously affected by the radiation (increasing the apparent temperature at the hot junction) and the gas flow (reducing the apparent temperature at the hot junction), it was evaluated as the most proper way to get an indication of the surface temperature. This type of recording was previously done and evaluated by Tran et al. and Werther [197, 205] and results were used for the estimation of the film temperature in contact with the specimen. Recorded characteristics during the experiments comprise observations, photo and video documentation, temperature recordings of the TCs within the specimen (if applicable), the char layer surface regression and the mass loss. For the temperature recordings of the internal TCs, the system DARWIN was used which recorded temperatures with a frequency of 0.5 Hz. The active current of the heat panel was recorded with a frequency of 1 Hz. The remaining measurements were done with variable frequency depending on their characteristics between 10 Hz (e.g. for the gas temperature and LC readings) and 50 Hz (e.g. for the dynamic pressure above the specimen's surface). The observations included the smoke production, the charring of the surface, the time of ignition, the position of the surface TCs (on the specimen's surface or in formed char layer cracks), the surface regression and the visible extinction of flaming and glowing combustion (if applicable). The experiments were performed with a previously defined external heat flux, the corresponding set point of the heat panel was either set and changed manually during the duration of the experiment or automatically changed in accordance to a previously defined surface temperature (mean of two TCs). The surface of the specimen was adjusted manually to be flush with the combustion chamber's lower surface; the adjustment was made based on an approximated mean loss of the surface. Eventually observed deviations from a parallel surface regression were noted in the protocol of the experiment. When the experiment was terminated, the heat panel and the gas flow was shut down, the specimen removed from the FANCI setup, eventually available TCs cut and the specimen's mass recorded. Subsequently, the specimen was carefully extinguished with water. Finally, the specimen was left for drying and the aluminium coating was removed by a heating fan, see Figure 3.12 (b). Subsequently, the geometry of the specimen was
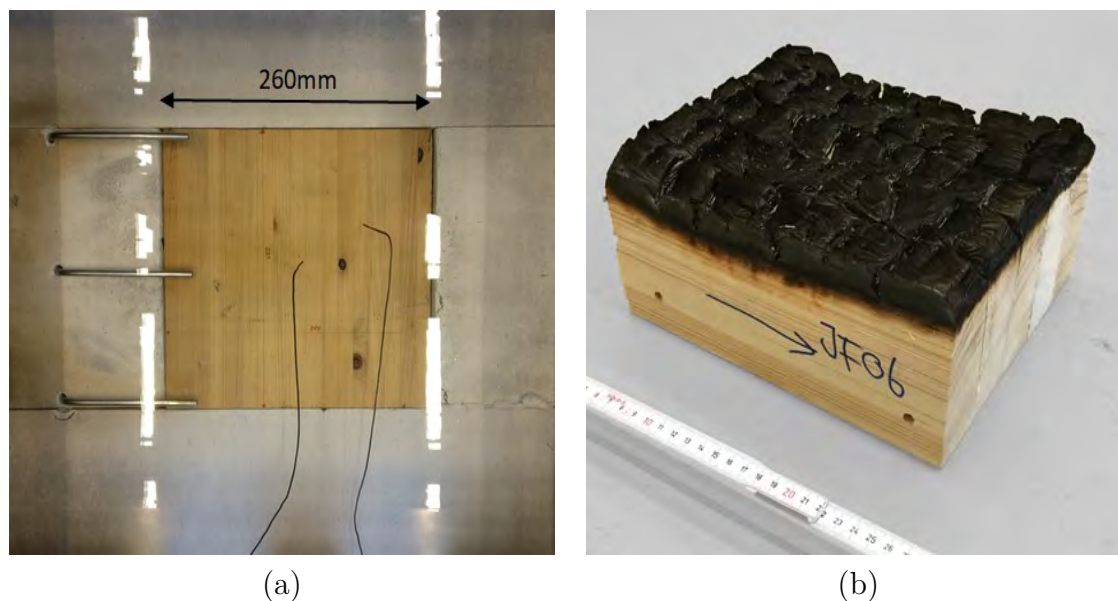
Figure 3.12: Pressure sensors above the specimen (a) and a specimen after exposure (b).

assessed with and without the char layer. In series JF, the specimens were re-conditioned to 12% EMC to determine the mass of the char layer while for other experiments, the char layer mass was determined directly by drying of the collected char layer material.

Several calibration experiments were done with non-combustible specimens which had a HFS, a standard PT, a heat flux PT and a small wire TC installed. Two different water cooled HFS of type Schmidth-Boelter were used to confirm the heat flux estimations using the current. The agreement between both HFS was good and the estimation agreed well with the estimation using the current above 10 kW/m² but poor with respect to the estimation of the current below 5 kW/m².

3.3.4 Results

The results from the HP experiments are the change of the cross section, the mass loss, temperature measurements as function of the gas flow environment (ht and mt) and the external heat flux applied. An overview of the results is provided in Table 3.6. The results are summarised below with respect to the temperature results, the determination of the residual virgin cross section and the char layer regression.

Temperature measurements. For specimens with instrumented beams, the temperature recordings were used to determine the progress of charring during the exposure. For the determination of the charring rate by the temperature readings of the TCs, the location of the 300°C isotherm was estimated individually for every TC exceeding 300°C. In general, at least three TCs in the same depth were installed and used to estimate the
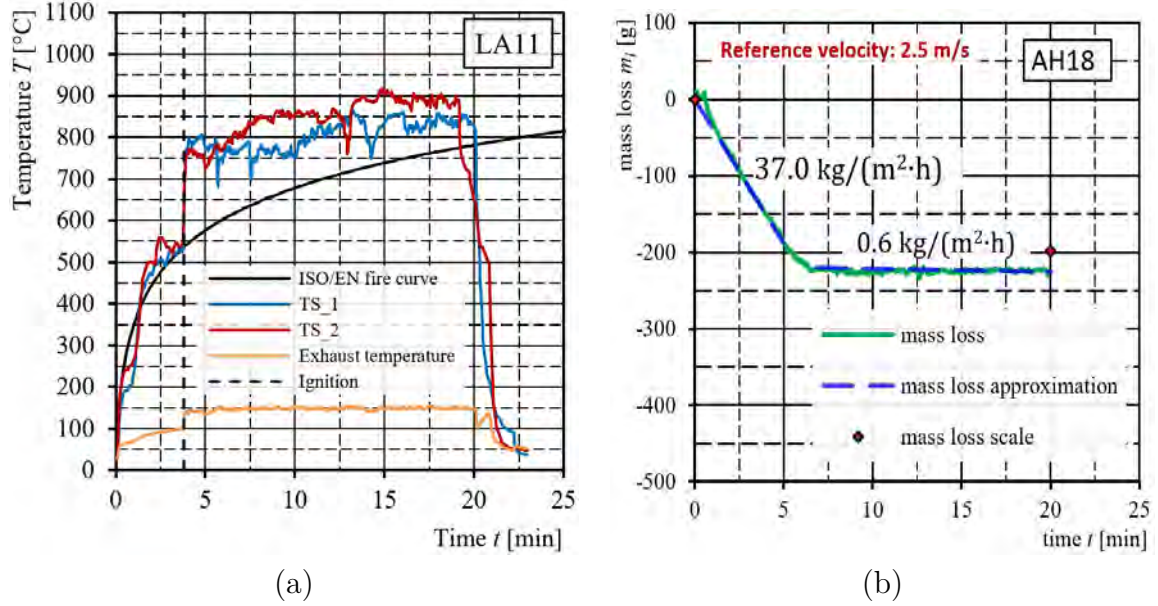
Figure 3.13: Examples of experimental results: Compartment temperatures (a) and mass loss measurements (b). Images by L. Ackermann and A. Hägerli and A. Spichtig.

mean value for the charring time at the default depth of the TCs. Using the inlet and the exhaust temperature, the gas temperature in the compartment was estimated as all three wire TCs in the combustion unit, unit III in Figure 3.9, were clearly affected by the radiation from the radiant heat panel. Together with the surface temperature measurements, they were used to estimate the film temperature as suggested by Wickström [209] using the average of the gas and surface temperature, see Eq. 3.3.

$$T_{fi} = \frac{T_g - T_s}{2} \tag{3.3}$$

where
T_{fi} is the film temperature, in K or °C;
T_g is the gas temperature, in K or °C;
T_s is the surface temperature, in K or °C.

Cross section. The geometry of the specimens was assessed after the experiments to determine the total residual section after exposure, i.e. the remaining virgin section with the attached char layer, and, the virgin section after the manual removal of the charred thickness. The residual cross-section and the remaining virgin cross-section were estimated applying three different methodologies: (i) hand measurements, (ii) manual scanning and manual post-processing and (iii) manual 3D-scanning and automatic post-processing. For (i) and (ii), the envelope above the char layer was estimated intuitively between char
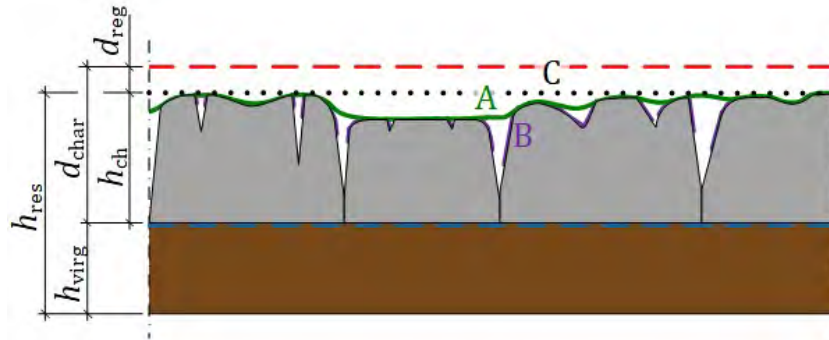
Figure 3.14: Char layer structure with the envelope curve (A), "deep sections" (B) and the effective surface level (c). Other definitions used than in Figure 2.7.

layer pieces above the char layer cracks, see Figure 3.14. For (iii), the median was used to determine an approximate similar result as the estimations of the envelope for the residual section including the char layer.

In the future, for the estimation of the remaining cross-section by 3D-scanning, it is intended to use NURBS (non-uniform rational basis splines) to allow for a more controllable process and avoid the uncontrolled recording of "deep sections" in cracks, see purple marked areas in (B) in Figure 3.14. The "deep sections" result from the 3D-scanning and are dependent on the photographers position from various angles, recognising the cracks to a certain, undefined extent [170]. To limit the falsification of the effective surface level of the char layer by "deep sections", the use of the median value was evaluated and found insignificantly different from the mean value defined by the envelope curve. While manual measurements were performed in the first six series, the techniques were compared with the 3D-scanning in series 7. The deviation between the methods was found to be insignificant. Consequently, in the series 8 and series 9, the estimation of the cross-sections was done without saw cutting only by 3D-scanning. In all series, eventually apparent edge effects were excluded from the estimation of the cross-section's geometry. Regardless of the method, the residual cross section and the remaining virgin cross-section was used to determine the char layer surface regression (rate), the charring depth and rate and, consequently, the thickness of the char layer respectively. For some characteristics, multiple ways for the determination were performed, e.g. the charring by means of TC readings and the residual virgin cross section. In general, a good agreement of the methods was achieved. An example of the estimation of the accuracy of the char layer regression is shown in Figure 3.15 (a) where observations during the experiments are compared to the measurements of the residual cross section including the char layer after the experiment; the measurements obtained after the experiment were considered more reliable and used for further analysis. The char layer surface regression rates determined for all experiments in ht and mt environments are plotted in Figure 3.15 (b).

		1	2	3	4	5	6	7
		Series no.	Series ID	$T_{fi,mean}$[1] [°C] min|max	$\beta_{ch,mean}$ [mm/min] min|max	$\rho_{ch,0}$[1] [min] min|max	$\beta_{wood,mean}$ [mm/min] min|max	Δm [kg/m³] min|max
4		1	CF	165|420	0.3|0.8	n.a.	0.9|1.3	n.a.
5		2	MH	n.a.	0.4|0.9	35|80	1.1|1.8	n.a.
6		3	TR	n.a.	0.5|1.2	n.a.	1.4|1.9	32|58
7		4	DW	255|405	0.5|0.9	n.a.	1.3|1.8	28|47
8		5	AT1	355|560	0.4|1.5	65|90	1.0|2.3	21|44
9		6	LA	390|520	0.3|1.8	45|100	1.2|2.2	29|48
10		7	JF	405|485	0.0|1.8	40|85	0.6|1.4	25|34
11		8	AT2	n.a.	0.4|1.8	50|80	0.5|1.6	29|43
12		9	AH/AS	135|470	0.0|1.8	70|175	0.0|2.0[2]	3|37[2]
13		10	FH	120|230	0.0|1.4	100|220	0.0|0.7[2]	1|3[2]

n.a.   not available
1)   rounded (steps 5)
2)   values for the reduced exposure level given

Table 3.6: Overview of results of the experimental series in the FANCI setup.
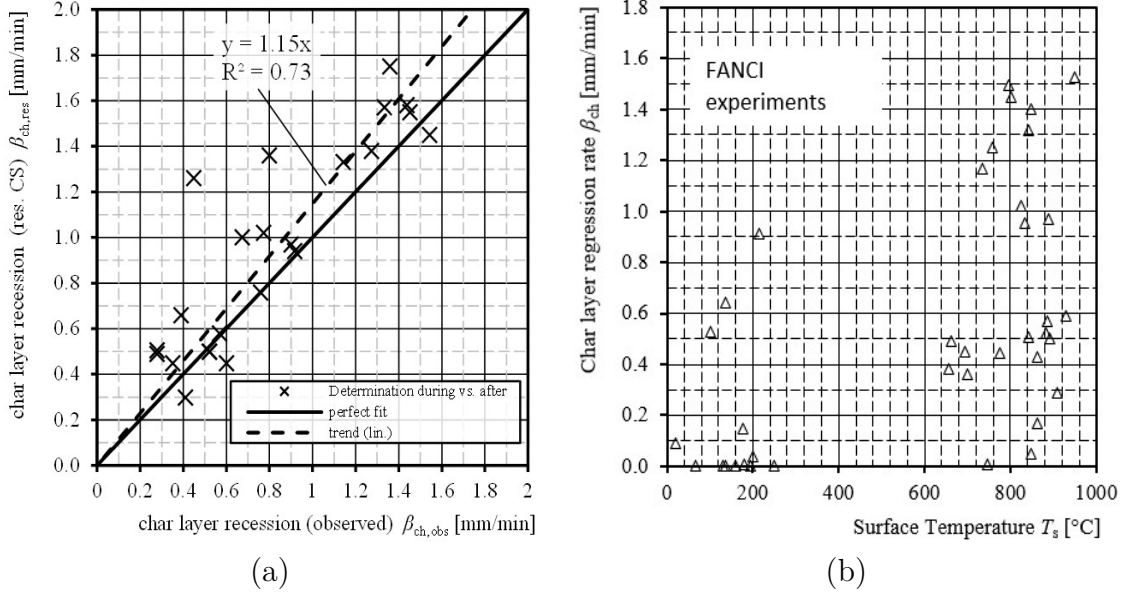
Figure 3.15: Analysis results of the char layer regression. Correlation between the observed rate during the experiment and the determined rate using the residual cross section after the experiment including the linear trend using the least squared method (a) and the correlation with the surface temperature (b).

Char layer density. The density of the char layer (yield) was determined as mean value over the char layer thickness, i.e. a bulk density. The char layer volume V_{ch} was determined as bulk volume using the loss of the total thickness and the residual virgin wood section respectively, i.e. the char layer thickness h_{ch}, and the exposed surface area of the specimen, compare Figure 2.7. By the use of the dry bulk density, the cracks and char layerpockets are taken into account. In contrast to Spearpoint et al. [186], the char layer density is found to be dependent on the thickness rather than a heat flux. The mass of the char layer material was determined either indirectly by the difference of the (re-conditioned) mass of the specimen after removal of the char layer after the experiment and the mass of the original specimen before the experiment, or, directly by drying the char layer material in an electrical oven at 105°C. The dry density of the char layer referring to 0% MC was estimated applying the simple relationships given in Eq. 3.4 and 3.5 respectively. The summary of the density measurements is included in Table 3.6 (Column 4).

$$\rho_{ch,0} = \frac{m_{t=0,12} - m_{virgin,12}}{V_{ch}} \tag{3.4}$$

$$\rho_{ch,0} = \frac{m_{ch,0}}{V_{ch}} \tag{3.5}$$

where

$\rho_{ch,0}$	is the dry bulk density of the char layer, in kg/m³;
m	is the actual mass of the specimen, in kg;
$t = 0, 12$	is the index referring to the specimen at the time before the exposure at 12% MC;
$virgin, 12$	is the index referring to the remaining virgin wood section of the specimen after the exposure at 12% MC;
V_{ch}	is the bulk volume of the char layer equal to $d_{char} \cdot A_{exp}$, in m³.

3.3.5 Main findings

The main findings of the presented experiments concern many parameters which can be utilised for the improvement of future experiments and the estimation of a specimen's contribution to the fire:

- The FANCI setup was capable to describe and isolate relevant characteristics;

- The behaviour of the specimens was different depending on the characteristics of the turbulent environment;

- Depending on the fire exposure conditions a significant char layer surface regression could be observed;

- The char layer density at the end of the experiment varied significantly between about 50 kg/m³ and 200 kg/m³.

- The char layer thickness at the end of the experiment varied between about 5 mm and 20 mm;

- The effect of changed reference gas velocity, i.e. the set-point velocity at the inflow had significant effect on the behaviour of the specimen and the environment in the combustion unit;

- The type of exposure with respect to the standard deviation of the gas velocity had a significant effect on the results; Consequently, the results were grouped in moderately turbulent (mt) and highly turbulent (ht);

- The HFS (Schmidt-Boelter type) delivered measurements which were depending on the imposed gas flow indicating the sensitivity to convective heat transfer;

- The HFS (Schmidt-Boelter type) delivered unreliable measurements in regions below 10 kW/m³ which is of significant interest for the description of the self-extinguishing behaviour;

- The ambient current delivered reliable information for the external heat flux over the complete range applied;

- The PT tested to deliver comparative values to the HFS could deliver reasonable results using modified calibration parameters in the heating phase while in the cooling phase significant deviations to the other measurement techniques were observed;

- Various measurement techniques can be applied for the measurement of the residual virgin section; the use of rulers, manual scanning technique using photographs or scanners or 3D-scanning delivers reliable results. It is recommended to always compare any advanced contactless measurement technique with traditional measurement techniques.

3.4 Investigation of the char layer [2]

The structural fire design in currently available product approvals, e.g. ETAs, and the typical design processes following design standards, e.g. the fire part of Eurocode 5 [35], is based on the evaluation of the load-bearing capacity in standard fire. Limited models are available to determine design fires when a combustible structure contributes to the definition of the particular compartment fire.

Recently, some researchers proposed a fixed fitting factor for ventilation controlled fires in the steady state burning phase and explained the factor with the external combustion [26, 22]. This is consistent with other research where observations during exterior compartment experiments implied that a significant share of the combustible gases created by the pyrolysis combust not in the compartment but at the facade where sufficient oxygen is available, e.g. Maag [117] and first quantifications by Hakkarainen [74]. The fitting factor should not be understood as the combustion efficiency factor when structural timber in significantly involved in compartment fires, normally set to $\chi = 0.8$ [33]. The reduction of the structural fire load to 30% until the maximum compartment temperature is reached is based on the comparison of the HRR prediction comprising of the interior and the structural fire load [22].

The experimental campaign in this Chapter follows an alternative approach, which focuses in general on the energy balance in charring building components and in particular on the formation of a new material, the char layer. The results show that energy is stored temporarily in the char layer until the conditions in the compartment environment allow for a further combustion. In experiments, a representative char layer has been formed, the analysis of this material is presented in this Chapter. A fire exposure of 120 min has been chosen as it creates a char layer thickness of about the same thickness as during an entire fire duration, previously described as damage, see Brandon [22].

---

[2]Parts of this Section are content of a journal publication [180]

3.4.1 Particular research question

The heat content of wood is well researched and a recent approach proposal uses a heat content for "structural timber" to consider its contribution to the fire for members with a typical moisture content of massive timber members in heated indoor environments. Thus, a contribution of structural elements as function of the charring depth can be taken into account as structural fire load, i.e. 7 MJ/m^2 per mm charring depth and a corresponding factor for the HRR. Similar to the approach by Brandon [22], a reduction factor can be applied to allow for the consideration of the combustion characteristics in compartment fires of structural timber in general and in particular of the char layer. However, the approach may be over simplified and relies on the concept of charring rates of the structural timber only. While the charring rates are essential for the calculation of the remaining virgin layer and can be used for the prediction of the load-bearing capacity, they might offer a limited validity with respect to the prediction of the fire dynamics. To solve the fire dynamics, it seems that five major properties are needed:

1. The heat stored in the original material, i.e. the heat content of wood, the moisture content and the density; it can be assumed that this knowledge is available;

2. The conversion rate of wood into the char layer including the creation of combustible, volatile gases as byproduct; it can be assumed that this is described by the charring rate;

3. The regression of the surface (char recession or surface regression); limited information is available with respect to this point, thus, this property is studied in another part of this study, see Chapter 3.3;

4. The heat stored in the thermally modified layer, the created char layer; i.e. the heat content of the char layer and the density; barely no information is available with respect to this point.

Answering the bullet Point 4 of this list is the particular research content of this Chapter, i.e. (1) the density and (2) the heat content to draw conclusions about the heat content of the char layer to increase the knowledge in this area and contribute to the knowledge about the fire dynamics in compartments with structural timber.

3.4.2 Material and equipment

In total, six spruce beams were selected from a stock of spruce beams which has been stored in the climate room at ETH Zürich at 65% RH to reach an EMC of 12%. The beams were machine planed, manually cut and edgewise glued with one-component polyurethane adhesive to create two STP specimens with an exposed timber surface of 200 mm × 390 mm (length × width). The beams which had been selected for the analysis after the fire exposure, b18 and b47, had densities of 445 kg/m^3 and 454 kg/m^3, respectively.
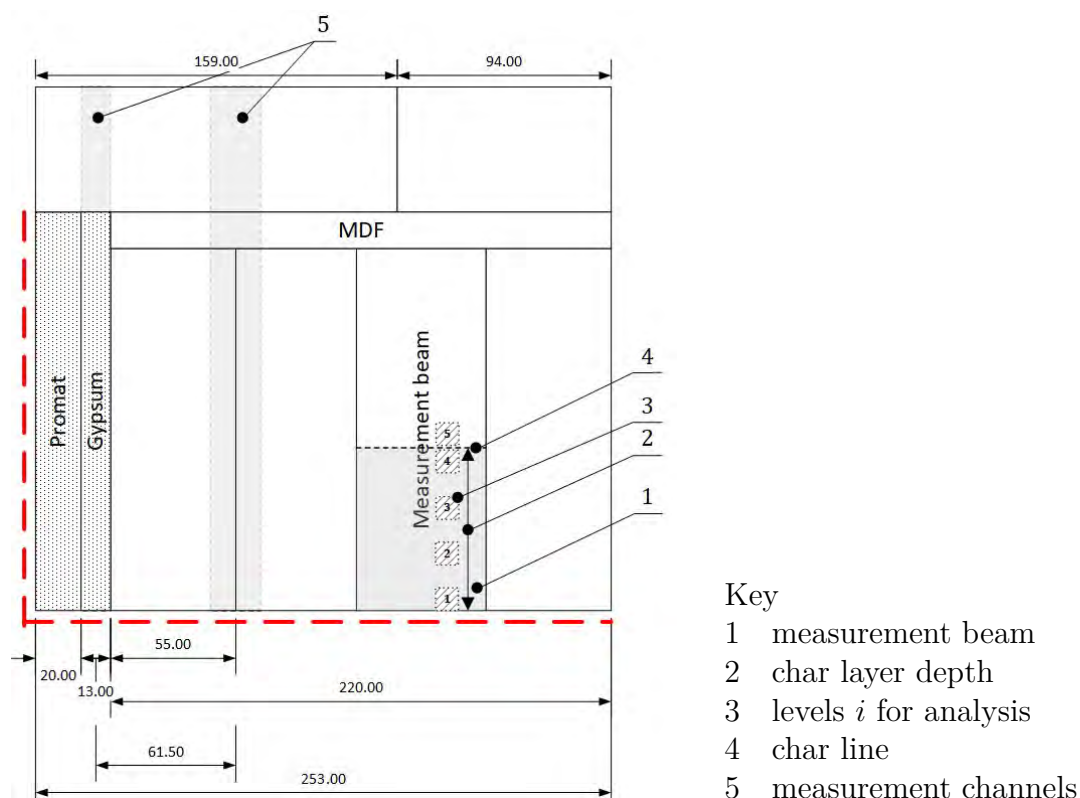
Figure 3.16: Cross section of specimens BC1 and BC2 (dimensions in mm). Own figure.

The timber specimen was protected on one side by a double layer gypsum based fire protection system and on the other side by a CLT panel, which analysis was content of another study, a drawing is provided in Figure 3.16. Both specimens were designed with two vertical channels to allow the installation of a pitot tube and a bi-directional pressure sensor at the exposed surface.

3.4.3 Methods

Initially, the two specimens were fire exposed, subsequently material was prepared for the analysis. The analysis comprised the preparation of representative levels distributed over the depth of the char layer, the density measurements and, finally, the bomb calorimetry analysis. All three steps are described in the following.

Fire exposure of the specimens. The horizontally arranged specimens were standard fire exposed on their lower side at in an oil fired model scale fire resistance furnace on two consecutive days at MPA Stuttgart. Directly after the fire exposure of 120 min, the furnace was turned off, the specimen removed and carefully extinguished with water and transported to ETH Zürich where the specimens were disassembled.
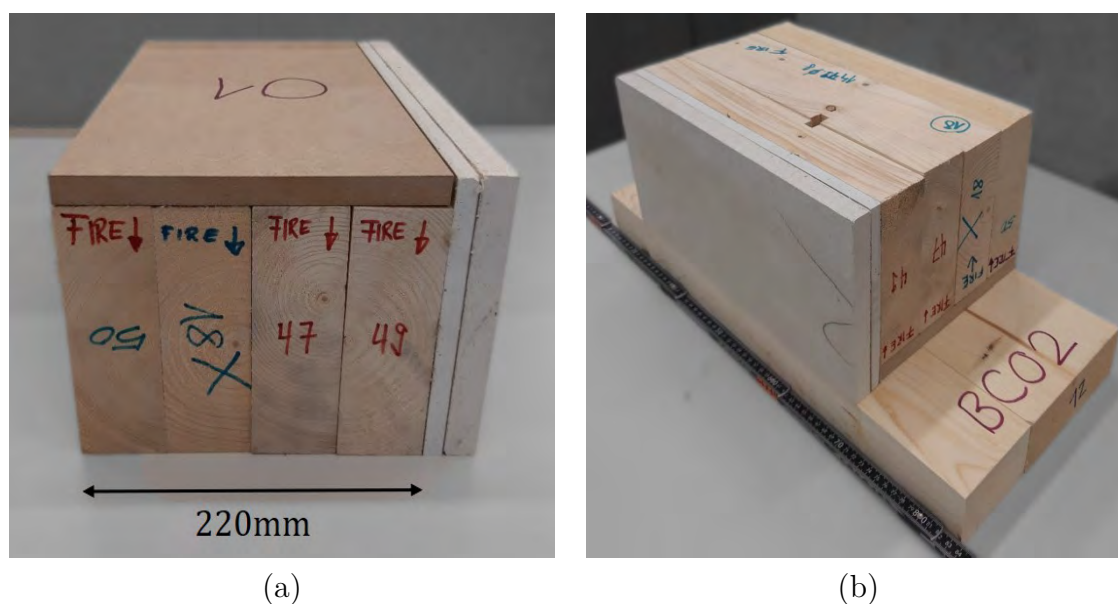
Figure 3.17: Specimen BC1 (a) and BC2 (b) under assembly. Images by F. Hirzel.

Preparation of the sample material. The previously selected beams were cut out of the specimens, cautiously placed in a frame and returned to the climate room where they were dried from extinguishing water until they reached mass equilibrium indicating an EMC of 12% in the section of the virgin wood. The length sections showed a typical variation of the charred surface, the char line, char expansion and char recession and the occurrence of cracks and voids, see Figures 3.18 and 3.19 (a). For the further analysis sample material was defined in five levels considering the challenging extraction process of the char layer. Five levels with sufficient depth and distance were defined over the char layer depth, see Figures 3.16 and 3.19. Level $i = 1$ had a variable thickness; lost volume due to char recession or increased volume due to char expansion was included in this level. The blade thickness used in the cutting process of 0.65 mm was considered in the extraction procedure and the actual thickness of the levels of 10 mm was checked for the mixed levels $i = 4$ and $i = 5$, see Figure 3.20. The accuracy of the procedure was evaluated as sufficient as the mean of four measurements per level was about 9.9 mm. After cutting, sample material was collected in glass containers and left in an electrical oven (Salvis A.G. Luzern) at 105°C for drying, see Figure 3.20. The sample material was used to measure the bulk density and to produce samples for the heat content analysis. In addition, the dry density of the virgin wood sections, i.e. beyond level $i = 5$, was determined to 404.9 kg/m^3 (BC1-b18) and 397.6 kg/m^3 (BC2-b47).

Besides the material obtained from the specimens BC1 and BC2 further char material was included in the campaign. Char material originated from the HP experiments in the FANCI setup described in Section 3.3, a full-scale furnace experiment performed at VTT (Finland) and reference char production in a muffle kiln was included. Furthermore,
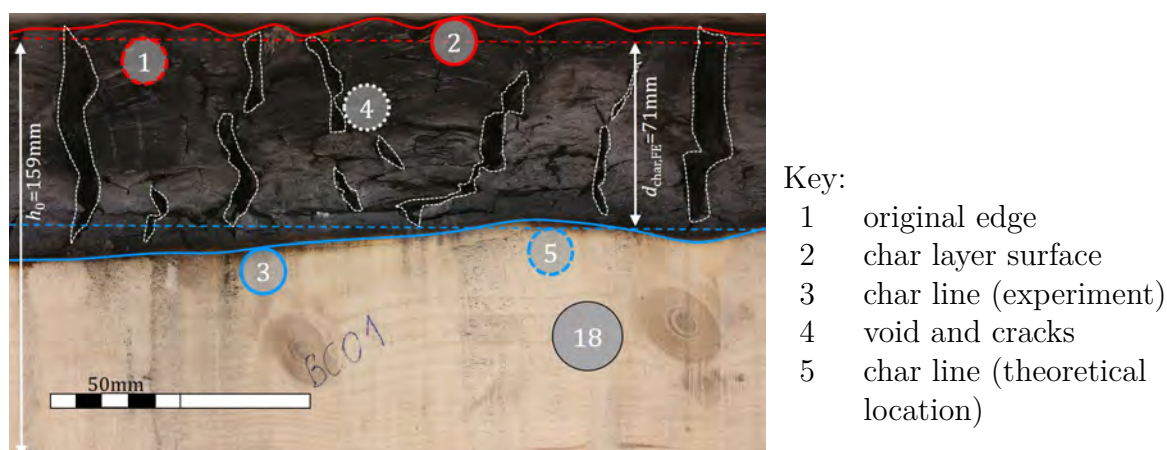
Figure 3.18: Length section of beam 18 (specimen BC1) after fire exposure. Own image.

uncharred reference material from leftover material was prepared. As the other material of BC1 and BC2, it was stored at 105°C for drying.

Production of reference char material. This part of the analysis comprised the production of char layer from the material previously used to determine the density of the levels. A muffle kiln was used to produce char layer from the wood material as done in an industrial process; two series were done. In CP0, the set-point temperature was set to 275°C, subsequently, the compartment temperature increased within hours to approximately 300°C indicating the exothermic reaction within the samples. The samples of series CP1 were of levels $i = 1$ to $i = 4$ with a dimensions 145 mm × 53.5 mm × 10 mm. The samples were individually wrapped in aluminium foil to limit the oxygen access and to allow for easier handling in the monitored pyrolysis process. The sample material was marked inside with paper cuts as the marking was expected to disappear in the heating process. For the production of the reference material, series CP1, the set point of the muffle kiln was chosen slightly lower in the beginning. Initially, a set-point temperature of 230°C was held constant for 48 h, but further increased after the checking of the material's characteristic as the material had still a significant resistance against breakage by hand. The set-point temperature was increased in steps to 275°C, see Figure 3.22 (b). After about five days, reaching about 57% of the dry mass, the sample L1 was investigated further. Breakage by hand was possible in both directions, i.e. cross and lengthwise with respect to the fibre direction. The colouring of the material was in general charred black with some red reflections. After re-packing, all samples were re-inserted in the muffle kiln. The pyrolysis process was terminated when the mass loss indicated a mass loss relative mass of 45% (relative to the standard density with 12% EMC) was achieved. After the production of the charred reference material, the samples of series CP1 were stored in the drying furnace at 105°C. Exemplary, reference material of level $i = 3$ was selected for further analysis of the heat content of series CP1. On the day of the bomb calorimetry
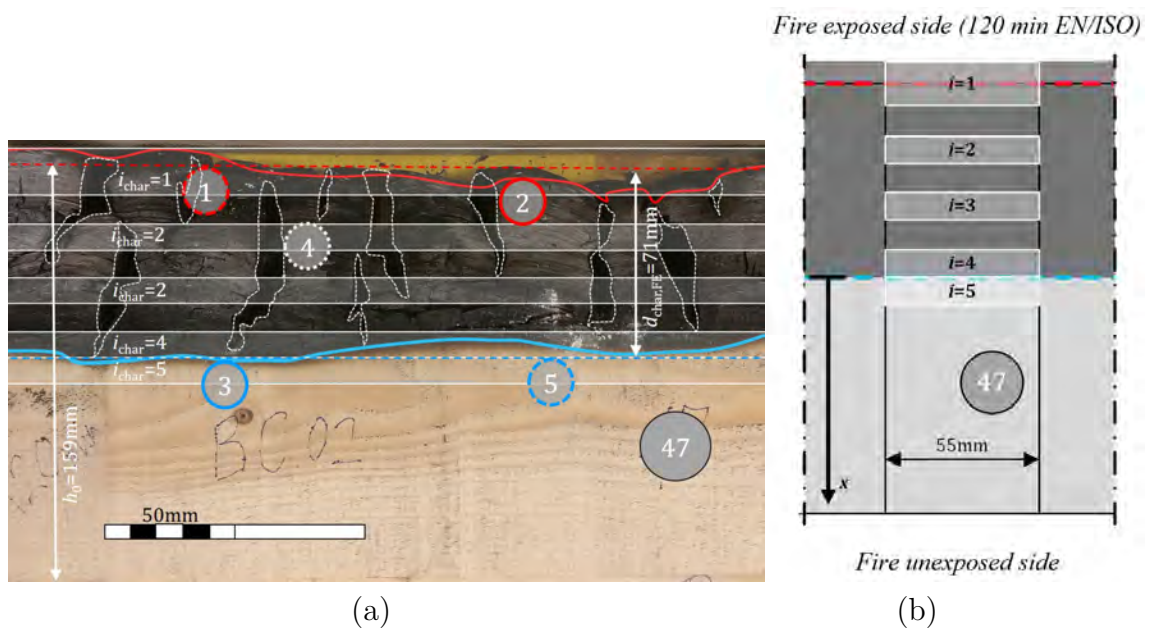
Figure 3.19: Length section of beam 47 (specimen BC2) after fire exposure; key as in Figure 3.18. Own images.
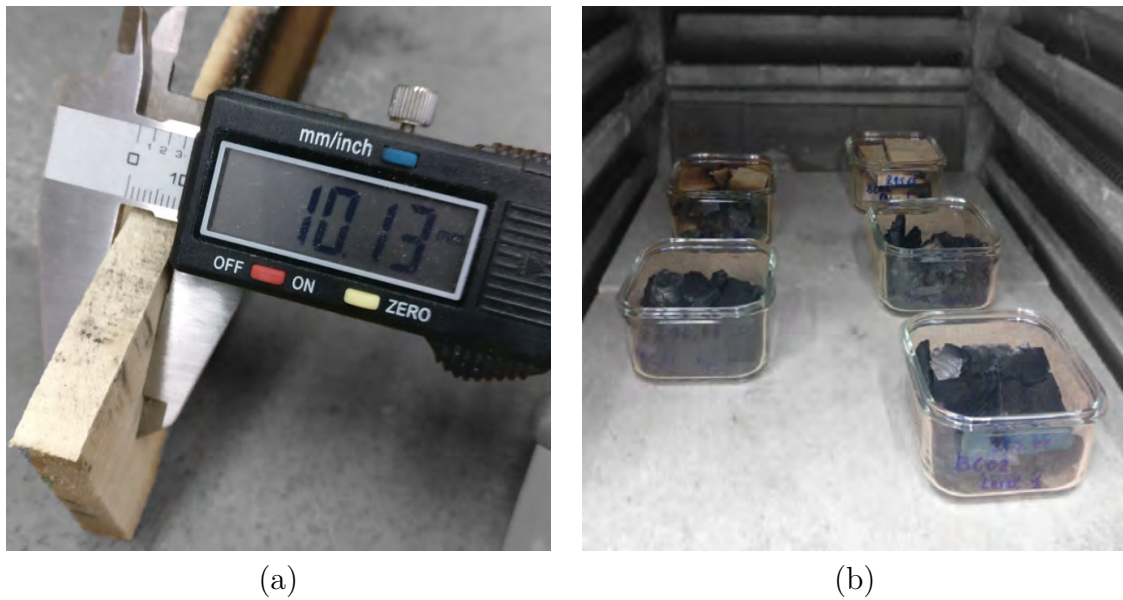
Figure 3.20: Verification of the default thickness of the mixed level $i = 5$ (a) and drying storage of the sample material in an electrical oven (b). Own images.

analysis, the material CP1-L3 was transported to the lab in a sealed container and a tested in triplicate as the other material.

Bomb calorimetry. After constant mass conditions were achieved in the drying process, bomb calorimetry analysis was conducted with all selected sample material to derive the heat content (UHV) of the char layer. The analysis was performed at ETH Zürich using two quasi-adiabatic bomb calorimeters. The oven dried sample material was transported in the sealed containers to the chemistry lab where the analysis was performed. For the analysis, the sample material was carefully blended in the container and moved to a porcelain mortar where the material was crushed and blended again. For samples including wood from levels $i = 4$ and $i = 5$ and for the reference wood material, sample cubes with about 1.0 g were used without any further preparation (e.g. pestling, pill production). The char material in powder form was filled in two gelatin capsules. The filled gelatin capsules were then placed in the combustion cup, see Figure 3.21 (a). A fuse wire was brought in contact with the sample in the cup and inserted in the stainless steel bomb, see Figure 3.21 (b), which was closed and charged with oxygen. Subsequently, the bomb was inserted in de-ionised water at about room temperature. After reaching an approximately constant temperature, the bomb was electrically ignited and the following temperature rise was measured until no further temperature increase was detected (ca. 600 sec). A typical temperature increase was about $\Delta T = 1.5$ K. About 90 samples were analysed including the calibration runs with the gelatin capsule material as compound to assess the heat capacity of the bomb calorimeter system, C_v, later used in the determination of the sample's heat content. For the gelatin capsules, a combustion energy of $\Delta_c U = -18.23$ kJ/g [126] was considered. Exemplary, a temperature graph of a bomb calorimetry test is shown in Figure 3.22, complementary data is given in the associated IBK report [165].

3.4.4 Results

The results from the analysis of the levels of the previously fire exposed specimens are the density and the heat content. The results are summarised below.

Density. The results of the analysis refer to the theoretically derived location of the char line following the levels shown in Figure 3.19 (b). The results comprise the bulk densities of the levels located in the char layer and the partly decomposed level $i = 5$ which is located directly beyond the char line and can be expected that it exceeded 200°C. In general, the relative average bulk density of the charred levels $i = 1$ to $i = 4$ was determined to 26% and 23% of the dry density of the source material for BC1-b18 and BC2-b47 respectively. The density of the level $i = 5$ heated above 200°C was determined to 92% and 80% of the dry density of the source material for BC1-b18 and BC2-b47 respectively. The results for the determination of the bulk density (absolute and

(a)

(b)
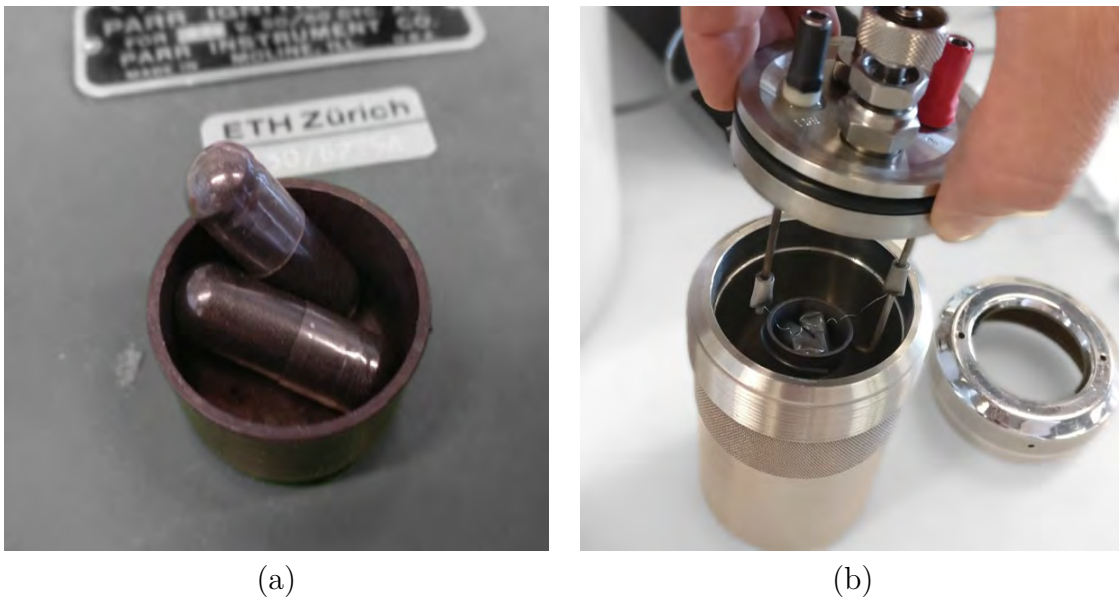
Figure 3.21: Filled gelatin capsules in a combustion cup (a) and inserting the prepared sample in the bomb (b). Own images.

(b)
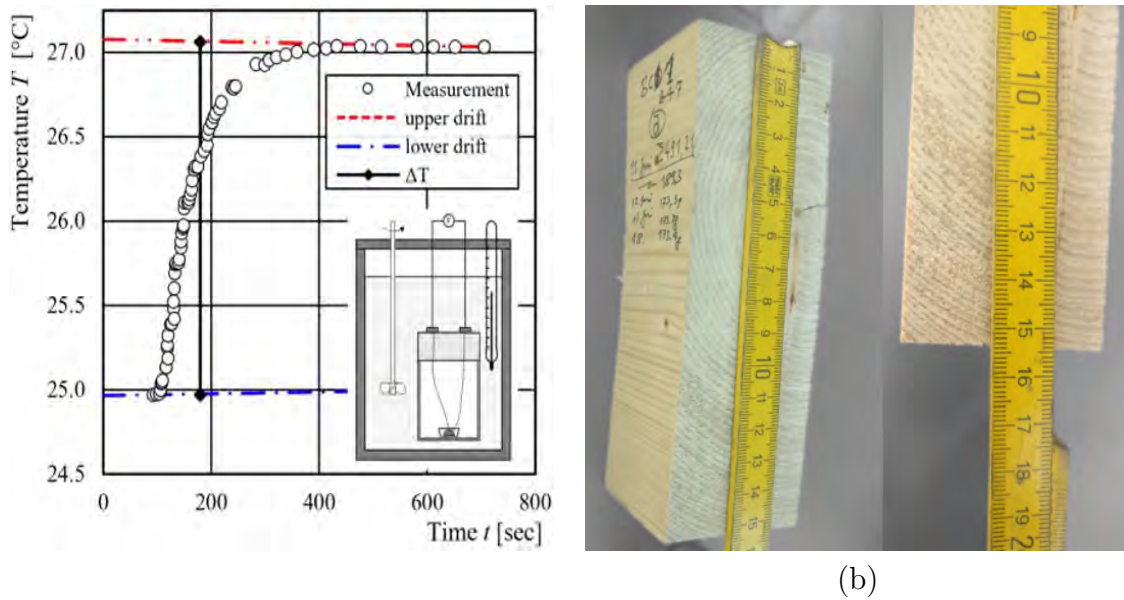
Figure 3.22: Example of the evaluation of the temperature rise of bomb calorimetry readings (a) and the dried reference material (b). Own figure and image.

Level i		1	2	3	4	5	remaining virgin section
experienced temperature[1]		>300°C (charred levels)				<300°C	<200°C
BC1-b18	absolute [kg/m³]	94.6	89.0	79.3	205.6	363.9	397.6
	relative [-]	0.24	0.22	0.20	0.52	0.92	1.00
BC2-b47	absolute [kg/m³]	53.0	104.3	104.4	156.5	324.7	404.9
	relative [-]	0.13	0.26	0.26	0.39	0.80	1.00
mean	absolute [kg/m³]	73.8	96.7	91.9	181.0	344.3	401.3
	relative [-]	0.18	0.24	0.23	0.45	0.86	1.00
mean	relative [-]	0.28				0.86	1.00
		0.20				1.00	
		0.40					1.00

[1] according to the temperature predictions (FEM simulations)

Table 3.7: Absolute and relative bulk densities (0% EMC) for all levels of specimens BC1 and BC2 and the virgin wood beam.

Level i	1	2	3	4	5	mean
Determined dry density (0% EMC)	395.0	386.1	372.3	385.6	371.2	382.1
relative density ($\frac{\rho_i}{\rho_{mean}}$) [-]	1.03	1.01	0.97	1.01	0.97	1.00
Calculated standard density (12% MC)	442.4	432.5	417.0	431.9	415.7	427.9

Table 3.8: Determined and calculated densities [kg/m³] of the reference material (five levels) made from b18.

relative) are given in Table 3.7, absolute values are plotted in Figure 3.23 (a), the density profile determined in this analysis shows results significantly different from zero near the fire exposed edge. Apparently, this is in contradiction to the BEC-model following the suggestions in Eurocode 5 [180, 35], the material properties communicated by Law et al. [111], see Figure 2.6.

The reference density of the levels of the fire exposed specimens was determined by means of reference material from leftovers from the production of specimens BC1 and BC2. Remaining cuts from the beams b18 and b47 were oven dried at 105°C and the dry density measured. The cutting process was performed similar to the process described above but the process was less critical due to the undamaged material. The thickness of the five levels (mean 9.98 mm; 16 measurements) was checked after the manual cutting process with the band saw. For the determination of the reference densities of the levels, see Table 3.8, the default volume at 12% EMC was taken into account.

Series	Experiment type	n	H_u	STD
		[-]	[MJ/kg]	
BC	Model scale (furnace MPA)	28	29.64	3.09
model-scale	Model scale (furnace VKF)	3	29.93[1]	-[2]
full-scale	Full scale (furnace VTT)	1	33.00	-[2]
bench-scale	Bench scale (heat panel setup)	6	29.24	0.63
CP	Muffle kiln	3	24.52	-[2]
[1] one outlier excluded				
[2] not determined due to low number of samples n				

Table 3.9: Average heat content and further details of analysed series.

Heat content. The average heat content of the all char specimens was 30.24 MJ/kg (STD 2.76 MJ/kg, $n = 37$), the average heat content of specimens of the level $i = 5$ directly below the char line was determined to 21.35 MJ/kg (STD 0.31 MJ/kg, $n = 3$) and the heat content of the uncharred source material (location level $i = 1$,i.e. 10 mm thick material at the fire exposed edge of beam b18) to 19.86 MJ/kg (STD 0.88 MJ/kg, $n = 6$). The results of the char specimens included six samples of heat panel experiments (series 10 in Section 3.3) which were exposed initially to a high exposure level followed by an exposure to allow extinction at various gas flows (reference gas flow 1 m/s and 5 m/s) whereby results were corresponding to the char samples from series BC. Results from the series CP1 (char production in a muffle kiln; material taken after 8 days) were significantly less, see Table 3.9. The results for the heat content agree very well with the corresponding values for char layer reported in the literature, see eg. Francis [56]. The average heat content of the series CP-1 was determined to 24.5 MJ/kg (average) significantly lower than for the samples produced from material which has been exposed to standard fire, compare Table 3.9.

3.4.5   Main findings

The main findings of the presented experiments concern many parameters which can be utilised for the improvement of future experiments and the estimation of a specimen's contribution to the fire:

- The methodology presented in this Section worked well to describe and isolate relevant characteristics;

- The char layer proved to be a sensitive structure during the cutting process, moist cutting (applied in Section 3.5) could improve the procedure;

- The char layer exhibited a mean density (yield) between 8% and 28% of dry wood for different specimens;
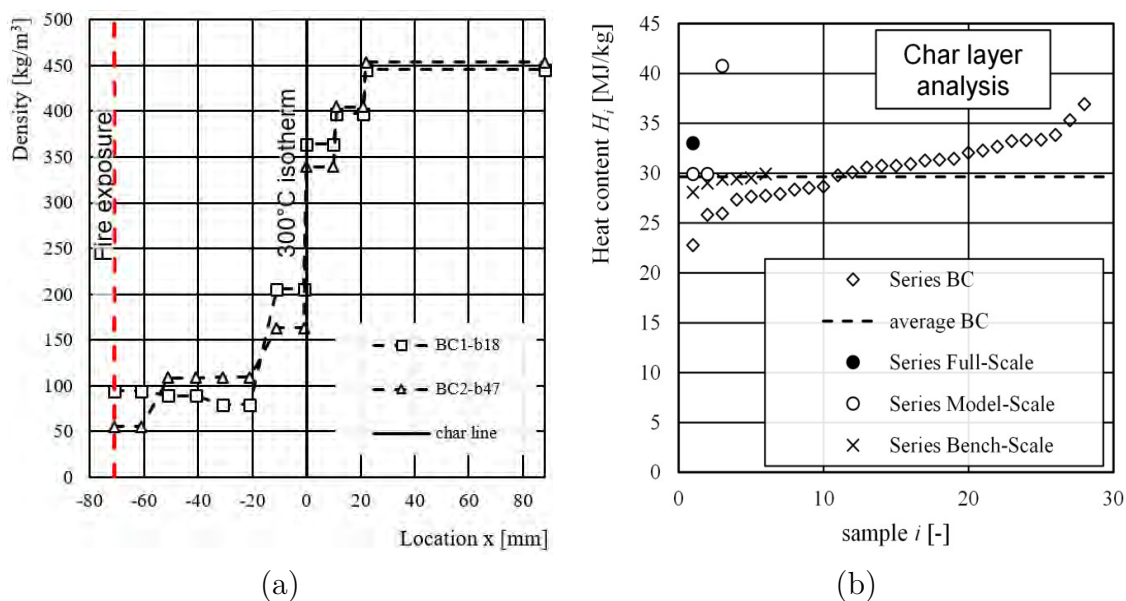
Figure 3.23: Derived density profiles of BC1-b18 and BC2-b47 as specified in Table 3.7 (a) and derived heat content (char only) of the bomb calorimetry for all results as summarised in Table 3.9 (b). Own figures.

- The char layer analysed in details (mean density 28%) exhibited a density profile ranging between about 15% and about 50% with respect to the dry wood material;

- The virgin wood level directly below the char line exhibited a reduction of the density which could be lumped to the char layer;

- The heat content of the char layer was in the range of industrially produced char coal, a heat content (for the dry material) of about 31 MJ/kg was determined;

- The heat content of samples analysed in this campaign did not vary with respect to the origin, char layer material from furnace tests and heat panel experiments delivered similar results.

3.5 Behaviour of structural timber in compartment fires

One model scale compartment experiment was performed at ETH Zürich with a compartment made from CLT. The experiment CI 30 was performed by the team of IBK and led by M. Kleinhenz, the author of this thesis was involved in all design steps and was responsible to contribute with tasks that fit the purpose of this thesis. During the experiment, the structural timber was left unprotected on all five surfaces to allow for

the creation of a char layer in a real fire created by the wood crib used to represent the movable fire load, by the structure and the ventilation through to the single opening. The fully developed fire was terminated manually after about 30 min.

3.5.1 Particular research question

In Section 3.4, the char layer was investigated with respect to its heat content and its density which are essential elements of the fire dynamics of compartments where timber structures are involved. This input will be later used for the development of the TiCHS-model, see Chapter 6. The char layer material used for the analysis of the heat content presented in Section 3.4 was taken from furnace tests and experiments and from the FANCI experiments which exhibit a significantly different fire exposure. In the analysis, no char layer material originated from a compartment fire. Thus, a compartment experiment was initiated to complete the picture with respect to the origin of the char layer material. Besides the measurements presented here, further recordings were taken, among others, the mass loss, the temperature distribution in the compartment, the heat conducted away from the compartment through the incombustible floor, the location of the neutral height in the ventilation opening, the flame height and the gas velocity at the ceiling and the rear wall in the compartment.

3.5.2 Material and equipment

A cube with edge length of 500 mm was designed with an opening share of about 40% of the face wall. The enclosure was designed with five elements of 120 mm thick CLT elements with a symmetrical layup of layers with an individual thickness of 40 mm. A lintel of about 100 mm was designed to allow the accumulation of hot gases near the ceiling. The wall elements were arranged with their outer layer in vertical direction. With the exception of the reveal and the exterior surface above the ventilation opening, all surfaces remained unprotected. A wood crib with a floor area of 240 mm × 240 mm with 12 full layers of 5 sticks each was designed and located in a rear corner of the compartment. The wood crib (2.4 kg) was designed for a free burning time of about 11 min, a pre-test resulted confirmed about 14 min duration measured from the placement of the fire starter under the crib. The density of the CLT panels used was determined to about 465 kg/m^3 at 10% MC. The MC of the CLT elements was measured to 10% at the day of the experiment.

Three load cells were arranged under a frame which formed the incombustible base layer of the compartment together with a double layered mineral based building board. Between the 20 mm thick boards, two wire thermocouples were located (installation: laid-in). A TC tree was installed in the centre of the compartment comprising of nine thermocouples, see Figure 2.13 (a). Centric on the ceiling and the rear wall bi-directional velocity probes similar to the one proposed by McCaffrey et al. [122] with an outer diameter of 12 mm were installed to measure the dynamic pressure and determine the gas
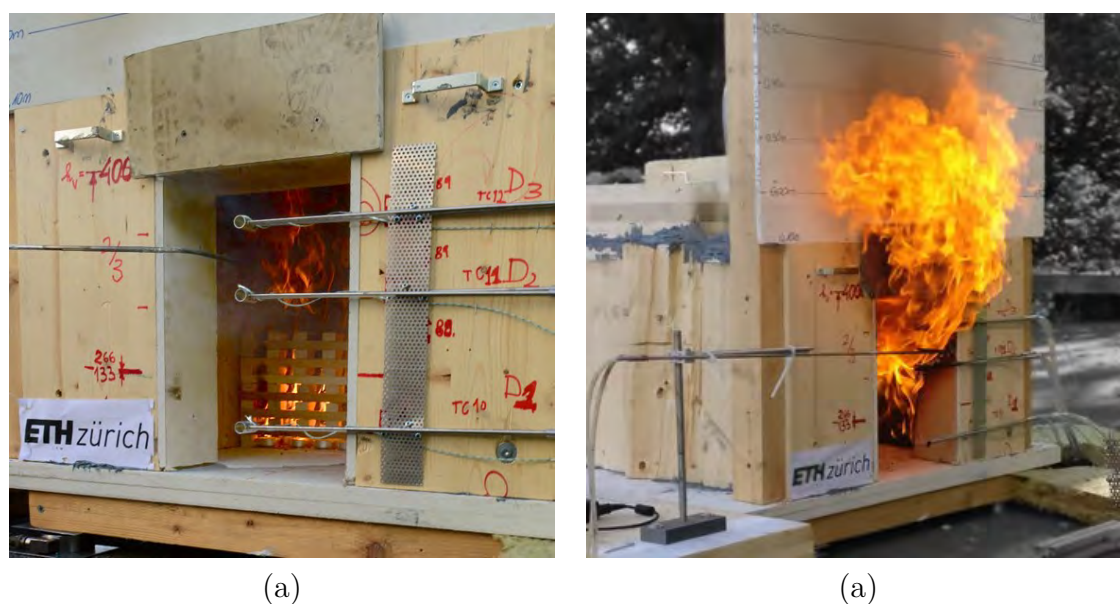
Figure 3.24: Wood crib short before its complete ignition at about 3 min (a) and fully developed fire at about 6 min after ignition of the wood crib (b). Own images.

velocity at the corresponding surfaces. Three further bi-directional velocity probes were positioned in the expected in- and outflow section of the ventilation opening while for the detection of the neutral layer a manually guided dynamic pressure probe was used.

3.5.3 Experiment

The experiment was performed in open space on a day with very low wind speeds (predicted max. wind speed 3 m/s; measured wind speed <1 m/s) and with an exterior temperature of about 17°C. For ignition, a custom-made igniting device was used, which allowed the utilisation of all continuous vertical channels of the wood crib. It took about 3 min to ignite the entire crib, 30 s later, the first flames appeared exterior of the compartment. After the full burning of the crib, the compartment fire grew and reached flashover within about 3 min. Subsequently, significant exterior flaming was observed, indicating a ventilation controlled fire, see Figure 3.24 (b). After 32 min, measured from the ignition of the crib, the experiment was manually terminated. The timing was chosen to prevent falling-off of charring layers. A custom-made water spray extinguisher was used to terminate the fire. In the following, the compartment was disassembled on site and the successfully accomplished extinguishment verified. Then, the CLT elements were transported carefully to the workshop where they were cut for further analysis of the charred sections.

3.5.4 Analysis

All holohedral CLT elements were selected for the analysis of the cross section with respect to the residual virgin section thickness, the char layer thickness and its density respectively. Cross section specimens were taken from the elements to estimate the progress of the charring with respect to the geometrical char layer properties and its mass. By default, three specimens were taken from all four CLT elements. For the right wall, further specimens were cut from the top and bottom of the wall, i.e. specimens RB and RT. The numbering followed the expected gas flow direction during the fully developed fire, see Figure 3.25. The cutting process was performed manually using a band saw. In total, 14 specimens were cut for further analysis; all sections exhibited a charred, outer layer comprising two adjacent lamellae including one gap. In a first step, the geometry of the specimens was recorded manually with a sliding caliper and a ruler, see Figure 3.25 (b). The mean values of the recordings were used for the analysis of the section dimensions. This analysis comprised the measurements of (1) the residual virgin wood thickness, (2) the total remaining section thickness and (3) the area of the specimen, by default 133 mm × 170 mm. Using (1), and the original thickness of the CLT, the charring depth d_{char} was assessed. Using (1) and (2), the thickness of the char layer h_{ch} was determined. Subsequently, the char layer was removed manually, all char material collected in aluminium containers and the material dried at 105°C for three days until mass consistency was achieved. After removal of the char layer, the measurements of the residual virgin wood section was confirmed randomly for three specimens to exclude potential errors of the char line detection when the char layer was attached.

3.5.5 Results

The results presented here are those obtained by the analysis described in Section 3.5.4 which cover elements analysed for the associated research question of this PhD thesis only. The summary of the measurements, grouped for the specimen's location with respect to the height is given in Table 3.10. Results show a charring behaviour with a typical range $d_{char} = 23.1 \pm 3.7$ mm. The significant span is due to the minimum and maximum values detected in the bottom (RB) and the lower wall regions (L1). The reduced charring in the regions of the compartment's edges are clearly visible comparing the mean results for the specimens RT and RB, $d_{char,T+B} = 19.8$ mm with the mean of the wall specimens, $d_{char,walls} = 23.5$ mm. The density of the char layer was determined using the actual charring depth of the particular specimen and reached between 22% and 26% of the estimated dry wood density of the source material (423 kg/m³).

The readings of the TC tree in the compartment was used to follow the temperature development in the compartment, see Figure 3.26 (a). The average compartment temperature exceeded 300°C at about 2 min and 600°C at about 6 min; neglecting the lowest TC, the latter level would be exceeded 20 s earlier which is about the time when exterior flaming was observed. It should be noted that the lowest TC in a height of about 30 mm
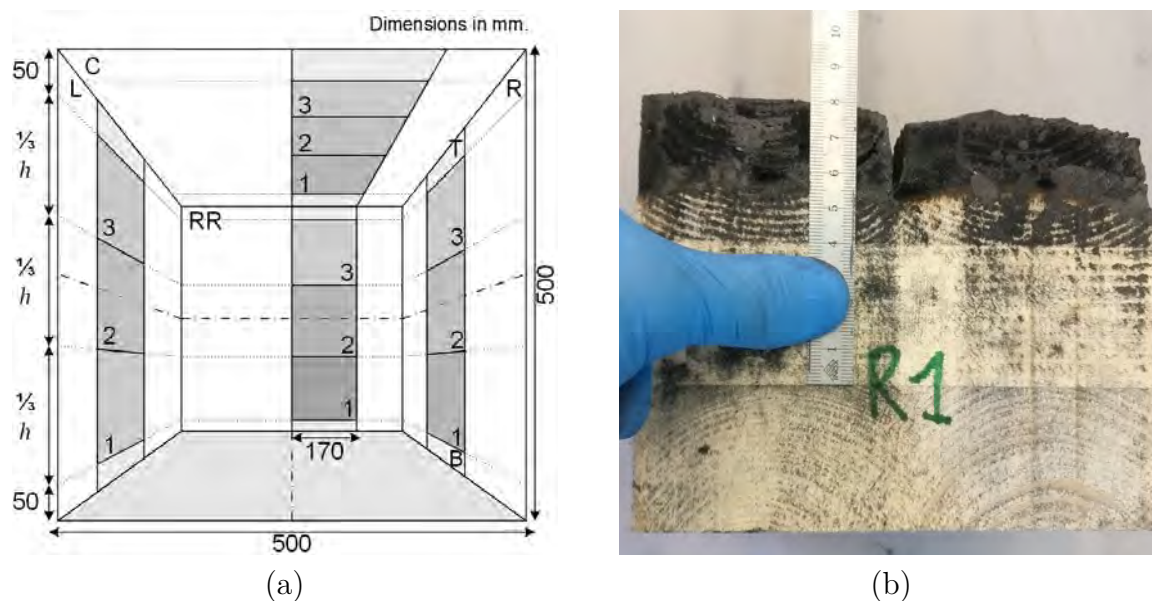
Figure 3.25: Location and identifier for the specimens (a) and section of specimen R1 (b). Own images.

reaches temperature levels of the TC positions in the upper region of the compartment. From this observation, it can be concluded that a nearly uniform temperature distribution is reached deviating from full-scale compartment experiments where the lower region thermocouples remain about 100 to 200 K below the upper region's TCs [190]. Consequently, it should be observed that compartment experiments of various scales should be compared with care. The compartment, similar in its geometry to those tested by Gorska [67], exhibited slightly lower temperature close to the ceiling, see readings for TC9 (20 mm below the ceiling surface; grey curve) in Figure 3.26 (a). The reduction of the temperature in the upper region was previously linked by Gorska to the creation of a significant amount of gases created from the pyrolysis of the structural timber. Consequently, Gorska proposed the use of a three zone model for compartments with exposed structural timber. In the experiment presented here, the amount of structural timber reached a maximum possible value, i.e. about 230% of the floor area. Observing the limited difference between the temperatures of the top region (TC9), the observation can not be supported. The TCs in between the base layer boards experienced a temperature increase of about 300 K showing a significant heating of the incombustible floor. This is in contrast to the assumption of some calculation model to exclude the floor surface from the enclosure surface [196]. As the TCs schow significant heating of the floor, it contributes to the reduction of the heat in the compartment as suggested in Eurocode 1 [34]. In Figure 3.26 (a), the total mass loss is shown which was determined to 13.06 kg.

A simplified energy balance can be developed utilizing the input presented here. Using the average charring depth of about 24 mm and the density of the structural timber,

Location	d_{char} [mm]	h_{ch} [mm]	d_{ch} [mm]	$\rho_{ch,0}$ [kg/m³]
ceiling	24.1 ± 0.7	24.4 ± 0.9	<0	101.3 ± 6.3
RT	21.4	27.6	<0	n.a.
wall 3	23.6 ± 0.7	25.9 ± 1.2	<0	103.5 ± 0.4
wall 2	23.2 ± 1.3	25.3 ± 0.6	<0	96.6 ± 4.4
wall 1	23.8 ± 1.3	22.4 ± 0.9	1.4	90.5 ± 3.7
RB	18.1	15.8	2.3	n.a.

n.a.   not available

Table 3.10: Average values for charring depth d_{char}, char layer thickness h_{ch}, char layer surface regression depth d_{ch} and dry density of the char layer $\rho_{ch,0}$.

the CLT panels, of 465 kg/m³ at 10% MC, the default heat content of dry wood of 17.5 MJ/kg, the contribution to the fuel load due to the wood crib can be determined to about 40 MJ while the charred wood volume and corresponding mass respectively would result in an total energy amount of 180 MJ. However, using the default heat content of the char layer of 31 MJ/kg determined in Section 3.4, the contribution of the structural timber reduces to about 100 MJ which corresponds to an structural fire load density related to the exposed timber surface of 3.5 MJ/m² per mm char layer depth or about 45 kW/m². This value for the smouldering contribution is similar to the value reported by Rezka [151, 20]. Thus, the contribution by smouldering is at the upper limit of the wide range of previously communicated results, see Section 2.3.36. The released total contribution by the structural timber is 2.5 times higher than of the movable fire load but only 55% of the energy when only the charring depth would be considered. This energy balance is further developed in the TiCHS-model, see Chapter 6. The determined gas velocities are plotted in Figure 3.26 (b); on average, the ceiling and the rear wall experienced similar gas velocities, i.e. about 2.0 m/s.

3.5.6   Main findings

The main findings of the presented experiment concern many parameters which can be utilised for the improvement of future experiments and the estimation of a specimen's contribution to the fire:

- The experimental setup presented in this Section worked well to describe and isolate relevant characteristics;

- The fire development was significantly extended by the structural timber surfaces;

- The gas flow distribution in the ventilation opening could not be holistically described with three sensors only;
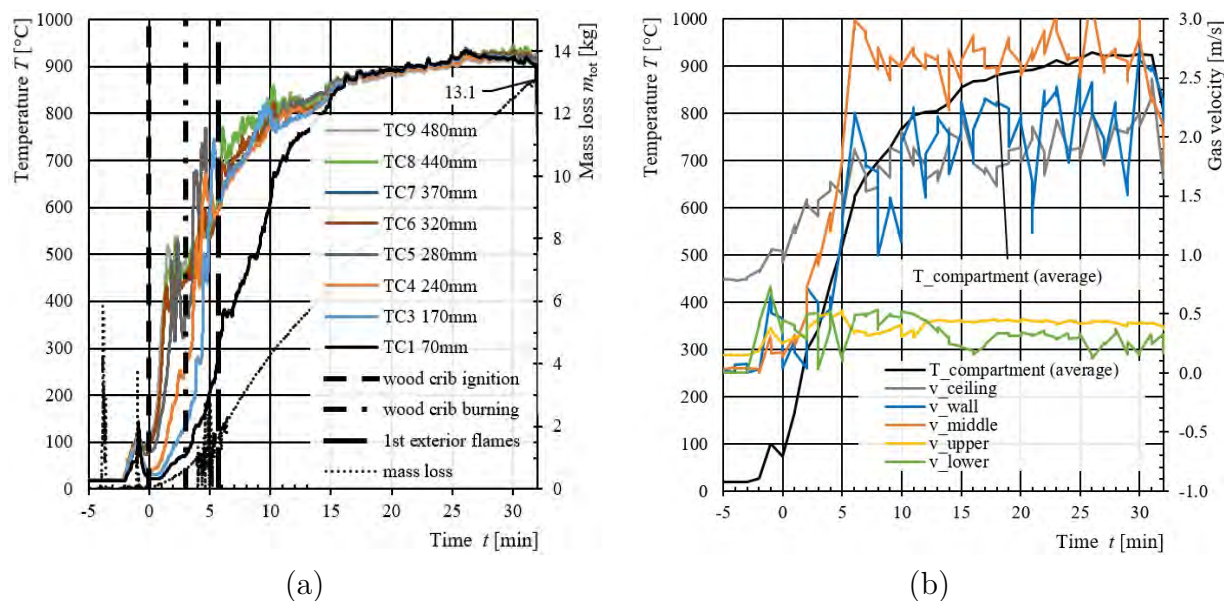
Figure 3.26: Temperature development in the compartment including the mass loss (a) and the estimated gas velocities at the five positions (b). Own figures.

- The gas flow near the surfaces of wall and ceiling was determined to be about 2.0 m/s;

- The char layer exhibited densities between 20% and 26% of dry wood;

- The char layer in the lower wall, mid-height and upper region had mean densities of approximately 90 kg/m^3, 95 kg/m^3 and of 105 kg/m^3, respectively, while the mean for the ceiling was about 100 kg/m^3.

- Using the default heat content of the char layer determined in Section 3.4, on average, the structural timber surfaces delivered a contribution to the fire of 45 kW/m^2 by the char layer combustion (derived by the decay of the material).

3.6   Summary of this Chapter

Four experimental campaigns have been conducted and are presented in this Chapter. The experiments were conducted (1) in fire resistance furnaces, (2) in the costume made FANCI setup using an electrical quick response heat panel, (3) in a fire resistance furnaces with extended analysis including a bomb calorimeter focusing on the char layer formed and (4) in a small scale compartment with exposed structural timber. The directly determined results are given in the particular Sections of this Chapter. The results are used in the following, to estimate the different behaviour of combustible and non-combustible products in fire resistance furnaces, see Chapter 4, and, to develop a timber charring

and heat storage model, see Chapter 6. The most important results of this Chapter were the heat flux measurements in the furnaces using a HFS at various locations and positions which were in accordance to those determined by the PT, the characteristics of the furnace environment with respect to the oxygen measurements and the related gas velocities near the specimen's surface, the char layer densities and the heat content of the char layer material. In accordance to the procedures presented in this Chapter, for future experiments and tests in the research field of fire dynamics of compartments with exposed structural timber, it is highly recommended to highlight the need to estimate the characteristics of the char layer, especially its mass and its thickness throughout the duration of the experiments.

Chapter 4

Thermal exposure and fire exposure of structural timber [1]

---

[1]Parts of this Section are content of (journal) publications [162, 167, 176, 174, 173, 179]

4.1 General - Acknowledgement of contributions

This Chapter was a result of many activities within the framework of COST FP1404 (`www.costfp1404.com`) including intense discussions with Prof. L. Bisby, Prof. U. Wickström and experts from other universities and institutes, especially N. Werther at TU Munich (Germany) and D. Brandon, D. Lange and J. Sjöström at RISE (Sweden). Their support in one or other ways is kindly acknowledged as well as the support from the team at IBK, ETH Zürich including the master students T. Rizzi, M. Hächler and D. Werlen who executed some comparison modelling and experiments together with the author of this thesis.

4.2 Overview of the topic

Recently, the standard fire resistance testing has been questioned for combustible products as the thermal exposure may be (1) different due to the combustible surfaces leading to surface flaming and (2) different from that in compartment fires [110]. Today's fire resistance test methodologies were already developed before 1900 based on experience with ad-hoc testing of various building components made from various building materials including timber [83]. After a standard time-temperature curve was found, it was later related to fire loads available in compartments, which would be consumed in a fire for domestic buildings after about one hour [84]. While in fire resistance testing, in Europe, the plate thermometer is used to describe the thermal exposure, in fire safety engineering, preferably heat flux sensors (HFS) are used.

This part of the thesis compares available data with complementary data of experiments performed by the author and the group at IBK Zürich. The comparison focuses on the thermal exposure of combustible and non-combustible building components, the usage and technical background of the PT and the HFS to measure heat fluxes in fires and similarities and differences of furnace environments to compartment fire environments.

4.3 Methodology

As the literature with respect to fire resistance or fire safety engineering focuses often on non-combustibles, fire experiments in fire resistance furnaces with timber floor specimens were studied and compared to measurements of experiments with non-combustible specimens. The experimental campaign comprised initially unprotected specimens with a combustible surface (specimens C) but, further, a specimen with a non-combustible surface (NC). Looking at building materials, timber (specimens) exhibit a low material density (ld) compared to non-combustible building materials like concrete specimens, taken in the following as reference, show a comparably high density (hd). In the experimental campaign, specimens C and NC with ld and hd were included, temperatures and

heat fluxes were analysed at and near the surface of specimens with its lower side fire-exposed in a fire resistance furnace following established rules given in EN 1363-1 [37]. However, the tests were performed as experiments, i.e. with additional measurements to serve scientific purposes rather than testing for certification. Measurements from PT and TC temperature sensors and of a HFS at two locations (variation of the horizontal coordinate) and various positions (variation of the distance to the fire-exposed surface; variation of the vertical coordinate) were compared with each other. The oxygen concentration is considered relevant for flaming combustion and seems to require special consideration in the current discussion. Consequently, the oxygen concentration in the furnace at various positions including the exhaust was measured as oxygen would be essentially needed for the combustion when a combustible specimen is fire-exposed. Furthermore, the fuel consumption was assessed by the measurements of the furnace fuel and the mass loss of the timber specimens. For complimentary reasons, the theory of heat transfer from a fire compartment was studied with focus on timber in comparison to concrete to define the "thermal exposure".

4.4   Limitation

In this Chapter, the question of the thermal exposure in standard fire test furnaces is answered and the thermal exposure in fire resistance testing furnaces is linked to typically ventilation controlled post-flashover fires. Thus, this Chapter focuses on the fire dynamics of (furnace) compartments rather than the load-bearing or separating function in the fire situation. Further, other important characteristics as the fire spread, growth and cooling phase including the change of the fire duration is not investigated here.

4.5   Introduction - Scope of this chapter

Fire resistance tests are used today to provide comparable measures of building products' response to fire with respect to several functions such as separating or load bearing functions. Tests on structural elements are standardised based on its purpose, for example walls, floors, beams or columns. In general these are pass/fail tests performed to assess the fulfilment of acceptance criteria expressed as a certain fire duration, e.g. 60 min, with optional specification documents for extended application. The thermal load is controlled by a temperature sensor to follow a so-called standard time-temperature curve defined in e.g. EN 1363-1/ISO 834-1 (referred to EN/ISO in this thesis) or ASTM E119 [5, 37, 85]. Besides the slight difference of the curves, see Figure 2.2, the type and number of control devices are different for the two standards. While EN/ISO used a standardised insulated metal device (plate thermometers, PT) for controlling thermal exposure, the corresponding ASTM standard requires for thermocouples in a protection tube. Without specifying the use of it, the ASTM standard recommends in addition to record the fuel consumption

for any test. The fuel consumption to fire the furnace is less when testing combustible products compared to non-combustible products. This became obvious during the renaissance of fire resistance tests with combustible specimens in the last years after the successful introduction of cross-laminated timber (CLT) as solid timber floor or wall elements on the market. Fuel consumptions of an oil-fired furnace are given in Figure 4.1. In Figure 4.1, tests with solid timber products analysed further in this study are indicated with round markers. Most likely based on this different amount of fuel needed to follow the standard fire time temperature curve some have recently concluded that the thermal exposure of CLT is different in fire resistance tests compared to non-combustible products [110]. As fire resistance testing is an essential element in the current framework of fire resistance it is important to follow up the comments which is done in the following.
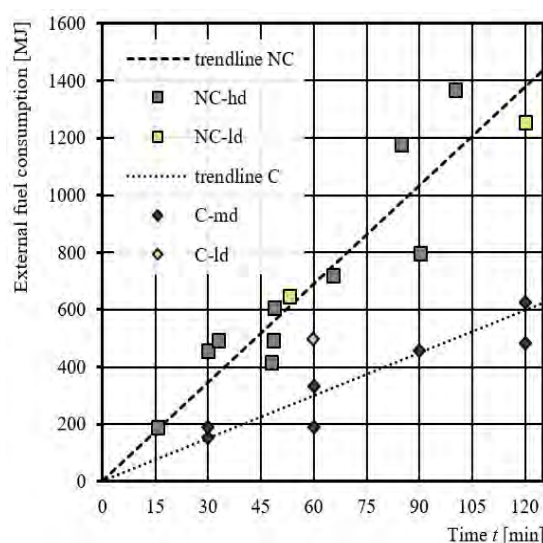
Figure 4.1: The burner fuel used by the VKF furnace to follow the EN/ISO temperature (external fuel) with different types of specimens: Combustible (C), non-combustible (NC), high density (hd) and low density (ld) specimens. Own figure.

4.6 The definition of heat transfer and heat flux measurements in fires

In this Section, the theory of the incident heat flux, the absorbed heat flux and the heat flux measurements is summarised. In addition, appropriate thermal boundary conditions and its use in fire engineering are briefly presented and special consideration is given to the fire resistance testing environments and wood (based) products in particular. Further, typical values in the literature are given which are later used in the analysis for comparison of the experimental results obtained in the corresponding campaign.

The thermal exposure is sometimes used in the literature without giving a clear definition. In the literature, the expressions "fire exposure" or, apparently more general, "thermal exposure" are frequently used to describe the accidental loading case "fire", which needs to be addressed for most structures independently of the building material [34]. Both terms seem to be well accepted within the field of fire safety engineering, but it often remains unclear what the mentioned heat fluxes refer to and which thermal boundary conditions are valid assumptions; although apparently very important, the SFPE Handbook [81] does not deliver a definition for the term thermal exposure. Some literature is available discussing a similar term, the thermal load, e.g. [148].

While heat transfer within a solid, i.e. conduction, is a comparatively simple problem that can be solved applying appropriate material properties that vary with its temperature, the heat transfer from air to a solid is of more complex nature. If a solid's surface is exposed to a heat source, e.g. a fire, the heat transfer from and through a gas to a solid is to be solved. This problem is of increased complexity but essential for fire safety engineering [209]. In the following, the conduction, radiation, convection and the thermal boundary conditions are presented before the terminology is widened for an approach to define "thermal exposure".

Conduction. Conduction is the heat transfer within a solid and is defined as transmission of heat through a solid from places with higher temperature to places with lower temperature [81]. This heat transfer can be described using the Fourier's law of heat conduction. The law for one-dimensional conduction along the axis x (depth) can be written in differential form as

$$\dot{q}''_{cond} = -k \frac{\delta T}{\delta x} \tag{4.1}$$

where
$\dot{q}''_{cond}$ is the rate of conductive heat flux per unit area, in W/m^2;
T is the temperature, in K;
x is the distance normal to the solid's surface, in m;
k is the thermal conductivity of the solid, in W/(m $\cdot$ K).

In structural engineering, the response of the structure to a fire is of great interest. The strength of structural materials correlates with the increase of the material's temperature. Thus, structural engineers focus often on the determination of the temperature distribution within the structural member, the solid. For timber, a building material consisting of several chemical compounds such as lignin, cellulose and water, thermal modelling is often done using so-called effective material properties. These properties are typically obtained by calibration to a certain heating rate, an exposure scenario. Thus, these effective material properties are not automatically appropriate for other heating rates than those used for the calibration. For example, the fire part of Eurocode 5 [35] gives thermal material properties originally calibrated backwards from temperature measurements in timber members exposed to standard fire [105]; the application using deviating heating

rates is not restricted but it remains unclear if the application is justified. However, these effective material properties for timber are considered valid for (initially) protected timber, i.e. when a timber member is indirectly fire-exposed through a fire protection system, e.g. a gypsum plasterboard. In the case of an encapsulated timber member, in a fire, the protected but heated timber surface receives a reduced heating rate - or heat flux - and would definitely experience heating deviating from standard fire exposure. The comparison of fire test results with initially protected timber members and simulations using effective material properties given in Eurocode 5 resulted in a good agreement as shown e.g. by Tiso et al. [195].

Convection. The heat exchange from a gaseous substrate, e.g. air, and the surface of a solid is called convection. To allow heat transfer due to convection a difference between a surface temperature and its surrounding gas temperature is needed. The (local) heat flux due to convection to the surface can be described as
temperature and its surrounding gas temperature is needed. A local heat flux due to convection can be described as

$$\dot{q}''_{conv} = h_c \left(T_g - T_s \right) \tag{4.2}$$

where

$\dot{q}''_{conv}$ is the rate of convective heat flux per unit area, in W/m^2;

h_c is the convective heat transfer coefficient, in $W/(m^2 \cdot K)$;

T_g is the gas temperature, in K;

T_s is the surface temperature, in K.

It should be noted that all variables in Eq. 4.2 are typically variables changing with time. The convective heat transfer is significantly dependent on the material's (thermal) properties as the surface characteristics influence the heat transfer coefficient. The surface temperature is depending on the material of the solid as significant heat may be conducted away from the surface to the cooler parts of the solid. For fire-exposed timber, it should be noted that the calculation of the heat transfer coefficient h_c in Eq. 4.2 may be a difficult task, considering the geometrical changes (shrinking and cracking of the surface). A further challenging task is the prediction of the surface temperature, which might be affected by invisible smouldering combustion of the char layer; flaming combustion may cause further influence of the surface depending on the flame geometry and the orientation of the surface. The determination of the heat transfer coefficient h_c should take into account the characteristics of the gas flow over the surface in contact with the gaseous environment (e.g. laminar or turbulent flow, natural or forced convection). Depending on the flow characteristics, consideration should be further given to the specimen's length with respect to the gas flow.

The convection can led to a significant convective heat flux into structural elements if the envelope, i.e. the surface temperature of the enclosure elements of a compartment is significantly cooler than the gas, i.e. the gas temperature, within the compartment.

During the fully developed phase of a compartment fire this could for example occur if the envelope of the compartment is highly thermally conductive, e.g. made from metal. In contrast, for inert envelope materials the difference between the gas temperature and the surface temperatures is usually small and convection usually does not play a significant role. Timber might be considered as an insulating material, and with the formation of a char layer, the insulating characteristics increase further. Indicative surface temperature measurements, presented in Chapter 3, show that the surface temperature of fire-exposed timber in a furnace experiment is about the control temperature of the furnace. Consequently, in this case, the assumption of the control temperature at the surface of the solid is justifiable.

Radiation. The exchange of thermal energy by radiation does not require any (gaseous) material between the emitting and receiving object, the radiation is transferred by electromagnetic waves [81, 209]. When an object inhibits a temperature higher than 0 K it will emit radiation. In general, any object may simultaneously absorb and emit radiation. The upper boundary of the emitted radiation, or, the emitted radiant heat flux origins from a perfectly black body and is given by the Stefan-Boltzmann law:

$$\dot{q}''_{emi,max} = \sigma \cdot T_r^4 \tag{4.3}$$

where
$\dot{q}''_{emi,max}$ is the rate of emitted radiant heat flux of a black body per unit area, in W/m^2;
σ is the Stefan-Boltzmann constant, $5.67 \cdot 10^{-8}$ in W/(m$^2 \cdot$ K^4);
T_r is the incident black body radiation temperature, in K.

To consider the actual emitting body, the emissivity $\varepsilon < 1$ can be introduced to consider that only a fraction of the black body's radiant heat flux will be emitted:

$$\dot{q}''_{emi,ef} = \varepsilon \cdot \sigma \cdot T_r^4 \tag{4.4}$$

where
$\dot{q}''_{inc}$ is the rate of emitted radiant heat flux per unit area, in W/m^2;
ε is the surface emissivity, in FSE, typically between 0.7 and 0.9 [209];
σ is the Stefan-Boltzmann constant, $5.67 \cdot 10^{-8}$ in W/(m$^2 \cdot$ K^4);
T_r is the incident black body radiation temperature, in K.

In general, the incident radiant heat flux arriving at a receiver's body surface is the sum of a single or multiple emitting bodies with their individual emissivity, typically different surface orientations and radiation temperature. Thus, introducing a view factor (sometimes referred to as configuration, shape or angle factor), the incident radiant heat flux can be defined considering the surface's characteristics with respect to the emissivity and a view factors to:

$$\dot{q}''_{inc} = \varepsilon_i \cdot F_{j-i} \cdot \sigma \cdot T_r^4 \tag{4.5}$$

where

$\dot{q}''_{inc}$ is the rate of incident radiant heat flux per unit area, in W/m^2;

ε_i is the surface emissivity of the body i , in FSE, typically between 0.7 and 0.9;

F_{j-i} view factor from surface j to surface i;

σ is the Stefan-Boltzmann constant, $5.67 \cdot 10^{-8}$ in W/(m$^2 \cdot$ K^4);

T_r is the incident black body radiation temperature, in K.

For further information about the view factors, corresponding literature should be consulted, e.g. Wickström [209]; for simplicity reasons, the view factor is not further discussed and set to unity in the following.

Absorbed radiant heat flux. The absorbed radiant heat flux by a solid's surface is a fraction of the incident radiant heat flux defined in Eq. 4.5. Introducing an absorptivity α for a surface correspondingly to the emissivity ε, the absorbed radiant heat flux can be defined as:

$$\dot{q}''_{abs} = \alpha \cdot \dot{q}''_{inc} \tag{4.6}$$

where

$\dot{q}''_{abs}$ is the rate of absorbed radiant heat flux per unit area, in W/m^2;

α is the surface absorptivity, in FSE, typically between 0.7 and 0.9;

$\dot{q}''_{inc}$ is the rate of incident radiant heat flux per unit area, in W/m^2.

The net radiant heat flux to a surface. The net radiant heat flux to a surface is equivalent to the sum of the counteracting flows of the absorbed radiant heat flux by the surface and the emitted radiant heat flux from the surface. Considering the Kirchhoff's identity, i.e. the absorptivity and the emissivity of a surface can be assumed equal, the heat balance at the surface can be expressed to define the net radiant surface to a solid's surface:

$$\dot{q}''_{rad} = \dot{q}''_{abs} - \dot{q}''_{emi} = \alpha \cdot \dot{q}''_{inc} - \varepsilon \cdot \sigma \cdot T_r^4 = \varepsilon \cdot \dot{q}''_{inc} - \varepsilon \cdot \sigma \cdot T_r^4 \tag{4.7}$$

and finally

$$\dot{q}''_{rad} = \varepsilon \cdot \left(\dot{q}''_{inc} - \sigma \cdot T_s^4 \right) \tag{4.8}$$

where

$\dot{q}''_{rad}$ is the rate of the net radiant heat flux per unit area, in W/m^2.

ε is the surface emissivity , in FSE, typically between 0.7 and 0.9;

σ is the Stefan-Boltzmann constant, $5.67 \cdot 10^{-8}$ in W/(m$^2 \cdot$ K^4);

T_s is the surface temperature, in K.

It is worth having a closer look at the black body radiation temperature used in the equations above and in particular in Eq. 4.5. Assuming two different radiating bodies and omitting the view factor, i.e. setting it equal to unity, the following can be stated for the two bodies in energy balance:

$$T_r = \sqrt[4]{\frac{\varepsilon_i \cdot T_i^4}{\sigma}} \tag{4.9}$$

where

T_r is the incident black body radiation temperature, in K;

ε_i is the surface emissivity of the body i , in FSE, typically between 0.7 and 0.9;

F_{j-i} view factor from surface j to surface i;

σ is the Stefan-Boltzmann constant, $5.67 \cdot 10^{-8}$ in W/(m$^2 \cdot$ K^4);

T_i is the surface temperature of the body i , in K.

In a more general form, Eq. 4.9 is given by Wickström [209] with a notifiable interpretation: The temperature T_r, can be described as the temperature a surface would get which is in radiation equilibrium with the incident radiant heat flux, i.e. no heat is transferred to or from its surface neither by convection or conduction. It should be noted that the relationship in Eq. 4.9 is typically used in practice to "translate" compartment temperatures under a not further defined radiant heat flux. This is correctly speaking only valid if the compartment temperature would be equal to the surface temperature and the material is an inert body. Typically, fire-exposed timber exhibits an insulating char layer on the fire-exposed side which can be considered as such, thus, the latter can be considered as fulfilled while the former should still be verified. The described situation may be studied as the concept of the adiabatic surface temperature in corresponding literature, e.g. Wickström [209].

The incident radiant heat flux in the literature. In the literature, the incident radiant heat flux measured in fire resistance furnaces is provided in some references and considered valid in any case for non-combustibles ranging up to about 125 kW/m^2, 150 kW/m^2, 180 kW/m^2 at about 60 min, 90 min and 120 min, respectively, during EN/ISO standard fire exposure. In contrast, in the literature focusing on timber, low values with max. 50 kW/m^2 in compartment fires were reported by Rezka et al. [20, 151].

4.7 Thermal boundary conditions

The heat fluxes by convection and radiation may be used to determine the temperature distribution in a solid exposed to a heat source. To do so, it is essential to apply a thermal boundary condition. There are three kinds of thermal boundary conditions (BC) whereby an appropriate thermal BC is to be used to solve the resulting differential equations [209]. The three thermal BCs are the following:

(i) Prescribed surface temperature: the first kind of thermal BC, also called the "Dirichlet boundary condition", means that a surface temperature is prescribed. In FSE, this thermal BC may only be used for materials of low density and thermal conductivity, then the surface temperature is approximated by the (furnace) compartment temperature. For highly conductive materials (e.g. steel), the convective flow from the surface would reduce the surface temperature and may create a significant temperature difference between the compartment and the surface of the solid. For comparison purposes, thermal simulations of an infinitely wide solid made from wood material exposed to standard fire have been executed with the FE software Abaqus [183], see Figure 4.3 (a). Firstly, the thermal exposure was simulated prescribing a time-temperature curve on the surface elements, alternatively, the same default time-temperature was prescribed at the surface allowing the surface to re-emit and absorb alternatively a certain share. Both cases represent about the 1st kind of thermal BC (broken lines) and about the 3rd kind of thermal BC (continuous curves) in Figure 4.3 (a).
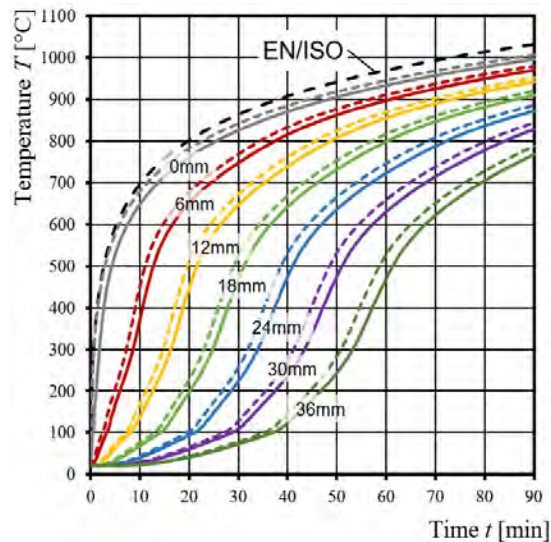
Figure 4.2: Simulated temperatures in various depths of a one-sided infinite wide wood specimen with (a) prescribed surface temperature (broken lines) and (b) a prescribed compartment temperature (continuous lines) when exposed to EN/ISO standard fire and corresponding incident radiant heat flux calculated acc. to Eq. 4.5. Temperature readings are given for depths every 6 mm. Image by T. Rizi.

(ii) Prescribed surface heat flux: the 2nd kind of thermal BC, also called the "Neumann boundary condition", only considers a surface heat flux prescribed at the solid's exposed boundary. This would mean that the surface heat flux is equal to the heat flux being conducted away from the surface into the solid. This BC is not

applicable in FSE but carelessly used by many fire engineers [82]. In this case, the difference between the surface temperature and the ambient environment are neglected. Depending on the material under investigation, this implies a risk for wrong conclusions when the solid's surface temperature and its interaction with the (cold) environment is not further considered. E.g., the 2nd kind of thermal BC is applied often for calculations and the interpretation of cone-calorimeter tests where its validity should be carefully assessed as with the applications for fire compartment calculations. Typically, the surface characteristics including the temperature and the temperature difference to the compartment influence the heat transfer to the solid, thus, the 3rd kind of thermal boundary condition is applicable. For comparison purposes, thermal simulations were performed for a prescribed surface heat flux of 35 kW/m^2 and for a variable surface heat flux derived with the EN/ISO time-temperature curve and Eq. 4.5. Infinitely wide solids made from wood and concrete with the FE software Abaqus [183] were simulated, see Figure 4.3 (b). The heat flux absorbed from the surface of the solid for wood (green curves) and concrete (red curves) are shown. For both, the prescribed constant surface heat flux and the variable surface heat flux, it is apparent that the absorbed heat flux is strongly dependent on the material's thermal properties and a function of the time due to the different change of the temperatures of the individual elements in the solid.
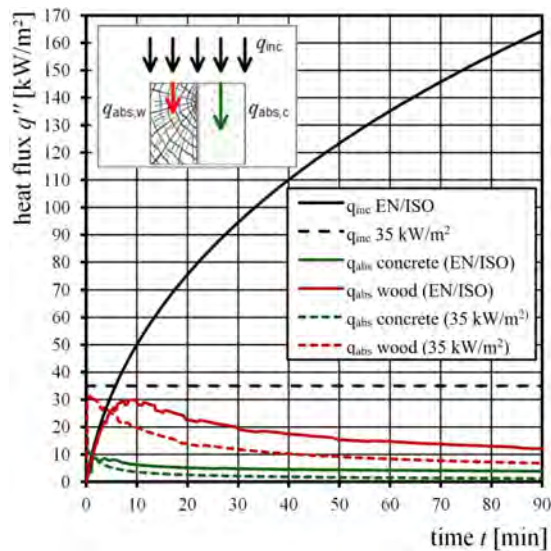
Figure 4.3: Incident radiant heat flux for a black body radiation temperature following EN/ISO standard fire and corresponding incident radiant heat flux calculated acc. to Eq. 4.5 (continuous lines) and a constant level of 35 kW/m^2 (broken lines) with the calculated corresponding absorbed heat flux for wood and concrete. Image by T. Rizi.

(iii) Natural boundary condition: The 3$^{\text{rd}}$ kind of thermal BC, also called the Robin boundary condition or the mixed boundary condition, means that the heat flux to a surface depends on the temperature difference between the surrounding (fire) environment and the surface temperature. In its most general form, this thermal BC comprises prescribed convection and radiation conditions and different radiation and gas temperatures. The appropriate heat flux according to the third kind of BC is obtained by superimposing radiation and convection to the total heat flux as follows:

$$\dot{q}''_{tot} = \dot{q}''_{rad} + \dot{q}''_{conv} \tag{4.10}$$

and using Eq. 4.6 and Eq. 4.2

$$\dot{q}''_{tot} = \varepsilon \cdot \left(\dot{q}''_{inc} - \sigma \cdot T_s^4 \right) + h_c \left(T_g - T_s \right) \tag{4.11}$$

and furthermore inserting Eq. 4.5

$$\dot{q}''_{tot} = \varepsilon \cdot \left(\varepsilon_i \cdot \sigma \cdot T_r^4 - \sigma \cdot T_s^4 \right) + h_c \left(T_g - T_s \right) \tag{4.12}$$

$$\dot{q}''_{tot} = \varepsilon \cdot \sigma \cdot \left(T_r^4 - T_s^4 \right) + h_c \left(T_g - T_s \right) \tag{4.13}$$

where
$\dot{q}''_{tot}$ is the rate of the total heat flux to a surface, in W/m^2;
ε is the surface emissivity, in FSE, typically between 0.7 and 0.9;
σ is the Stefan-Boltzmann constant, $5.67 \cdot 10^{-8}$ in W/(m$^2 \cdot$ K^4);
h_c is the convective heat transfer coefficient, in W/(m$^2 \cdot$ K);
T_g is the gas temperature, in K;
T_r is the incident black body radiation temperature, in K;
T_s is the surface temperature, in K.

In the fire situation, the natural boundary condition given in Eq. 4.13 can be simplified as the radiation temperature and the gas temperature can be assumed equal to an introduced fire temperature, also used in Eurocode 1 [34]:

$$\dot{q}''_{tot} = \varepsilon \cdot \sigma \cdot \left(T_f^4 - T_s^4 \right) + h_c \left(T_f - T_s \right) \tag{4.14}$$

However, it should be noted that the estimation of the surface temperature is still required. For a timber specimen, this might be a complex task where potential smouldering combustion might influence the surface temperature depending on the particular environment in the test, experiment or compartment.

Thermal boundary condition "Heat Flux"   In FSE, it is often referred to "the thermal boundary condition heat flux" which can not be definitely associated with one of the above listed three thermal boundary conditions given by physics. Wickström [209]

discusses the limitations given by the associated use. Applying this practice, it is assumed that the surface of the body under consideration is kept at ambient temperature. Then, the heat balance would become independent on the surface temperature of the exposed solid. Wickström points out that this procedure accuracy is highly dependent on the assumptions of the emissivity and the conductive heat transfer coefficient.

Thus, the application of this approach should be carefully executed. It can be concluded, that this approach might be a reasonable simplification in practice. However, to determine material properties or important characteristics such as the self-extinguishment of timber, this simplified approach may lead to large uncertainties.

Typically, in FSE practice, a radiative heat flux (density) is predicted, originating from e.g. a fire source. Consequently, the surface heat flux at a load-bearing member's surface is derived considering the relative orientation and location of the member to the fire. This surface heat flux is then used in finite element calculations neglecting the fact that losses or convective heat transfer at the member's surface may be incorrectly modelled. Consequently, the heating of the specimen is incorrectly predicted and the determination of the load-bearing capacity is not valid. The approach of the thermal boundary condition "heat flux" is further used for the determination of material characteristics, e.g. the ignition of wood in cone calorimeters. In this case, radiative feedback from the flames and the heat transfer to and from the gaseous environment are neglected. Typically, a significant scatter of test results is reported. Finally, these results are generally applied in practice, neglecting the theory of heat transfer.

4.8   Heat flux measurements in fire resistance tests

Direct measurements of the heat flux to a surface, $\dot{q}''_{tot}$, within a fire compartment are not possible in practice as it depends on the exposed material, its surface and its geometry and the response of the exposed surface. Measurements made with sensors are valid for the particular specifications (body temperature, surface characteristics, geometry) and cannot be transferred directly to other materials. Generalisation of the sensor measurements to other materials, other geometries or, in general, other products implies the acceptance of a physically flawed transfer. When measurements are taken, the following three questions should be considered:

(1)   What influences the measurements?

(2)   What type of heat flux should be described? and

(3)   Which kind of the thermal exposure or heat flux is considered?

The background for these questions can be found in Section 4.6, reasons are the variegated definitions and usage of the heat flux. Confronted with the task of heat flux measurements, typically, water-cooled Schmidt-Boelter type heat flux gauges (HFS) are used; an example is shown in Figure 4.4 [147]. These devices measure a voltage created in a sensor due to a

heated surface which can be translated by the device to a heat flux. Typically, provided calibrations claim that the sensors can show either an absorbed heat flux or an incident radiant heat flux. While the exposed surface of the HFS has a sensor area with high emissivity due to its black blink coating, the highly conductive body is cooled to induce a heat flux along the depth of the sensor. The cooling is achieved by cooling water channelled through the sensor's body. According to the sensor's patent, the measurement voltage resulting from the temperature difference is converted to an incident radiant heat flux using calibration factors. While the cooling water is typically constant at about 300 K, the temperature at the exposed surface is likely to exceed 500 K while the gas temperature in a fire compartment temperature may exceed 1300 K. Due to the significant difference between the gas temperature and the sensor's surface temperature, this type of sensors are highly sensitive to convective heat transfer when placed in fire compartments or hot gases, compare Eq. 4.2. As the convective part can not be foreseen in a calibration process and accordingly corrected for all situations, a sum of heat transfer by radiation and convection to the cooled surface is likely to be measured. The convective part of Eq. 4.13, is often neglected when HFSs are used, e.g. by Sultan [192]. Depending on the actual gas temperature level this procedure can be questioned as the temperature difference $(T_g - T_s)$ in Eq. 4.2 may lead to a considerable measurement error if the absorbed heat flux of the HFS is increased by the convective heat flux. Another source of the uncertainty is the convective heat transfer coefficient which is complex to estimate depending on gas flow characteristics at the surface of the sensor. While for free convection a limit for the convective heat transfer coefficient of about $10 \text{ W}/(\text{m}^2 \cdot \text{K})$ can be specified, it can reach at least five times this value for forced convection [189], i.e. when the gas motion is externally imposed [81]. It should be noted, that, replacing the HFS with a test specimen, an undefined boundary arises as the surface temperature of the specimen in question remains unknown and is likely to be different from the HFS. Using the above specified maxima for the temperature difference and the heat transfer coefficient it can be calculated that a maximum error exceeding 30% can be determined by comparing both terms of Eq. 4.14:

$$\frac{h_c \left(T_f - T_s\right)}{\varepsilon \cdot \sigma \cdot \left(T_f^4 - T_s^4\right)} = \frac{50 \cdot (1300 - 500)}{0.8 \cdot 5.67 \cdot 10^{-8} \cdot (1300^4 - 500^4)} = \frac{40000}{126717} = 0.32 \qquad (4.15)$$

Apparently, the error is strongly dependent on the gas flow characteristics due to the large influence of the convective heat transfer coefficient. In fully-developed fires, a 50% reduction of the convective heat transfer coefficient from $50 \text{ W}/(\text{m}^2 \cdot \text{K})$ to $25 \text{ W}/(\text{m}^2 \cdot \text{K})$ can be expected as suggested in Eurocode 1 [34]; consequently, the error reduces but exhibits still about 15%. It is only when the HFS is used in environments with gas temperatures about equal to the surface temperature of the sensor that the error would be negligible, especially when using the water cooled HFS in fire environments, the results should be considered as such, evaluated with care and an error estimation given.

Measurements in mm
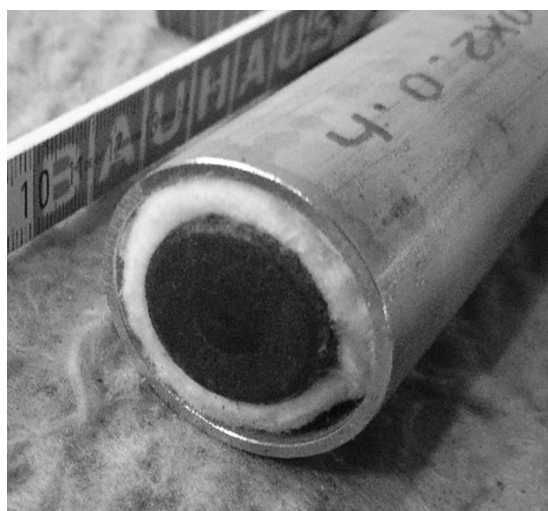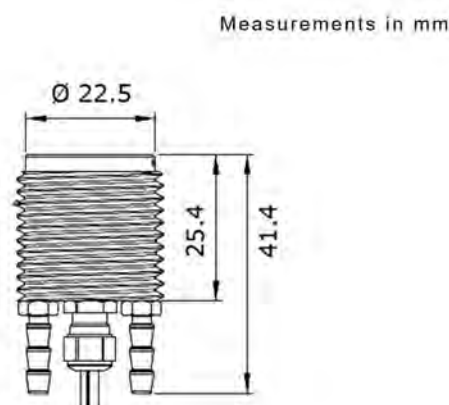
Own image.   Image by Hukseflux.

(a)   (b)

Figure 4.4: HFS installed in a low conductive steel pipe with ceramic fibre insulation (a) and end elevation of the HFS (b).

To document the level of thermal exposures, Babrauskas [8] collected results of heat flux measurements of furnaces which were controlled using the EN/ISO [37, 85] or ASTM [5] standard fire exposure. It can be assumed that sensors of Schmidt-Boelter type were used. The difference between the two standardised time-temperature curves is very limited, see Figure 2.2 (a), thus, the analysis of heat flux measurement for both cases was considered justified in this thesis. For the heat flux measurements, a considerable scatter of up to about ± 25 kW/m²can be observed, see Section 4.5. However, in a general sense, the provided data tend to follow the incident radiant heat flux calculated according to Eq. 4.5, by substituting the corresponding time-temperature curves for the black body radiation temperature. Although the data presented in Babrauskas [8] were collected for a study to estimate limits of charring of wood, it remains unclear whether the data were obtained in fire resistance furnaces with combustible or non-combustible materials. In another study, different devices were compared to control fire resistance furnaces [192], see Figure 2.2 (b). Testing non-combustible floor elements, HFGs of Schmidt-Boelter type have been inserted with their sensor surface flush with the fire-exposed surface. In the experimental campaign by Sultan [192], the temperature control devices were either PTs according to EN/ISO, shielded thermocouples according to ASTM, bare bead thermocouples and a modified PT with increased insulation. The determined lowest and highest heat flux measurements of the available four tests are shown in Figure 4.5 (b). By trend, the results agree with data of Babrauskas [8] shown in Figure 4.5 (a) and, further, with the incident radiant heat flux calculated using Eq. 4.5 with the acceptance of an expected large scatter. Sultan concluded that HFS measurements indicated about 10% higher levels of the typically measured incident radiant heat flux. As discussed above in this section, and shown in

Eq. 4.15, one can concluded that this overestimation represents the error due to the convection of Eq. 4.14 and demonstrated in Eq. 4.15. That the default incident radiant heat flux obtained using Eq. 4.5 is strictly speaking only valid for a perfect black body had not been considered by Sultan [192]. However, as the data appears, the resulting error seems to be within an acceptable error range: it should be noted, that the agreement between the measurements and the simplified prediction of the incident radiant heat flux by Eq. 4.5 is fair when exposure levels are roughly evaluated; However, for specific conclusions and accurate calculations the use of the obtained data may be limited.

(a)   (b)
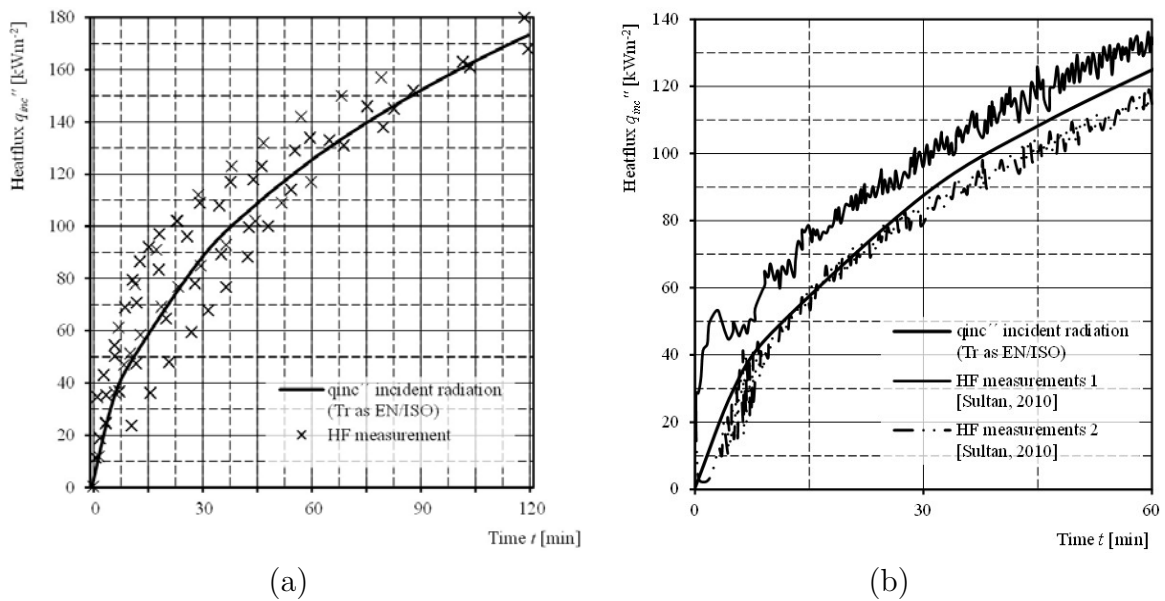
Figure 4.5: Measured heat flux in wall furnaces during standard fire tests acc. to ISO 834 and ASTM E119 [5] modified from Babrauskas [8] and the calculated heat flux using Eq. 4.5: (a) Measured heat flux in two furnaces during tests acc. to ASTM E119 [5] with upper and lower bounds modified from Sultan [192] and the calculated heat flux using Eq. 4.5 (b). Own figures.

The PT measures a temperature of a thermally well-defined body. In Europe, the PT is used to control a furnace environment [37] which is characterised by a high radiative environment with simultaneously high gas temperatures. The PTs are relatively large sensors and therefore less sensitive to convection, the surface temperature is close to the gas temperature which makes the device less sensitive to the heat transfer coefficient which is complex to determine . The PT measures in principle the temperature of surface in equilibrium due to radiation and convection assuming that the conduction away from the solid's surface is negligible. However, the device has an inertia which causes a time delay, and for practical reasons it is not possible to avoid heat losses by conduction from the measuring surface. Häggkvist et al. showed that PT measurements can be used to calculate an incident radiant heat flux with additional measurements of the gas

temperature and physically justifiable factors [73, 154]. According to Häggkvist et al., the incident radiant heat flux can be calculated as:

$$\dot{q}''_{inc} = \sigma \cdot T_{PT}^4 + \frac{(h_{PT} + K_{PT}) \cdot (T_{PT} - T_g)}{\varepsilon_{PT}} + \frac{C_{PT} \frac{dT_{PT}}{dt}}{\varepsilon_{PT}} \tag{4.16}$$

where

$\dot{q}''_{inc}$ is the rate of the total heat flux to a surface, in W/m^2;

σ is the Stefan-Boltzmann constant, $5.67 \cdot 10^{-8}$ in $W/(m^2 \cdot K^4)$;

T_{PT} is the temperature of the PT, in K;

ε_{PT} is the surface emissivity of the PT,

h_{PT} is the convective heat transfer coefficient of the PT, in $W/(m^2 \cdot K)$;

K_{PT} is the correction coefficient for conduction losses of the PT, in $W/(m^2 \cdot K)$;

T_g is the gas temperature, in K;

C_{PT} is the lumped heat capacity of the PT, in $J/(m^2 \cdot K)$;

dt is the time derivate, in sec.

In Eq. 4.16 the second and third term are correction terms for the heat losses and the device's inertia causing a delay when the temperature changes. In general, measurements of a PT together with Eq. 4.16 could be used also in environments deviating from fire to calculate an incident radiant heat flux which could replace the sensitive HFS in its typical application [210].

4.9 Furnace experiments

4.9.1 General

The available heat flux measurements of the incident radiant heat flux from literature shown in Figure 2.2 (b) were taken from fire resistance tests of specimens with non-combustible materials [8] and not further specified materials [192], shown in Figure 2.2 (a). Until today, no corresponding information is available for combustible materials in the literature. To extend the available data set, nine experiments were performed in a standard fire resistance furnace with additional instrumentation, see Table 4.1. The instrumentation of the furnace and the specimens exceeded the standard requirements mainly to address the purpose of this study, analysing the compartment environment of furnaces when combustible specimens are exposed. Beside heat flux measurements with a HFS, oxygen concentration measurements were taken. Measurements were taken at different locations and positions. Furthermore, a large number of temperature measurements within the specimens were taken to follow the temperature gradient and progression of the charring within the solid. Experiments were performed in the model scale furnace at VKF ZIP AG (formerly part of Empa, Swiss Federal Laboratories for Materials Science and

Test no.	1	2	3	4	5	6	7	8	9
Test ID	CLT 01	CLT 02	CLT 03	CLT 04	CLT 05	CLT 06	CLT 07	STP I	STP II
Exposure time [min]	60	120	120	90	120	120	120	120	130[1)]
Oxygen measurements	none			surface	surface, centre of furnace, exhaust				
1)	initially protected by a non-combustible fire protection system; failure induced at ca. 100 min								

Table 4.1: Overview of fire resistance experiments performed for this study.

Technology) in Switzerland with solid timber panels (STPs) and cross-laminated timber (CLT) elements as floor specimens.

4.9.2 Material and equipment

In 2017, a series of furnace experiments were performed by ETH Zürich with various specimens, see Chapter 3. In the following, nine experiments relevant for the topic of this thesis are discussed. The specimens were produced on site out of spruce lamellae either orientated edgewise (STP) or crosswise (CLT) by means of various adhesives. Prior to the exposure using the EN/ISO standard fire time-temperature curve, all specimens were stored in a climate room to reach an EMC of 12%. At the day of the experiment, the MC was verified measuring the electrical resistance. The model scale furnace (inner measures 1000 mm × 800 mm ×1000 mm) at VKF is an oil fired furnace, both burners are located at one shorter side, diagonally opposite the exhaust opening in the bottom of the furnace. A schematic section view is presented in Figure 4.6 (a). In all experiments, the temperature was controlled using five PTs situated 100 mm beyond the exposed surface of the specimen uniformly distributed over the area with a minimum centre distance to the furnace walls of 250 mm. The mean value of the temperature readings of the PT were used to control the furnace temperature to follow the standard fire time-temperature curve. Examples of the control temperature (mean) in comparison to the accepted tolerances according to EN 1363-1 are given for the first three experiments in Figure 4.6 (b).

Key:
a... specimen   d... HFS
b... oil burner   e... PT
c... furnace window   f... fitting insulation

(a)   (b)
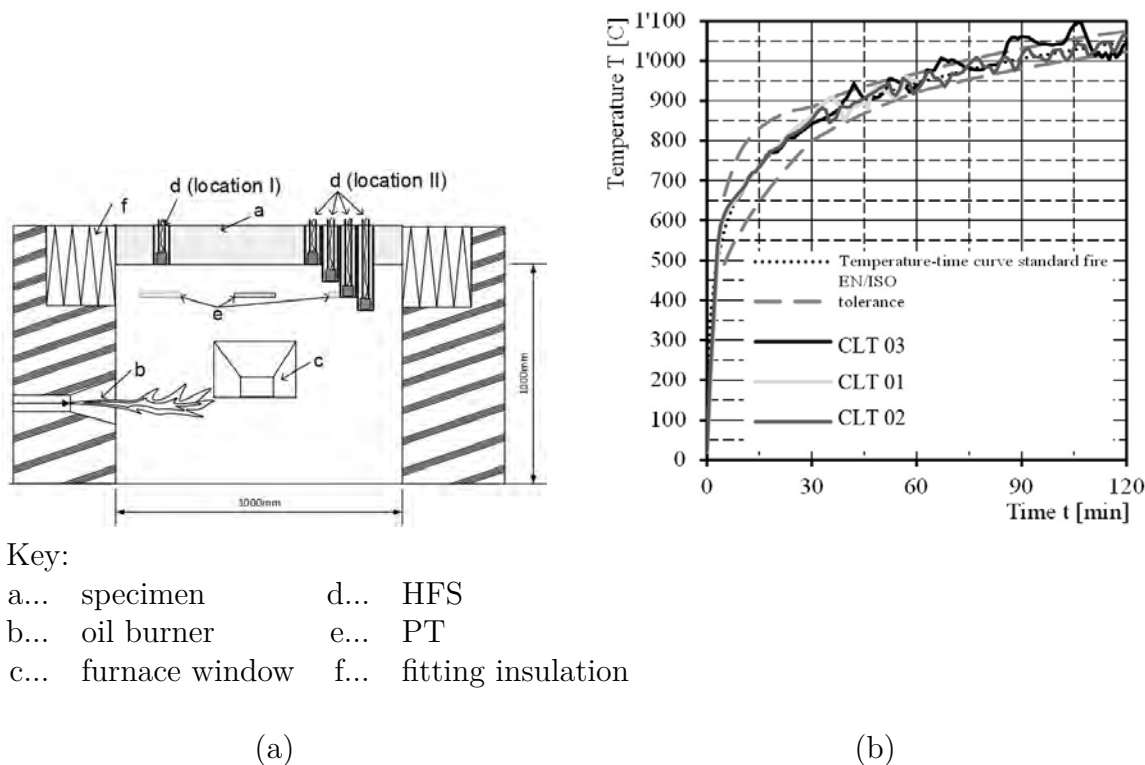
Figure 4.6: End elevation of the model scale furnace with the indicated location and position of burners, PTs and heat flux sensor (details enlarged) (a) and furnace control temperature of experiments CLT 01 to CLT 03 (b). Own figures.

Three experiments were terminated after 60 min, 90 min and 130 min, respectively, while the remaining six experiments lasted 120 min, see Table 4.1. Longer duration than found in the literature were chosen as many fire resistance tests with timber products in the literature last only up to 90 min with respect to national fire regulations. Additional measurements exceeding the requirements of EN 1363-1 [37] were taken to allow conclusions with respect to the thermal exposure of the fire-exposed specimens, i.e. combustible materials: the additional measurements were, (i) the fuel oil consumption, (ii) the heat flux measurements with a HFS (calibrated for the incident radiation heat flux), (iii) the mass loss of the specimens, (iv) oxygen concentration, (v) the furnace gas temperature, (vi) the exposed surface temperature, (vii) the temperature distribution within the specimens. Details of these measurements were as follows.

(i) The burner fuel consumption (fuel oil) was measured as suggested in ASTM (rate and total);

(ii) HFS measurements were performed using a HFS of Schmidt-Boelter type, insulated and inserted in a low conductive steel pipe, see Figure 4.4. Measurement locations and positions were chosen with respect to the burners and the PT so that measure-

ments of the sensor are not disturbed by the PT. Four different positions (depths) were chosen for the HFS at the location II. (1) One position was to place the sensor surface at the same height as the PT and (2) another with the sensor flush with the exposed surface of the specimen. Further positions were defined by (3) 40 mm above and (4) 40 mm below the PT. It should be noted that the position flush with the surface (1) was changed when the surface coordinate changed (e.g. due to char layer surface regression), the fit was adjusted manually by means of observations performed through both, oppositely arranged furnace windows. A further variation of the location of the HFS was chosen to check whether the incident radiant heat flux is different above the flame in the burner region (location I) or the region away from the burner (location II). Measurements and data were collected manually throughout the testing. Measurements were taken regularly every two to four minutes. The channels through the specimens where measurements were taken were always sealed with either the HFS or a plug to keep the furnace' integrity.

(iii) The mass loss of the specimens was measured with a scale before and after the experiment. The time between the termination of the experiment and the weighing was less than 90 seconds followed by the extinguishment of minor flames and the smouldering char layer. Instrumentation and fixing devices were considered in the mass estimations.

(iv) The oxygen concentration was measured with probes installed at either the surface only (CLT 4) or at three different extraction points. A membrane pump was used to extract the sample gas from the heated environment. The measurements were taken with an electrochemical sensor which required that the sample gas had to be cooled before the analysis. A heat exchanger was used to achieve suitable sample gas temperature below 50°C which caused a delay of the measurements of about 60 sec which was considered in the interpretation of the results. The gas flow through the sampling system was controlled throughout the duration of the experiments. The extraction points were in the furnace compartment (centre location, centre height), the exhaust channel (approx. 1000 mm from the exhaust opening in the bottom of the furnace) and the surface of the specimens. If a change of the surface coordinate was observed, this probe's position (depth) was adjusted accordingly.

(v) The furnace gas temperature was measured by two wire thermocouples (type K, glass fibre insulated) with welded junctions. The conductor area was in total 0.5 mm^2. For every experiment, the wires were replaced.

(vi) Temperature measurements within the specimens were made with thermocouples (type K, glass fibre insulated) with a conductor area of 0.5 mm^2. The thermocouples were installed during the production (see Figure 4.7) following the requirements given in EN 1363-1 [37] to address the low conductivity of the specimen material; accordingly, wires had a minimum length of 50 mm parallel to the isotherms. For

comparison reasons, thermocouples were further drilled in from the unexposed side, results of the comparison have been published in Fahrni et al. [53].

Figure 4.7: Wire thermocouples of CLT ($0.5\,\text{mm}^2$ conductor area) attached to lamellae before the bonding process in a hydraulic press. Own image.

4.9.3   Results of the furnace experiments

The Results of the furnace experiment are presented below with respect to the measurements listed in Section 4.9 above.

(i) In the starting phase of up to about half an hour, both burners were used in all experiments. Except for with STP II, the experiment with the non-combustible fire protection system, one of the two burner was alternately turned off after about 30 min to avoid excessive temperatures in the furnace. The burner fuel consumed, indicated as external fuel consumption, ranged from about 9 litres (CTL 01, 60 min) to 32 litres (STP II, 130 min). Results are shown in Table 4.2 together with the mass loss of the specimens, see (iv).

(ii) The incident radiant heat flux measured with the HFS was done approximately every two to four minutes, readings from all measurements are given in Figure 4.8 for all tests. In Figure 4.8 measurements taken during the experiment STP II with the non-combustible surface are indicated with squares. In the experiment CLT 03, the location of the HFS was varied between locations I and II, in the burner region and away from it, shown in Figure 4.9 (a) Measurements were taken consecutively at both locations with a time difference of less than 0.9±0.3 min. At 41 min the shift of

Test ID	CLT 01	CLT 02	CLT 03	CLT 04	CLT 05	CLT 06	CLT 07	STP I	STP II
Exposure time [min]	60	120	120	90	120	120	120	120	130
Mass loss [kg]	14.4	27.6	40.7	28.4	22.6	23.7	25.3	22.0	6.0
Fuel consumption [litre]	8.8	16.5	12.7	17.0	13.0	19.0	18.0	20.0	32.0

Table 4.2: Individual mass loss of the specimens, and fuel oil consumption of experiments performed in this study.

the burners was performed which led to inconsistency of the measurements. In the experiment STP I, the position (depth) of the HFS was changed between the upper position "U" flush with the specimen surface, at a medium position "M" 40 mm above the PT and at a lower position "L" 40 mm below the PT, see Figure 4.9 (b). For the upper position, the sensor's depth was checked visually, so that its exposed surface was flush with the exposed surface of the specimen.
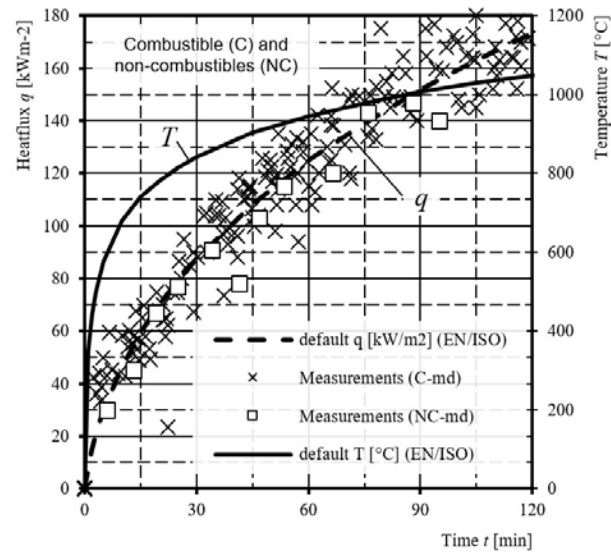
Figure 4.8: Incident radiant heat flux measured by the HFS for all experiments and corresponding default flux for EN/ISO standard time-temperature exposure determined by Eq. 4.5. Own figure.

| (a) | (b) |
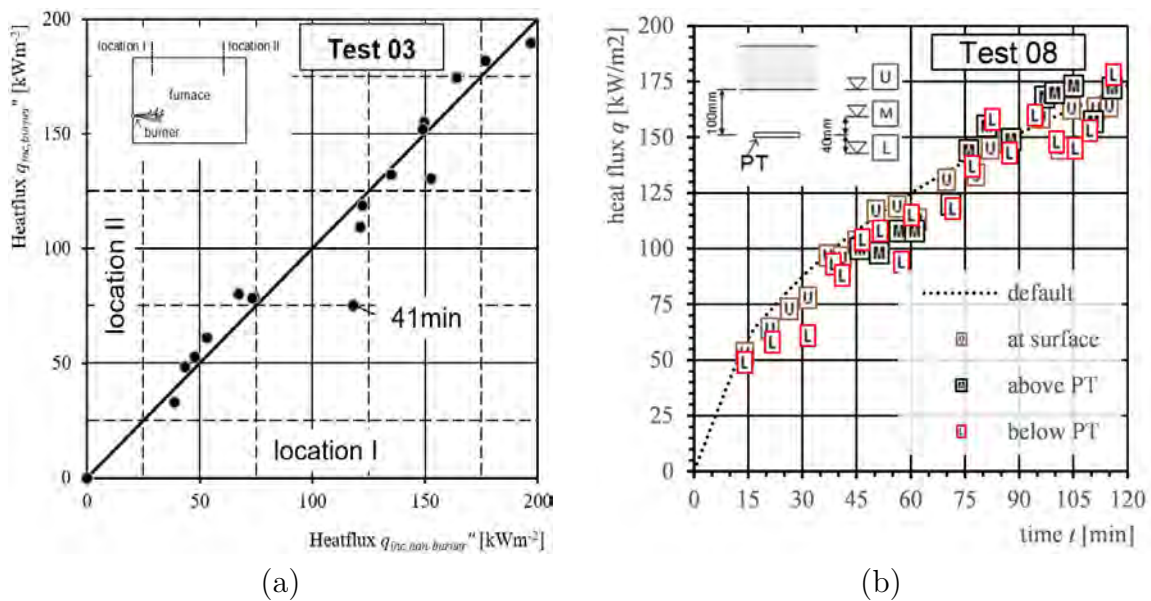
Figure 4.9: Measured incident radiant heat flux by the HFS for CLT 03 (Test 03) and STP I (Test 08). At two locations (a) and at three positions: at the specimen's surface "U", above the PT "M" and below the PT "L" (b). Own figures.

(iii) For comparison reasons, the incident radiant heat flux was determined based on recordings of the PT temperature (mean) together with the measured gas temperature

as described by Häggkvist et al. [73]. Results of experiments CLT 01 to CLT 03 are shown in Figure 4.10 together with corresponding results of the HFS, indicated as "HF by HFS".
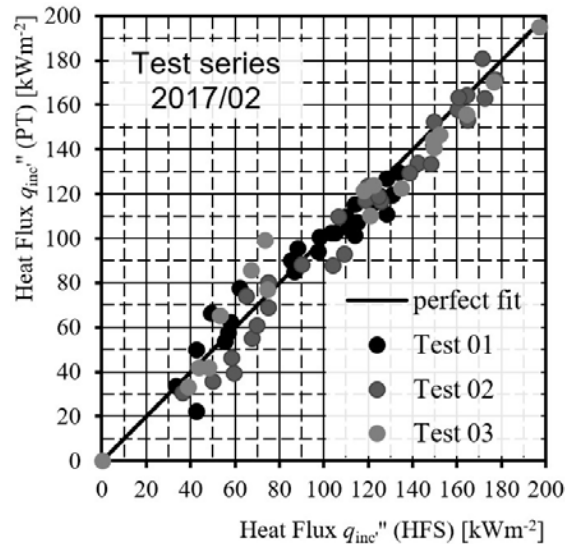
Figure 4.10: Incident radiant heat flux for experiments CLT 01 to CLT 03 (Test 01 to Test 03). Comparison of results measured by the HFS and a PT. Own figure.

(iv) The mass loss was estimated by comparing the specimen's mass before the experiment and directly after the experiment before extinguishing. In this campaign, the mass loss of the timber due to charring was determined to about 6 kg to 41 kg respectively. Differences can be explained by the different test durations, the lay-up of the product in combination with the adhesives used and the availability of a fire protection system. Results are shown in Table 4.2.

(v) Measurements of the oxygen concentration were taken at various positions resulting in different groups of data in all experiments. Figure 4.11 (a) shows oxygen concentration during the exposure near the specimen's surface and in the exhaust for the experiment CLT 04 (Test 04). In subsequent experiment, the probe position was adjusted to follow the change of the exposed surface (char layer expansion or regression, charring layer fall-off). The measurements for the experiment STP II (Test 09) with an initially protected specimen are plotted in Figure 4.11 (b), where the shift from a non-combustible specimen (NC) to a combustible specimen (C) is indicated with a vertical double bar. The change of the oxygen concentration due to the reaction of combustible products released from the suddenly fire-exposed surface and the burners can be noticed in Figure 4.11 (b) after the failure of the protection system at about 100 min. The oxygen concentration at the surface and

in the furnace drops to a value close to zero after the failure of the protection system at about 100 min.
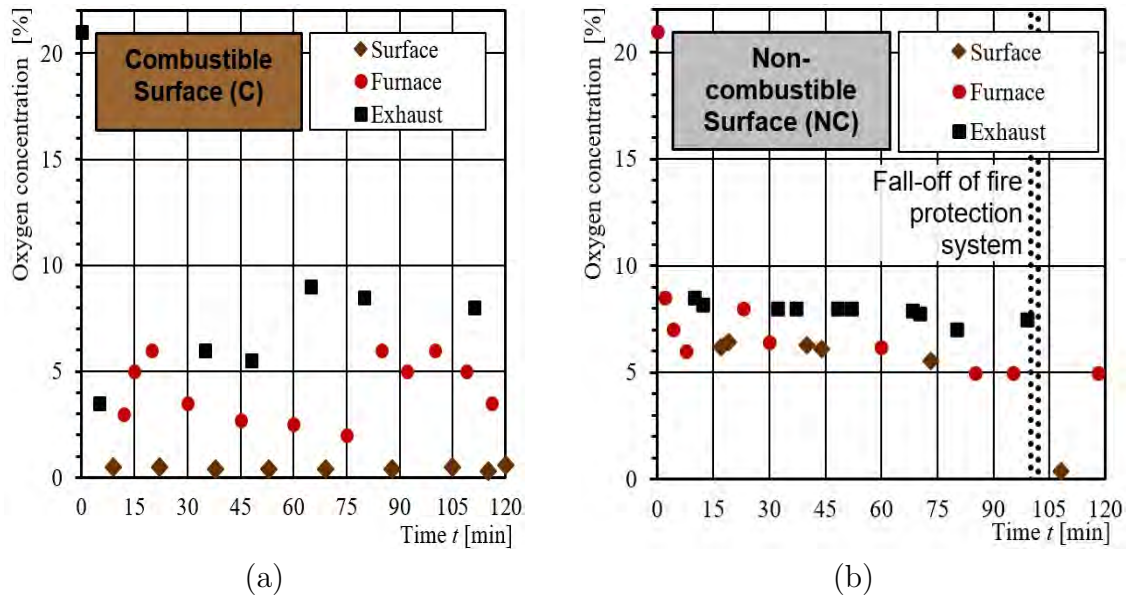
Figure 4.11: Oxygen concentration at several locations. Test 04 (CLT 04): the extraction point was 5 mm below the specimen's exposed surface at the start of the exposure (a). Test 09 (STP II): the extraction point was held flush with the specimen's surface and later adjusted to the changed depth (b). Own figures.

(vi) The temperature readings within the specimens were used to assess the actual charring depth associated with the charring temperature of 300°C suggested in Eurocode 5 [35]. For comparison reasons, charring rates determined in this campaign were only compared to literature when no failure of the charring layers was observed. In general, the charring rate allows a comparison of the furnace performance as the one-dimensional charring rate of $\beta_0 = 0.65$ mm/min is widely accepted for spruce wood. Mean values of all measurements in equal depths were used to determine the results for the charring depth and charring rate respectively. Figure 4.12 gives the assessed charring depth for the experiments CLT 02 and CLT 07 where no fall-off of charring layers was observed with the linear charring rate for solid timber given in [35]. In addition to the temperature readings, the (mean) thickness of the residual virgin cross-section was determined to complete the data set, see Figure 3.5 which was found to be in good agreement with the wire thermocouples installed parallel to the isotherms close to their hot junctions.
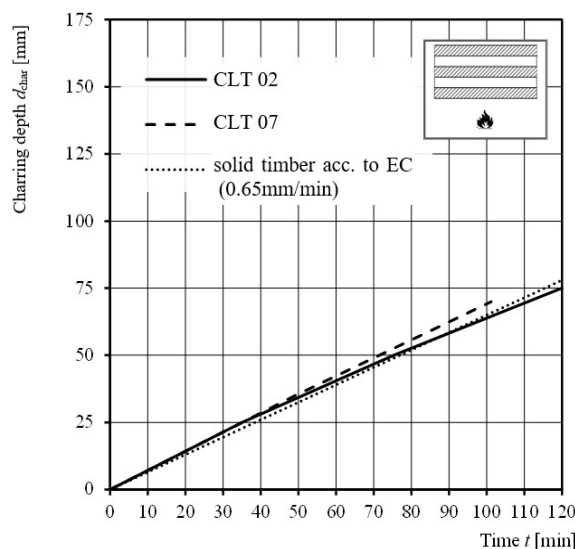
Figure 4.12: Determined charring rate for the specimens CLT 02 and CLT 07 in comparison to the one-dimensional charring rate for solid timber in Eurocode 5. Own figure.

4.10   From thermal exposure to fire exposure

Below, the results of the fire resistance experiments with combustible specimens, CLT 01 to CLT 07 and STP I (Test 01 to Test 08) and STP II (Test 09) where a non-combustible specimen was converted into a combustible during the exposure in a furnace experiment, are analysed with respect to the differences and similarities in a) furnace tests and experiments and b) post-flashover fires in compartments..

4.10.1   Thermal exposure of combustibles and non-combustibles in fire resistance tests

Heat flux measurements. The available results for the incident radiant heat flux measurements in fire resistance furnaces were taken from the scientific literature, shown in Figure 4.5, and their lower and upper boundaries identified. While these readings have been taken most likely during tests with non-combustible building elements, this work extends the data with HFS measurements in fire resistance furnaces when combustible specimens are exposed. The results from an experimental campaign comprising nine experiments are presented in comparison to the boundaries from literature results. The additional data from this work are provided firstly as HFS measurements, considered as the incident radiant heat flux and, secondly, as the determined incident radiant heat flux by means of the PT and gas temperature measurements. The comparison is provided over the exposure duration of 120 min in comparison to a default incident radiant heat flux for the EN/ISO time temperature curve following to Eq. 4.5 in Figure 4.13.
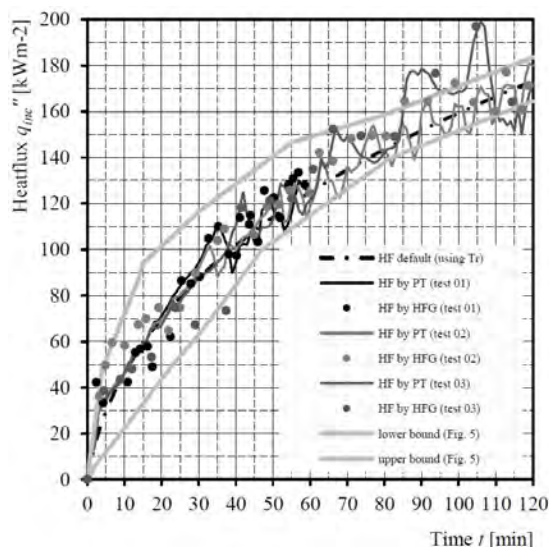
Figure 4.13: Heat flux measurements by PTs (HF by PT) and a sensor (HF by HFG) of experiments CLT 01 to CLT 03 and default curve for EN/ISO standard time-temperature exposure determined by Eq. 4.5 and lower and upper bound for values collected in the literature. Own figure.

Figure 4.13 shows that there is no evidence that combustible products receive less incident radiant heat flux when tested in fire resistance furnaces which are controlled by PT. It should be noted that the values reported in the literature and the readings of this study vary within boundaries of ± 25 kW/m^2. Furthermore, it should be noted that successive HFS readings with very limited time shift may vary considerable as well. The large variation of the HFS readings should be considered when the behaviour of specimens under the particular exposure is related to a certain incident radiant heat flux. A possible source of the significant variation might be the sensitive convection term (second term of the right side in Eq. 4.14) as, the measured readings are, physically speaking, only valid for the measurement device providing a certain emissivity, roughness and length and surface temperature. The HFS might be calibrated to show the incident radiant heat flux but this is only valid in a certain application range. The general application for another material, another surface or, generally, to certain building element with different thermal properties or surface characteristics, or more specifically to timber with a unique characterisation of the charred layer's surface including cracking and possible smouldering effects is physically not correct. In the experimental campaign, a variation of the location of the HFS was investigated, i.e. the area of the burners (location I) and away from the burners (location II), see Figure 4.6 (a). One could expect higher measurements above the burners where flaming occurs. However, no evidence for this was found, measurements of both locations are in very good agreement, see Figure 4.6 (b). Considering the apparent stability of the radiation and the measurement at 41 min where a change of the

furnace burners affected the HFS readings to a limited but recognisable amount, it can be concluded that the radiation from the furnace envelope is superior compared to the radiation of the burner flames. Comparing the burning of timber elements at ambient conditions, e.g. under cone heaters or other radiant sources, one can observe that flaming combustion occurs at and near the surface depending on the environment conditions (for cone calorimeter tests, the investigated variable is mainly the external heat flux and the time), while in environments with limited oxygen, e.g. a furnace, no surface flaming can be observed. In the case of surface burning, it is apparent that the flames would create additional energy radiating back to the specimens' surface. As in fire resistance furnaces, PTs are installed 100 mm away from a test or experimental specimen, one could conclude that combustible specimens receive more radiation as the PT-or a non-combustible specimen. Thus, in this study, the position (depth in the furnace) of the HFS was varied, measurements flush with the specimens surface (upper position "U") were completed with measurements 40 mm above and behind the PT (middle position "M") and 40 mm before or in front of the PT (lower position "L"). Results are plotted in Figure 4.9 (b) and show that there is no evidence that the incident radiant heat flux is increased due to flaming not detected by the PT. It can be observed that in earlier phases of the experiments, the heat flux measurements below the PT "L" are about 10% lower compared to the measurement at the combustible's surface "U". Observations during the early phase of the experiments did not show any surface flaming in this early phase. Measurements taken at about 45 min don't show any difference, some subsequent measurements of the lower position "L" show higher measurements. In general, no clear trend of the measurements can be observed. Overall, all measurements are in agreement with the default curve.

Oxygen concentration. The oxygen concentration was measured as the furnace compartment environment may or may not provide sufficient oxygen concentration to allow for flaming combustion, see Section 2.3.19. Sample gas was extracted from positions at and near the surface of the specimen and analysed with respect to the oxygen concentration. The intention was to investigate combustion near the measurements and the potential of flaming near the specimens' surface behind the PT. Jervis found a minimum required oxygen concentration for flaming combustion significantly above 5% typically provided in fire resistance furnaces [89]. Oxygen concentration at different positions are shown for the experiment CLT 04 (Test 04) and STP II (Test 09), an initially protected timber specimen, in Figure 4.11. From the measurements, it can be concluded that some oxidation occurs at and near the surface of the timber specimens as the average oxygen of the furnace environment of 5% drops to less than 1% at the specimen's surface. This trend of reduction of the oxygen concentration was further observed during a full scale furnace experiment with an additional specimen (STP III, see Figure 3.1 (b)). For STP III, exposed for 90 min, the oxygen concentration was measured with a paramagnetic analysis device directly at the timber surface. Results showed oxygen concentrations of less than 2% [109, 173]. The experiment CLT 04 was the only experiment with a fixed position of the oxygen probe to analyse the oxygen concentration approximately 5 mm below the

surface. Up to about 60 min, the oxygen is consistently below 1% while it increases in the second half of the two-hour test to values up to 5%. It can be assumed that this increase is in relation to the increasing distance to the surface due to surface regression which was estimated for this experiment to about 20 mm at the end of the experiment. Consequently, in subsequent experiments, the probe position was adjusted to follow eventual changes of the exposed surface due to char layer regression or fall-off of charring layers of CLT specimens. These experiments confirmed, that experiments with combustible surfaces - all experiments except STP II (Test 09) - exhibited oxygen concentrations at the surface below 1% throughout the entire duration of the fire exposure.

Oxygen concentration and heat flux measurements. It should be noted that any flaming combustion releases heat energy. If surface flaming, i.e. flaming combustion at the specimen's surface would occur, the heat flux measurements should indicate higher measurement in this regions. Simultaneously, the oxygen concentration should indicate a proper environment. However, oxygen measurements might represent an interrupted cadence as flaming combustion would in turn consume oxygen and lower concentration in the sample gas. Thus, the measurements in the reference case, i.e. for the non-combustible specimen or in the centre of the compartment are of importance. The heat flux measurements in different positions (depths) should be read together with the oxygen measurements near the surface and in the furnace. With both measurement types, the potential flaming behind the PT can be investigated. It seems that any flaming near the surface is contributing insignificantly to the overall thermal exposure most likely due to the low availability of oxygen of about 5% in the furnace (measured in the centre to be representative for the furnace environment rather than detecting flames near the surface). Other studies with bench-scale test methods show that for flaming combustion oxygen levels of higher than 14% are needed [89] which confirms that a typical fire resistance furnace environment, observed to exhibit an oxygen concentration of about 5%, will not allow for flaming combustion. It is assumed that volatile pyrolysis products produced during the charring process of the timber specimen, ignite near the burner where oxygen is blown into the compartment. With respect to the HFS measurements in positions other than flush with the surface, the measurement technique should be discussed. It is expected that the sensitivity to convective heat transfer of the sensor embedded in the wide specimen for the upper measurements (flush with the surface) and inside the furnace is different. Finally , it should be noted that all measurements shown in Figure 4.9 (b) are in good agreement with the overall trend of the incident radiant heat flux determined by Eq. 4.5, see Figure 4.5.

Fuel consumption. The analysis of the fuel consumption for resistance fire tests should be executed with care. In the following, the fuel consumption is considered as the sum of the fuel used by the furnace (burner fuel) and the fuel by a combustible specimen as structural fuel. This sum is considered as energy consumption As the geometry and

thermal inertia of fire testing furnaces vary significantly comparison should be done only for the same furnace and the same durations. To analyse the different furnace burner fuel oil consumption, data of 26 tests and experiments performed in the model scale furnace at VKF were collected; available data for the VKF full scale furnace significantly exceed the observed trends for combustible and non-combustible specimens. Results are presented for tests with combustible (C) and non-combustible (NC) products as shown in Figure 4.1. Further, one data-set for a STP with a non-combustible fire protection system applied to the timber specimen is included in Figure 4.1 (STP II, Test 09). To estimate the shares of the fuel used by its origin, the energy content was assumed to be 18 MJ/l for oil fuel and 18.5 MJ/kg for dry wood fuel and the corresponding value for a reduced MC in accordance with Eurocode 1 [34] applying Eq. (11).

$$\Delta H_{w,u} = \frac{\Delta H_{w,0} \cdot (100 - u) - 2.44 \cdot u}{100} \tag{4.17}$$

where

$\Delta H_{w,u}$ is the heat content of wood at the actual moisture content, in MJ/kg;
$\Delta H_{w,0}$ is the heat content of dry wood, in MJ/kg;
u is the initial moisture content of the wood specimen, in %.

The mass loss of the CLT and STP specimens was directly used to estimate the energy contribution released in the furnaces. Implicitly, the procedure assumes that the material of the char layer does not exhibit any mass. As shown in Chapter 3.4, in general, this assumption is not valid as the char layer exhibits (i) a remaining mass and a signification higher heat content than wood (factor ~1.6) which has to be taken into account for a correct assessment of the energy balance. A correct energy balance of the charring structural timber including the heat storage in the char layer is presented by the development of the TiCHS model, see Chapter 6. However, for the energy balance investigated here, mainly CLT specimens have been analysed which showed partly failure of the bond line integrity, i.e. fall-off of charring layers. Thus, it was not possible to reliably estimate the remaining char layer mass as most of the failed char layer combusted in the bottom of the furnace during the experiment or after the termination of the experiment. Consequently, the entire mass loss was considered as energy contribution related to the heat content by the wood only. For the energy analysis presented here, (1) the corresponding heat content provided by the combustible specimen and (2) the burner fuel provided were estimated for experiments with a standard fire exposure of 120 min. Individual results of both contributions (1) and (2), were calculated and compared to the linear trend determined for non-combustible specimens presented in Figure 4.1. Figure 4.1 shows that the total fuel used, i.e. the external fuel to fire the furnace (burner fuel oil) and the fuel corresponding to the heat content provided by the specimens, reach about only 80% of the trend line for non-combustible (NC-hd) products tested (100% equals 1380 MJ at 120 min), see linear trend line in Figure 4.1. Any further reduction to the energy stored in the char layer would increase the difference. In any case, the remaining difference can be explained by the different thermal inertia of the materials. The fuel recordings indicated with NC-hd
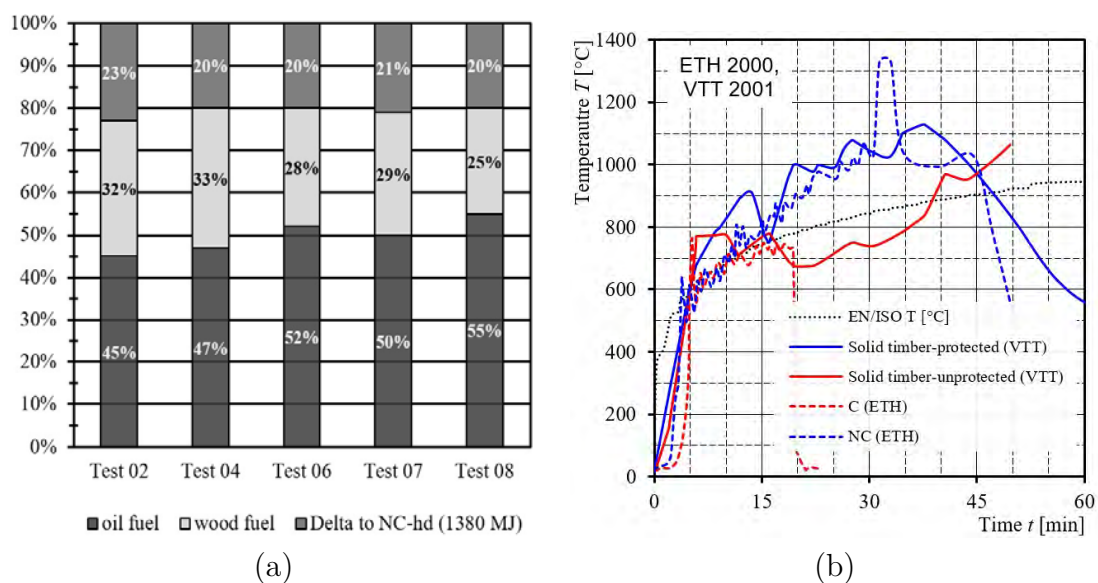
Figure 4.14: Percentage of burner fuel and wood fuel used during experiments of 120 min in a fire resistance furnace at VKF with combustible, low density specimens and difference to the estimated value for a non-combustible high density specimen (a), and temperature measurements of compartment experiments for combustible surfaces(C) and non-combustible surfaces (NC) modified from [117, 74] (b). Own figures.

in Figure 4.1 (a). represent concrete slabs with approximately double thermal inertia compared to wood. To check the variations, the experiment STP II (Test 09) was performed with a timber specimen but with an applied medium density fire protection system (780 kg/m³) on its exposed surface. With this type of protection, the start of charring was delayed until about 100 min, which was verified with three TCs in the interlayer. The consumed burner oil at failure of the protection system corresponds to about 80% of the trend line for non-combustibles (NC-hd), see Figure 4.1 (a). Apparently, after the manually induced fall-off of the fire protection system, the corresponding consumption of the burner oil reduces as the combustible specimen starts to contribute to the total fuel. That the fuel consumption of furnaces is significantly depending on the thermal properties of the specimen exposed to the fire was shown about 50 years ago [76]. Thus, in general, it should not be a surprise that the total energy consumed in furnace tests are below those of non-combustible high density products.

4.11 Structural timber fire-exposed in furnaces and compartments

In Section 4.10.1, it was shown that combustible products provide fuel when exposed to fire in a furnace, and, thus, decrease the external fuel (burner oil) needed to fire a furnace

to follow a defined time-temperature curve. For fires in compartments where structural timber surfaces are left unprotected, it is therefore expected that structural timber will contribute to compartment fires. In the following, the temperature development and the exterior flaming will be compared for compartment with combustible and non-combustible surfaces. Subsequently, the compartment environment will be compared in furnaces and compartment fires.

The first studies which observed and compared and quantified the effect of the combustible surfaces on the fire development were done in the 2000 at ETH Zürich, and 2001 at VTT, Finland [117, 60, 58, 74].

Analysing the temperature-time curves in fire compartments, e.g. Figure 4.14 (b), it can be observed that a steep temperature rise can be expected for compartments with combustible surfaces similar to EN/ISO standard fire is applied, regardless the combustibility of the surface. As shown by Hakkarainen [74], temperatures in the compartment experiment remained below those of the parametric fire design applied to the actual compartment. By trend, temperature measurements showed, that the maximum temperature to be expected is of similar, or of slightly higher magnitude than for compartments experiments with non-combustible surfaces, temperature measurements of the compartment experiments with combustible surfaces and non-combustible surfaces are given in Figure 4.14 (b) where nearly similar temperature developments can be observed. Theoretically, a difference can be explained by the thermal inertia as structural timber elements act as an insulation material where a low amount of heat can be conducted to the solid's inside, and, further, stored in the building components. The apparent limitation of the difference can be explained by the limiting oxygen access for combustion in the compartment which does not allow for a higher heat release rate in the compartment fires (interior HRR) for ventilation controlled (VC) fires. Ventilation controlled fires are compartment fires where the combustion rate inside the compartment is governed by the limited access to air and consequently to oxygen due to the limited compartment opening which allows for the exchange of fresh air and (hot) combustion gases. That the majority of severe compartment fires are VC is well researched [81].

While the temperatures were reached similar temperatures with about 1100°C in fire compartments with non-combustible and combustible interior compartment surfaces (protected and unprotected solid timber [117, 74]), a significant difference was observed exterior the compartment at the facade: For the experiments with combustible interior surfaces, an exterior plume appeared, see Figure 4.15. Observing the extreme differences also documented in [58, 60, 74, 117] and shown as HFS measurements at the level of the window above the fire compartment, see Figure 4.16 (a), the effect of the increased fuel load due to the combustible interior surfaces is apparent. A fist approach to estimate the increased fire loads by structural timber was mentioned by Friquin-Leikanger [62]. Friquin-Leikanger proposed to estimate in a first step the design fire for a particular compartment, e.g. using the parametric design fires implemented in Eurocode 1 [34] . Subsequently, the movable fire load should be increased by the structural fuel load corresponding to the charring depth estimated by Eurocode 5 [35]. Thus, the total fire load
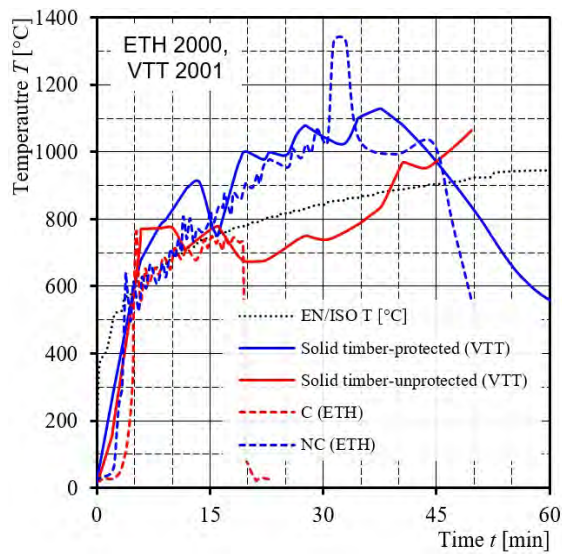
Figure 4.15:   HFS measurements at the window above the fire compartment for compartment experiments with and without exposed structural timber modified from [74] (a) Exterior plume in front of a window at a compartment fire experiment 7 min after fire ignition with interior combustible surfaces (left, own figure) and non-combustible surfaces (right) [117] (b). Own figure (left), Figure by T. Maag (right).

would be the sum from the movable fire load and the structural fire load corresponding to the parametric fire design:

$$Q_{tot} = Q_{mov} + Q_{st} \tag{4.18}$$

where

Q_{tot} is the total fire load , in MJ;
Q_{mov} is the movable fire load according to the compartment occupancy, in MJ;
Q_{st} is the fire load of the structural timber, in MJ/m².

whereby the structural fire load provided by structural timber can be defined by:

$$Q_{st} = E_{st} \cdot d_{char,para} \cdot A_{st} \tag{4.19}$$

where

Q_{st} is the fire load of the structural timber, in MJ;
E_{st} is the energy per cubic metre structural wood, in MJ/m³;
$d_{char,para}$ is the charring depth corresponding to the parametric fire design, in m;
A_{st} is the surface of the structural timber, in m².

In the following, the indicated approach by Firquin-Leikanger [62] is applied to VC fires. Following well-established design procedures, an increased total fire load which comprises the movable fire load (defined by the occupancy) and the structural fire load (defined by the thickness of the char layer), see Eq. 4.19 and 4.18, respectively, the fire duration would be significantly longer as the combustion in the compartment would be limited by the ventilation opening. Exemplarily, for the standard ISO fire room (8.6 m² floor area, 46 m² enclosure surface) where all surfaces would be made from solid wood, the approximate additional fire load due to charring in a 60 min fire would correspond to a fire load of about 1700 MJ/m². This value corresponds approximately to a library occupancy considering the 80% fractile [34]. However, from the compartment experiments referenced in the literature and mentioned here, it is apparent that a significant amount of the volatiles created in the compartment will combust exterior, leading to a significant exterior heat release. This increased heat release, the external combustion and the longer flaming at the compartment's exterior at the facade respectively are currently addressed qualitatively by the limitation of the combustible surfaces depending on the building class (e.g. Germany [17, 16]), limitation of combustible elements on the exterior of a building (e.g. Sweden [21]) or material specifications and special fire stops in ventilated the facade systems (e.g. Switzerland [181, 28]). A more recent approach developed further the aforementioned proposed methodology based on a series of compartment experiments. It was found that about 70% of the created structural fire load corresponding to the created charring depth, combust outside, see Brandon [22]. Recently, the approach by Brandon [22] was discussed and further developed [180] based on the findings presented in Chapter 3.4.
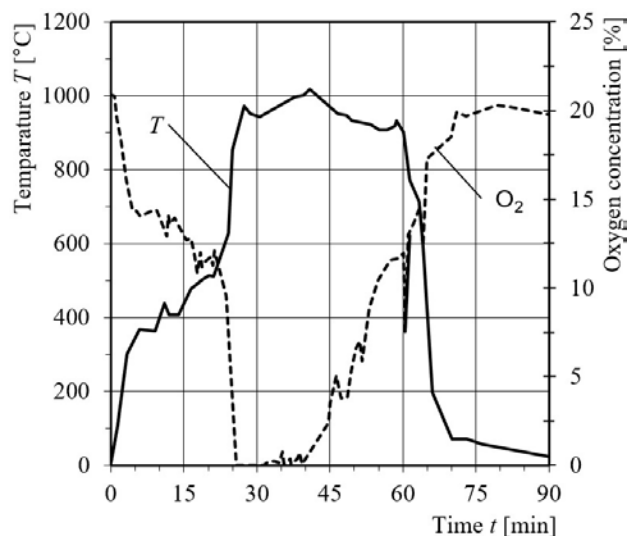
Figure 4.16: Compartment temperature and oxygen concentration in a compartment fire experiment modified from Lennon et al. [112].

Comparing the oxygen concentration in fire testing furnaces and compartment fires, the following can be concluded. For specimens exposed to fire in furnaces, previously presented for combustible and non-combustible products in Figure 4.11, a concentration of approximately 5% can be expected which is in compliance with regulations of [37]. This is in agreement with the literature where for furnace tests in a model scale furnace oxygen concentrations lower than 6% were reported [55]. Correspondingly, recent data from full-scale furnaces complete this trend [109]. From simulations applying zone-models or field models, it is well known that VC fires exhibit a lean environment as the movable fuel, typically arranged on the floors, tend to consume most of the oxygen provided by the air inflow. Available measurements of the oxygen concentrations in compartment experiments confirm the physics behind this description of the environment during the fully developed fire, e.g. Figure 4.16. After an initial rise of the temperature to about 400°C, the temperature increase is limited until the windows were punched to initiate a flash-over fire at approximately 25 min. Parallel to the temperature increase to about 1000°C, the oxygen level drops to levels near zero until the temperature starts to fall before extinguishing work were initiated at about 60 min.

Both test conditions, the maximum temperature and the limitation of oxygen reflect the conditions in an under-ventilated fire compartment. Relating the increased fire load in fire compartments with combustible products, described by Eq. 4.19 and 4.18 respectively, with the reduced amount of burner fuel needed in fire resistance furnace when combustible products are fire-exposed, one could conclude that the fire duration in a compartment would be extended accordingly. However, from observations and measurements during compartment fire experiments it is known that a considerable amount of the combustible

gases will leave the compartment unignited, which may reduce the extended fire duration to a certain amount. While Brandon proposed a corresponding reduction of the structural fire load in the steady-state phase by fitting calculations to measurements to 0.3 [22], Schmid et al. analysed the heat stored in the char layer and could verify a reduction between about 0.4 and 0.7 [180].

With respect to the decay phase it seems to be important to discuss whether combustible products would undergo sustained burning or self-extinguish. From many fire resistance tests it is known that timber member would self-extinguish when left on the furnace. E.g., recently this was shown even for long standard fire exposure when a solid timber deck in a full-scale standard fire test of 120 min was left on the furnace. Already some minutes after it was observed that no sustained flaming occurred, temperatures dropped significantly despite the fact that the heated furnace walls were still emitting considerable amount of energy. This self-extinguishing behaviour is also known from certification tests where test labs leave the specimens on the furnace after the test termination rather than extinguish them with water. Contrary, other research showed that induced air flow into the furnace compartment is able to influence the load bearing behaviour of timber elements [98] and that air flow has an impact on the potential for self-extinguishment [43] and influences the charring of timber [168, 176]. Consequently considering, the thermal exposure as independent of a specimen's material, to describe the exposure conditions of a combustible specimen in an improved way, the gas characteristics, i.e. the movement of the gas and the oxygen concentration, should be further considered. Thus, it seems apparent that, exceeding the thermal exposure, the term "fire exposure" should be introduced which comprises the thermal exposure and the gas characteristics of the environment.

4.12 Summary of this Chapter

The obtained results agree well with the literature, however, discussing the physics it is shown that heat flux measurement should be used with special care. It can be concluded that the thermal exposure observed in fire resistance tests is a reasonable measure to describe post-flashover fires, and that, in fire resistance testing furnaces, the thermal exposure of combustibles is as for non-combustibles. The lower amount of fuels required when testing combustible products can be related to, firstly, the contribution by the product itself, and (a) the lower thermal inertia typically observed for combustible products. Both conclusions indicate longer fire durations in real fires when the movable load is defined. It should be highlighted, that a considerable amount of created combustible gases would not burn in the compartment but outside.

In this Chapter, the physics of heat transfer was summarised with special consideration of structural timber. While the mixed boundary condition is observed in many applications in FSE, the first boundary condition may be applicable for fire-exposed timber as it acts as an isolating material. Furnace experiments were presented where water cooled heat flux sensor (HFS) measurements were performed in different positions (depths) and

locations and compared to results available in the literature. In general, a large scatter ($\pm 25 \text{ kW/m}^2$) was observed in the literature and of measurements performed in this study but the trend follows a simplified default curve between zero and 180 kW/m^2 at 120 min. No difference was found for combustible and non-combustible surfaces. No difference was found for measurements of different positions, most likely due to the limited oxygen content which does not allow flaming combustion at the surface of the timber in a oxygen limited furnace compartment. Heat flux measurements behind the plate thermometer (PT) are not higher behind the PT than in front of the furnace control device as no flaming combustion is possible due to the low oxygen concentration which can be observed also in compartment fires preventing additional heating. A source of uncertainty is the measurement technique per se as HFS measurements include (i) the absorbed radiant heat flux (ii) minus the emitted radiant heat flux (iii) plus the heat flux by convection. The convective part, (iii), cannot be estimated easily for environments with high gas temperature. In contrast, for plate thermometers (PT) at high gas temperatures, the convective part is negligible. The oxygen concentration in compartments fires is as low as in furnaces which explains that a considerable amount of the pyrolysis gases will burn outside of a ventilation controlled compartment fire. Thus, it was concluded that furnace tests are a proper mean to test combustible products as for non-combustibles as the thermal exposure can be expected to be equal and the oxygen levels are close to zero in both cases. The reduced burner fuel consumption in fire resistance tests with combustibles can be explained by the lower thermal inertia of wood compared to e.g. concrete and the contribution by the combustible specimen. This additional fire load may increase the combustion time in a compartment fire but a considerable share of this additional fire load will burn outside of the compartment which is currently addressed in various ways by regulations. Limited design tools are currently available to estimate the additional duration. Referring to the initial question if combustibles receive a different thermal exposure, the following can be concluded: Thermal exposure can be defined as exposure to an incident radiant heat flux and a gas temperature. From the literature and the test results presented here, it can be concluded that (1) the thermal exposure of combustible materials is not different from non-combustibles when tested in furnaces and (2) that the thermal exposure of combustible products in the post flashover phase of ventilation controlled compartment fires is similar to the thermal exposure in fire resistance tests. Due to the sensitivity of combustible materials to the oxygen concentration in the environment at their surfaces, it seems obvious that the gas characteristics should be further considered, thus, the term of "fire exposure" comprising the thermal exposure and the gas characteristics of the environment is defined here.

The comparison of the energy balance of furnaces is a complex task as the thermal response (e.g. the inertia of the furnace walls) of the furnaces in consideration may be significantly different. Comparing results from the burner fuel consumption may be done considering the mass loss of the specimen. However, for components producing a char layer, for a deeper analysis, the stored energy content of the char layer with an eventually higher heat content per unit mass might be relevant, see Sections 3.4 and 6.

Chapter 5

Contribution of structural timber to the fire dynamics in compartment fires [1]

5.1 General

This Chapter is subdivided in two parts. The first part, Section 5.2, provides the theoretical determination of structural fire load, potentially available to contribute to the fire dynamics in compartments. In the second part, Section 5.3, the analysis of experimental data is presented where the combustion behaviour of structural timber in compartment fire is studied. In the second part, the overall characteristics of compartment fires are investigated with the focus of the associated behaviour of exposed timber structures considering the theoretical background derived in the first part. Both parts are used as input for the modelling of fires in compartments with structural timber fuel, in Chapter 6.

Parts of this Chapter are based on experiments described in Chapter 3, which were performed by the team of IBK at ETH Zürich supported by numerous students, and on data and material provided by N. Werther (TU Munich, Germany), D. Brandon (RISE, Sweden) and A. Just (RISE, Sweden and Taltech, Estonia). Related publications were drafted together with the team of IBK at ETH Zürich together with N. Werther, D. Brandon, A. Just and F. Richter (London Imperial and University of California, Berkeley).

5.2 Fuel by structural timber

5.2.1 General

Fire safety engineers use the heat release rates (HRR) of products as one of the most important parameters for the modelling of fires [97]. Correspondingly, structural engineers specialised in fire resistance design use the charring rates to describe the performance of structural timber elements exposed to fire. The basic input values to the fire resistance design models are typically one dimensional charring rates for various products or assemblies. They have been derived empirically and are, in the majority of cases, related to a default temperature-time exposure, typically, the EN/ISO standard fire curve [37, 85]. Some studies investigated the HRR of wood products in the cone calorimeter, however, the testing environment defers significantly from conditions in a compartment fire. Only limited studies tried to connect the HRR with a charring rate such as Crielaard et. al [43].

Assuming that the charring rates are well researched, an apparent approach would be to directly determine the HRR by wood products using the charring rate based on the energy content of wood. The heat content - sometimes referred to as energy content, caloric or heating value - of wood is between about 15 MJ/kg and 20 MJ/kg. The range can be explained by the moisture content and the wood species which may show a variation of the wood component resin. Typically, the species also show a significance difference in their densities, e.g. poplar 350 kg/m^3 and oak 680 kg/m^3. Typically, in Europe softwood species are used for structural timber which exhibits a mean density between 350 kg/m^3 and 520 kg/m^3 for the strength classes C 14 and C 50, respectively, at 12% equilibrium moisture content [36]. A corresponding dry density can be derived using

well established empirical relationships. Consequently, for the determination of structural fuel load, fuel load density and further the HRR, respectively, several characteristics and their corresponding modification are needed. The assumptions and conditions, partly visualised in Figure 5.1 are listed here and presented in the following:

(1)   a reference heat content for dry wood material of 17.5 MJ/kg;

(2)   a reference density of 450 kg/m^3;

(3)   an reference moisture content: 10%.

For the modification to meet actual material properties, the following correction factors are assumed:

(4)   a modification factor for deviations of the dry density (dry): α_ρ;

(5)   a modification factor to consider the moisture content: α_{MC};

Further, the contribution of the timber structure to the total fire load (density) and the HRR are dependent on:

(6)   the area of exposed surfaces or structural timber: A_{st};

(7)   the actual charring rate: β_{st}.

To address the typical combustion efficiency losses observed from compartment fires and, in additions, the combustion behaviour of structural timber in compartment fires, two corrections are presented:

(8)   a factor to consider the combustion efficiency of the fuel: χ;

(9)   a factor to consider the combustion behaviour of the structural timber: α_{st}.

5.2.2   Reference heat content

The energy content, in the following referred to as the heating content of a material can be described using a higher or upper and lower heating value, HHV/UHV and LHV, respectively. The HHV, also known as gross calorific value, describes the heat released during the combustion process if all combustion products reach again the initial temperature after the combustion process is completed. Thus, for the HHV, the vaporisation and re-condensation of water are included in this consideration. Contrary, the LHV, also known as net calorific value, considers the energy required to vaporise the water only. Thus, the LHV is relevant if the re-condensation of the water occurs exterior of the system which is relevant for most of the considerations in fire safety engineering. The heat content of wood is well researched and documented in the literature [30, 63] and further
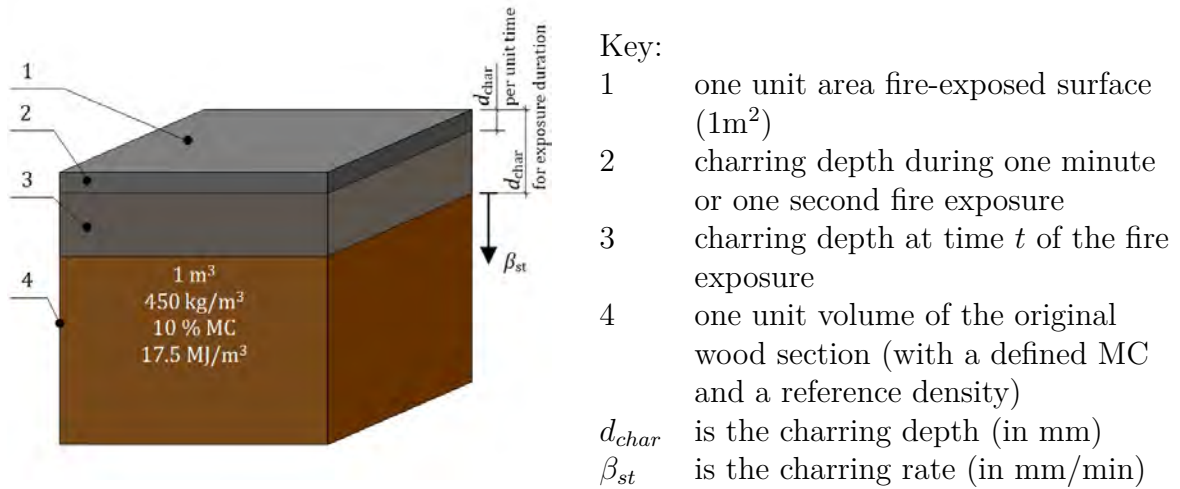
Figure 5.1: Assumptions for the estimation of the fire load by structural timber. Own figure.

specified in fire design standards, e.g. Eurocode 1 [34]. In general, a dependency on the species can be observed which can be traced back to the different shares of the main macroscopic components, i.e. the chemical composition. A difference in the heat content is documented for softwood and hardwood which can be traced back to the higher share of lignin [68]. The lignin content differs significantly for softwood and hardwood respectively, see Figure 5.2, though the reader is advised these are not automatically valid for all wood species.

5.2.3 Reference density

It should be considered, that the mean density of wood specified e.g. in EN 338 [36] relates to the normal condition (20°C, 65% RH) for inducing 12% MC in wood. In fire design, for the movable fire load, typically, a the 80% fractile value is applied to take into account the large scatter of the distribution of the movable fire load for an occupancy. Apparently, the timber material properties, including the density, exhibit a certain scatter. The aforementioned reference density of 450 kg/m³ at 10% EMC corresponds the strength class C45 taking into account the mean value; the 80% fractile value would correspond to a class of about C24, a typically used class. However, it should be considered that the fractile value should address the uncertainties of the distribution of the fire load, which is not the case for structural timber as all elements are fabricated, arranged and exposed in a well-defined way. Thus, it is assumed that the mean value of the density of structural density can be applied. The correction for the density α_ρ allows the consideration of other densities than the reference density of 450 kg/m³ with a simple relationship given in Eq. 5.1 while the factor is equal to unity, $\alpha_\rho = 1.0$, for the reference case.

$$\alpha_\rho = \frac{\rho}{450} \tag{5.1}$$

where

α_ρ is the correction coefficient for the density (dry);

ρ is the actual dry density, in kg/m^3.

5.2.4   Reference moisture content

The correction for the moisture content is intended to account for the lower net caloric value for moist wood. The fire design is expected to be done for compartments representing for an occupancy of residential or office use providing a comfortable indoor climate. Thus, the herein arranged structural timber is exposed to an indoor climate. Depending on the exterior climate and the heating, wood exposed to indoor climates show an equilibrium moisture content (EMC) of about 5% to 10% for a relative humidity of 25% and 55% at 21°C, see Glass et al. [66]. However, massive timber members may show a significantly delayed response time and experience seldom a moisture content below 10% EMC [75, 64]. Accordingly, the determination of the reduced net calorific value for 10% MC follows [34]. The development of the correction coefficient can be derived following Eq. 5.2 and is provided graphically in Figure 5.2. For the reference moisture content it can be determined to $\alpha_{MC} = 0.89$.

$$\alpha_{MC} = \frac{17.5 \cdot (1 - 0.01 \cdot u) - 0.025 \cdot u}{17.5} \tag{5.2}$$

where

α_{MC} is the correction coefficient for the moisture content;

u is the moisture content expressed as percentage of dry weight.

5.2.5   Combustible surface area

Apparently, the surface area of structural timber is a significant parameter when the contribution to the fire in a compartment should be assessed. The unprotected surface area of structural timber is assumed to be involved in the fire dynamics with respect to the contribution to the fire load. As introduced in European standards, e.g Eurocode 1 [34], the contributing area is related to the floor area of the fire compartment. Therefore, a corresponding factor is introduced defining the ratio of the floor area to the surface of the structural timber as in Eq. 5.3:

$$\alpha_{A,i} = \frac{A_{st,i}}{A_f} \tag{5.3}$$
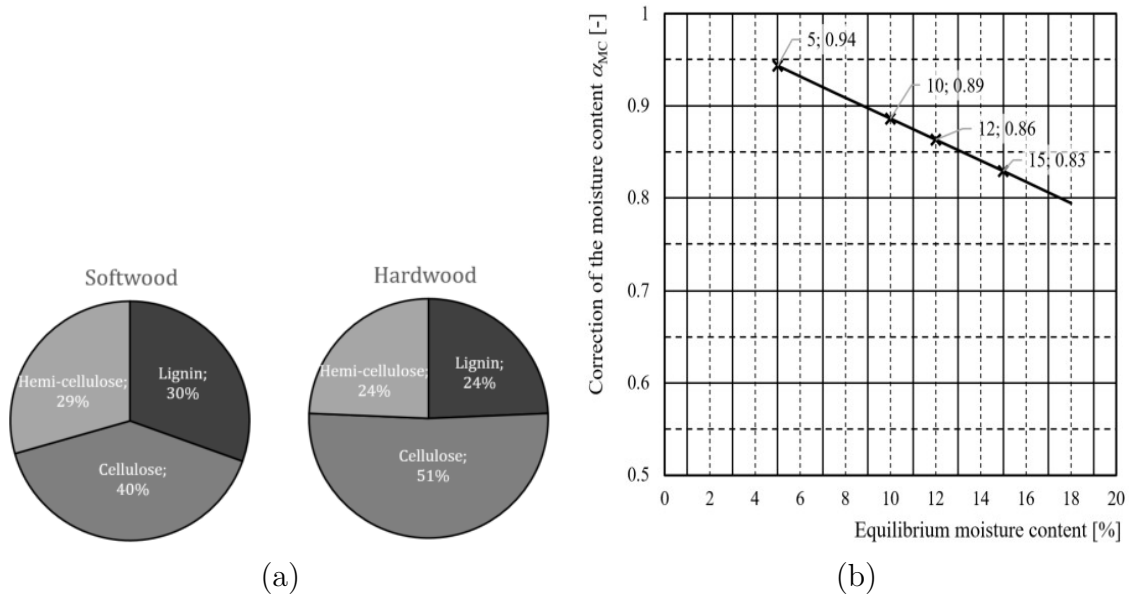
Figure 5.2: Main components of soft and hard wood (a) and correction coefficient α_{MC} for the moisture content of structural timber (b). Own figures.

where

α_A is the correlation coefficient for the structural timber surfaces;

i is the zone $i = 1$ to 3;

A_{st} is the surface of structural timber, in m²;

A_f is the compartment floor area, in m².

For later discussions, it should be noted that three zones have been introduced in Eq. 5.3, i.e. the (1) ceiling, the (2) upper and (3) lower zone. Wall elements are considered in zones (2) and (3). The sectioning in zones allows on one hand to account for the different oxygen concentration in the upper and lower zone and, on the other hand, the different heat transfer coefficients for vertical and horizontal surfaces. In general, the factor α_A is not constant during an entire fire duration as eventually applied fire protection may fail protecting the initially protected surfaces from charring by falling-off. Eurocode 5 [35] further recognises a situation where charring occurs behind an applied fire protection system, i.e. a not fully encapsulated member. As recognised from standard fire , in this situation from the start of charring to fall-off of the fire protection system, a 30% reduction of the charring rate might be assumed, considered by a factor α_{pr}. Thus, Eq. 5.3 can then be extended to:

$$\alpha_{A,i} = \frac{\alpha_{pr} \cdot A_{st,i}}{A_f} \tag{5.4}$$

where

α_{pr} is the correction coefficient for the protected but not entirely encapsulated structural timber surfaces, $\alpha_{pr} = 0.7$ for protected but charring timber surfaces.

5.2.6   Charring rate

The charring rate is the rate of the conversion of structural timber in the char layer; it reduced the virgin wood section able to carry loads. The charring rate is considered to be a proper measure to describe the contribution to the structural fire load proposed by various authors [22, 124]. In the simplest case, there is only one charring depth to be considered in a compartment. Correspondingly, in this case, there is only one description for the charring rate. At that point it should be highlighted, that, contrary to the simplified design rules available for standard fire, in general, the charring rate is not constant for general design fires. The charring rates have been empirically determined for standard fire and for parametric fires. Recently, an improved proposal for a general determination of charring depth has been made by Werther [205]. The proposal has similarities to a cumulative radiant energy method (CRE) [134], but uses the compartment temperature as correlated variable. The regressions are based on fire tests with various heating regimes. Two regression functions have been suggested by Werther [205, 206], given in Eq. 5.5 and 5.6:

$$d_{char,upper} = \left(\frac{kT}{4.4 \cdot 10^5}\right)^{\frac{1}{1.35}}$$ (5.5)

$$d_{char,lower} = \left(\frac{kT}{1.35 \cdot 10^5}\right)^{\frac{1}{1.6}}$$ (5.6)

where

$d_{char,upper}$ is the charring depth (upper boundary); in mm;
$d_{char,lower}$ is the charring depth (lower boundary); in mm;
kT is the cumulative thermal impact described by the temperature, in ($K^2 \cdot min$).

It should be noted that the upper and lower bound have been originally developed to allow best fit in the heating phase (upper boundary, Eq. 5.5) and the entire fire development (lower boundary Eq. 5.6), respectively. For the development of the TiCHS model, the correlation with respect to the best fit for the entire fire development was considered relevant. For the use in the structural fire design, in the current revision of Eurocode 5 [40], a mean value has been proposed, see Eq. 2.4. These correlations allow the designer to predict a charring depth based on any design fire, e.g. a compartment temperature. Figure 5.3 (a) shows the prediction of the charring depth for a temperature prediction according to the German national Annex of Eurocode 1 [48] assuming the start of charring when the compartment temperature exceeds 300°C. Deriving the
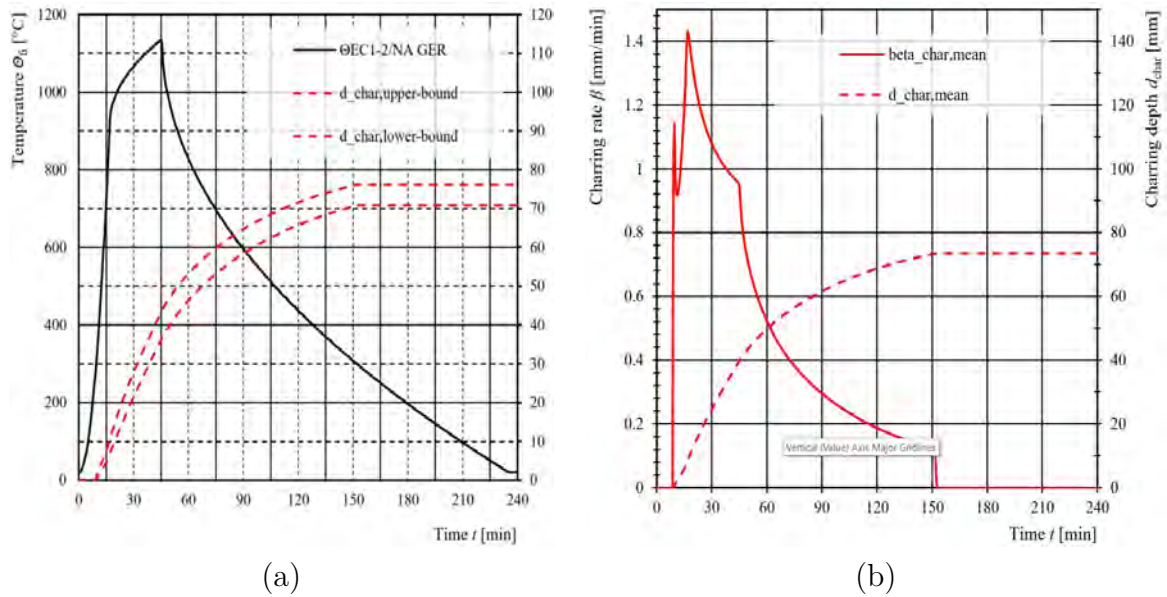
Figure 5.3: Time-temperature curve for a parametric fire design according to Eurocode (GER) [48] and the charring depth according to the cumulative temperature charring model. Charring depth for a non-standard fire (a) and development of the corresponding charring rate (b). Own figures.

equation with respect to time allows the determination of the charring rate at any time. Figure 5.3 (b) shows the development of the mean charring rate according to Eq. 2.4 and its derivative. It is apparent that the charring rate is not a constant value but experiences a significant variation over the time with various phases. The charring rate shows peaks directly after the ignition and, subsequently, a reduction of the charring rate parallel to the development of a char layer followed by a reduction of the charring rate corresponding to a significantly different temperature development in the cooling phase.

5.2.7 Heat Release Rate

In this Section, the energy content of fire-exposed timber and the associated available energy for heat production will be discussed and developed into the HRR, based on the characteristics and factors presented in the previous Sections 5.2.2 to 5.2.6. Considering the energy stored in dry timber, i.e. 17.5 MJ/kg and a reference density assumed to 450 kg/m³, the specific HRR of dry timber, i.e. with zero moisture content, can be determined to:

$$\dot{s}_0'' = \frac{H_{u,0} \cdot \rho_0}{60} = 0.13 \tag{5.7}$$

and further, including the correction for the density and the moisture content:

$$\dot{s}''_w = \dot{s}''_0 \cdot \alpha_\rho \cdot \alpha_{MC} \tag{5.8}$$

and simplified for structural timber, assumed to exhibit a MC of 10%:

$$\dot{s}''_{10} = 0.12 \cdot \alpha_\rho \tag{5.9}$$

where
$\dot{s}''_0$ is the specific HRR of dry wood for one mm charring per minute, in MW/m² · mm/min;
$\dot{s}''_{10}$ is the specific HRR for structural timber for one mm charring per minute, in MW/m² · mm/min.

Using Eq. 5.9 it should be considered that for the fire design, the HRR should further consider a combustion efficiency χ which is normally set to a value between 0.7 and 0.9. Commonly, for cellulosic type fuels the combustion efficiency is set to $\chi = 0.8$. Considering this combustion efficiency, the effective HRR of structural timber given in Eq.5.9 would decrease further. However, as the structural fuel load might be concentrated with the movable fire load, it is not integrated in the specific HRR $\dot{s}''_{10}$.

The possibilities for a comparison with direct measurements is limited as the testing conditions seem to significantly influence the determined HRR values and, further, that wood specific characteristics, i.e. the charring rates, are often not measured. If sensors are installed to follow the temperature development throughout the specimen, they are often incorrectly installed, compare Fahrni et al. [53]. Standard cone-calorimeter test with spruce panelling showed a HRR between 0.22 MW/m² and 0.24 MW/m², similar single burning item (SBI) tests with spruce wood resulted in slightly lower HRR of 0.22 MW/m² [211]. The authors mentioned that these values should be applicable for fuel-controlled fires and omit to specify (i) charring rates, (ii) the mass loss rates and (iii) the time to burn-through. Burn-through is understood as the time when the 20 mm thick panelling would be consumed which would allow the determination of a mean charring rate. It remains unclear if the values are maximum, mean or values during a steady state burning phase. Considering a HRR of structural timber of $\dot{s}''_{10} = 0.12$ and a combustion efficiency of $\chi = 0.8$, the corresponding charring rates would be up to about 2.5 mm/min. The higher values in the SBI test may result from the vertical arrangement of the specimen. In the following compartment experiment, Wilk et al. [211] determined a HRR of the same cladding type between 0.15 MW/m² and 0.18 MW/m² which corresponds to charring rates of 1.6 mm/min and 1.9 mm/min, respectively, using the above mentioned relationships. As indicated before, no further details about the charring rates are given which makes it impossible to determine whether the specified HRR are peak values, mean values or values in the steady burning state. Further use of the values is limited as they are in contradiction to the recorded structural HRR over 45 min implying a mean charring rate of 0.44 mm/min based on the 20 mm thick timber cladding and assumed burn-trough.

5.2.8 Structural fire load

The structural fire load provided by timber members can be determined corresponding to the volume of the structural timber involved in the fire. This is done taken into account the characteristics and factors presented in the previous Sections 5.2.2 to 5.2.6. Considering the energy stored in dry timber, i.e. 17.5 MJ/kg and a reference density assumed to 450 kg/m^3, the specific fire load of dry timber, i.e. with zero moisture content, can be determined to:

$$s_0 = H_{u,0} \cdot \rho_0 = 7.88 \tag{5.10}$$

and further, including the correction for the density and the moisture content:

$$s_w = s_0 \cdot \alpha_\rho \cdot \alpha_{MC} \tag{5.11}$$

and simplified for structural timber, assumed to exhibit a MC of 10%:

$$s_{10} = 6.98 \cdot \alpha_\rho \tag{5.12}$$

where
s_0 is the specific structural fire load of dry wood for one mm section depth, in MW/m^2 per mm/min;
s_{10} is the specific structural fire load of structural wood with a moisture content as expected for heated indoor climates for one mm section depth, in MW/m^2 per mm/min.

Thus, considering a simplification with a fixed density for structural timber, which should cover the majority of construction, the structural fire load can be rounded to 7.0 MJ/m^2 per mm structural timber. This value is higher than the value of 5.39 MJ/m^2 per mm charring depth proposed by Schmid and Brandon et al. [175]. The lower value origins from measurements by Crielaard [42] who determined this value simultaneously with the measurements of the charring rate during a nearly steady state burning of a test specimen in a cone calorimeter set to 75 kW/m^2 external radiant heat flux. Comparing both values, the following ratio would be determined:

$$c = 5.39/7.0 = 0.77 \tag{5.13}$$

consequently, expressed for an effective specific structural fire load, to:

$$s_{10,ef} = c \cdot s_{10} \tag{5.14}$$

and, finally, explicitly considering the combustion efficiency to:

$$s_{10,ef} = \chi \cdot \alpha_{st} \cdot s_{10} \tag{5.15}$$

where

$s_{10,ef}$ is the effective specific structural fire load of structural wood with a moisture content as expected for heated indoor climates for one mm section depth, in MW/m^2 · mm/min;

s_{10} is the specific structural fire load of structural wood with a moisture content as expected for heated indoor climates for one mm section depth, in MW/m^2 · mm/min;

c is the factor to describe the combustion efficiency and the combustion behaviour of structural timber forming a char layer which is able to store heat;

χ is the factor to describe the combustion efficiency in compartment fires based on the type of fuel load;

α_{st} is the factor to describe the combustion behaviour of structural timber in compartment.

The factor representing the afore presented ratio of $c = 0.77$ agrees well with the combustion efficiency used for cellulosic fuel loads, set to $\chi = 0.8$, see Chapter 5.2.7. The higher value of 7.0 MJ/m^2 per mm can be interpreted as value associated with the complete combustion of the energy content of wood while the lower value, 5.39 MJ/m^2 per mm, seems to be an effective value. In the following, the factor c will be investigated. It is claimed that the factor is the product of $\alpha_{st} \cdot \chi$ describing the heat storage with the individual factor α_{st}.

5.3 Combustion behaviour of structural timber

5.3.1 General

A specification for the correction with respect to the combustion characteristics of structural timber is more complex than the previously mentioned correction factors. Contrary to a combustion efficiency $\chi = 0.8$ to describe incomplete combustion (e.g. creation of soot) of fire fuel, the factor α_c should consider the formation and involvement of a new material, i.e. the char layer, in the fire dynamics of a compartment fire. The char layer is formed and consumed in various phases of the fire. In the literature, the appearance of such a factor can be traced back to the first compartment fire experiments with exposed structural timber where a significant exterior plume was observed for the compartment tests and the total HRR measured [117, 74]. Hakkarainen [74] tried to quantify the structural fire load released and estimated the exterior HRR. She estimated the exterior burning of 50% for a compartment with exposed structural timber (experiment VTT-T1). Later, Brandon [22] proposed a fitting factor based on the HRR measurements developed for a large number of compartment experiments, comparing them to predictions. Until the maximum compartment temperature was reached, a factor $c_B = 0.3$ was

introduced to reduce the structural timber fuel which Brandon quantified based on the charring depth [22]. Thus, in the steady-state burning phase of a ventilation controlled fire, only 30% of the potential structural timber fuel would contribute to the HRR inside the fire compartment and the temperature development, respectively. From Brandon [22], it remains unclear for which wood densities the factor is valid and if other corrections or modifications were considered. Thus, it was not explicitly stated if the heat content of wood has been reduced already by 20% due to incomplete combustion typically described by $\chi = 0.8$ for cellulosic based fuels, or, the actual moisture content of wood, α_{MC} described above, reducing the heating value of wood. The actual proposal in the current revision of Eurocode 5 [40], expected to be implemented in the revised Eurocode 1, systematically considers the influencing parameters for the moisture content, the density of structural wood and the combustion efficiency. As it is assumed that future development will be able to describe α_{st}, this factor has been already implemented for the calculation of the structural fire load and the HRR, respectively. By default, it is suggested to set the factor conservatively to $\alpha_{st} = 1.0$ [40].

5.3.2   Method

To analyse the existence of factor conservatively to α_{st} and estimate the order of magnitudes of the factor, a two-step approach was performed. In a first step, the energy content in a char layer, corresponding to the potential heat released to a compartment was analysed. To allow for the estimation of the stored energy, the density and the heat content of the char layer were developed and subsequently considered. In a second step, the fire dynamics documented for compartment experiments was studied when structural timber was involved in the fire dynamics.

5.3.3   Analysis of the heat content stored in the char layer

The total energy stored in a material can be assessed using the heat content and the corresponding mass of the solid. In the following, this was done for the char layer which was related to the virgin wood. A default heat content for the char layer material was derived by bomb calorimetry analysis in Section 3.4. Furthermore, distinct density gradient was developed for two examples, see Figure 3.23. The associated temperature profile for the examples, previously fire-exposed to EN/ISO standard fire, was developed. This was done using the thermal material properties of Eurocode 5 [35]. The material properties in Annex B of Eurocode 5 have been derived originally with respect to this exposure. The model is designated as BEC-model in the following. The temperature gradient was derived for this one-dimensional situation with the software SAFIR [61] and is presented with the associated density profile in Figure 5.4. For comparison reasons, the results are overlaid with data from the literature [159, 158]. In addition, the temperature history for the five levels analysed in Section 3.4 are given Figure 5.5 (a). For the temperature gradients, it should be observed from the measurements and the predictions that some
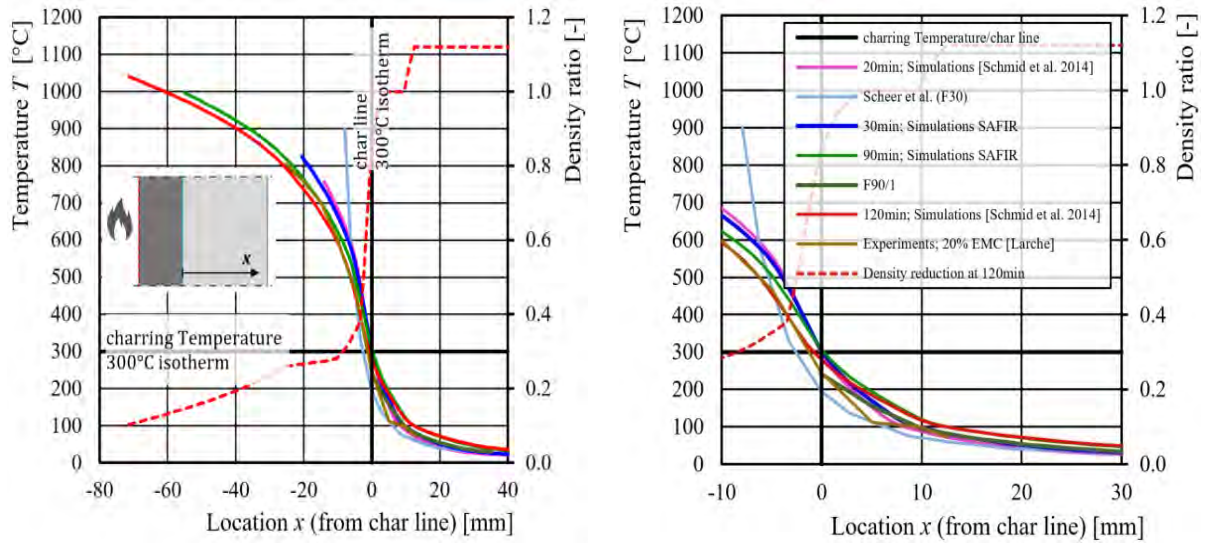
Figure 5.4: Temperature gradient of a fire exposed timber section by simulations and the associated density of the section according to literature and the BEC-model. Own figures.

mass loss occurs in the wood section near the char line, i.e. depths heated above 200°C. For simplicity reasons it is aimed for accounting all mass losses in the char layer only. Consequently, the mean mass of the char layer, was reduced from 23% to 22% as indicated by Line 3 in Figure 5.5 (b).

Utilising the data from experiments and the BEC-model, an energy balance was set up. The energy of the lost section, associated to the virgin wood and determined using the charring depth, was compared to the energy stored in the char layer. An energy analysis for charred structural timber in furnaces was done and compared to simulation data, see Table 5.1. Subsequently, the ratio for the effective combustion factor, i.a. a totally effective factor was determined, see Table 5.1 Line 8. Assuming a combustion efficiency of $\chi = 0.8$ for cellulosic based fuels, the corresponding factor associated with the char combustion or, the combustion of structural timber respectively, was derived, see Table 5.1 Line 8. All results for the combustion factor c and the char combustion factor, respectively, exhibit in the significantly large range of about 0.39 to 0.85 and exceed the value $c_B = 0.3$ proposed by Brandon [22]. However, the char layer in compartment fires may significantly deviate from those derived in Table 5.1. Subsequently, compartment experiments were investigated to analyse the combustion behaviour of structural timber with respect to α_{st}.

1	2	3	4	5	6	7	8	9
	Characteristic	Symbol	Unit	BEC-model EC [35, 61]	STP I VKF	STP III RISE	BC1 MPA	BC2 MPA
Material	Source							
Structural timber	Considered depth	$d_{char,60min}$	[mm]	36	37	37	38	37
	Corrected calorific value	$\Delta H_{st,10}$	[MJ/kg^3]	16	16	16	16	16
	Potential energy contribution	$E_{st,60min}$	[MJ/m^2]	248	253	260	235	239
Char layer	Determined calorific value	ΔH_{ch}	[MJ/kg^3]	31	31	31	31	31
	Energy storage	$E_{st,60min}$	[MJ/m^2]	91	39	93	123	123
	Combustion factor (total)	$c = \alpha_{st} \cdot \chi$	[-]	0.51	0.68	0.51	0.38	0.39
	Char combustion factor	α_{st}	[-]	0.63	0.85	0.64	0.48	0.49

Table 5.1: Energy analysis of charred structural timber sections. Stimulated results (Column 5) and results from furnace experiments (Columns 6 to 9).
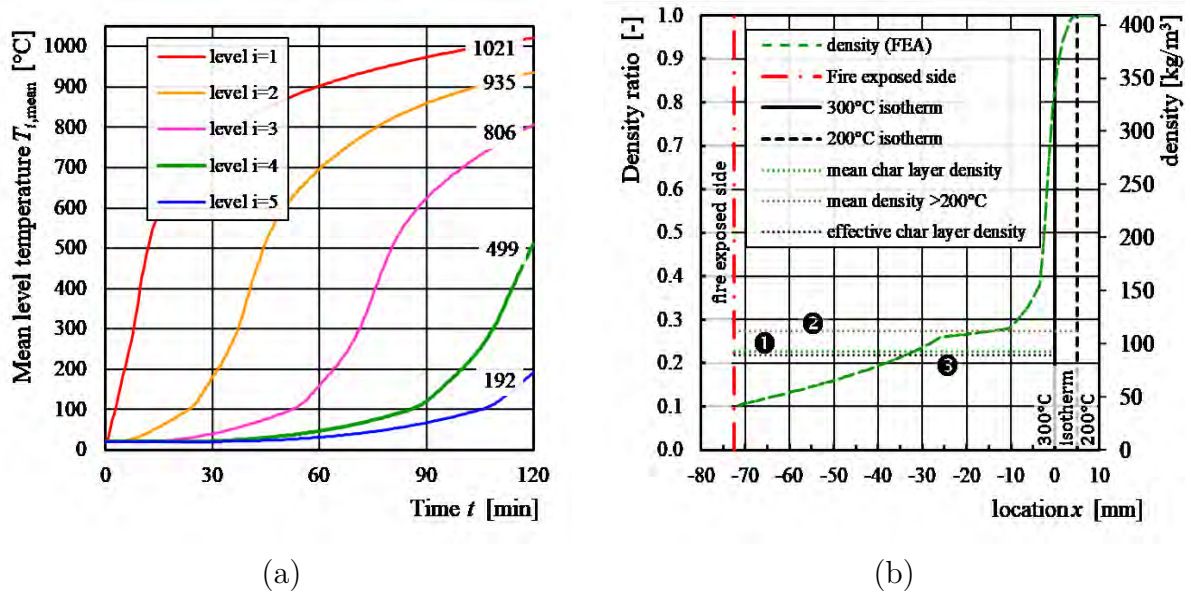
Figure 5.5: Means of the simulated nodal FEA temperature history of all five levels analysed in Section 3.4 including the final mean temperature at 120 min (a). Development of the effective density of the char layer; (1) Mean density of the heated depth exceeding 300°C, (2) exceeding 200°C and (3) lumped to the char layer only (b). Own figures.

5.3.4 Analysis of the combustion behaviour of structural timber in compartment fires

In this Section, the analysis is presented which was performed for compartment experiment campaigns where structural timber was involved in the fire dynamics. Consequently, the heat release is analysed of compartments with movable fuel load and with and without structural timber providing additional fuel by the combustible surfaces. Recently, compartment experiments with combustible surfaces came into focus of the fire safety engineering community, summarized e.g. by Östman et al. [141]. While, previous experiments with structural fire load were generally extinguished manually, most recent experiments focused on the capability to reach burnout. For some products with glued layers (i.e. cross-laminated timber; CLT), failure of the bond line integrity was observed in the fire situation. Subsequently, falling charring layers not able to stick to the walls or floors were able to fuel the compartment fire resulting in a cyclic burning, i.e. multiple flash overs and multiple decay phases. In this study, products acting as solid wood are studied and for experiments showing these type of failure, only the phases before the failure of the glue line integrity will be considered. An interesting experimental approach was used by McGregor and Medina [123, 125] when they performed experiments in identical compartments (floor area ca. 16 m^2) with and without the involvement of combustible surfaces of structural timber. Consequently, it was possible to isolate the contribution of
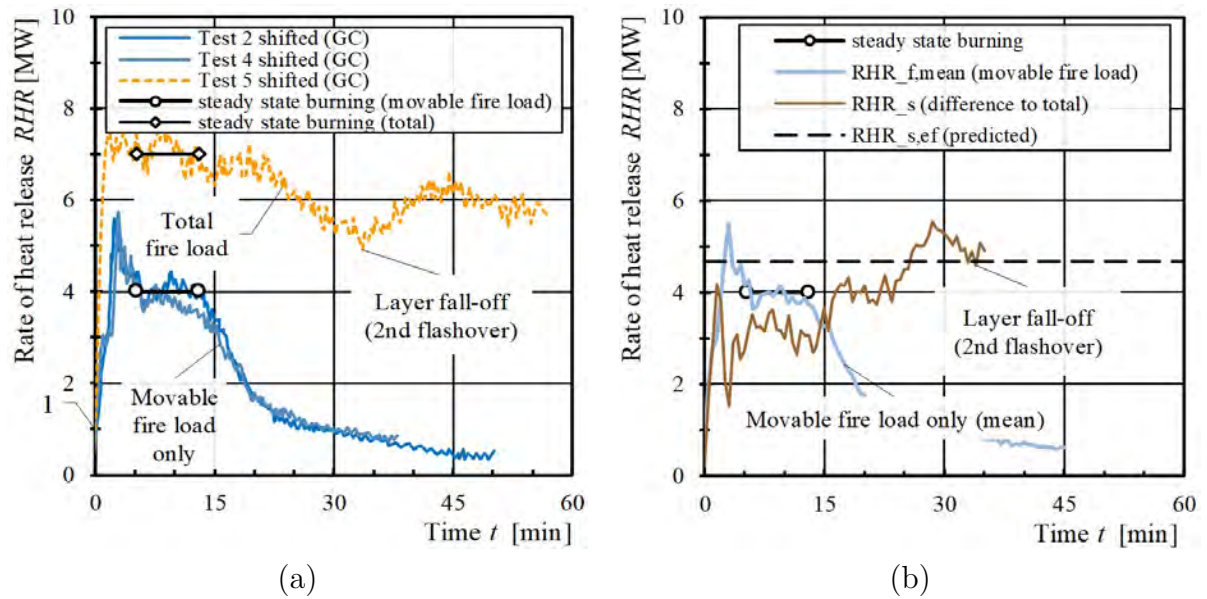
Figure 5.6: HRR of experiments by McGregor [123] summarized in Table 5.2 (a) and shifted average of experiments with movable fire load from (a) and the derived difference to the total HRR assigned to the combustible surfaces (b). Own figures.

the timber structure using the total rate of heat release measured with an industrial cone calorimeter. By an industrial cone calorimeter the rate of HRR can be determined based on the consumed oxygen when analysing the extracted combustion gases. The accuracy of such a measurement system was estimated by Dahlberg [46] who could specify a confidence interval with max. 16%. Table 5.2 reports selected measurements of experiments by McGregor [123] and Su et al. [190] where movable fire load was used.

The HRR of the reported experiments by McGregor [123] are plotted in Figure 5.6 whereby the curves have been shifted through the of 1 MW-point considered as flash-over point in time to allow for an improved comparison. Further, in Figure 10, the phase of the steady state burning is marked for experiments without the contribution of structural timber. The reported charring rates by McGregor [123] can not be used directly as the installation of the sheathed thermocouple sensors (highly conductive material) in the direction of the heat flux in the timber member (insulating substrate) gives significantly unreliable results as shown by Fahrni et al. [53]. The error is apparent as a charring rate of 0.85 mm/min based on measurements is significantly lower than 1 mm/min determined by observations, i.e. the fall-off of the 35 mm thick first layer of the CLT after about 34 min apparent in the HRR measurements in Figure 10. The higher charring rate was confirmed by the measurements of the virgin cross-section after the experiment. The results for the analysis of the compartment experiments show the combustion factor in ranges between about 0.5 and 0.8, see Table 5.2 Lines 8 and 9.

	Variable	Symbol	Unit	GC (Test 2) Ia	GC (Test 4) Ib	GC (Test 5) VI	JS (Test 1-1) II	JS (Test 1-4) IV
Experiment Characteristic								
Timber Structure	Exposed structural timber	A_{st}	[m²]	-	-	54	-	42
	Estimated charring rate	β_{st}	[mm/min]	-	-	1.0	-	0.9
Measurements	Peak rate	$HRR_{tot,max}$	[MW]	5.5	5.7	7.6	9.0	13.2
	Steady state phase	HRR_{tot}	[MW]	4.0	4.0	7.0	5.8	7.5
Predictions	Eq. 5.9	HRR_{st}	[MW]	-	-	5.8	-	4.2
Results	Char combustion factor	$c = \alpha_{st} \cdot \chi$	[-]	-	-	0.64	-	0.51
	Char combustion factor	α_{st}	[-]	-	-	0.80	-	0.63

Table 5.2: Energy release analysis of two compartment experiments campaigns by McGregor and Su et al. [123, 190].

5.4   Summary of this Chapter

In this Chapter, the heat release rate (HRR) of compartments with exposed structural timber surfaces is discussed. In total, three different approaches are presented. Firstly, a comparison of the available default heat content of structural wood and the HRR measured in cone calorimeter tests reported in the literature. It appears that a ratio of 0.8 could be observed, similar to the combustion efficiency coefficient for cellulosic based fires. This would mean, that 20% of the available energy would not be combusted or released as heat energy. It remains unclear if a further reduction is needed to account for the combustion behaviour of timber, which is considered in this thesis as the sum of the pyrolysis of wood, the creation of the char layer as (temporary) energy or heat storage. Secondly, an energy analysis of a fire exposed timber section is presented. Data from simulations and experiments are utilised and compared with each other. Thus, the density profile is superimposed with the default heat content of structural wood. The corresponding results show that, exceeding the combustion efficiency factor, a further reduction is justified to take into account the combustion behaviour of structural timber. This reduction was determined to be between about 15% and 50% which accounts for the heat storage in the char layer. Finally, the HRRs of two compartment experiments are compared for the cases where a compartment fire was investigated with and without the contribution of structural timber. The results verify the existence of a factor to describe the combustion behaviour. The factor α_{st} was observed to reduce the HRR by structural timber in the fully developed phase of a fire between about 20% and 35%. The bond line integrity of the structural timber remains as strict requirement for these values. It should be noted that this factor, considered here as a mean value, is not expected to be constant for, neither all compartment geometries, ventilation conditions nor the share of exposed structural timber surfaces. Furthermore, it should be noted that the stored heat may be released at a later, potentially unfavourable stage of the fire. The variability of the factor to consider the combustion behaviour is investigated with the TiCHS-model developed in Chapter 6.

Chapter 6

The Timber Charring and Heat Storage model [1]

---

[1]Parts of this Section are content of (journal) publications [178, 166]

6.1 General

In this Chapter, a model is developed to predict the contribution of the structural timber to the fire dynamics in a compartment fire. This Chapter is divided in three parts, Section 6.2 describes the elements of a framework to account for the behaviour of timber in compartment fires; Section 6.3.1 describes the development of the model, and Section 6.4 presents the application of the model on compartment fires including a validation using experimental data. The validation of model parameter used in the developed model and the model Validation are presented in this Chapter.

Previously, in Chapter 5, the main input for the consideration of structural timber has been presented. While most of the input are apparent when systematically analysing the fuel provided by structural timber, the parameter to consider the combustion behaviour of structural timber is not satisfactorily solved. Previously, rough estimates for an exterior combustion have been observed by Hakkarainen [74], followed later by a constant factor fitted to a large series of compartment experiments by Brandon [22]. Wade et al. [202] presented the use of a parameter study of costume-set factors to consider a fuel access. All mentioned methodologies experience shortcomings as the use of constants might imply conservative or non-conservative results. A further drawback is that they are generally not fit for application in draft situation, which might be a decisive case for timber structure in cross-ventilated fires.

The Timber Charring and Heat Storage model, in short TiCHS-model, is designed as a framework to combine various elements considered responsible for the description of a structural timber contributing to a compartment fire. Previously, see Section 5.3, it was aimed for determine a factor for the consideration the structural timber's contribution in fire compartments resulting in a large range of possible reductions between about 10 and 85% of the potential energy release by structural timber. Using the TiCHS-model, the risk to over or underestimate the combustion behaviour of structural timber by constant factors for the description of the combustion characteristics should be reduced. In the following, the development of the TiCHS-model is presented. To apply the TiCHS-model, inputs for the description of the fire in a compartment are needed, which comprise mainly the environment with respect to the gas flow into and inside the compartment. Some simplified engineering approaches are given whenever needed which imply areas for further development. Although the TiCHS framework is a simplified model which allows for manual calculation, the use of an automated process is recommended. The validation of the TiCHS-model is performed by three steps.

6.2 Structure of TiCHS

The TiCHS-model is a heat storage model providing information about the heat stored in a timber section for a duration of the the fire exposure. The model describes the decay of the original material, namely structural timber, to the char layer which subsequently

goes into decay. The decay process is described as the loss of mass corresponding to the heat release. The conversion process from structural timber is dependent on the available heat only, regardless of the availability of oxygen. In its actual form of the TiCHS-model, the cumulative temperature correlation model for the description of charring is implemented. The decay process of the char layer is dependent on the heat that can be activated by the compartment environment. The released heat is dependent on the fire exposure of the char layer surface which includes the thermal exposure and the gas characteristics. In the following, the elements of the TiCHS-model are presented and discussed. The determination of the elements with respect to the energy E_i are determined for the reference properties described in Section 5.2.7. By default, the unit used to depict the heat stored or released is the volumetric unit megajoule per square meter per mm, e in $MJ/(m^2 \cdot mm)$, which appeared to be a practical approach when dealing with the structural fire load as density measure i.e. related to an area) and the pyrolysis of timber, typically described by a rate expressed as millimetre per minute (mm/min).

6.2.1 Energy in structural timber

The heat content of structural timber is as presented previously in Chapter 5 considered by $e_{st} = 7.0$ $MJ/(m^2 \cdot mm)$ corresponding to about $E_{st} = 15.6$ MJ/kg. This energy content is considered as the starting value E_0 for the energy analysis in the following. The value is valid for the referenced structural timber made from softwood with 10% MC and a density of 450 kg/m^3. For deviating density or other species this value can be adopted with an apropriate modification factor.

6.2.2 Release of combustible volatiles during conversion of the structural timber to the char layer

During the decomposition of structural timber into char material, a certain potential heat amount is released. This potential heat is released as combustible volatiles considered to be oxygenated hydrocarbons, responsible for the flaming combustion during the pyrolysis process if sufficient oxygen is available. Previously, the condition for the flaming combustion with 15% oxygen was discussed, see Section 2.3.19. The corresponding value to consider the amount of combustibles created during the creation of the char layer was taken from literature discussing the industrial production of char coal where the particular energy is described to about 6% of the heat content of wood. The relevant MC is not described by Bunbury [30], thus, a 0% MC is assumed for the referenced heat of combustion although it is likely that Bunbury referred to a significantly higher MC as the production of char coal from wood containing 20% MC is presented [30]. Referring to the reference heat content of 10% MC, the share considered for the heat released is equivalent to about $E_{vol} = 1.1$ MJ/kg, equivalent to $e_{vol} = 0.5$ $MJ/(m^2 \cdot mm)$ or about $\dot{q}''_{vol} = 8.0$ $MJ/(m^2 \cdot mm/min)$ to allow the description of the released potential HRR with respect to the actual conversion process described by the charring rate. This value

should not be misunderstood as the maximum contribution to the combustion of structural timber as the various stages of the char layer decomposition creates combustible volatiles.
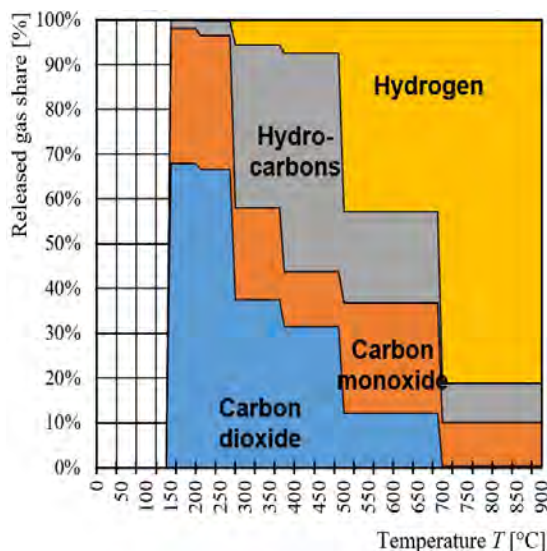
Figure 6.1: Gaseous products produced during wood distillation according to Bunbury [30]. Own figure.

6.2.3 Conversion energy

To modify or convert the structural timber into char material, a certain energy is required and lost for the system. The conversion process is understood as endothermic process. This conversion energy - or heat - is assumed to be higher than the latent heat of vaporisation, ΔH_v [187]. Typically, ΔH_v is considered together with the energy required to heat the solid from its initial temperature to the reaction temperature. The heat of gasification, see Eq. 2.5, has been researched for various materials including wood. The effect of the significant difference between typically investigated small scale samples and the structural timber remains unclear. It can be expected that the increased solid material affects the integral term in Eq. 2.5 and, consequently, the results of any analysis performed. Any influence of the sample's or specimen's size is not further considered in this thesis and a conservative value chosen for the conversion energy, $E_{con} = 1.4$ MJ/kg, as indicated within Table 2.2, corresponding to $e_{con} = 0.6$ MJ/(m$^2 \cdot$ mm). Considering E_{vol} and E_{conv}, the remaining energy similar to the potential heat in the section can be derived. If no further decomposition of the char layer has occurred, the maximum energy available in the char layer can be determined by its density (yield) and the default heat content previously determined to 31 MJ/kg. For fire retardant treated structural timber, this value should be reviewed as Levan reported an increased heat storage capacity of the

char layer for some products [113]. The reduced energy available after the conversion E_i corresponds to an energy yield or degree of exploitation of about 85%. This energy yield, understood as the product of the default heat content of the char layer density, represents the degree of exploitation. The degree of exploitation depends on the pyrolysis process efficiency which, in turn, is dependent on the heating rate, the gas flow, the particle size, the pressure, the process temperature, the reactor type and further details documented in energy research for char coal production [2, 7, 30, 185]. Exemplarily, the optimum process temperature is reported to be 500°C but for high exploitation degrees it is essential to allow re-merging of the charred material with the hydrocarbons to allow for an absorption. In practice, energy yields below 70% are considered reasonable [191], which would increase the losses from the conversion to char layer material to $E_{con} = 4.7$ MJ/kg. It should be noted that this high value would still be lower than the maximum value for the heat of gasification reported in the literature, as reported in Table 2.2. The decrease is not further followed up but considered to contribute to the conservativeness of the model. The low value for E_{con} considered in the TiCHS-model is conservative as the complementary energy remains available for the heat release, i.e. about $E_3 = 13.1$ MJ/kg.

6.2.4 Charring of the virgin wood section

The charring process, i.e. the modification from virgin wood to the char layer material is the basic process which defines the aforementioned parts of TiCHS, the conversion energy and the release of combustible volatiles. The progression of the char line into the virgin section of the structural timber is described by the charring rate β_{st}. In the TiCHS-model, an advanced charring model developed by Werther [205] is implemented which is also proposed as the cumulative temperature model for charring in the actual revision of Eurocode 5 [40]. To estimate the charring depth, the proposed upper boundary equation representing the correlation over the entire fire duration, Eq. 5.5 is taken into account in the TiCHS-model. The corresponding charring rate can be obtained by its time derivative. A kinetic model may substitute the charring model in the future. The reason for the implementation of the cumulative temperature model for charring is the robustness of the model, which included larger timber sections in its validation, compared to bench scale specimens and that it is validated against experiments under fire exposure in oxygen lean environments.

6.2.5 Decomposition of the char layer

The decomposition of the char layer comprises the smouldering and glowing combustion. The decomposition, also referred to as char oxidation, is the exothermic reaction of the char layer which is responsible for the release of the heat from the char layer. By smouldering and glowing, the char layer is further decomposed under the release of combustible volatiles, mainly hydrocarbons, carbon monoxide and hydrogen, see Figure 6.1. As shown in Section 3.4, the char layer exhibits a default heat content of 31 MJ/kg.

Consequently, the density reduction is corresponding to the smouldering and glowing combustion of the char layer when flaming is not observed. In this thesis, it is assumed that the smouldering and glowing contribution is governed by the oxygen contact intensity and the imposed heat flux. This energy contributes to the heating of the compartment depending on the fire exposure of the surface. Looking at the fire-exposed timber section, it should be highlighted that, the smouldering and glowing combustion provides a heat source related to the decay of the char layer. Consequently, E_{dec}, is superimposed with the external heat flux and the resulting conduction which reaches the virgin wood section at the char line. In the empirical charring models currently used, the contribution by the smouldering and glowing combustion is considered indirectly as they are developed under similar fire exposures. The typically referenced fire exposure is the EN/ISO standard fire and the furnace environment, i.e. the gas characteristics in terms of oxygen contact intensity. From these tests it is known that the char layer exhibits a certain thickness and density. E.g. for the EN/ISO standard fire exposure, the density was determined to be 24% on average over the depth of the char layer, compare Table 3.8. All losses in density correspond to the contribution to smouldering and glowing of the char layer representative for the particular fire exposure. The smouldering and glowing combustion has a weak dependency on the oxygen concentration of the environment as documented in the literature, see Section 2.3.36. From the experiments conducted in the framework of this thesis, the quantitative contribution by smouldering and glowing was observed to be dependent on the fire exposure at the specimens exposed surface.

6.2.6 Char layer surface regression

The char layer surface regression describes the volumetric change of the char layer, see Figure 2.7. While the char layer thickness h_{ch} is increased by the charring rate, it gets decreased by the char regression rate β_{ch} or the corresponding depth d_{ch}. The char layer surface regression is considered in this thesis as last stage of the char layer oxidation and considered separately as it appeared as a different characteristic in the experiments performed in the framework of this thesis. By the char layer surface regression, the residual heat content E_{res}, corresponding to the available energy yield in the char layer, is released. The char layer surface regression was observed to be significantly correlated to the gas characteristics, the velocity and the turbidity environment. From furnace experiments insignificant char6.3.1 layer surface regression can be expected while the FANCI experiments allowed to measure this characteristic explicitly.

6.2.7 Governing conditions

It should be highlighted that the endothermic reaction to thermally modify the structural timber into the char layer including the simultaneous release of combustible volatiles is only governed by the temperature regardless the availability of oxygen. Thus, a certain amount of gaseous fuel load will be made available regardless the type of compartment

fire, i.e. fuel controlled (FC) or ventilation controlled (VC). This means, the heat corresponding to energy of the volatiles will only be released if the essentially needed oxygen is provided. Thus, the exothermic reaction might be completed as late as the combustible volatiles reach sufficient oxygen exterior the fire compartment. For the initially created combustible volatiles, a VC compartment fire provides no limitation for the HRR, understood as the sum of the interior and exterior combustion in connection with a compartment fire. Interestingly, this merely temperature dependency has not been discussed for other fire loads where the decomposition of the solid and the creation of combustible volatiles, respectively, might be found to be controlled by temperature only. Typically, for fully developed compartment fires (without the contribution or interaction with structural timber), it is expected that a VC fire goes into decay when 70% of the movable fire load is consumed. However, it seems to be illogical that a solid fuel load, e.g. a polyurethane based sofa, would react differently to high temperatures in presence or absence of oxygen. Brandon et al. observed that the decay phase was introduced significantly before 70% of the arranged fuel load was consumed [23].

For the smouldering and glowing combustion of the char, less oxygen originating from the compartment is required depending on the compartment temperature as described in Section 2.3.47. This is most likely caused by the incomplete, typical, reaction product of char layer decomposition, i.e. carbon monoxide which represents a combustible gas. Lange et al. [109] reported the detection of significant carbon monoxide concentrations close to the surface of a STP in fire resistance furnaces providing an oxygen concentration of about 5%. It should be noted that the oxygen distribution in fire compartments is not entirely solved yet, thus, it should be highlighted that the oxygen concentration of the lower zone is clearly boosted by the inflowing air oxygen concentration but further the upper zone is not completely oxygen depleted. This is commonly addressed by setting a minimum oxygen concentration in fire simulation software packages, e.g. by the zone model CFAST to 1.5% [91].

6.2.8   Heat content of the char layer

The previously mentioned elements of the TiCHS-model,E_{vol}, E_{dec} and β_{st} can be used to describe the available heat content in a wood section and schematic view of the heat stored in a structural timber section can be put together. An example is shown in Figure 6.3 where a timber section is presented which has been exposed to its left side for 120 min EN/ISO standard fire. In Figure 6.3, the previously presented elements are arranged with respect to the material's density and energy content of a wood section which was analysed previously as described in Section 3.4.

The heated surface is represented by the broken bar at the location -71 mm while the 300°C isotherm, the char line, is located at 0 mm. The charring depth of 71 mm corresponds to a section exposed for 120 min to EN/ISO standard fire. The location was simulated with the thermal properties of wood given in Eurocode 5 [35] using the software SAFIR [61], referred to as BEC-model, see Chapter 5.
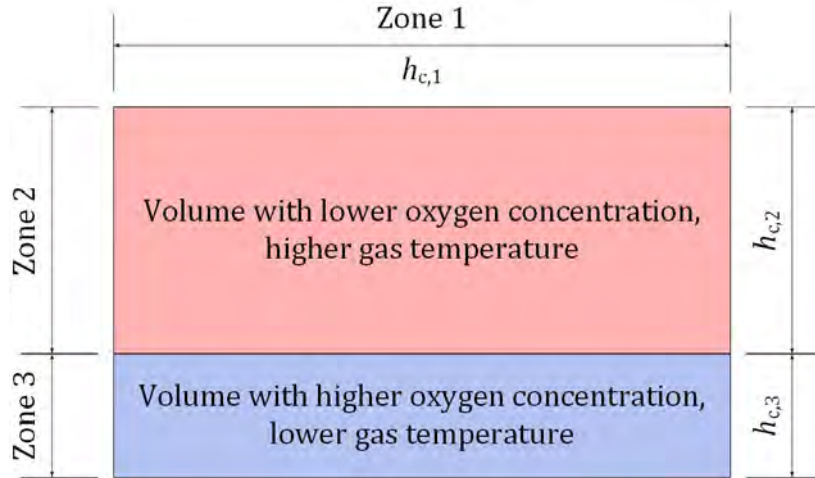
Figure 6.2: Assumed zones in the TiCHS-model in a compartment with with a post-flashover fire with two temperature zones and three different fire exposure zones. Own figure.

In Figure 6.3 the heat content of the timber section is represented by the horizontal brown line at 7 MJ/m^2 per mm section depth, see Eq. 5.12. The actual material energy yield of the material which was heated above 200°C is represented by the black curve. By combining the energy diverging from the wood energy, for the actual case, an average can be calculated to $e_{res} = 3.4$ MJ//m^2 per mm, indicated as grey horizontal line to the left of the char line. It represents the remaining energy in the char layer after 120 min exposure in the furnace. The reduction from 7 MJ/m^2 per mm to 6.0 MJ/m^{2}per mm accounts for the conversion to the char layer E_{conv} while the difference between the horizontal brown and blue lines represents the heat released during the conversion to the char layer, E_{conv}. On the left side of the char line, the area indicated by E_{ch} between the grey and red horizontal lines represents the energy content available for the heat release by smouldering and glowing combustion (decay of the char layer material). In the exemplarily discussed experiment, presented in Figure 6.3, the smouldering and glowing contribution can be determined as the difference between the red and the grey line. Following the specific heat content of the exposed section, the five energy expressions can be set together as:

$$e_{ch} = e_{st} - e_{vol} - e_{conv} - e_{res} \tag{6.1}$$

and for the actual example as:

$$e_{ch} = 7.0 - 0.5 - 0.6 - 3.4 = 2.5 \tag{6.2}$$

and consequently, assuming a charring rate of $\beta_{st} = 1$ mm/min:

$$\dot{q}''_{ch} = e_{dec} \cdot \beta_{st} \cdot \frac{1000}{60} = 42.0 \tag{6.3}$$
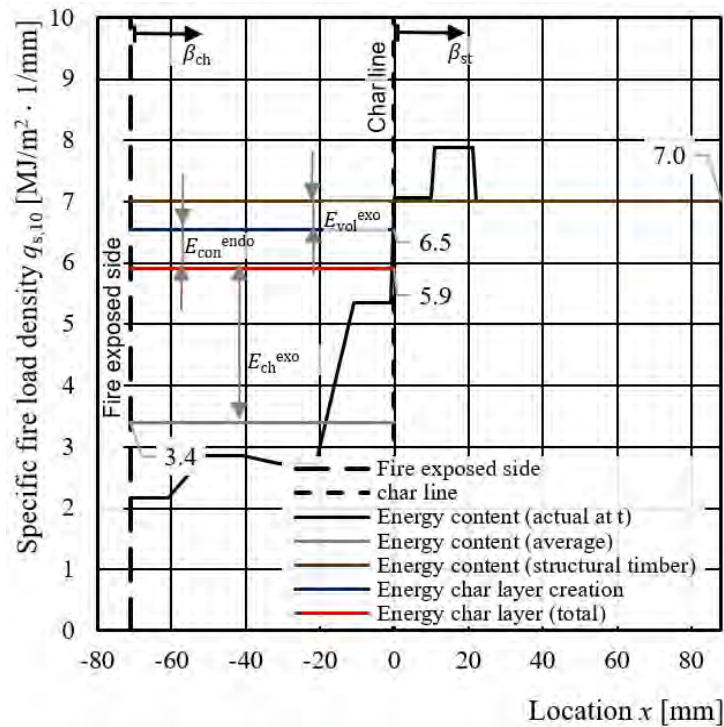
Figure 6.3: Application of the TiCHS-model to a fire-exposed timber section. Heat content of wood and char layer plotted as specific fire load density available for release during pyrolysis and smouldering and glowing combustion. Own figure.

where
$\dot{q}''_{ch}$ is the contribution by smouldering and glowing combustion, in kW/m^2.

6.3 Development of the TiCHS-model

6.3.1 General

In the following, the results from the FANCI experiments presented in Section 3.3 are evaluated with respect to the elements of the TiCHS-framework presented in Sections 6.2.1 to 6.2.6. Typically, experiments with radiant heat sources are evaluated with respect to the effect of energy source, sometimes expressed (incorrectly) as $\dot{q}''_{ext}$, $\dot{q}''_{abs}$ or $\dot{q}''_{inc}$, but often referred back to a value measured by a water-cooled HFS, $\dot{q}''_{HFS}$. As presented previously in Figure 2.9, for wood specimens a large number of research is available investigating the charring behaviour as function $\dot{q}''_{HFS}$. [197, 143]. Besides the charring rates, further characteristics of timber were evaluated using $\dot{q}''_{HFS}$ which risks neglecting a potential contribution by a material's combustion [43, 51, 3, 120]. While the estimation should be generally carefully discussed with respect to the description of the thermal exposure, see

Chapter 4, for charring materials, this traditional approach should be avoided. For timber as charring material which forms a significant char layer on the exposed side, apparently, the contribution by smouldering and glowing combustion should be estimated further. For the analysis below, it is assumed that the char surface has an emissivity close to 1.0, compare 2.1.

6.3.2 Parameter validation of elements used in the TiCHS-model

In this Section, the validation of the choice of input parameters is presented. This will be done on the basis of the FANCI experiments presented previously in Section 3.3. The FANCI consists of a radiant heat source in a closed channel where a controlled gas flow is used to apply realistic environments on a charring specimen. The FANCI experiments allowed to measure and analyse the parameters described earlier in Section 6.2, summarized in Table 3.6. Following the TiCHS-model, various elements should be considered to give a more holistic picture of structural timber exposed to heat, e.g. experiments performed under radiant heat sources. These elements can be expressed as:

1. the conversion energy E_{conv} as lost amount of energy (endothermic);

2. the release of energy by combustible volatiles E_{vol} as heat flux $\dot{q}''_{vol}$ (exothermic);

3. the release of energy by smouldering and glowing combustion described by the decay of the char layer material E_{ch} as heat flux $\dot{q}''_{ch}$ (exothermic);

4. the release of energy by char layer regression E_{reg} as heat flux $\dot{q}''_{reg}$ (exothermic);

5. the loss of energy due to convection as heat flux $\dot{q}''_{conv}$ (exothermic) as the surface temperature exhibited higher temperatures than the film temperature.

Following the heat content of the exposed section, the five energy expressions can be described per unit time, thus, expressed as heat flux. Superimposing the elements with the external heat flux, they can be combined as:

$$\dot{q}''_{sum} = \dot{q}''_{ext} + \dot{q}''_{vol} + \dot{q}''_{ch} + \dot{q}''_{reg} - \dot{q}''_{conv} \tag{6.4}$$

Eq. 6.4 describes the heat flux at the char line excluding the conduction into the uncharred timber and radiation losses of the surface. In a final step, the result of Eq. 6.4 is correlated to the charring rate, which is an effect from the conducted heat into the solid. The absorptivity of the char layer is assumed to be close to 1.0 which is reasonable as reported values in the literature show values of about 0.95 for the char layer. The losses due to convection are depending on the gas temperature and the surface temperature which were both measured in the FANCI experiments and used to determine the losses considering the turbulent environment in the setup as suggested by Wickström [209]. In

Figure 6.4 (a), the traditional approach to correlate the result to an external heat flux $\dot{q}''_{ext}$ is performed which showed a certain but weak dependency of the charring rate β_{st} on the variable. Taking into account the sum of the heat fluxes presented in Eq. 6.4, the correlation could be significantly improved as shown in Figure 2.9 (b). From the improvement of the correlation from a correlation of about $R^2 \sim 0.5$ to $R^2 \sim 0.9$, as shown in Figure 2.9, it can be concluded that the parameters are correctly identified. The heat flux relevant to describe charring rates up to about 2.15 mm/min exceeds 280 kW/m^2. In general, it can be concluded that the parameters should be determined when the behaviour of combustibles are investigated and a char layer is involved in the response of the material. It was shown that the parameters can be captured in experiments studying the behaviour of fire-exposed timber. The release and assumed flaming combustion of the volatiles during the conversion process, $\dot{q}''_{vol}$, and the losses due to the convective heat transfer $\dot{q}''_{conv}$, were observed to be of minor order of magnitude. In contrast, the smouldering and glowing combustion $\dot{q}''_{ch}$ and the final consumption of parts in contact with the environments, i.e. the char layer regression, $\dot{q}''_{reg}$ are of significant order of magnitude. Apparently, the improvement of the correlation shown in Figure 2.9 requires further input than the rather simple approach to measure or estimate the incident radiant heat flux. Contrary to experiments, in the design process, the measurement of these additional input is not always easy or even possible. In the following, the char layer combustion, decisive for the oxidation of the char layer by $\dot{q}''_{ch}$ and $\dot{q}''_{reg}$ are developed for the TiCHS-model. Subsequently, it will be applied on furnace tests and, finally, on compartment fires.
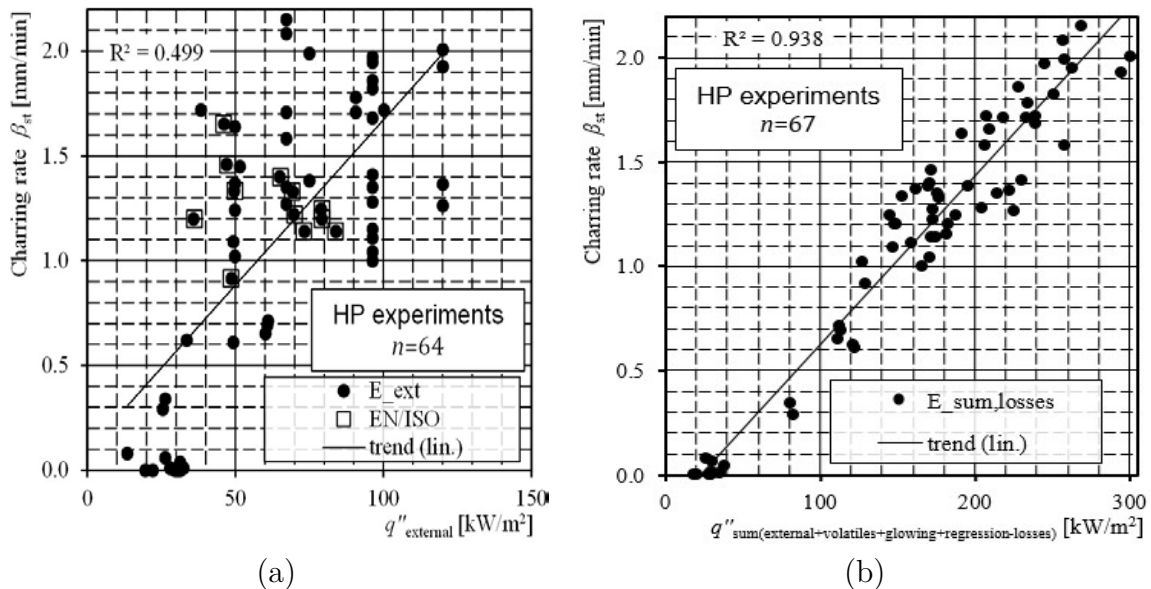
Figure 6.4: Analysis of charring rate observed in the FANCI experiments. Correlation with the external heat flux (a) and correlation with the sum of heat fluxes (b). Own figures.

6.3.3 Char layer combustion

The decay of the char layer material (oxidation including smouldering and glowing combustion) is considered to be the most relevant characteristic attributed to the char layer formed on structural timber. From the analysis of the Eq. 6.4 with respect to the results of the FANCI experiments, it is the most significant contribution exceeding the external heat flux. The exothermic reaction is assumed to occur when the oxygen concentration at the surface, is higher than 2%. In general, it is concluded that the smouldering reaction for lower heat fluxes is chemistry driven rather than driven by the incident heat flux. Following the literature dealing with smouldering combustion, the decisive turning point can be predicted by the Damköhler number Da. In general, this number describes the chemical reaction of materials. Four types are available including Da_{tur} for a turbulent environment, typically used in the combustion science. Da_{tur} describes the relationship between a material flow and an associated chemical reaction. Richter [152] presented the use of the relationship of the char layer thickness and the thermal diffusivity from the material in his description of Da_{tur}. However, the concept of the Damköhler number was not further followed up except from the following important input for the influence to describe the reaction by:

1. the thickness of the char layer;

2. the diffusivity of the char layer;

3. the characteristics of the material (gas) flow.

The elements are described in the following with respect to the findings in the FANCI experiments and its application in the TiCHS-model. Subsequently measures to describe the gas flow and relationships to predict the smouldering and glowing combustion are presented.

Thickness of the char layer. The thickness of the char layer represents the volume for potentially storing energy. Thus, it is of significant importance to estimate the char layer thickness, h_{ch} in Figure 2.7. It is governed primarily by the charring depth d_{ch} which can be estimated using e.g. the cumulative temperature charring model, see Section 2.3.10 and Eq. 2.4, respectively. As indicated in Figure 2.7, the char layer may experience a reduction of its thickness by d_{ch}. In the literature, various values for the char layer regression are mentioned [62, 214, 175]. It is assumed that the surface regression occurs primarily in oxygen rich environment. A limit of 15% was reported for the occurrence of the char layer regression [175]. By the consumption of a certain depth near the char layer surface, d_{ch}, a corresponding heat amount is released. The amount of the heat is described in the TiCHS-model by e_{res} and its corresponding heat release rate by $\dot{q}''_{reg}$. In the FANCI experiments, the char layer surface regression was measured for the experiments performed under various exposure conditions described by the external heat flux, the gas velocity and the degree of turbulence of the environment. The

degree of turbulence is considered in this work as linked to the standard deviation of the mean gas velocity. Consequently, experiments were grouped in highly turbulent (ht) and moderately turbulent (mt) environments. The mainly horizontal shift of the original surface was observed to be about linear over the time of exposure in the experiments and reached levels up to 1.8 mm/min. Significant differences were observed for the char layer regression rate in turbulent and moderately turbulent environments, thus, both groups were analysed separately. The char layer regression rates were observed with rates up to 0.6 mm/min for mt environments and 1.8 mm/min for ht environments. The correlation of the char layer regression rate was tested with the external heat flux $\dot{q}''_{inc}$ and found to be non-existent ($R^2 < 0.1$). Figure 6.5 (a) shows the dependency of the charring rate with respect to the external heat flux. A similar, insignificant correlation was found with the char layer density ($R^2 < 0.1$). An improved correlation was found for the hot gas velocity at the specimen's surface, see Figure 6.5 (b). The dependency indicate the dependency mentioned above for the input to the Damköhler number of the gas flow. Consequently, the apparent dependency of the char layer surface regression on the hot gas velocity was described with linear trends by manual fitting. Apparently, the variation of the char layer regression depending on the gas velocity is rather weak. Subsequently, the correlation for the char layer regression rate and the surface temperature (Series 9; 11 data points) was tested where a high correlation coefficient was observed ($R^2 \sim 0.8$). Due to the limited number of data points and the difficulty to estimate the surface temperature in practice, this was not further followed up. At the moment it is not entirely solved to what extent the surface regression is a separate characteristic from the smouldering and glowing combustion of the char layer. However, experiments could verify that the char yield drops drastically from a certain density to zero rather than a smooth, continuous decay to zero density, as compared to Section 3.4. A potential improvement is the description of the dependency of the char layer surface regression on the available oxygen. From furnace tests and experiments, performed at about 5% oxygen concentration, it is known that no or very limited char layer surface regression occurs. The linear relationships presented in Figure 6.5 (b) are given to:

$$\beta_{ch,0,ht} = \left(\frac{1}{5}v_{hot} + 1/4\right) \cdot \alpha_{ox} \tag{6.5}$$

$$\beta_{ch,0,mt} = \left(\frac{1}{10}v_{hot} - 1/8\right) \cdot \alpha_{ox} \tag{6.6}$$

where
$\beta_{ch,0}$ is the surface regression rate of the char layer, in mm/min;
ht is the index for highly turbulent environments;
mt is the index for moderately turbulent environments;
v_0 is the hot gas velocity in, in m/s;
α_{ox} is the factor to consider reduced oxygen concentration.
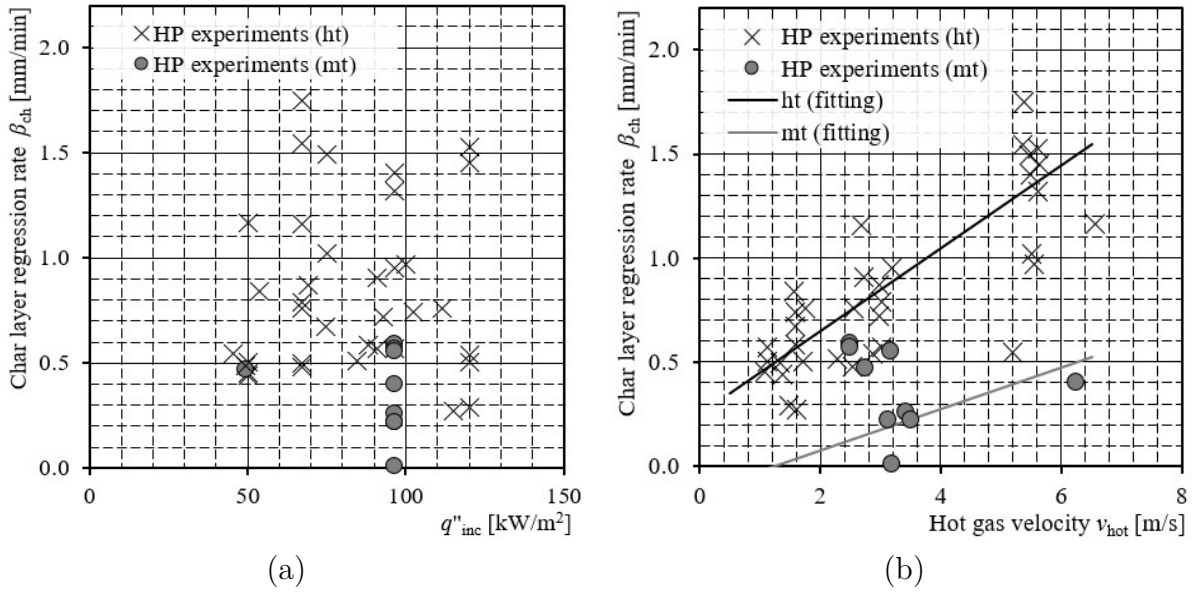
Figure 6.5: Development of the correlation for char layer surface regression rate. The correlation with the external heat flux (a) and the hot gas velocity (b). Own figures.

Diffusivity of the char layer. As previously reported, the char layer volume, in this thesis considered as bulk volume with a bulk density, contains cracks and voids. The cracks, visible at the surface, seem to follow a certain pattern [213] also observed in the 3D-scanning of the char layer surface [170]. From the observations after fire exposure for different fire durations, insignificant changes of the pattern can be reported. Thus, it was concluded that the mass of the char layer pieces decreases at the expense of the increased porosity. Subsequently, it was concluded that the diffusivity can be described sufficiently by the bulk density of the char layer. Analysing the results of the FANCI experiments, a clear trend of the char layer density with respect to its thickness was observed, see Figure 6.6 (a). Consequently, a power curve was determined to describe the apparent correlation to:

$$\rho_{ch,0} = 228 \cdot h_{ch}^{-0.45} \tag{6.7}$$

which can be further simplified to

$$\rho_{ch,0} = \frac{230}{\sqrt{h_{ch}}} \tag{6.8}$$

where
$\rho_{ch,0}$ is the (dry) char layer density, in kg/m^3;
h_{ch} is the char layer thickness, in mm.

The developed relationship, described above as power curve, was tested against the experimentally determined data from the various sources. A similar looking power curve was found by Spearpoint et al. [186] to describe the correlation between the char yield (referred to as char fraction) as function of a heat flux ratio (convective gain vs. radiative loss). The data considered in this work for the determination are (i) the FANCI experiments presented in Section 3.3, (ii) the furnace experiments presented in Section 3.2, and, (iii) the compartment experiment CI 30 presented in Section 3.5. The data series of the furnace tests was extended by experimental performed by Fahrni [52] which are presented with analysis performed with respect to the TiCHS-model in Table 3.2. The results, plotted in Figure 6.6 (b), show a good agreement. It should be observed that the fit of the data with the trend is reduced for, both, the furnace experiments, presented as black dots, and the compartment experiment. For both groups, the Eq. 6.7 clearly underestimates the apparent char layer density. Discussing the relationships presented in the paragraph, it can be stated that the char layer density seems to be a function of the depth as its heat content can be activated by the environment to a limited extent only. The deeper analysis of the char layer density profile performed in Section 3.4 resulting in the yield profile with significantly denser regions away from the exposed surface provided in Figure 3.23 (a) underpin this hypothesis.

(a)   (b)
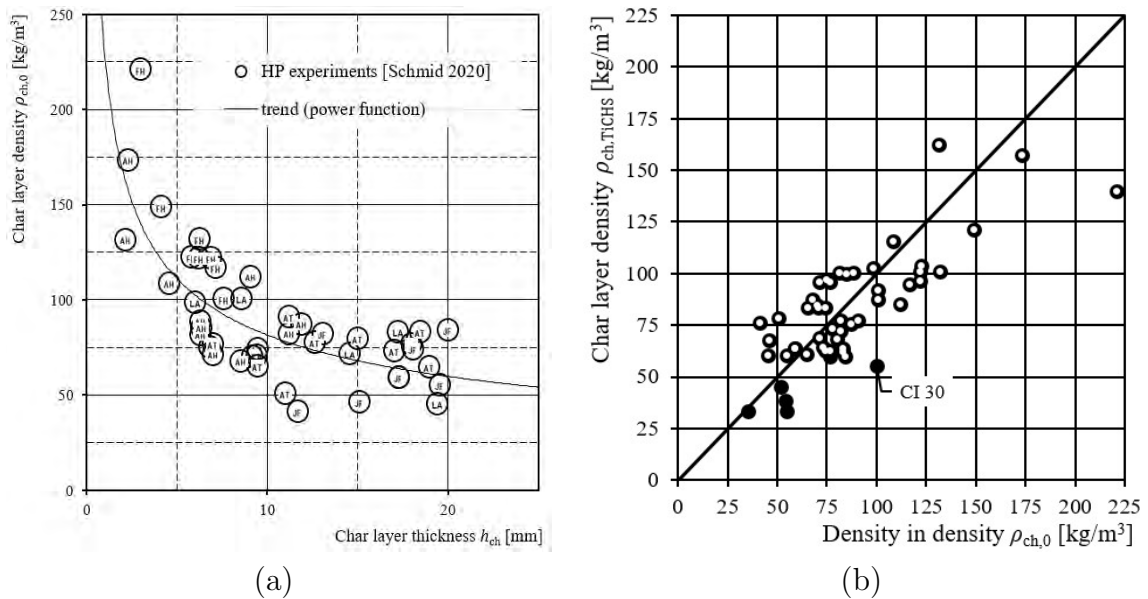
Figure 6.6: Determined char layer density. Plotted as function of the char layer thickness (a) and the correlation Eq. 6.7 tested for the FANCI experiments (hollow dots) including furnace experiments (black dots) and the compartment experiment CI 30. Own figures.

Gas flow. In this work, the gas flow characteristics are assumed to be described by (i) the gas velocity, (ii) its standard deviation (STD) and (iii) the oxygen concentration. Ohlemiller [140] concluded that the decay of the char layer material (smouldering) is more reactive to the gas velocity than the oxygen concentration, see Section 2.3.36. Thus, it seems apparent to test the experimental results for the decay of the char layer material, representative for the smouldering and glowing combustion, starting with the gas velocity. The three characteristics are investigated in the following with respect to the influence of experimental results with respect to the combustion behaviour of the char layer.

In the fire situation, the characteristics of the air change at the entrance in the compartment with respect to (i) the flow section area, (ii) the density in accordance to the expansion of the gas due to heating and (c) the oxygen concentration due to the combustion processes in the compartment. The description of the flow characteristics into and within a fire compartment is of highly complex nature which has not been addressed further in the actual thesis, detailed information can be found in the relevant literature, e.g. the SFPE handbook [81]. As the model requires input with respect to a), b) and c) simplified assumptions were taken which follow in parts well recognised models used in engineering, presented by e.g. Drysdale [49]. From steady state assumptions, the division of the inflow and the outflow through a compartment opening is well established. As the majority of the fire loads available in compartments and investigated in the past are of cellulosic nature, the assumption was considered as valid also for compartments with a significant share exposed timber surfaces. Relationships for the gas velocity at the inflow section (i.e. the lower third of the ventilation opening) can be utilized to describe the mass flow into the compartment. Drysdale [49] specifies typical gas velocities in a range of about 5 m/s to 10 m/s without referring to either the in- or outflow section nor combustion zones in the compartment. Madrzykovski [118] indicated that this order of magnitude can be assumed for the hot gas velocities. In the small scale experiment described in Section 3.5, a significantly lower gas velocities near the surfaces of about 2 m/s was determined, see Figure 3.26. However, it is assumed that this characteristic scales with the actual geometry. The derived velocities in the CI 30 experiment were found to be different from full-scale experiments by Su et al. [190] where the maximum gas velocity was measured near the ceiling of 4 m/s, $STD(v) = 0.5$ m/s, see Figure 6.7.

In the furnace experiments conducted in the framework of this thesis, measurements of the gas velocity near the specimen's surface and the density of the char layer after the exposure were made. The reduction of density can be considered as measure of the smouldering and glowing combustion during the exposure.

The experiments in the FANCI, described in Section 3.3, were performed at ambient condition with an oxygen concentration as in ambient air, i.e. about 21% per volume or about 23% per mass. The applied gas velocities were between about 1 m/s 8 m/s (hot gas velocity). The turbulent environment was considered as moderately turbulent (mt) and highly turbulent (ht) indicating a significantly different standard deviation of the gas velocity, see Figure 3.10. For the FANCI experiments it seems apparent that the $STD(v)$ has a significant impact on the decomposition of the char layer, i.e. smouldering
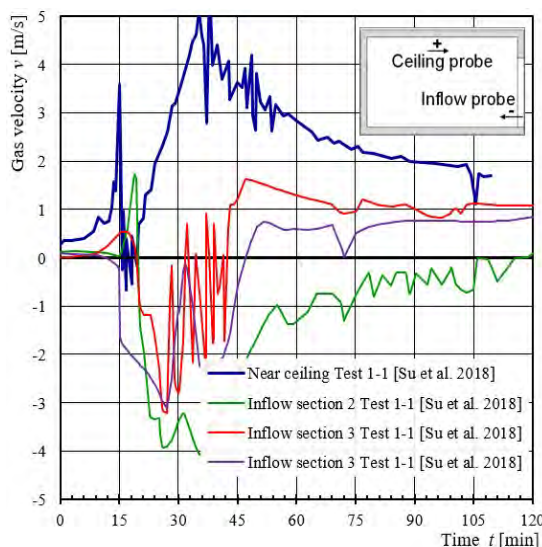
(a)

Figure 6.7: Gas velocities in a compartment test near the ceiling and in the inflow section, Test 1-1 by Su et al. [190]. Own figure.

and glowing combustion. Consequently, the results were analysed separately for mt and ht. For the series no. 12 (series FH/AS; mt), the trend line for the char layer surface regression is plotted in Figure 8.1 (a). The correlation of the char layer surface regression was further tested against the standard deviation $STD(v)$ with a similar correlation fit ($R^2 \sim 0.44$). The slightly reduced correlation might be explained as the results were previously grouped with respect to the STD, i.e. in mt and ht. The correlation was further tested for the variable of the char layer density. Extending the data of the moderately turbulent results by further experimental data shows significantly improved correlation of about ($R^2 \sim 0.79$) for both characteristics, v_{hot} and $STD(v)$, see Figures 8.1 (a) and (b), respectively. As previously indicated, it can be assumed that the char layer reaction, i.e. its decay, may be dependent on the STD. Thus, the coefficient of variation of the hot gas velocity $CV(v) = STD(v)/v_{mean}$ was tested for a correlation with the char layer surface regression which was found insufficient, see Figure 8.1 (c). Consequently, a measure to describe the gas flow conditions relevant for the char layer smouldering and glowing contribution was developed.

Degree of turbulence. From the analysed results above it is apparent that the smouldering and glowing combustion seems to be dependent on the characteristics of the gas velocity. Various approaches were tested including the standard deviation and the coefficient of variation. Results were of limited significance. Consequently, for the description of the gas velocity a measure, the degree of turbulence, DOT was introduced. The DOT
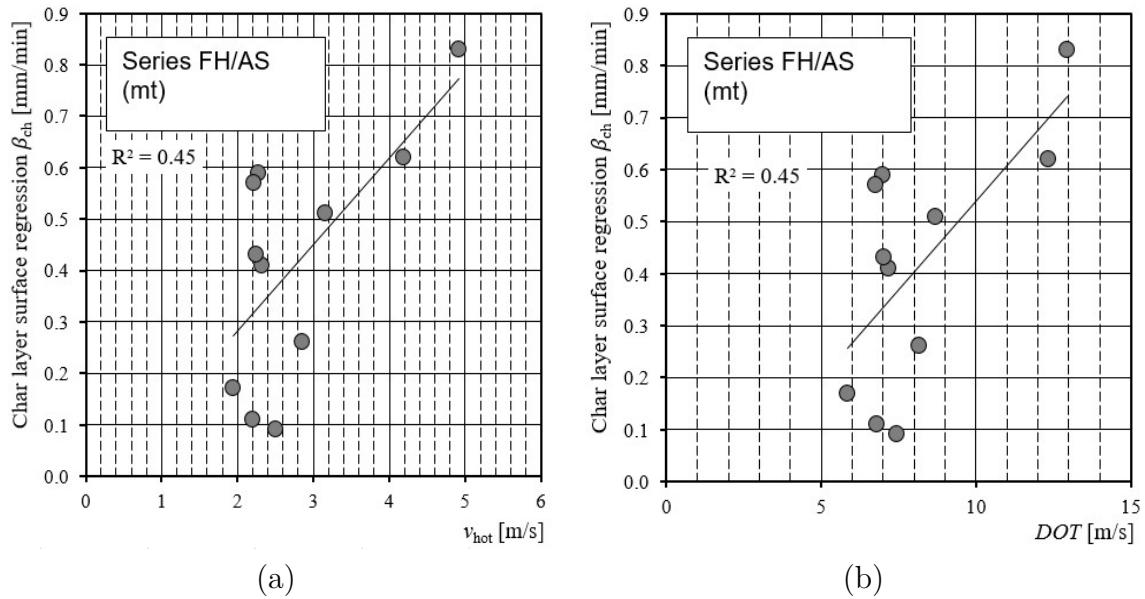
Figure 6.8: Char layer surface regression correlated to the hot gas velocity (a) and correlated to DOT (b). Own figures.

is defined as presented in Eq. 6.9:

$$DOT = v_{hot} + 2 \cdot STD(v_{hot)} \tag{6.9}$$

where

DOT degree of turbulence, in m/s.
v_{hot} is the hot gas velocity near the fire exposed surface, in m/s;
STD is the standard deviation, in m/s.

For the previously presented relationship of the char layer surface regression, the DOT does not improve the prediction, see Figure 6.3.3. However, for most of the characteristics, it was observed that the regression coefficient (method of least squares) increases when characteristics which are refereed to the smouldering and glowing combustion are correlated with DOT. In Figure 6.9 (a) the char layer density is described as function of DOT for experimental results from various sources. It should be considered that the char layer density was previously described already as function of its thickness. A deeper analysis of the char yields from FANCI experiments and yields from the furnace and compartment material showed a noticeable underestimation of the char layer density, previously shown in Figure 6.6. The inclusion of data from further sources would allow the determination of a similar relationship as specified in Eq. 6.7. The consideration of results from the compartment and furnace experiments would lead to a shift of the previously developed trend. It seems that the more realistic environments are less capable to activate
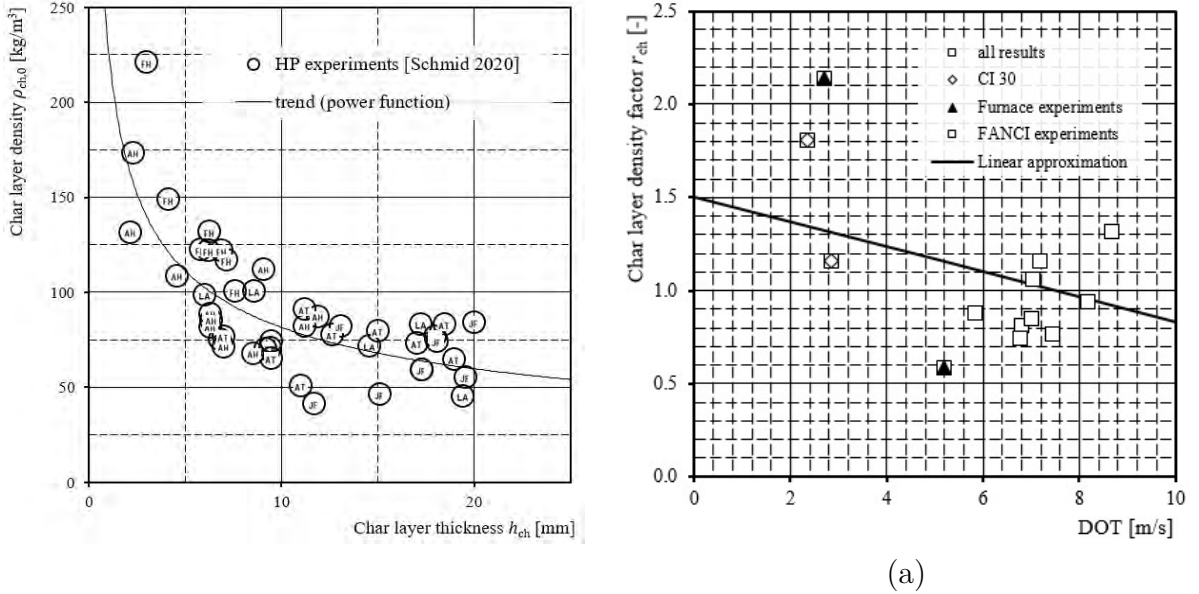
Figure 6.9: Correlation of the char layer density with the DOT (a) and the development of the correction factor for the char yield as function of the DOT (b). Own figures.

the smouldering combustion in the char layer which might be traced back to the forced convention in the FANCI experiments. To describe the modification of the char yield, a modification factor was developed to take into account the apparent differences in the activation of the char layer combustion and in the FANCI experiments and furnace and compartment experiments, respectively:

$$r_{ch} = 1.5 - \frac{DOT}{15} \tag{6.10}$$

where

r_{ch} is the modification factor for the char yield;
DOT degree of turbulence, in m/s.

The development of the modification factor r_{ch} is shown in Figure 6.9 (b). The fit of the regression line might be underestimated as only FANCI experiments were included where the pitot tubes near the specimen's surface have been installed.

Smouldering and glowing combustion. In this work, the combustion of the char layer is assumed to occur in two steps. After the creation of the char layer, the oxidation can be described by (i) the decomposition of the char layer material which reduces its density depending on the fire exposure at the surface. In a second step, (ii) the char layer surface regression of the char layer material reduces its volume and its depth, respectively. Thus, a certain depth at the exposed side is degraded to zero density. The two-step

approach follows the observations of the FANCI experiments where the depth of the char layer is governed by the charring rate and the char recession rate, respectively. It appears that both variables are depending on the fire exposure, understood as the incident heat flux, the gas temperature, losses at the surface and the gaseous environment understood as the gas velocity, the description of its turbulence and the oxygen concentration. The dependency may be direct or indirect. Further, the change of the density seems to exhibit a similar dependency on these variables. As previously performed for the char layer density and the char layer surface regression, in the following correlations for the smouldering and glowing are developed. In a first step, the analysis was performed for the results of the FANCI experiments, grouped with respect to their gaseous environment, moderately turbulent (mt) and highly turbulent (ht). Thus, the correlation for the characteristic of the smouldering and glowing combustion is further compared to the degree of turbulence, DOT. The analysis was tested for various parameters including the surface temperature, the thermal lag, i.e. the difference between the gas and surface temperature but not found to be significant. The analysis for the correlation of the smouldering and glowing combustion showed first trends when the correlation with the gas velocity was tested, see Figure 6.10 (a). Urban et al. investigated the surface temperature of ember subjected to air flow in a channel [198]. Increasing the gas velocity from 1 m/s to 5 m/s, the radiation energy, originally expressed in temperature, doubled from about 60 kW/m^2 to 120 kW/m^2. The heat flux values corresponding to the temperature were determined by means of Eq. 4.5. It is believed that differences to the results from the HP experiments are due to the different setup and the significantly different geometry of the specimens exposed. While Urban et al. used samples of max. diameter of about 16 mm, the specimens of the HP experiments were thermally thick. From the order of magnitude, the values agree well with the determination of the smouldering and glowing combustion in the HP experiments (Chapter 3). More reasonable results were found for the smouldering and glowing combustion depending on the product of the gas velocity and the external heat flux, see Figure 6.9 (a). Trends for the available data sets, mt and ht, were developed separately. It appears that the smouldering and glowing combustion for highly turbulent conditions represents the upper boundary and the smouldering and glowing combustion for moderately turbulent environments converges the latter for higher values of the independent variable. No minimum or maximum envelope curve was chosen to predict the HRR by the oxidation of the char layer by smouldering and glowing combustion as it is not self-evident that one of these cases would lead to an overall a conservative design. Thus, simplified relationships were developed.

It should be noted that the oxygen concentration is barely used as input in design equations. In the literature, it is reported that the smouldering combustion is insignificantly depending on the oxygen concentration of the environment, compare Section 2.3.47. However, in the experiments conducted in the framework of this thesis, i.e. in the FANCI experiments at ambient conditions with oxygen concentration of about 23% by mass and in the furnace experiments with about 6%, respectively, for similar gas velocities a different contribution of the char layer combustion, i.e. smouldering and glowing combustion,
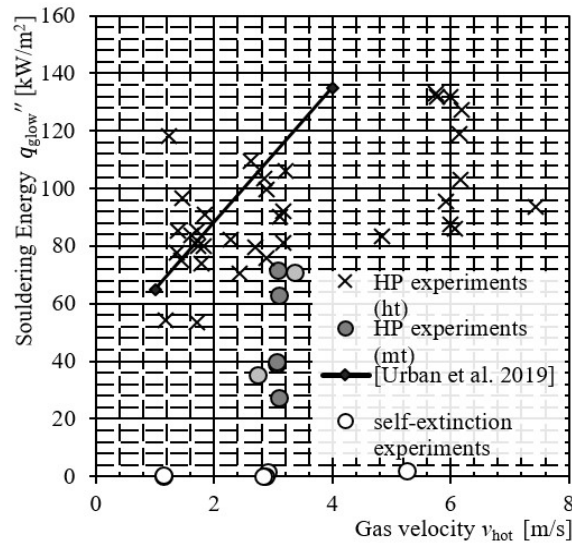
Figure 6.10: Analysis of the correlation for the char layer combustion. Own figure.

was found. This was measured and described by comparing the char yield. In Figure 6.11, results with similar gas velocities between 1.8 and 2.2 m/s are plotted. The relationships were plotted with respect to a mean external heat flux measured set in the FANCI experiments and estimated using Eq. 4.4 for the furnace experiments. The results from the FANCI experiments were taken from series with highly turbulent environments, which were considered similar to the environment of the exposure of STP I, compare Table 6.1, Column 8. A difference of about 3/4 was determined and a linear reduction factor r_{ox} developed in Eq. 6.11 for the combustion of the char layer in environments with reduced oxygen concentration.

$$r_{ox} = \frac{1}{1.5} + \frac{C_{ox}}{70} \tag{6.11}$$

where
r_{ox} is the modification factor for the smouldering and glowing combustion in oxygen lean environments;
C_{ox} is the oxygen concentration, in % by mass.
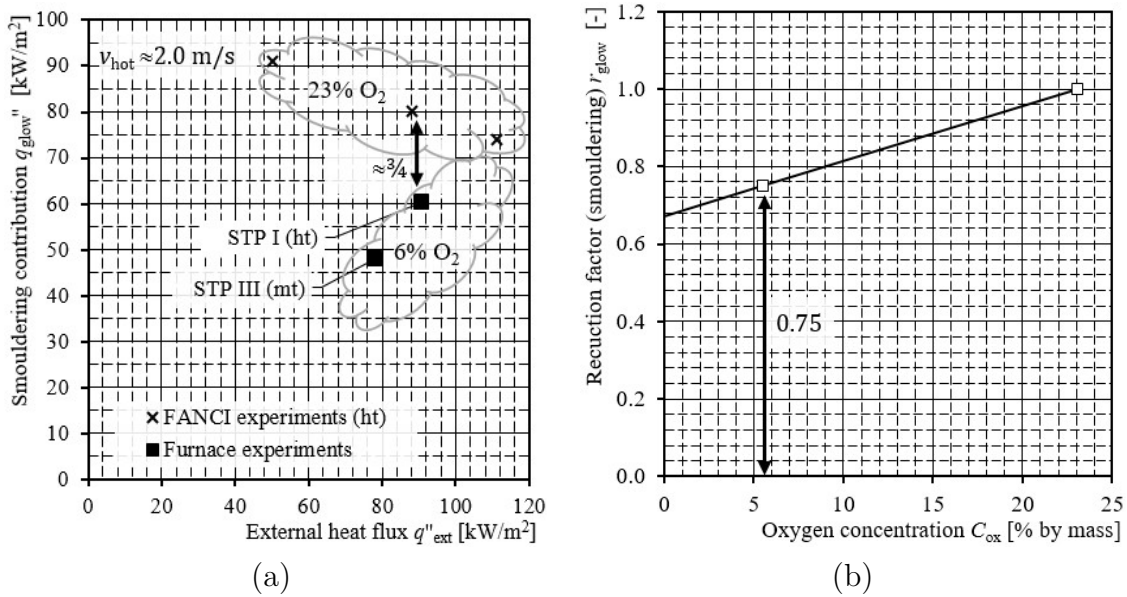
Figure 6.11: Development of the reduction for smouldering and glowing combustion in oxygen lean environments. Comparison of the char layer contribution to the fuel load at 6% and 23% environments (a) and the corresponding linear reduction factor (b).

6.3.4 TiCHS applied to furnace experiments

In the following, the presented relationships are applied to experimental data obtained from exposure of structural timber in standard fire resistance furnaces. Table 3.2 is extended using the methodology of the TiCHS-model. The contribution to the fire by smouldering of the char layer was estimated using the mass of the char layer. For the experiments in consideration, this yield was determined to a value between 9% and 19% as the average over the char layer depth. The smouldering and glowing contribution, understood equivalent to the decomposition of the char layer, for the experimental results was determined using the default energy content of the char layer of 31 MJ/kg, $\dot{q}''_{dec,experiment}$. The results are given in line 6 of Table 3.2 which contains further the input for Eq. 6.12.

$$\dot{q}''_{dec,experiment} = \left(V_{char} \cdot \rho_0 \cdot H_0 - m_{ch} \cdot H_{ch,0} \right) / t_{fi} \tag{6.12}$$

where

H_0	is the energy content of dry wood, 17.5 MJ/kg;
$\dot{q}''_{dec,experiment}$	is the contribution corresponding to the decomposition of the char layer due to smouldering and glowing combustion, in kW/m^2;
V_{char}	is the charred wood volume estimated using d_{char}, in m^3;
ρ_0	is the dry wood density;
$m_{ch,0}$	is the dry mass of the char layer;
$H_{ch,0}$	is the energy content of dry char layer material, 31.0 MJ/kg;
t_{fi}	is the time of fire exposure, in s.

In the following, the prediction of the smouldering and glowing combustion is compared for furnace experiments with the approach by the TiCHS-model. The latter was slightly modified to allow for a comparison as the conversion losses could not been determined for the experiments. Thus, the corresponding contribution was determined using the specific heat content of the char, available for smouldering and glowing combustion, see brown horizontal line in Figure 6.3, $e_{dec} = 7.0$ MJ/m^2 per mm. The maximum smouldering and glowing contribution by the char layer determined by the TiCHS-model corresponding to e_{res} is given in Table 6.1, Line 9. The direct estimation of the smouldering ang glowing using the measured mass of the char layer led to the comparison value given in Line 8. It should be noted, that the actual heat release due to the decomposition of the char layer $\dot{q}''_{dec}$ would be described by Eq. **??** which is depending on the variable heat flux. For the end of a 120 min fire exposure in a furnace (corresponding to about 1050°C furnace compartment temperature), the application of Eq. **??** would result in about $\dot{q}''_{dec} = 75$ kW/m^2.

6.4 TiCHS applied on compartment fires

6.4.1 General

The TiCHS-model is set up as framework to describe the contribution by structural timber to the fire dynamics in compartment fires. It accounts for the recently identified lacks of compartment models to consider the combustion behaviour of structural timber [180, 124], previously discussed in Section 5. It accounts also for the limitations of previously set fitting factors to address the share of the released energy interior of the compartment [22] or the required parameter study for the fuel access factors GER used by the B-RISK software [201, 202]. In the following, the predictions by the TiCHS-model will be compared to experimentally obtained results. The predicted contribution by structural timber is expressed by a structural heat release rate HRR_{st} which forms together with the HRR_f originating from the movable fire load the total fire load, HRR_{tot}. In the following validation process, predictions are performed for the structural heat release rate while the heat release rate from the movable fire load HRR_f will be taken from measurements of the corresponding compartment without the structural fire load provided by the structural

1	2	3	4	5	6	7	8	9	10
		STP 30	STP 60	STP 90	STP III	STP 120	STP I	BC1	BC2
test lab		VKF[1]	VKF[1]	VKF[1]	RISE	VKF[1]	VKF[2]	MPA	MPA
v_{mean}	[m/s]	n.a.	n.a.	n.a.	0.9[3]	n.a.	2.2	1.7	2.8
$STD(v)$	[m/s]	n.a.	n.a.	n.a.	0.9[3]	n.a.	1.5	0.9	0.8
$C_{ox,mean}$	[%]	n.a.	n.a.	n.a.	5%	n.a.	5%	n.a.[4]	n.a.
t_{fi}	[min]	30	60	90	90	120	120	120	120
$\rho_{st,0}$	[kg/m^3]	399.9	400.6	401.7	422.7	402.5	405.4	397.6	404.9
d_{char}	[mm]	20.1	37.5	54.5	55.2	75.0	73.3	71.0	71.0
$\rho_{ch,0}$	[kg/m^3]	76.5	51.9	53.9	81.2	54.7	35.2	117.1	109.3
$\rho_{st,0}/\rho_{ch,0}$	[-]	0.19	0.13	0.13	0.20	0.14	0.09	0.30	0.27
$\dot{q}''_{dec,experiment}$ [5]	[kW/m^2]	51.0	55.8	53.6	47.9	55.1	60.6	37.2	40.9
$\dot{q}''_{dec,model}$ [5]	[kW/m^2]	57.1	58.2	58.5	59.3	62.0	60.5	58.4	58.4

[1] Experiments performed and reported by Fahrni [52].
[2] Different furnace control procedure applied than other VKF experiments reported by Fahrni [52].
[3] In direction of the burners.
[4] Significant sooting of the furnace windows observed indicating insufficient oxygen supply.
[5] no losses considered.
n.a. not available.

Table 6.1: Comparison of the contribution by the char layer to the total fuel in furnace experiments.

timber. Typically, this has been achieved in the compartment experiments by sufficiently encapsulate the structural timber. In addition to the definition of the structural heat release rate HRR_{st}.

6.4.2 Limitations

In its current form, the TiCHS-model experience some limitations which are described in this section. The model aims for providing simplified engineering model with a reasonable accuracy, material and combustion science may provide in the future for improvements within the framework of the TiCHS-model. The TiCHS-model is a framework using elements to describe the heat storage within a structural timber. In this connection, an important characteristic is the charring model which describes the progress of the char line understood as initial conversion of wood to the char layer. Currently, the cumulative charring model described by Eq. 2.4 is considered as robust measure to estimate this element of the TiCHS-model. However, the eventually occurring char layer regression and the gas characteristics are indirectly accounted for and no information is available about the relevant conditions in the basic information, these characteristics were not measured in the furnace tests. In the future a kinetic model might be used, e.g. developed by Richter et al. who showed that the increased oxygen intensity might be considered by the modification of the heat transfer coefficient [153, 180]. Another limitation of the actual TiCHS-model is the simplified modelling of the phase before ignition and ignition criterion which is a pseudo criterion based on the 300°C limit given in Eurocode 5 [35]. Currently, no description of the temperature profile within the timber section is available, thus, the load-bearing capacity can not be directly determined. It should be highlighted that the TiCHS-model is intended for the prediction of the structural heat release rate HRR_{st}, while the HRR_f originating from the movable fire load and the compartment fire temperature is assumed to be determined by another model, e.g. by a zone or field model. In its current version, no consideration of the falling-off of charring layers is implemented due to the limitations of the charring model which is expected to exhibit reduced accuracy for a significant reduction of the char layer thickness. Surface flaming was not considered in the application of the TiCHS-model. In the actually used zone model, no radiative feedback of surface flaming to other elements than the origin was modelled. This can be justified with the good fit of the simulations of compartment experiments in the validation. However, for more narrow compartments, an effect is expected. As the TiCHS-model considers the fire exposure at the surface, an implementation of the contribution of surface flaming as external radiative heat flux to other surfaces is a minor development step.

6.4.3 Fire dynamics and the importance of the consideration of structural timber

In the following, the general assumptions for the prediction of the total heat release rate are presented. Schematically, the superimposition of the HRR by various sources is

provided in Figure 6.12. The contribution of the movable fire load by the interior relies on the well-recognised description of the fire dynamics in post-flashover compartment fires, documented in literature e.g. Drysdale [49]. After ignition, assumed at the origin, $t = 0$, the fire growth follows a t^2-fire [97]. In a t^2-fire, reaching the 1 MW point is defined by a fire-growth coefficient. To do so, Eurocode 1 [34] implemented the fire growth rate coefficient t_α, which should be set in accordance to the occupancy. Typically, $t_\alpha = 300$ s is used for residential or office occupancy, which might be modified to a shorter time if the fire spread on structural timber surfaces would lead to a faster fire growth. A difference combustible horizontal surfaces (ceilings) and combustible vertical surfaces (walls) is reasonable but not available. A potential fire retardant treatment is expected to slow the flame spread on the surface and, thus, the fire growth in such compartments. However, quantitative guidance is missing at the moment. McGregor observed ultrafast fire growth when combustible walls were located at the ignition source and the distance between walls was limited, i.e. $t_\alpha = 75$ s [123]. The importance of the distance between walls should be highlighted - especially when analysing the decay phase of a fire. Although any construction element of the enclosure, i.e. floors, walls and ceilings, would be heated in the growth phase and would emit energy in the cooling phase, combustible surfaces might represent a source for flaming combustion, compare 2.3.19. Consequently, surface flaming may superimpose the radiation from the component surface. Depending on the arrangement of further (combustible) elements, this situation would have impact on the fire dynamics in the compartment.

After the initial growth phase, the fire is expected to reach a certain maximum. Following available guidance, this maximum is corresponding to the limit of either the ventilation condition in the compartment (i.e. ventilation controlled, VC; limited by the compartment combustion capacity, CCC) or to the limit of the conversion of the (solid) fuel load to heat (i.e. fuel controlled; limit by the fuel load condition (FC). It should be noted that this approach is unreasonable if a temperature dependent decay of the interior (movable fire load) with a simultaneous creation of combustible volatiles is assumed as done for structural timber. In general, it would appear to be more reasonable to assume a decay (pyrolysis) of the solid fuel based on the the thermal exposure and the combustion of the bi-products depending on the fire exposure. Consequently, the total heat release, i.e. internal heat release and exterior heat release, is less affected by the compartment combustion capacity (CCC) as described by the currently available model, compare Figure 6.12. Special consideration should be materials that are able to create a substantial char layer, e.g. timber. Components of timber, i.e. the structural timber material and the char layer material, undergo pyrolysis depending on the thermal exposure also in inert conditions, then only a limited share of the stored energy is released as potential heat. The thermally modified layer, i.e. the char layer material, decompose with a certain delay, significantly depending on the compartment environment. It can be assumed that the application of the CCC as combustion limit represents a conservative approach for the fire development in a compartment as the heat release of the movable fuel occurs over a longer duration. Especially for structural timber this approach leads to increased charring and would be

generally conservative.

In reality, the temperature decay of the fire in the cooling phase is non-linear [97, 41], however, typically, a linear decay of the HRR in the cooling phase is assumed as suggested by Eurocode 1 and Zehfuss [48, 216]. In Figure 6.12, the above mentioned limits (CCC and FC) and description of the determined HRR for the movable fire load (blue and red curves) are presented for a typical example of a compartment fire. In addition, the structural HRR by the structural timber is implemented (brown curve). In this example it is derived for the compartment temperature corresponding on the temperature development based on the HRR by the movable fire load. The structural HRR was obtained by applying $\dot{s}''_{10} = 0.116$ MW/m^2 per mm/min, determined from Eq. 5.9. Directly superimposing both fuels, i.e. HRR_{st} and HRR_f, would result on one hand in conservative maximum temperature predictions, and, on the other hand, in the underestimation of the fire duration . Typically, for fires originating from cellulosic based fuels, a combustion efficiency of $\chi = 0.8$ is considered which means that 80% of the energy content will be effectively converted to heat due to losses of the incomplete combustion process.
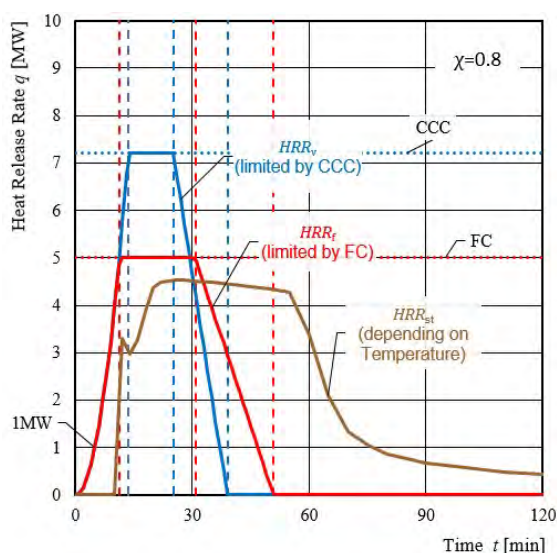
Figure 6.12: Superimposition of heat release rates by the movable fire load, limited either by the CCC or FC, and by the structural timber (schematic example). Own figure.

6.5 Validation of the TiCHS-model by compartment experiments

6.5.1 Selection of benchmark experiments and general assumptions

Compartment experiments were selected for the comparison of measurements obtained in the experiments with the TiCHS-model predictions. The selection was done based on the availability of measurements and settings of the compartment experiments. The three essential requirements comprise (i) the availability of data for the total HRR, (ii) the availability of compartment temperature recordings, and, (iii) the inclusion of the performance of a baseline experiment of the particular compartment. A baseline experiment is understood as compartment experiment with similar geometry and movable fire load design but with zero structural fuel load, the ceiling and all wall surfaces encapsulated. The report of the charring depths is taken into account for further comparison. The experiments under consideration are compartment experiment campaigns with CLT panels. The use of CLT products which exhibit bond line integrity throughout the fire duration would allow for an improved comparison but due to currently available product limitations such data are not available yet. In addition to experimental data, comparison to predictions presented by Wade et al. [202, 203] were made.

Subsequently, two experimental campaigns were identified appropriate for the validation of the TiCHS-model. The series have been performed and documented by McGregor and Su et.al. [123, 125, 190]. From the documented compartment experiments, a further selection was done to cover the range of combustible surfaces in the compartments. The description of the share of the combustible surface area is done as done usually for the movable fire load, thus referred to the floor area. usually referred to the selected two compartments and their details are specified in Table 6.5.1. It should be noted that in the experiments, various temperature measurements were taken. In the following the reported mean gas temperature measurements were considered as benchmark. Further it should be noted that the measurements of the HRR typically experience a time delay which was considered by shifting the 1 MW point manually to the flashover time observed by the temperature measurements.

To evaluate the actual proposal in the revised fire part of Eurocode 5 with respect to the consideration of the combustion behaviour of structural timber, the combustion behaviour factor α_{st} was determined for the analysed results. According to Eq. 5.9, assuming $\alpha_\rho = 1.0$, the following relationship was described:

$$0.12 \cdot \beta_{st} \cdot \alpha_{st} = \frac{HRR_{st}}{A_{st}} \tag{6.13}$$

Consequently, the modification factor can be determined by:

	1	2	3	4	5	6
1		Compart-ment area width[1)] $\times$ depth	Ventilation area[1)]	Exposed structural timber area	exposed elements	
2	ID.	A_f	A_v	A_{st}		Reference
3		[m $\times$ m]	[%]	[%]	c/w	
4	I	3.5 $\times$ 4.5	25	0	-	[123] Test 2 and 4
5	II	4.6 $\times$ 9.1	29	0	-	[190] Test 1-1
4	III	3.5 $\times$ 4.5	25	30	w	[125]
5	IV	4.6 $\times$ 9.1	29	100	c	[190] Test 1-4
7	V	3.5 $\times$ 4.5	25	145	w	[125]
8	VI	3.5 $\times$ 4.5	25	340	w, c	[123]

[1)] face wall related.

c   ceiling

w   wall(s)

Table 6.2: Overview of the compartment experiments included in the analysis.

$$\alpha_c = \frac{HRR_{st}}{A_{st} \cdot 0.12 \cdot \beta_{st}} \tag{6.14}$$

where

β_{st} is the actual charring rate, in mm/min;

α_{st} is the factor to consider the combustion behaviour of structural timber including the energy storage in the char layer and the potential heat release of the char layer, respectively;

HRR_{st} is the structural HRR, in MW;

A_{st} is the exposed surface area of structural timber, in m^2.

6.5.2   Baseline experiments

The baseline experiments (non-combustible surfaces; NC) for the validation were, Test 2 and Test 4 reported by McGreogor [123] and Test 1-1 reported by Su et al. [190]. The TiCHS-model applied on compartment fires baseline experiments were parts of compartment experiment campaigns where various shares of exposed structural timber surfaces were investigated. The compartment geometry by McGreogor and Medina [123, 125]

was similar to the compartments used by Hakkarainen [74] with a height of 2.5 m and floor area of about 16 m². The compartment's geometry was increased in the campaign by Su et al. [190] to a height of 2.7 m and floor area of about 42 m² to answer for more realistic conditions. In this thesis, the opening factor was not further specified. This is due to the actual discussion about the use of the opening factor and the exclusion of the floor area as suggested by Torero et al. [196] or the area of combustible surfaces as suggested by Gorska [67]. In this thesis, the opening is specified as the share of the front wall which was held constant for the baseline experiments and the subsequently conducted compartment tests, see Table 6.5.1, Column 4. Following the measurements of the gas velocity in Test 1-1, the velocity in the inflow section was set to 4.5 m/s which gave an overall good agreement for the hot gas velocity predicted, compare Figure 6.7.

6.5.3 Software

The software packages used for modelling the compartment temperature and the available oxygen were CFAST [91] and OZone [32]. Significantly different outcomes were observed modelling the benchmark experiments. The differences were with respect to the calculation time and the calculation results in general. From CFAST simulations the existence of two zones with respect to the temperature development and the oxygen concentrations were observed while the OZone simulations swiftly switched to the one-zone stage. This was followed up by the limitation of the oxygen depletion in the lower compartment zone for the TiCHS-model. From CFAST simulations, the temperature predictions reached unreasonable high limits exceeding 1800°C in the compartment. The implicitly consideration of the combustion efficiency by the reduction of the basic heat of combustion to about 70% led to a good agreement with the benchmark experiments in OZone. Contrary, the corresponding reduction would reach unreasonable low values for the heat of combustion in CFAST. The reduction of the combustion efficiency was estimated already by McGregor [123] and verified by Wade et al. [202] using B-Risk [201]. Consequently, the TiCHS-model was applied together with OZone using an effective heat of combustion of $\Delta H_{ef} = 12.1$ MJ/kg. In the modelling, no further reduction or limit for the combustion was introduced. Thus, the main objective of the software is the calculation of the internal combustion and the associated temperature development. The time steps in Ozone and the TiCHS-model were set to 1 min, the maximum simulated time was set to 150 min.

6.5.4 Compartment experiments I and II

For the validation process, the HRR was used from baseline experiments originating from two campaigns. Compartment experiment I, reported as Test 2 and Test 4 by McGregor [123], and, compartment experiment II, reported as Test 1-1 by Su et al. [190]. Input to the zone-model software was the HRR of the baseline experiments (NC), the compartment geometry and the definition of the wall material(s). Typically, the meas-

ured HRR by industrial calorimeters fluctuates. For simplicity reasons, an approximation of the total HRR was derived. Using the temperature predictions from the simulations (baseline simulation), the compartment temperatures was compared to the measured values. Results of the comparison of measured data and predictions for the temperature measurements of the baseline case of both experimental campaigns are given in Figure 6.13. The recording of the temperatures in experiment I stopped at about 47 min, thus, no further data is available after this point in time. A good agreement can be observed between the measured temperatures (grey curves) and the simulated temperatures. The so-defined HRR of the baseline cases were considered in the following simulations as the HRR from the movable fire load. They were superimposed with the predicted structural HRR provided by TiCHS-model. Further results are given for comparison reasons in Table 6.5.9.
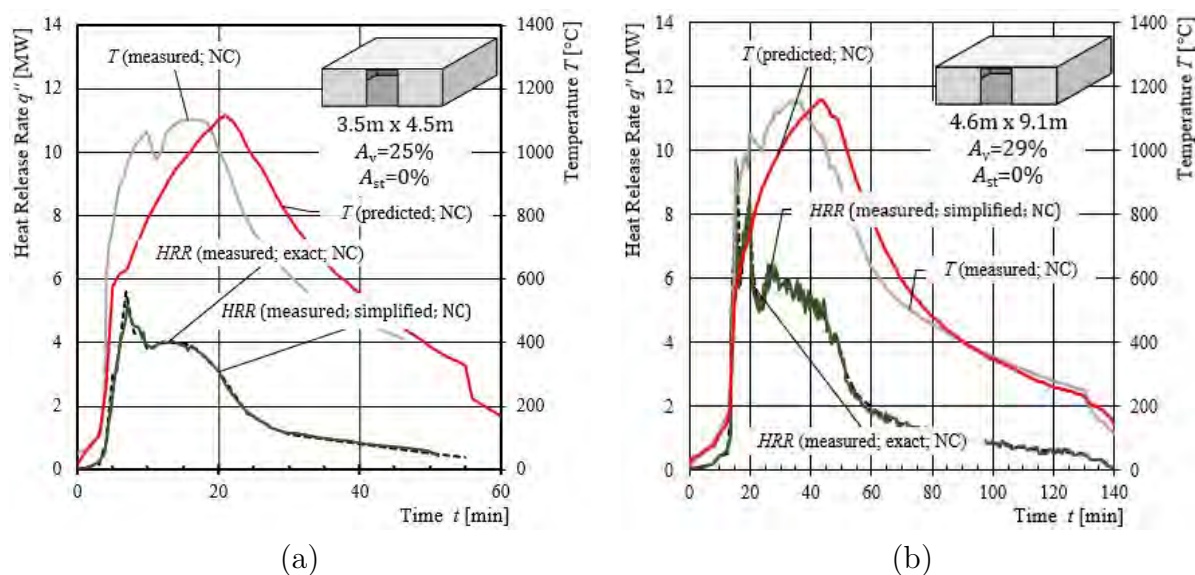
Figure 6.13: Results for compartment experiments and the baseline simulations. Experiment I (a) and experiment II (b). Own figures.

6.5.5 Compartment experiments III (30% exposed structural timber)

The rear wall of Compartment III, reported as Test 3 by Medina [125], was designed as unprotected structural timber element. Results for the HRR determined by the TiCHS-model and temperature simulations for the compartment III are plotted in Figure 6.14. It should be observed, that the HRR of the baseline (NC) was measured slightly higher than the HRR for the experiment III (C). Subsequently, temperatures of the baseline case (NC) and with the exposed rear wall agree well. In the experiment, the reported charring depth was between 21 mm and 44 mm. The simulated values with the TiCHS-model agree well

with the upper boundary, see Figure 6.15. Further results are given in Table 6.5.9

Figure 6.14: Results for compartment experiment III - predictions vs. measurements. Heat release rates (a) and temperatures (b). Own figures.

Figure 6.15: Results for compartment experiment III. Charring depth and the modification factor α_{st}. Own figure.

6.5.6 Compartment experiments IV (100% exposed structural timber)

The ceiling of Compartment IV, reported as Test 1-4 by Su et al. [190], was made from structural timber. Results for the HRR determined by the TiCHS-model and temperature simulations for the compartment III are plotted in Figure 6.16. In the experiment, partly fall-off of the CLT layers with respect to bond line integrity was observed. The experiment was terminated at about 53 min when charring layers fell-off and a signifiant re-growth of the fire was observed. The fall-off of parts of the CLT layers may be the cause for the increase of the HRR after 40 min which reduces the fit with the simulations results. The charring depth was simulated to reach about 78 mm, see Figure 6.17, while measurements indicated values between about 65 mm and 90 mm. The large scatter is most likely also due to the fall-off of charring layers which doesn't occur at once. Further results are given in Table 6.5.9, Row 8.

(a)   (b)

Figure 6.16: Results for compartment experiment IV - predictions vs. measurements. Heat release rates (a) and temperatures (b). Own figures.

Figure 6.17: Results for compartment experiment IV. Charring depth and the modification factor α_{st}.

6.5.7 Compartment experiments V (145% exposed structural timber)

Two opposite walls of Compartment V, reported as Test 2 by Medina [125], were designed as unprotected structural timber element. Results for the HRR determined by the TiCHS-model and temperature simulations for the Compartment V are plotted in Figure 6.18. In the experiment, after the initial decay between 30 min and 40 min, a re-growth of the fire was observed as the outer layer of the CLT elements fell-off. The experiment was terminated at about 60 min. Disregarding failure of the bond line integrity, the charring depth was simulated to reach about 54 mm, see Figure 6.19. This simulation result should be read with care as the decay seems to be suddenly initiated. Corresponding predictions by Wade [203] do not conclude a decay after 90 min.
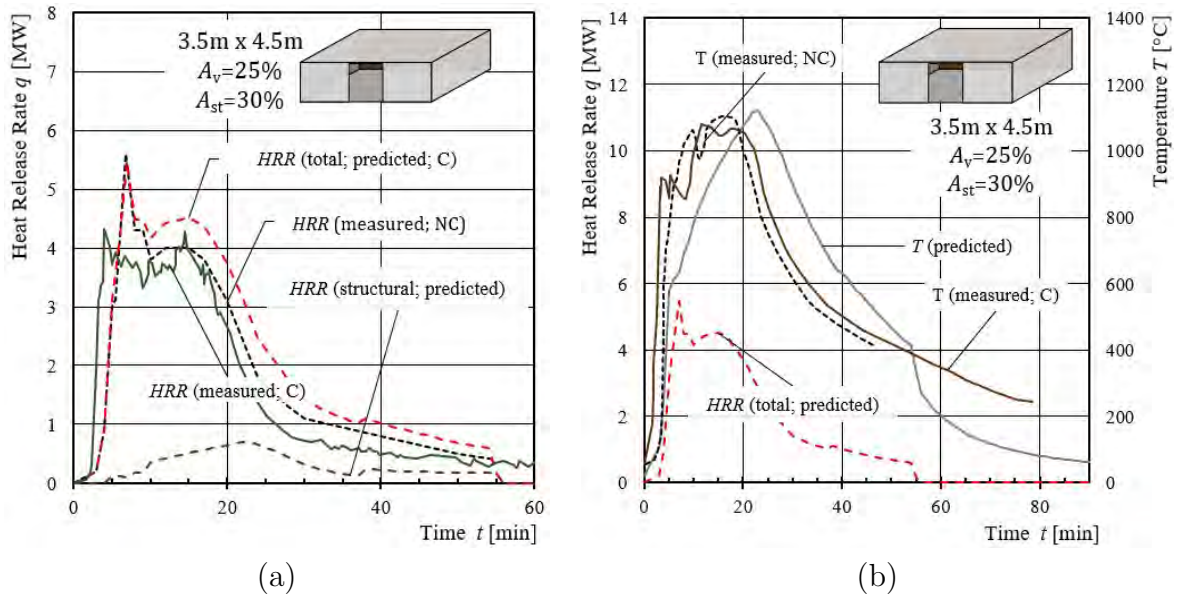
Figure 6.18: Results for compartment experiment V - predictions vs. measurements. Heat release rates (a) and temperatures (b).
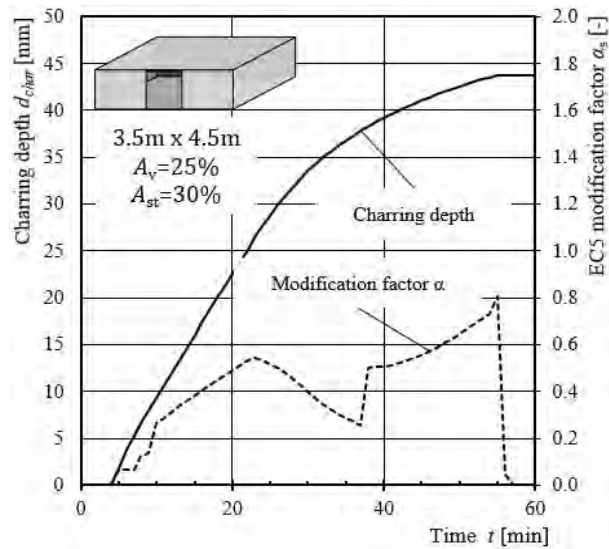

Figure 6.19: Results for compartment experiment V. Charring depth and the modification factor α_{st}.

6.5.8 Compartment experiments VI (340% exposed structural timber)

The entire enclosure surface of Compartment VII, reported as Test 5 by McGregor [123], were made from combustible materials. Results for the HRR determined by the TiCHS-model and temperature simulations for the Compartment VI are plotted in Figure 6.20. In the experiment, after the initial decay between 30 min and 40 min, a re-growth of the fire was observed as the outer layer of the CLT elements fell-off. Consequently, parallel courses of the curves end at about 40 min. The experiment was terminated at about 60 min. Disregarding failure of the bond line integrity, the charring depth was simulated to exceed about 85 mm at 90 min, see Figure 6.21. This simulation result should be read with care as no decay could be observed. Similarly, the predictions by Wade [203] do not conclude a decay neither. Simulations results presented in Figures 6.20 and 6.21 were simulated for a gas velocity in the inflow section of the ventilation opening with 4.5 m/s. The increase of the inflow gas velocity to 7.5 m/s resulted in more severe charring depths and increased the contribution of the char layer. It can be concluded that, (a) this compartment characteristics exhibiting this large share of combustible surfaces will most likely not go into decay, and, (b) that the increased gas velocity in the compartment is capable to boost the smouldering and glowing combustion of the structural timber which was observed increase to about 90 kW/m^2 in this case, compare Table 6.5.9, Column 7.
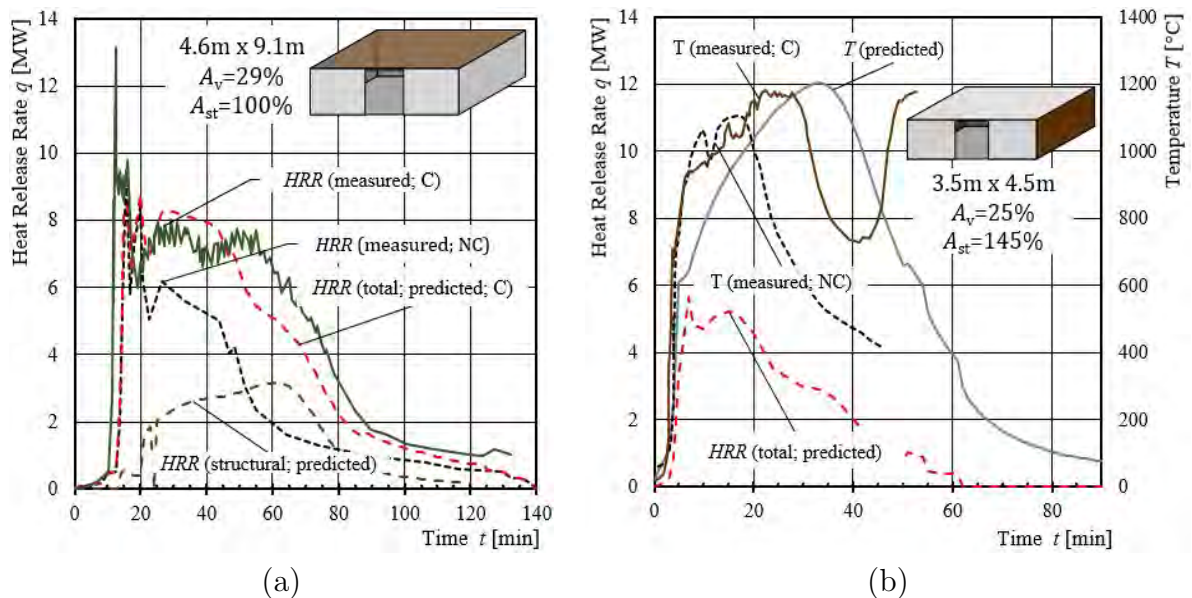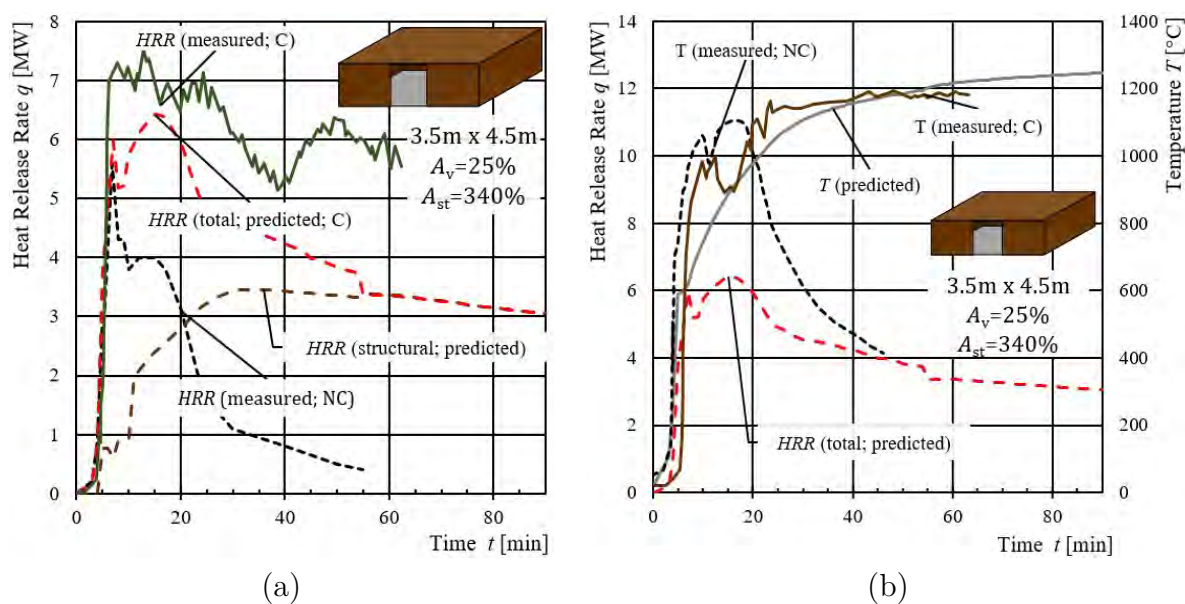

Figure 6.20: Results for compartment experiment VI - predictions vs. measurements. Heat release rates (a) and temperatures (b). Own figures.
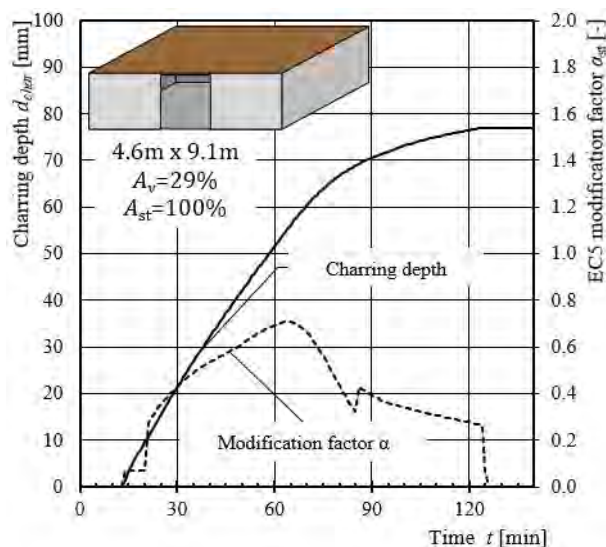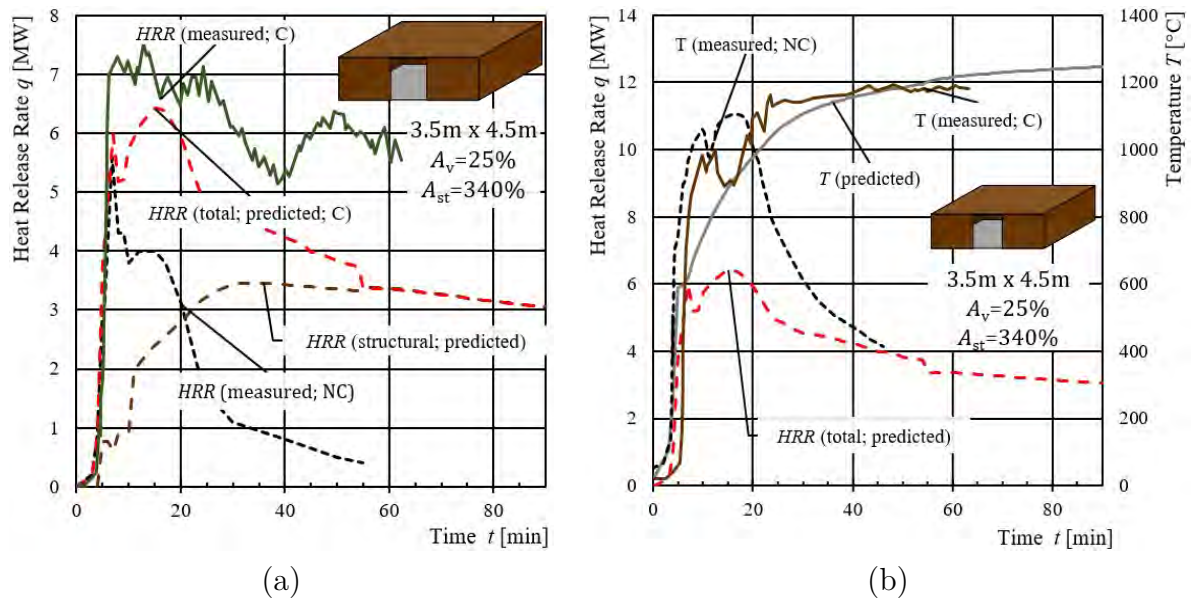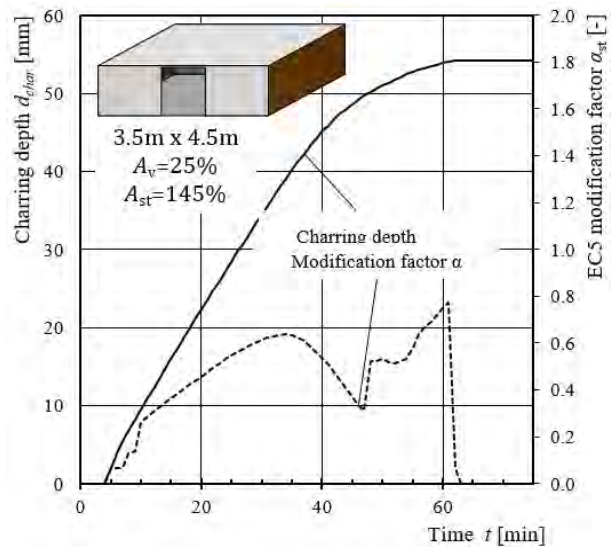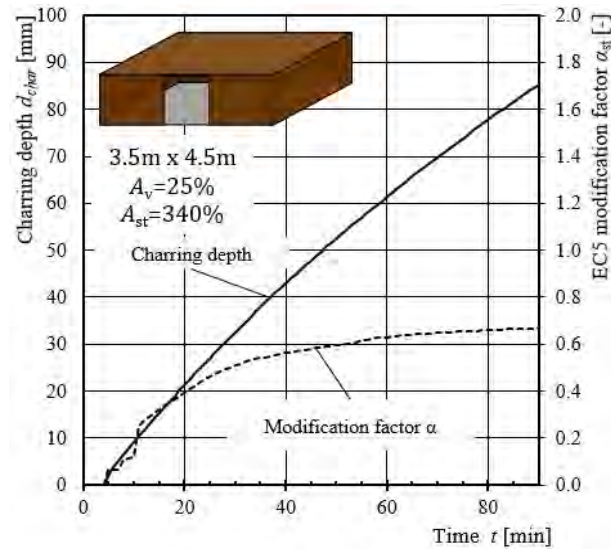
Figure 6.21: Results for compartment experiment VI. Charring depth and the modification factor α_{st}. Own figure.

6.5.9 Results of the validation simulations

Results with respect to the duration of the fully developed fire are given in Table 6.5.9, Column 2. The fully developed fire phase is considered to start at the time when the compartment temperature exceeds 600°C until the maximum temperature is reached. The duration of the decay phase, after the compartment temperature's peak until 300°C are reached is specified for the simulations and the compartment experiments in Table 6.5.9, Column 3. For the baseline case I (NC), the duration of the phase III was estimated by the simulation due to the lack of temperature measurements. In Column 4 and Column 5, the determined modification factors for the particular phase in accordance to Eq. 6.14. The modification factor is intended to correct Eq. 5.9 to take into account for the storage of energy in the char layer. In Column 8, the maximum determined heat release by smouldering and glowing combustion is specified. For the compartment experiments IV and VI, comparison values are included from the direct analysis of the compartment experiments reported in Section 5.3.4 and Table 5.2 Lines 8 and 9, respectively; a fairly good agreement can be stated.

	1		2	3	4	5	6	7
1	ID.	A_{st} [%]	t_{II} [min]	t_{III} [min]	$\alpha_{st,II,max}$ [-]	$\alpha_{st,III,max}$ [-]	d_{char} [mm]	$\dot{q}''_{dec}$ [kW/m^2]
2								
3								
4	I	-	(14)	(37[1])	-	-	-	-
5	II	-	(22)	(83)	-	-	-	-
6	III	30	19 (15)	33 (47)	0.55	0.80	43.8	85
7	IV	100	49 (27)	67 (120)	0.70 (0.63)	0.45	76.5	75
8	V	145	28 (19)	29 (n.a.)	0.65	0.80	55.2	90
9	VI	340	80 (n.a.)	28 (n.a.)	0.70 (0.80)	-[3]	>85.3[3]	75/90[2]

II fully developed fire phase after flashover

III decay phase

[1] based on simulations for the baseline compartment

[2] for about 50% increased gas velocity at the inflow section

[3] value for 90 min; no decay phase predicted

n.a. not available

Table 6.3: Overview of the results of the validation simulations by TiCHS. Values in brackets are derived from measurements.

6.6 Summary of this Chapter

In this Chapter, a model to predict the contribution of structural timber to the fire development in compartments is developed. The TiCHS-model is based on data obtained from various sources including the literature. The data originated from furnace experiments with applied instrumentation and measured characteristics exceeding standard testing and from experiments with the novel FANCI, which allowed the investigation of selected variables under controlled fire exposure. The fire exposure is understood as thermal exposure including the description of the gas characteristics. The key of the investigations presented in this Chapter is the empirical description of the char layer decomposition, which is a significantly different material from timber but has been left unconsidered in the majority of research projects studying the fire resistance of timber structures. The gas characteristics appear to be of significant influence for the smouldering and glowing combustion, which is subdivided in two characteristics, i.e. the decay of the char layer's bulk volume and the surface regression of the char layer. The TiCHS-model uses five elements to describe the contribution of structural timber to the fire. Improving the fit of correlations in the FANCI, it was shown that the five elements capture the relevant characteristics of fire-exposed timber. For the charring model, an existing model was taken from literature which appeared to give reasonable results validating the final

model against compartment experiments. Further relationships were developed by the analysis of the available data.

The application of the TiCHS-model is currently limited to products which create a stable char layer sticking to the virgin wood. This is valid for solid timber panels that exhibit no bond lines parallel to the exposed surface. The TiCHS-model allows for the prediction of the structural fire load and its corresponding HRR in fully developed fires (it is assumed that localized fires or travelling fires are not likely or are non-conservative for compartments with combustible ceilings). The TiCHS-model was tested with two zone models whereby the TiCHS-model recognises three zones with respect to the fire exposure. For all simulated compartment tests, a good agreement with the.experimental data was found. It is expected that the TiCHS-model can be refined in the future to implement further characteristics. From the presented results, it can be observed that the modification factor α_{st} implemented in the current draft of the fire part of Eurocode 5 [40] to describe the combustion behaviour of structural timber, reaches a maximum value of 0.7 in the second phase of the fire. In the decay phase, α_{st} increases to a maximum of 0.8. However, for the compartment with all surfaces made from structural timber, no decay phase was observed. The wind superimposition or draft situation may change the observed behaviour.

Chapter 7

Summary, conclusions and outlook

7.1 Motivation and approach

The introduction of panel type timber products such as solid timber panels (STPs) or cross-laminated timber (CLT) panels allowed for a competitive alternative to traditional construction elements made from cement based products. The cost competitiveness of the production of the panels is considered as a major advantage beside the dry construction technique with comparatively light weight products. It is expected that volumetric, pre-fabricated modules will advance the building tradition in this field in the next years. A further advantage seems to be the environmental benefit of the reduced carbon footprint resulting from bound carbon(dioxide) and reduced emissions during the production and transportation.

Before the turn of the millennium, a trend in relaxation of the building regulations could be observed with respect to wood based materials. Most likely, the decreasing number of fire accidents contributed to the relaxations as well [164]. It can be assumed that the implementation of common fire design rules for timber structures and the common framework for the description of the reaction to fire characteristics supported this trend. In parallel to this trend, the production numbers of panel type timber products increased due to the improved production techniques. Subsequently, the fire design rules developed for linear timber members, columns and beams, were extended to the panel type products. Founded on existing knowledge at this time, mainly originating from (semi-)empirical design models based on fire resistance testing of linear members, simplified design rules for CLT panels and STP were developed. This was done to answer the increased need for uncomplicated fire design as appreciated for linear timber members.

The change of the fire dynamics exterior and interior of compartments made from solid timber products was observed already in early studies around the turn of the millennium. Some building regulators noticed this and addressed the issue by the limitations for e.g. the design of facades or the share of exposed combustible surfaces [16, 17, 21]. The apparent increase of the available fire load in compartments was investigated in several compartment experiments to study the capability of fire brigades and sprinkler systems to successfully extinguish the fire applying traditional or slightly adopted techniques.

The successful implementation of the solid timber products in the market of mainly residential, low and medium rise buildings, was quickly exceeded. Multi-purpose and office buildings with compartment size exceeding 2000 m^2 in medium and high-rise building classes raised questions previously addressed by limited ambitions to investigate the applicability of the fire safety concepts, the fire fighting tactics and the structural fire design philosophy originally developed for non-combustible structural materials. It can be concluded that the technical possibilities exceeded those of the know how when it comes to the fire dynamics of compartments. Regardless of the question if the actual design framework is applicable to non-combustible structures only or not, several questions have been left unanswered so far. These questions comprise (i) the contribution of structural timber to a compartment fire (ii) the question if burnout - understood as self-extinguishment - can be expected and whether it should be required, or, if there are reasonable alternatives

existing. (iii) The limits for the applicability of actual fire fighting techniques on buildings including the suitability of the stay-put policy.

Up to now, compared to systematically organized studies of the fire resistance of linear elements in the 70s and 80s comprising several hundreds of furnace tests, limited effort was performed with panel type timber structures. On one hand, this can be traced back to the reliance of the extrapolation of characteristics and rules developed for linear members, the shift of the responsibility to the market and its demand for competitiveness, but, on the other hand, to the extreme costs of compartment experiments. Currently, a trend towards ad-hoc compartment experiments can be observed, which is the result of the lack in understanding the fire dynamics in compartments with exposed structural timber. For particular building projects, fire safety engineers and regulator's representatives ask explicitly for tests tailor made for the particular project. This may comprise the actual compartment size, the arrangement of openings or the particular product which is planned to be purchased. It is believed that with this methodology the relevant boundary conditions are well captured regardless of the low number of results, typically not more than one. In contrast, generally valid design models require the systematic investigation of isolated properties. To vary only one property at a time requires a lot of tests and increases the costs of typically available research and development budgets. In the work presented in this thesis, an alternative approach was followed up avoiding large or full-scale testing. The approach consisted of four campaigns (i) to (iv) with the aim of two major deliverables (v) and (vi):

(i) the design of a novel setup utilizing a quick-response radiant heat panel as heating source and the execution of about 80 experiments;

(ii) the performance and monitoring of furnace experiments with instrumentation and measurements exceeding standard testing;

(iii) the thorough analysis of the char layer material with respect to the stored energy;

(iv) the performance of a small-scale compartment experiment to validate conclusions from (i) to (iii);

(v) the analysis of the thermal exposure of combustible products in (furnace) fires and the definition of the term fire exposure;

(vi) the development of the Timber Charring and Heat Storage model based on the experiments and findings in (i) to (v).

7.2 Summary

FANCI experiments. The first experimental campaign that represents the core of this thesis were experiments in the Fire Apparatus for Non-standard heating and Charring

Investigation (FANCI), which was designed for this study. Aim of this campaign was the analysis of the timber's behaviour exposed to non-standard heating conditions in oxygen rich environments. Decisive characteristics of compartment fires were analysed and a costume made setup created to investigate isolated parameters. The FANCI allowed for the exposure of model-scale (timber) specimens to various environments with respect to the external heat flux and the gas characteristics. Typically used setups lack of the control of the gas flow above the specimens in the relevant order of magnitude. Designing the FANCI, significant effort was made to facilitate well-defined conditions with respect to the gas flow which could be monitored by means of various pressure sensors. The FANCI allowed to perform experiments (a) under different external heat fluxes which could be increasing, decreasing or constant, (b) under differently turbulent gas flows and (c) gas velocities. The following characteristics and measurements were possible to observe, analyse and measure or determine, respectively:

- the external heat flux, typically by means of the current and calibrated using heat flux sensor measurements;

- the gas temperature above the specimen;

- the surface temperature of the specimen;

- the mass loss of the specimens during the experiments;

- the temperature distribution across the specimens depth;

- the char layer surface regression;

- the gas velocity above the specimen;

- the turbulence of the gas.

After the experiments, the charring rate and the char layer density, sometimes referred to as yield, was determined. Using all mentioned measurements, the sum of the heat fluxes could be assessed. The sum was determined by, (1) the released volatiles during pyrolysis, (2) the decay of the char layer in the char layer bulk volume, divided in this work to (2a) the smouldering and glowing combustion inside the char layer and (2b) the char layer surface regression, and (3) the heat losses due to the temperature gradient at the specimen's surface. Consequently, the heat fluxes were determined at the char line exceeding 300 kW/m^2 leading to charring rates of up to about 2.5 mm/min. A char layer surface regression rate up to about 2.0 mm/min was observed. The aim of the analysis was the definition of the smouldering combustion of the char layer. Testing a large number of correlations, a measure for the description of the turbulence was found and defined as the degree of turbulence, which considers the gas velocity and its standard deviation. The latter should represent a measure of the agitation at the fire exposed timber surface.

Furnace experiments. The second experimental campaign consisted of the performance of furnace experiments. The main objective was the analysis of the thermal exposure of combustible products in comparison to non-combustible products. The secondary aims were the investigation of the validity of the execution of furnace tests with combustible products and the estimation of the surface flaming of timber specimens in furnaces. The campaign comprised experiments following the EN/ISO standard fire [37, 85] of combustible and one non-combustible specimen. The following characteristics and measurements were possible to observe, analyse and measure or determine respectively:

- the heat flux sensor (HFS) measurements at various locations and positions comprising locations above and away from the burner region and positions in level with and behind the control plate thermometers (PTs) and flush with the specimen's exposed surface;

- oxygen concentration measurements in the furnace compartment, more precisely, centric and close to the specimen's surface;

- the temperature on the fire exposed surface of the specimen;

- the internal temperature using various kinds and installations of temperature sensors;

- the mass loss of the specimens during the experiments;

- the burner fuel consumption of the specimens during the experiments;

- the char layer surface regression;

- the gas velocity at the fire exposed surface of the specimen;

- the standard deviation of the gas velocity;

Fire exposure. In the part of the thesis addressing the fire exposure, the question was investigated whether combustible products are exposed to different thermal exposure in furnace tests. It can be stated that no common definition of the term "thermal exposure" is available. While some structural engineers working in the field of fire resistance design expect a definition of a constant "load" it should rather be compared to a variable "wind load". It appears useful to define the thermal exposure as the correctly formed sum of the radiation and gas temperature of a solid. This requires the consideration of the mixed thermal boundary condition and the surface characteristics of the solid. Further, it is useful to extend the terminology by the term "fire exposure". For the description of combustion processes, comprising flaming and smouldering combustion, the proper description of the gaseous environment appears to be of significant importance. In the experiments and analysis performed in this thesis, it is concluded that the gaseous environment should be characterised by the gas velocity, its standard deviation and the oxygen concentration. Consequently, the conditions for flaming and smouldering combustion can be described.

While flaming combustion is significantly depending on the oxygen concentration, the glowing combustion appeared to be significantly depending on the gas velocity and its standard deviation.

Analysis of the char layer. The analysis of the char layer was performed with respect to its density profile and its heat content. The density profile was found to vary significantly over the depth with yields significantly different from zero at the fire exposed side, corresponding to a max. temperature of about 1050°C. Comparing results to further char layer material it was found that a significant variation of the char yield can be specified between about 10% and 30% of the dry wood material. Thus, it exceeds ranges specified in the literature. The bomb calorimetry analysis of char layer material extracted from various depths over the char layer showed fairly independent values for the heat content of about 31 MJ/kg. The assumption of the robustness of the value for the heat content was further supported by the inclusion of char layer material originating from FANCI experiments.

The TiCHS-model. The aim of the developed TiCHS-model is the prediction of the structural timber's contribution to a compartment fire. The TiCHS-model is intended to be used with a zone model. The TiCHS-model uses five elements to describe the heat storage and heat release of structural timber in a compartment fire. The relevance of the elements used in the TiCHS-model were validated using the measurements of the FANCI experiments. After the experiments, the charring rate, the char layer surface regression and the char layer density (yield) were determined as key input to describe the smouldering combustion, the combustion process attributed to the char layer. The TiCHS-model considers the conversion of the wood material to the char layer by an endothermic and an exothermic sub-step. The smouldering combustion is divided in two characteristics as observed in the experiment in all campaigns, i.e. the loss of char layer density considered as main smouldering process, and the char layer regression. The amount of smouldering combustion is directly dependent on the type of environment, i.e. moderately or highly turbulent, the hot gas velocity and the incident radiant heat flux. The amount of smouldering combustion is indirectly dependent on the char layer depth decisive for the maximum released heat for the particular environment. Using the elements of the TiCHS-model, the average contribution of the char layer's smouldering combustion in furnaces was determined to an average of between about 40 kW/m^2 and 60 kW/m^2 and up to 75 kW/m^2 using the prediction of the TiCHS-model. In the simulated compartments, these values increased to up to 90 kW/m^2. The differences seem to be depending on the gas velocity and the degree of turbulence defined in this thesis. A corresponding average in the small-scale compartment experiment performed in the last experimental campaign was determined to about 45 kW/m^2 which is about the same value mentioned in the literature for small-scale compartment tests [151]. As this value found to be dependent - among others - on the hot gas velocity, this value may be exceeded

significantly in peak values in real compartment fires.

Application of the TiCHS-model to compartment fires. The TiCHS-model was verified using data from compartment fires described in the literature [115, 123, 190]. Thereby, the TiCHS-model was used to predict the contribution by structural timber to the compartment fire. This was done by superimposing the heat release rate (HRR) by the structure with the HRR measured in the corresponding baseline compartment experiment. Scenarios with exposed surfaced between about 30% and 340% exposed structural timber surface with respect to the compartment floor area were analysed. A good agreement between the target HRR and the predicted total HRR by the TiCHS-model was achieved. The TiCHS-model delivers a good agreement with another prediction model developed by Wade [203] but seems to be more conservative in some cases. This might be be traced back to the description of the charring depth by the currently applied charring model. However, the TiCHS-model work without a parameter study of the fuel excess factor (GER) used by Wade but can directly predict the contribution by the structural timber based on the compartment environment.

7.3 Conclusions

The TiCHS-model. The main outcome of the thesis is the TiCHS-model, the Timber Charring and Heat Storage model to describe the contribution of structural timber to a compartment fire. The TiCHS-model uses input determined from the FANCI using a radiant heat panel, from furnace experiments, from a small-scale compartment test and the bomb calorimetry analysis of the char layer material. The TiCHS-model requires essentially input of the compartment's gas temperature and the oxygen concentration. Further, the TiCHS-model makes use of the incident radiant heat flux, the charring rate and the gas velocity at the exposed surface. The TiCHS-model uses a sub-model taken from Werther and Werther et al. [205, 206] to describe the charring depth of structural timber. The estimation of the gas velocity at the surfaces seems to be the most complex task but the performed calculations showed a certain robustness of the TiCHS-model's elements and the results to uncertainties. However, for the use in practice, it is recommended to include this parameter in a parameter study. Consequently, the model could be used to allow for predictions of the fire dynamics in draft situations. A dependency of the result for the charring depth on the gas velocity in the compartment could be observed. For this extended use, further validation is required.

Experimental work. It appeared to be of tremendous advantage to perform additional measurements in experiments which are typically performed as standard tests. Among others, it showed to be of enormous value to be able to estimate (a) the char layer's thickness including the char layer surface regression and (b) the bulk density of the char layer. At the time being it is assumed that mass loss measurements are considered as

standard measure even for standard fire resistance tests which can be easily conducted by deriving the differences of the mass before and after the experiment before extinguishing work. The additional properties allow for the estimation of the decay of the char layer (smouldering and glowing combustion) in the actual setup, regardless if a compartment experiment or a bench scale test has been performed.

7.4   Outlook

The TiCHS-model parameters.   In the current model, the smouldering and glowing combustion is considered dependent on the incident heat flux received by the structural timber and the hot gas velocity at its surface following a empirically estimated correlation function. The experimental results obtained with the FANCI allowed for a conservative approach and further data linking the extinguishment of the smouldering and glowing combustion with the incident radiant heat flux and the gas temperature seems to be essential. Further data-sets are needed to improve the correction of the three zones available in the TiCHS-model. Currently, the cumulative temperature charring model is implemented as sub-model in the TiCHS-model. Using a more general, e.g. kinetic charring model, the model accuracy may be increased.

The TiCHS-model setup.   The TiCHS-model is currently set up as independent ad-on for a common design tool for a zone model. Currently in some zone-models, e.g. OZONE [32] and CFAST [91] the option to allocate wood material to enclosure elements is available without the consideration of its combustibility. The actual implementation might be understood misleadingly and engineers might assume that the combustion of the structural timber and its contribution is considered. Thus, the creation of an add-on seems to be apparent. As the smouldering combustion seems to be depending on the gas characteristics, proper sub-models are required for the correct consideration of this characteristic. Surface flaming will be implemented based on the availability of the corresponding energy and the environmental conditions, respectively.

Compartment fire dynamics.   The overall compartment fire dynamics is typically analysed and described based on experiments with wood cribs. The wood elements of the wood cribs allow only for a limited creation of a char layer. The creation of the char layer is a significant difference from structural timber in a compartment fire. As described in the development of the TiCHS-model, the charring of the timber and the release of combustible volatiles is governed by the temperature as the temperature is responsible for a certain decay process regardless of the availability of oxygen. It seems unrealistic that more realistic fire loads such as polyurethane-based sofas produce combustible volatiles only if oxygen is available. In currently available design models, the decay is initiated at the point in time when 70% of the movable fire load is consumed. From recent compartment tests [123, 115, 23] a significantly earlier initial point of the decay phase was reported.

In general, structural timber members appear to respond more critically to longer heating with associated lower maximum temperatures rather than shorter heating with associated higher maximum temperatures. This can be observed for experiments investigating the corresponding zero-strength-layer which was observed to increase to 16 mm for bending members [108]. Thus, it is expected that especially timber buildings may profit from more realistic, eventually variable decay points.

Experimenting work. It is expected that the TiCHS-model will be further developed and refined. Subsequently, a re-validation of the model will be needed with an extended data-set. The availability of validation data for design models but also for the determination of characteristics related to the structural fire design of timber structures is of societal and industrial interest and should be followed up. Currently, the TimFix (pre-project) is setting up a framework for such a testing and experimental database, which should be released online under http://www.fsuw.com/. This pre-project is funded by CEI-Bois (The European Confederation of Woodworking Industries) bringing together important European industries to improve the research environment. Besides the aim to make data available, further data should be created with respect to draft and cross-draft and superimposed wind situations, which might reduce the robustness of calculation results obtained so far. The outcome is expected to allow for the improved validation of the future design models.

Bibliography

[1] Jitendra Agarwal, Marco Haberland, Milan Holickỳ, Miroslav Sykora, and Sven Thelandersson. Robustness of structures: Lessons from failures. *Structural Engineering International*, 22(1):105–111, 2012.

[2] Michael Jerry Antal, William S. Mok, Gabor Varhegyi, and Tamas Szekely. Review of methods for improving the yield of charcoal from biomass. *Energy & Fuels*, 4(3):221–225, 1990.

[3] Snorri Mar Arnorsson, Rory M. Hadden, and Angus Laws. The variability of critical mass loss rate at auto-extinction. *Fire Technology*, 2020.

[4] APA-The Engineered Wood Association. *Standard for Performance-Rated Cross-Laminated Timber, ANSI/APA PRG 320*, 2011.

[5] ASTM. ASTM E 119: Standard Test Methods for Fire Tests of Building Construction and Materials. *American Standard*, 2012.

[6] ASTM. E 2058-13, Standard Test Methods for Measurement of Synthetic Polymer Material Flammability Using a Fire Propagation Apparatus (FPA). *ASTM International, West Conshohocken*, 2013.

[7] Tevfik Aysu and M. Maşuk Küçük. Biomass pyrolysis in a fixed-bed reactor: effects of pyrolysis parameters on product yields and characterization of products. *Energy*, 64:1002–1025, 2014.

[8] Vytenis Babrauskas. Charring rate of wood as a tool for fire investigations. *Fire Safety Journal*, 40(6):528–554, 2005.

[9] Vytenis Babrauskas and Robert Brady Williamson. The historical basis of fire resistance testing-Part I. *Fire Technology*, 14(3):184–194, 1978.

[10] Vytenis Babrauskas and Robert Brady Williamson. The historical basis of fire resistance testing-Part II. *Fire Technology*, 14(4):304–316, 1978.

[11] Robert W. Balluffi, Samuel M. Allen, and W. Craig Carter. *Kinetics of materials*. John Wiley & Sons, 2005.

[12] C. Bamford, J. Crank, and D. Malan. The combustion of wood. Part I. In *Mathematical Proceedings of the Cambridge Philosophical Society*, volume 42, pages 166–182. Cambridge University Press, 1946.

[13] Vito Barbraukas. Ignition of wood - A review of the state of the Art. *Interflam Conference*, 2001.

[14] Alastair Bartlett, Rory Hadden, and Luke Bisby. A review of factors affecting the burning behaviour of wood for application to tall timber construction. *Fire technology (chief editor: L. Bisby)*, 55(1):1–49, 2019.

[15] Alastair Bartlett, Rory Hadden, Juan Hidalgo, et al. Auto-extinction of engineered timber: Application to compartment fires with exposed timber surfaces. *Fire safety journal*, 91:407–413, 2017.

[16] Bauministerkonferenz. Muster Richtlinie ueber brandschutztechnische Anforderungen an hochfeuerhemmende Bauteile in Holzbauweise (model guideline for fire protective requirements on multi-storey buildings made of timber). *Fachministerkonferenzen*, 2004.

[17] Bauministerkonferenz. Musterbauordnung (model building code). *Fachministerkonferenzen*, 2016.

[18] BCA. Technical Guidance Note 29. *Building Control Alliance (Online document)*, 2020.

[19] Beck. Thermocouple Temperature Disturbances in Low Conductivity Materials. 1962.

[20] Mohamed Naceur Belgacem and Antonio Pizzi. *Lignocellulosic Fibers and Wood Handbook: Renewable Materials for Today's Environment*. John Wiley & Sons, 2016.

[21] Boverket. BBR-BFS 2011:6. *BBR (Swedish Building Regulations)*, 2011.

[22] Daniel Brandon. Engineering methods for structural fire design of wood buildings: Structural integrity during a full natural fire. *Brandforsk*, 2018.

[23] Daniel Brandon and Johan Anderson. Wind effect on internal and external compartment fire exposure, RISE Report 2017:72. Technical report, RISE Research Institutes of Sweden AB, 2018.

[24] Daniel Brandon and Christian Dagenais. Fire Safety Challenges of Tall Wood Buildings–Phase 2: Task 5–Experimental Study of Delamination of Cross Laminated Timber (CLT) in Fire. *National Fire Protection Association. NFPA report: FPRF-2018-05*, 2018.

[25] Daniel Brandon, Alar Just, David Lange, and Mattia Tiso. Parametric fire design zero-strength-layers and charring rates. In *Proceedings of INTER (Meeting Kyoto)*, volume 18, 2017.

[26] Daniel Brandon, Koji Kagiya, and Tuula Hakkarainen. Performance based design for mass timber structures in fire Design-Calculation Example (N214-07). *COST FP1404 Dissemination Document*, 2018. 938.

[27] Daniel Brandon, Johan Sjöstrom, and Alastair Temple. Fire Safe implementation of visible mass timber in tall buildings - Report 1: Test plan & justification. *RISE Report 2020:10*, 19, 2020.

[28] Lignum-Dokumentation Brandschutz. 7.1 Aussenwände-Konstruktion und Bekleidungen. *Lignum, Zürich*, 2009.

[29] John Buckley. Fire investigation for the University of Nottingham jubilee campus. *Nottinghamshire Fire and Rescue Service*, 7:1147–1158, 2015.

[30] H. M. Bunbury. *Die bei der trockenen Destillation des Holzes erhaltenen Handelsprodukte.* Springer, 1925.

[31] Paulo B. Cachim and Jean-Marc Franssen. Assessment of Eurocode 5 charring rate calculation methods. *Fire technology*, 46(1):169, 2010.

[32] J. F. Cadorin, D. Pintea, and J. M. Franssen. *The Design Fire Tool OZone V2.0-Theoretical Description and Validation on Experimental Fire Tests.* University of Liege, Belgium, 2001.

[33] CEN. EN 1990: Eurocode: Basis of structural design. Technical report, European Committee for Standardization (CEN), Brussels, Belgium, 2002.

[34] CEN. EN 1991-1-2: Eurocode 1: Actions on structures Part 1-2: General actions: Actions on structures exposed to fire. *European Standard*, page 62, 2002.

[35] CEN. EN 1995-1-2: Eurocode 5: Design of timber structures - Part 1-2: General-Structural fire design. *European Standard*, page 80, 2004.

[36] CEN. EN 338: Structural timber-Strength classes. *European Standard*, 2009.

[37] CEN. EN 1363-1: Fire resistance tests - Part 1: General requirements. *European Standard*, page 55, 2012.

[38] CEN. EN 13381-: Test methods for determining the contribution to the fire resistance of structural members - Part 7: Applied protection to timber members. *European Standard*, 2019.

[39] CEN. EN 13381: Test methods for determining the contribution to the fire resistance of structural members. Applied protection to timber members . *European Standard*, 2019.

[40] CEN. EN 1995-1-2: Eurocode 5 - Design of timber structures: Part 1-2: General - Structural fire design, Draft for Revision April 2020. *European Standard*, 2020.

[41] Zhengrong Chen. *Design fires for motels and hotels*. PhD thesis, Carleton University, 2009.

[42] Roy Crielaard. Self-extinguishment of cross-laminated timber. Master's thesis, Delft University of Technology, Faculty of Civil Engineering and Geosciences, March 2015.

[43] Roy Crielaard, Jan-Willem van de Kuilen, Karel Terwel, Geert Ravenshorst, and Pascal Steenbakkers. Self-extinguishment of cross-laminated timber. *Fire Safety Journal*, 105:244–260, 2019.

[44] Christian Dagenais. *Assessing the Fire Integrity Performance of Cross-Laminated Timber Floor Panel-to-Panel Joints*. PhD thesis, Carleton University, 2016.

[45] Christian Dagenais and Lindsay Ranger. Revisiting Heat Delamination Characteristics of Adhesives in Cross-Laminated Timber. In *World Conference on Timber Engineering*, 2018.

[46] Martin Dahlberg. The SP Industry Calorimeter - For rate of: heat release measurements upto 10 MW. Technical Report SP Report 1992:43, Swedish National Testing and Research Institute - Fire Technology, 1992. no. 925.

[47] Susan Deeny, Barbara Lane, Rory Hadden, and Andrew Laurence. Fire safety design in modern timber buildings. *The Structural Engineer: journal of the Institution of Structural Engineer*, 96(1):48–53, 2018.

[48] DIN. DIN EN 1991-1-2/NA: Eurocode 1: Einwirkungen auf Tragwerke - Teil 1-2: Allgemeine Einwirkungen - Brandeinwirkungen auf Tragwerke - National Annex. *Deutsches Insitut fÃŒr Normung (DIN)*, 2010.

[49] Dougal Drysdale. *An introduction to fire dynamics*. John Wiley & Sons, 2011.

[50] J. Dunham, W. O'Connor, S. Ingberg, B. Thorud, and Ch. Diener. Fire-Resistance Classification of Building Materials. *Building Materials and Structures, Report BMS92, Report of the Subcommittee on Fire-Resistance Classifications of the Central Housing Committee, National Bureau of Standards*, 1942.

[51] Richard Emberley, Arne Inghelbrecht, Zeyu Yu, and José L. Torero. Self-extinction of timber. *Proceedings of the Combustion Institute*, 36(2):3055–3062, 2017.

[52] Reto Fahri. *Reliability-based code calibration for timber in fire.* PhD thesis, ETH ZÃŒrich, Switzerland, 2020.

[53] Reto Fahrni, Joachim Schmid, Michael Klippel, and Andrea Frangi. Correct temperature measurements in fire exposed wood. In *World Conference on Timber Engineering (WCTE 2018)*, pages MAT–O9. ETH Zurich, Institute of Structural Engineering (IBK), 2018.

[54] Roger Feasey. Post-flashover design fires. *University of Canterbury*, 1999.

[55] Jochen Fornather and Konrad Bergmeister. Versuchsbericht-Kleinbrandversuchsreihe 1-Teil 2 (KBV 1/2): Versuche mit Rissen. *Universität für Bodenkultur, Institut für konstruktiven Ingenieurbau, Vienna*, 2001.

[56] Wilfrid Francis and Martin C. Peters. *Fuels and fuel technology: a summarized manual.* Elsevier, 1980.

[57] Andrea Frangi, Marco Bertocchi, Sebastian Clauß, and Peter Niemz. Mechanical behaviour of finger joints at elevated temperatures. *Wood science and technology*, 46(5):793–812, 2012.

[58] Andrea Frangi, Giovanna Bochicchio, Ario Ceccotti, and Marco Pio Lauriola. Natural full-scale fire test on a 3 storey XLam timber building. In *Proceedings of the 10th World Conference on Timber Engineering*, pages 2–5, 2008.

[59] Andrea Frangi and Mario Fontana. Charring rates and temperature profiles of wood sections. *Fire and Materials*, 27(2):91–102, 2003.

[60] Andrea Frangi and Mario Fontana. Fire performance of timber structures under natural fire conditions. *Fire Safety Science*, 8:279–290, 2005.

[61] Jean-Marc Franssen and Thomas Gernay. Users manual for SAFIR 2019 - A computer program for analysis of structures subjected to fire. 2019.

[62] Kathinka Leikanger Friquin. *Charring rates of heavy timber structures for Fire Safety Design: A study of the charring rates under various fire exposures and the influencing factors.* PhD thesis, NTNU (Norges teknisk-naturvitenskapelige universitet), Institutt for bygg- og miljoteknikk, 2010.

[63] Richard Gann and Raymond Friedman. *Principles of fire behavior and combustion.* Jones & Bartlett Publishers, 2013.

[64] Konstantin Ganster, Andreas Ringhofer, and Gerhard Schickhofer. Experimentelle und numerische Untersuchungen des hygrothermischen Verhaltens von Brettsperrholz am Beispiel einer Außenwand. *Bauphysik*, 41(5):252–268, 2019.

[65] Helmut Glaser. Vereinfachte Berechnung der Dampfdiffusion durch geschichtete Wände bei Ausscheidung von Wasser und Eis. *Kältetechnik*, 10(11):358–364, 1958.

[66] Samuel V Glass and Samuel L Zelinka. Moisture relations and physical properties of wood. *Wood handbook: wood as an engineering material: chapter 4. Centennial ed. General technical report FPL; GTR-190. Madison, WI: US Dept. of Agriculture, Forest Service, Forest Products Laboratory, 2010: p. 4.1-4.19.*, 190:4–1, 2010.

[67] Carmen Gorska Putynska. *Fire dynamics in multi-scale timber compartments*. PhD thesis, The University of Queensland, Australia, 2019.

[68] Björn Günther, Kathrin Gebauer, Robert Barkowski, Michael Rosenthal, and Claus-Thomas Bues. Calorific value of selected wood species and wood products. *European Journal of Wood and Wood Products*, 70(5):755–757, 2012.

[69] Judith Hackitt. Building a safer future - Independent review of building regulations and fire safety: final report. *UK Gov*, 2018.

[70] Rory Hadden. *Smouldering and self-sustaining reactions in solids: an experimental approach*. PhD thesis, School of BRE Centre for Fire Safety Engineering, 2011.

[71] Rory Hadden, Alastair Bartlett, Juan Hidalgo, et al. Effects of exposed cross laminated timber on compartment fire dynamics. *Fire Safety Journal*, 91:480–489, 2017.

[72] Sven Hadvig. Charring of wood in building fires. *Technical University of Denmark Press, Lyngby*, 1981.

[73] Andreas Häggkvist, Johan Sjöström, and Ulf Wickström. Using plate thermometer measurements to calculate incident heat radiation. *Journal of fire sciences*, 31(2):166–177, 2013.

[74] Tuula Hakkarainen. Post-flashover fires in light and heavy timber construction compartments. *Journal of fire sciences*, 20(2):133–175, 2002.

[75] Stéphane Hameury and Tor Lundström. Contribution of indoor exposed massive wood to a good indoor climate: in situ measurement campaign. *Energy and buildings*, 36(3):281–292, 2004.

[76] T. Z. Harmathy. Design of fire test furnaces. *Fire Technology*, 5(2):140–150, 1969.

[77] Peter Häupl, Martin Homann, Christian Kölzow, et al. *Lehrbuch der Bauphysik: Schall-Wärme-Feuchte-Licht-Brand-Klima*. Springer-Verlag, 2017.

[78] M. Hellwig. Time-resolved analysis of the fuelwood combustion process. Zum Abbrand von Holzbrennstoffen unter besonderer Berücksichtigung der zeitlichen Abläufe (in German). 1988.

[79] Gunnar Heskestad. Engineering relations for fire plumes. *Fire Safety Journal*, 7(1):25–32, 1984.

[80] Matthew Hoehler, Joseph Su, Pier-Simon Lafrance, et al. Fire Safety Challenges of Tall Wood Buildings: Large-scale Cross-laminated Timber Compartment Fire Tests. In *SiF 2018-The 10th International Conference on Structures in Fire, Belfast, UK*. New University of Ulster, 2018.

[81] Morgan Hurley, Daniel T. Gottuk, John R. Hall, et al. *SFPE handbook of fire protection engineering*. Springer, 2015.

[82] F. P. Incorpera, D. P. DeWitt, T. L. Bergman, and A. S. Lavine. Fundamentals of heat and mass transfer. *John Wiley & Sons*, 3:749–751, 1996.

[83] Simon H. Ingberg. Fire tests of building columns. *Technologic Papers of the Bureau of Standards*, 1921.

[84] Simon H. Ingberg. Tests of the severity of building fires. *NFPA Quarterly*, 22(1):43–61, 1928.

[85] ISO. ISO 834-1: Fire-Resistance Tests - Elements of Building Construction - Part 1: General Requirements. *International Standard Association (ISO)*, 1999.

[86] ISO. ISO 5660-1: Reaction-to-fire tests–heat release, smoke production and mass loss rate–Part 1: heat release rate (cone calorimeter method) and smoke production rate (dynamic measurement). *International Organization for Standardization (Geneva, Switzerland)*, 2015.

[87] ISO. ISO 13943: Fire safety. Vocabulary. *International Standard Association (ISO)*, 2017.

[88] Marc Janssens. Modeling of the thermal degradation of structural wood members exposed to fire. *Fire and materials*, 28(2-4):199–207, 2004.

[89] Freddy Xavier Jervis Calle. *Application of fire calorimetry to understand factors affecting flammability of cellulosic material: Pine needles, tree leaves and chipboard*. PhD thesis, 2012.

[90] Nils Johansson and Madelene Ekholm. Variation in results due to user effects in a simulation with FDS. *Fire technology*, 54(1):97–116, 2018.

[91] Walter W Jones, Richard D Peacock, Glenn P Forney, and Paul A Reneke. *CFAST-Consolidated Model of Fire Growth and Smoke Transport (Version 6)*, 2005.

[92] Allan Jowsey. *Fire imposed heat fluxes for structural analysis*. PhD thesis, UoE, 2006. JS-XLS element no 693.

[93] Alar Just. *Structural fire design of timber frame assemblies insulated by glass wool and covered by gypsum plasterboards.* PhD thesis, TalTech University, Estonia, 2010.

[94] Koji Kagiya, Yuji Hasemi, Doggun Nam, et al. Investigation of a Large Wooden Gymnasium Fire-Its documentation, estimation of the fire scenario by experiments and evaluation of the structural properties of surviving timber elements. *Fire Safety Science*, 7:1147–1158, 2003.

[95] Bo Källsner and Jürgen König. Thermal and mechanical properties of timber and some other materials used in light timber frame construction. In *Proceedings of CIB W18*, volume 18, 2000.

[96] Kunio Kawagoe. Fire Behaviour in Rooms. *Building Research Institute, Ministry of Construction*, 27, 1958.

[97] Hyeong-Jin Kim and David G. Lilley. Heat release rates of burning items in fires. *Journal of propulsion and power*, 18(4):866–870, 2002.

[98] H. Kinjo, T. Hirashima, S. Yusa, T. Horio, and T. Matsumoto. Fire performance, including the cooling phase, of structural glued laminated timber beams. *Journal of Structural Fire Engineering*, 2016.

[99] Max Klar. *Technologie der Holzverkohlung: unter besonderer Berücksichtigung der Herstellung von sämtlichen Halb-und Ganzfabrikaten aus den Erstlingsdestillaten.* J. Springer, 1910.

[100] Michael Klippel and Andrea Frangi. Fire tests on finger-jointed timber boards - Test Report. *IBK Report*, (354), 2014.

[101] Michael Klippel and Andrea Frangi. Fire safety of glued-laminated timber beams in bending. *Journal of Structural Engineering*, 143(7):04017052, 2017.

[102] Michael Klippel, Joachim Schmid, Reto Fahrni, and Andrea Frangi. Assessing the adhesive performance in CLT exposed to fire. In *World Conference on Timber Engineering (WCTE 2018)*, 2018.

[103] Michael Klippel, Joachim Schmid, Reto Fahrni, Miriam Kleinhenz, and Andrea Frangi. Vorschlag einer Standardprüfmethode für Brettsperrholz im Brandfall. *Bautechnik*, 96(11):824–831, 2019.

[104] Michael Klippel, Joachim Schmid, and Andrea Frangi. Fire design of CLT. In *Proceedings of the Joint Conference of COST Actions FP1402 & FP1404; KTH Building Materials, Cross Laminated Timber–a Competitive Wood Product for Visionary and Fire Safe Buildings*, pages 101–122, 2016.

[105] Jürgen König. Structural fire design according to Eurocode 5-design rules and their background. *Fire and Materials: An International Journal*, 29(3):147–163, 2005.

[106] Jürgen König. Fire exposed simply supported wooden I-joist in floor assemblies, 2006.

[107] Jürgen König and Lars Walleij. One-dimensional charring of timber exposed to standard and parametric fires in initially protected and non-protected fire situations. *Trätek-Swedish Institute for Wood Technology Research*, 9908029, 1999.

[108] David Lange, Lars Boström, Joachim Schmid, and Joakim Albrektsson. The reduced cross section method applied to glulam timber exposed to non-standard fire curves. *Fire technology*, 51(6):1311–1340, 2015.

[109] David Lange, Johan Sjöström, Joachim Schmid, Daniel Brandon, and Juan Hidalgo. A Comparison of the Conditions in a Fire Resistance Furnace When Testing Combustible and Non-combustible Construction. *Fire technology*, pages 1–34, 2020.

[110] Angus Law and Rory Hadden. Burnout means burnout. *SFPE Europe Q*, 1:2017, 2017.

[111] Angus Law and Rory Hadden. We need to talk about timber: fire safety design in tall buildings. *The Physics Teacher*, 98(3):10–15, 2020.

[112] T. Lennon, M. Bullock, and V. Enjily. The fire resistance of medium-rise timber frame buildings. In *World Conference on Timber Engineering*, 2000.

[113] Susan L. LeVan. Chemistry of fire retardancy. 1984.

[114] Kaiyuan Li. The role of char cracking in timber fires. *COST Action FP1404 STSM Report N253-06*, 2016.

[115] Xiao Li, Xia Zhang, George Hadjisophocleous, and Cameron McGregor. Experimental study of combustible and non-combustible construction in a natural fire. *Fire Technology*, 51(6):1447–1474, 2015.

[116] Albert Lingens. *Untersuchung des Abbrandes und der Brandgase ausgewählter Holzarten in Abhängigkeit vom chemischen und strukturellen Holzaufbau.* PhD thesis, 2003. JS-XLS element no 331.

[117] Trond Maag and Mario Fontana. *Brandversuche an Modulhotels in Holzbauweise (in German)*, volume 250. ETH Zurich, 2000.

[118] D. M. Madrzykowski and S. Kerber. Fire Fighting Tactics Under Wind Driven Fire Conditions: 7-Story Building Experiments. Technical report, 2009.

[119] Tiziano Maffei. *Kinetic model of coal combustion.* PhD thesis, Politecnico di Milano, 2013.

[120] Cristian Maluk, Luke Bisby, Michal Krajcovic, and Jose Luis Torero. A heat-transfer rate inducing system (H-TRIS) test method. *Fire Safety Journal*, 105:307–319, 2019.

[121] B. J. McCaffrey and G. Heskestad. A Robust Bidirectional Low-Velocity Probe for Flame and Fire Application. *Combustion and Flame*, (26):125–127, 1976.

[122] B. J. McCaffrey and G. Heskestad. A robust bidirectional low-velocity probe for flame and fire application. *Combustion and flame*, 26:125–127, 1976.

[123] Cameron McGregor. Contribution of cross laminated timber panels to room fires. Master's thesis, Carleton University, 2013.

[124] R. McNamee, J. Zehfuss, A. Bartlett, et al. Enclosure Fire Dynamics with a combustible ceilling. *INTERFLAM 2019 proceedings*, 2019.

[125] Alejandro Ramon Medina Hevia. Fire resistance of partially protected cross-laminated timber rooms. Master's thesis, Carleton University, 2015.

[126] Erich Meister. *Grundpraktikum Physikalische Chemie: Theorie und Experimente.* vdf Hochschulverlag AG, 2012.

[127] Vivian Merk, Munish Chanana, Sabyasachi Gaan, and Ingo Burgert. Mineralization of wood by calcium carbonate insertion for improved flame retardancy. *Holzforschung (Publisher: De Gruyter)*, 70(9):867–876, 2016.

[128] Eskko Mikkola. Charring of wood. *Tutkimuksia-Valtion Teknillinen Tutkimuskeskus*, 1990.

[129] Jean-Christophe Mindeguia, Guillaume Cueff, Virginie Dréan, and Gildas Auguin. Simulation of charring depth of timber structures when exposed to non-standard fire curves. *Journal of Structural Fire Engineering*, 2018.

[130] David Morrisset, Rory Hadden, Alastair Bartlett, Angus Law, and Richard Emberley. Time dependent contribution of char oxidation and flame heat feedback on the mass loss rate of timber. *Fire Safety Journal*, page 103058, 2020.

[131] Swedish Civil Contingencies Agency (MSB). IDA database Evaluation of fatalities in buildings, 2019.

[132] Newman. Multi-directional flow Probe assembly for Fire Application. 1987.

[133] Ralph M Nussbaum. The effect of low concentration fire retardant impregnations on wood charring rate and char yield. *Journal of Fire Sciences*, 6(4):290–307, 1988.

[134] Nyman. Predicting fire resistance performance of drywall construction exposed to parametric design fires - a review. 2008.

[135] Goverment UK of GB. Fire accident database Evaluation of fatalities in buildings, 2019.

[136] Ministry of Works. Fire Grading of Buildings - Part 1: General Principles an Structural Precautions. Technical report, Joing Committee of the building research board of the department of scientific & industrial research and of the fire offices' committee, 1946.

[137] R. A. Ogle and J. L. Schumacher. Fire patterns on upholstered furniture: Smoldering versus flaming combustion. *Fire Technology*, 34(3):247–265, 1998.

[138] T. Ohlemiller and W. Shaub. Products of wood smolder and their relation to wood-burning stoves. Technical report, National Bureau of Standards, Washington, DC (USA). Center for Fire Research, 1988.

[139] T. J. Ohlemiller. Smoldering combustion propagation on solid wood. *Fire Safety Science*, 3:565–574, 1991.

[140] T. J. Ohlemiller. Smoldering combustion. *SFPE handbook of fire protection engineering*, 3, 2002.

[141] Birgit Ostman and Daniel Brandon. Fire Safety Challenges of Tall Wood Buildings-Phase 2-Task 1-Literature Review. Technical report, FPRF (Fire Protection Research Foundation), 2016.

[142] Birgit Östman, Esko Mikkola, Rene Stein, et al. Fire safety in timber buildings. *Technical guideline for Europe. SP Report 2010*, 19, 2010.

[143] Birgit Östman and Lazaros Tsantaridis. Correlation between cone calorimeter data and time to flashover in the room fire test. *Fire and Materials*, 18(4):205–209, 1994.

[144] Birgit A.-L. Östman and Lazarous D. Tsantaridis. Heat release and classification of fire retardant wood products. *Fire and materials*, 19(6):253–258, 1995.

[145] William J. Parker. Prediction of the heat release rate of wood. *Fire Safety Science*, 1:207–216, 1986.

[146] R. V. Petrella. The mass burning rate and mass transfer number of selected polymers, wood, and organic liquids. *Polymer-Plastics Technology and Engineering*, 13(1):83–103, 1979.

[147] William M. Pitts, Annageri V. Murthy, John L. de Ris, et al. Round robin study of total heat flux gauge calibration at fire laboratories. *Fire Safety Journal*, 41(6):459–475, 2006.

[148] C Gorska Putynska, A Law, and JL Torero. An investigation into the effect of exposed timber on thermal load. In *24th Australasian Conference on the Mechanics of Structures and Materials*, 2016.

[149] Egle Rackauskaite, Catherine Hamel, Angus Law, and Guillermo Rein. Improved formulation of travelling fires and application to concrete and steel structures. In *Structures*, volume 3, pages 250–260. Elsevier, 2015.

[150] Rein, Guillermo and Torero, José L. and Jahn, Wolfram and Stern-Gottfried, Jamie and Ryder, Noah L. and Desanghere, Sylvain and Lázaro, Mariano and Mowrer, Frederick and Coles, Andrew and Joyeux, Daniel and others. Round-robin study of a priori modelling predictions of the Dalmarnock Fire Test One. *Fire Safety Journal*, 44(4):590–602, 2009.

[151] Robert Rezka and Jose Torero. Wood and Fibres: Properties. *Book: Lignocellulosic Fibers and Wood Handbook*, 2016.

[152] Franz Richter. *Computational investigation of the timber response to fire.* PhD thesis, 2019.

[153] Franz Richter and Guillermo Rein. A multiscale model of wood pyrolysis in fire to study the roles of chemistry and heat transfer at the mesoscale. *Combustion and Flame*, 216:316–325, 2020.

[154] Amanda P. Robbins and Peter Clive Robert Collier. *Heat flux measurements: experiments and modelling.* BRANZ, 2009.

[155] E. O. Sachs. Suggested standards of fire resistance. In *Report on Proceedings of the International Fire Prevention Congress*, pages 6–11, 1903.

[156] Wilhelm Sandermann and Hans Augustin. Chemische Untersuchungen über die thermische Zersetzung von Holz erste Mitteilung - Stand der Forschung. *Holz als Roh-und Werkstoff*, 21(7):256, 1963. 1050.

[157] Erwin L. Schaffer. Strength validation and fire endurance of glued-laminated timber beams. 467, 1986.

[158] C. Scheer, Th. Knauf, and C. Meyer-Ottens. Rechnerische Brandschutzbemessung unbekleideter Holzbauteile. *Bautechnik (Berlin)*, 69(4):179–189, 1992.

[159] Claus Scheer and Mandy Peter. *Holz-Brandschutz-Handbuch.* John Wiley & Sons, 2009.

[160] Joachim Schmid. Background document of prEN 13381-7; Test methods for determining the contribution to the fire resistance of structural members: Part 7; Applied protection to timber members. 2013.

[161] Joachim Schmid. Thermal exposure of combustible products in furnace tests. *COST Action FP1404 STSM Report N259-06*, 2018.

[162] Joachim Schmid, Daniel Brandon, Norman Werther, and Michael Klippel. Thermal exposure of wood in standard fire resistance tests. *Fire safety journal*, 107:179–185, 2019.

[163] Joachim Schmid, Reto Fahrni, Andrea Frangi, et al. Determination of design fires in compartments with combustible structure-modification of existing design equations. *Proceedings INTER International Network on Timber Engineering Research*, 52:509–511, 2019.

[164] Joachim Schmid, Reto Fahrni, Michael Klippel, and Alar Just. Fire design of timber structures–actual design and outlook: Estrategias de protección al fuego–Diseño y apariencia. In *1º Fórum de Construcción con Madera (FMC 2019)*, pages 65–77. Forum Holzbau (Pamplona), 2019.

[165] Joachim Schmid, Reto Fahrni, Michael Klippel, Miriam Kleinhenz, and Andrea Frangi. Fire tests to provide input for soliving the fire dynamics of timber buildings. *IBK Report (in preparation)*, 2021.

[166] Joachim Schmid and Andrea Frangi. Structural timber in compartment fires - the timber charring an heat storage model. *Open Engineering (submitted 10/2020)*, January 2020.

[167] Joachim Schmid, Michael Klippel, Reto Fahrni, and Andrea Frangi. Brandeinwirkung auf Holzbauteile im Pruefofen und bei realen Braenden. *Bautechnik*, 95(8):524–534, 2018.

[168] Joachim Schmid, Michael Klippel, Reto Fahrni, and Andrea Frangi. Timber structures in the cooling phase - additional influence factors. *Proceedings INTER International Network on Timber Engineering Research*, 52, 2019.

[169] Joachim Schmid, Michael Klippel, Alar Just, and Andrea Frangi. Review and analysis of fire resistance tests of timber members in bending, tension and compression with respect to the Reduced Cross-Section Method. *Fire safety journal*, 68:81–99, 2014.

[170] Joachim Schmid, Michael Klippel, Martin Viertel, et al. Charing of Timber - Determination of the Resdual cross section and charring rates. *WCTE 2020*, 2021.

[171] Joachim Schmid, Jürgen König, and Alar Just. The reduced cross-section method for the design of timber structures exposed to fire-background, limitations and new developments. *Structural engineering international*, 22(4):514–522, 2012.

[172] Joachim Schmid, Jürgen König, and Jochen Köhler. Fire-exposed cross-laminated timber–modelling and tests. In *World Conference on Timber Engineering*, 2010.

[173] Joachim Schmid, David Lange, Johan Sjöstrom, et al. The Use of furnace tests to describe real fires of timber structures. *SIF 2018*, 2018.

[174] Joachim Schmid, David Lange, Johan Sjöström, et al. The use of furnace tests to describe real fires of timber structures. In *World Conference on Timber Engineering (WCTE 2018)*, 2018.

[175] Joachim Schmid, Alessandro Santomaso, Daniel Brandon, Ulf Wickström, and Andrea Frangi. Timber under Real Fire Conditions - The Influence of Oxygen Content and Gas Velocity on the Carring Behavior. *Structures in Fires 2016 (SIF'16)*, 2016.

[176] Joachim Schmid, Alessandro Santomaso, Daniel Brandon, Ulf Wickström, and Andrea Frangi. Timber under real fire conditions-the influence of oxygen content and gas velocity on the charring behavior. *Journal of Structural Fire Engineering*, 9(3):222–236, 2018.

[177] Joachim Schmid, Konstantinos Voulpiotis, Michael Klippel, et al. Robustness in fire - possibliities for tall timber buildings. 2021.

[178] Joachim Schmid, Norman Werther, and Andrea Frangi. The fire resistance of timber structures comparison of incombustible and combustible structures using extended design models. *Structures in Fires 2020 (SIF2020)*, 2020.

[179] Joachim Schmid, Norman Werther, Michael Klippel, and Andrea Frangi. Structural Fire Design-Statement on the Design of Cross-Laminated Timber (CLT). *Civil Engineering Research Journal*, 7(5):113–117, 2019.

[180] Joachim Schmid, Norman Werther, Franz Richter, and Andrea Frangi. Fire compartments with structural timber - Combustion characteristics in the steady-state phase. *submitted to: Fire Technology*, 2020.

[181] Yannick Schüdde. Swiss Structural Timber Construction-Fundamentals of Fire Safety Regulations: A Research on Public Wooden Buildings in Switzerland in Course of the European Public Wood Project. 2019.

[182] Merwin Sibulkin. Heat of gasification for pyrolysis of charring materials. In *Fire Safety Science: Proceedings of the First International Symposium*, pages 391–400, 1985.

[183] Dassault Systemes Simulia. Abaqus 6.12 documentation. *Providence, Rhode Island, US*, 261, 2012.

[184] D. Sinclair. RIBA Plan of Work 2013 overview. Technical report, Royal Institute of British Architects, 2013. xls-element no. 933.

[185] Ongama Soka and Oluwaseun Oyekola. A feasibility assessment of the production of char using the slow pyrolysis process. *Heliyon*, 6(7):e04346, 2020.

[186] M. Spearpoint and J. Quintiere. Predicting the burning of wood using an integral model. *Combustion and Flame*, 123(3):308–325, 2000.

[187] John E. J. Staggs. The heat of gasification of polymers. *Fire safety journal*, 39(8):711–720, 2004.

[188] René Steiger. *Mechanische Eigenschaften von Schweizer Fichten-Bauholz bei Biege-, Zug-, Druck-und kombinierter M/N Beanspruchung: Sortierung von Rund-und Schnittholz mittels Ultraschall*. PhD thesis, ETH Zurich, Switzerland, 1996.

[189] Carola Steinert. *Bestimmung der Wärmeübergangsbedingungen auf Bauteile im Brandfall: Abschlußbericht; Kennwort: Wärmeübergang*, volume 120. 1996.

[190] Joseph Su, Pier-Simon Lafrance, Matthew Hoehler, and Matthew Bundy. Fire Safety Challenges of Tall Wood Buildings - Phase 2: Task 2 & 3 - Cross Laminated Timber Compartment Fire Tests. Technical report, 2018.

[191] Yi Su, Yonghao Luo, Wenguang Wu, Yunliang Zhang, and Shanhui Zhao. Characteristics of pine wood oxidative pyrolysis: degradation behavior, carbon oxide production and heat properties. *Journal of Analytical and Applied Pyrolysis*, 98:137–143, 2012. 1021.

[192] Mohamed Sultan. Comparisons of temperature and heat flux in furnaces controlled by different types of temperature sensors. In *Advances in the State of the Art of Fire Testing*. ASTM International, 2010.

[193] A. Tewarson and R. Pion. Flammability of plastics - Burning intensity. *Combustion and Flame*, 26:85–103, 1976.

[194] V. Thi, M. Khelifa, M. El-Ganaoui, and Y. Rogaume. Finite element modelling of the pyrolysis of wet wood subjected to fire. *Fire Safety Journal*, 81:85–96, 2016.

[195] Mattia Tiso, Alar Just, J. Eberhardsteiner, W. Winter, and A. Fadai. Behaviour of insulation materials in timber frame assemblies exposed to fire. *EPS*, 45:45, 2016.

[196] José L. Torero, Agustin H. Majdalani, Cecilia Abecassis-Empis, and Adam Cowlard. Revisiting the compartment fire. In *Fire Safety Science - Proceedings of the 11th international Symposium*, volume 11, pages 28–45, 2014.

[197] Hao C. Tran and Robert H. White. Burning rate of solid wood measured in a heat release rate calorimeter. *Fire and materials*, 16(4):197–206, 1992.

[198] James L. Urban, Michela Vicariotto, Derek Dunn-Rankin, and A. Carlos Fernandez-Pello. Temperature measurement of glowing embers with color pyrometry. *Fire Technology*, 55(3):1013–1026, 2019.

[199] VDI/VDE. Temperature measurement in industry - Installation of thermometers; Technische Temperaturmessungen - Einbau von Thermometern. Technical report, Verein Deutscher Ingenieure e.V., Dusseldorf, Brussels, Belgium, 1994.

[200] VKF. BSV 2015: Explanatory report for consultation - Overall revision Swiss fire protection regulations. *VKF 11/01/2013, Association of cantonal fire insurance*, 2015.

[201] Colleen Wade, Gregory Baker, Kevin Frank, Roger Harrison, and Michael Spearpoint. B-RISK 2016User Guide and Technical Manual. 2016.

[202] Colleen Wade, Michael Spearpoint, Charles Fleischmann, Greg Baker, and Anthony Abu. Predicting the fire dynamics of exposed timber surfaces in compartments using a two-zone model. *Fire technology*, 54(4):893–920, 2018.

[203] Colleen Alice Wade. *A theoretical model of fully developed fire in mass timber enclosures.* PhD thesis, University of Canterbury, Christchurch, NZ, 2019.

[204] Houzhi Wang, Philip J. van Eyk, Paul R. Medwell, et al. Identification and quantitative analysis of smoldering and flaming combustion of radiata pine. *Energy & Fuels*, 30(9):7666–7677, 2016.

[205] Norman Werther. *Einflussgroeszen auf das Abbrandverhalten von Holzbauteilen und deren Beruecksichtigung in empirischen und numerischen Beurteilungsverfahren.* PhD thesis, TUM, Technical University Munich, 2016.

[206] Norman Werther and Carla Matthäus. Wärmeenergie und Holzfeuchte als Einflussgrößen auf das Abbrandverhalten von Holz. *Bautechnik*.

[207] Robert H. White. Charring rate of composite timber products. *Proceedings Wood and Fire Safety*, pages 353–363, 2000.

[208] Robert H. White and M. A. Dietenberger. Wood products: thermal degradation and fire. *Encyclopedia of materials: science and technology.[Sl]: Elsevier Science Ltd, c2001: Pages 9712-9716*, 2001.

[209] Ulf Wickström. *Temperature calculation in fire safety engineering.* Springer, 2016.

[210] Ulf Wickström, Johan Anderson, and Johan Sjöström. Measuring incident heat flux and adiabatic surface temperature with plate thermometers in ambient and high temperatures. *Fire and Materials*, 43(1):51–56, 2019.

[211] Erhardt Wilk, Ingolf Kotthoff, and Thomas Redmer. Der Brand in Räumen-Auswertung von Originalbrandversuchen im Vergleich mit analytischen Rechenverfahren-Teil 4. *Zeitschrift fur Forschung Technik und Management im Brandschutz*, (1), 2014.

[212] F. Williams. A review of flame extinction. *Fire Safety Journal*, 3(3):163–175, 1981.

[213] S. Winter and W. Meyn. Advanced Calculation method for the fire resistance of timber framed walls. *Proceedings of the CIB W18 meeting (Meeting 2009, Dubendorf, Switzerland)*, 2009.

[214] Chatani Yukiko and Kayunori Harada. Measurement of Char Oxidation of a Glue Laminated Timber Material heated by Cone Calorimeter. 2015. JS-XLS element no 643.

[215] Jochen Zehfuss. *Bemessung von Tragsystemen mehrgeschossiger Gebäude in Stahlbauweise für realistische Brandbeanspruchung*. PhD thesis, Technischen Universitaet Carolo-Wilhelmina zu Braunschweig, 2004. Nr. 885.

[216] Jochen Zehfuss and Dietmar Hosser. A parametric natural fire model for the structural fire design of multi-storey buildings. *Fire Safety Journal*, 42(2):115–126, 2007.

Chapter 8

Complementary data

8.1 Analysis of the char layer combustion

In this Annex, complementary information with respect to the analysis of the results in Chapters 5 and 6 is provided.

8.2 Convection coefficient in compartment fires

In the TiCHS-model, three zones are considered. The division was done to address the observations in the small scale compartment experiment which resulted in different densities of the char coal at the ceiling and on the walls. In general, for compartments it is expected that the behaviour of any member is different in the upper and lower zone, typically described by two-zone models. These zone-models know only two zones with respect to the combustion processes, e.g. the energy balance and the gas temperature and the oxygen concentration are evaluated for both zones. However, it appears that for combustible surfaces, their contribution to the fire is not only dependent to the fire exposure in terms of oxygen concentration in the particular zone but further to their orientation. Thus, different fire exposures can be expected for vertically or horizontally orientated. Consequently, the char yield and the charring rates may differ in compartment fires for walls and the ceiling. The TiCHS model follows the approach to introduce a factor with answers the different behaviour following the heat transfer by convection which is different for vertical and horizontal surfaces. In general, the convection in the compartment is caused by the significant gas density change due to the difference of the inflow air and the heated gas [209]. In general, the available relationships for the heat transfer coefficient are of empirical nature and can be estimated as given by Wickström to:

$$h_f = \frac{k \cdot C}{L} \left(Gr_f \cdot Pr_f \right)^m \tag{8.1}$$

where
h_f is the convective heat transfer coefficient, in $W/(m \cdot K)$;
k is the conductivity at the film temperature, in $W/(m \cdot K)$;
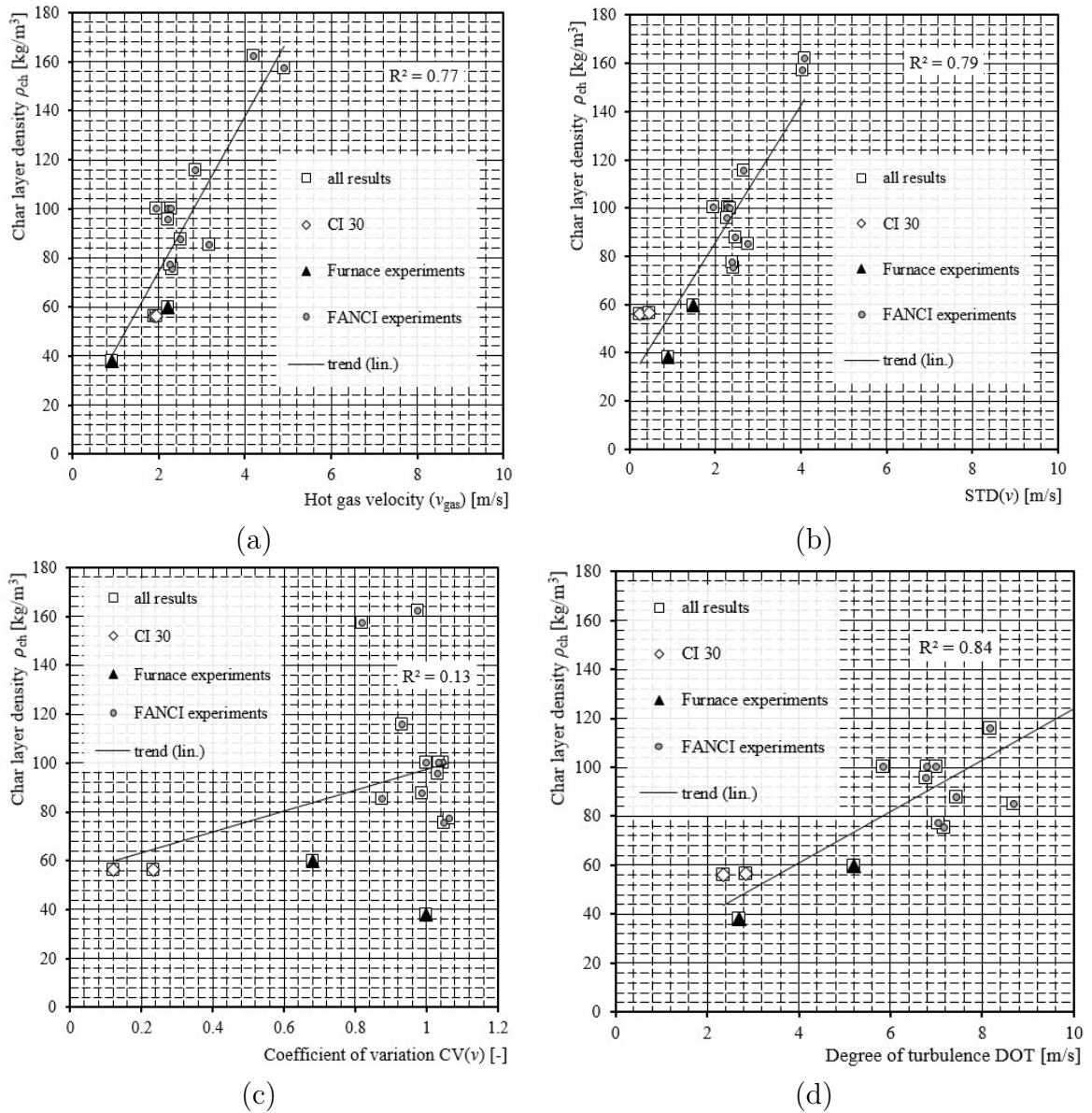L   is the characteristic length of the surface.

Figure 8.1: Char layer surface regression correlated to the hot gas velocity (a), correlated to $STD(v)$ (b), to $CV(v)$ (c) and to DOT. Own figures.
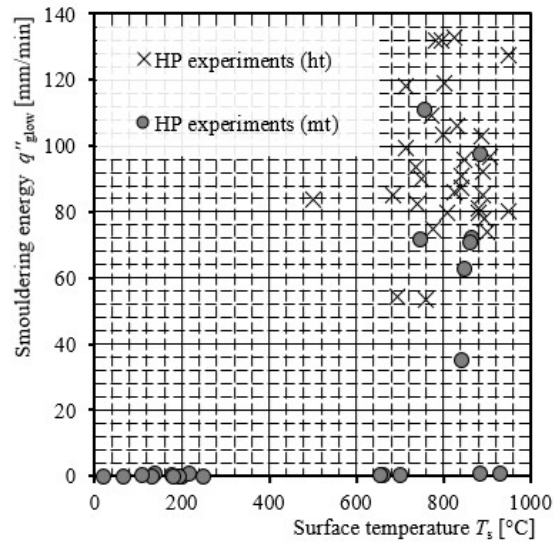
Figure 8.2: Smouldering combustion as function of the surface temperature. Own figure.

		1	2	3	4	5
1		location	ceiling	wall (mid-upper)	wall (lower)
2		zone i	1	2	3
3	$Pr \cdot Gr$	[-]	$5.0 \cdot 10^8$	$5.0 \cdot 10^{11}$	$5.0 \cdot 10^{10}$
4	k	[W/(m $\cdot$ K)]	0.09	0.09	0.08
5	m	[-]	0.25	0.33	0.25
6	C	[-]	0.59	0.13	0.27
7	L_{char}	[-]	2.5	2.5	0.93
8	$h_{c,i}$	[W/(m $\cdot$ K)]	3.3	38.2	12.7
9	$h_{c,i}/h_{c,1}$	[-]	1	12	4

Table 8.1: Determination of typical convection coefficients (absolute and relative) for a fire compartment. Input taken from Wickström [209].

Chapter 9

Curriculum Vitae 2020

Curriculum vitae

Joachim Schmid
Institut für Baukonstruktion IBK
ETH Zürich
Stefano-Franscini-Patz 5, 8093 Zürich, Switzerland

Profile

I have more than twelve years of experience in research of fire safety engineering and fire resistance design with the focus on combustible materials such as timber construction, with expertise several areas listed below. Besides standardisation, I have experience in drafting project application (national and European) as principal investigator of >2.0 M€ research grants (2009-2020). I had the opportunity to teach at Luleå Technical University (LTU, Sweden), Linnaeus University Växjö (LNU, Sweden), SP courses, ETH (Switzerland) and for industry events. I was Guest editor of the Fire Safety Journal (2017-2019), and could publication and review of technical papers as expert and member of the scientific committee for various international conferences.

Education

2006	Technical University of Vienna, TU Wien, Vienna, Austria *Master of Civil Engineering Science, March 2008*
1997	ORGn Anton-Krieger-Gasse, Vienna, Austria *Final exam at the public high school specialized in math and science, June 1997*

Research Positions

2015–	Research fellow, Project leader and PhD student at IBK, chair of timber structures, ETH Zürich, Switzerland
·	PhD "Natural fire design of timber structures" (2016-2020)
·	Chairmanship COST Action FP1404 (2014-2019)
·	Teaching (Fire Safety Engineering, Fire design of timber structures)
·	Standardisation (Revision of EN 1995-1-2; member of WG4 and PT4)
·	Project acquisition

2008–2014 SP Technical Research Institute of Sweden, Division of Wood Buildings (previously Trätek), Stockholm, Sweden

· Fire resistance testing in less than full scale

· Development of fire lab equipment and testing methods

· Responsible for accreditation for several testing methods

· Development of design rules for wood based materials and modeling

· Coordinator of education in the field of fire resistance for timber construction

· Standardisation (CEN/TC/250/SC5/WG4, CEN/TC/127/WG1/TG12)

Research Interests

Fire resistance of timber structures.

Fire dynamics (with focus on combustible building components).

Modeling and development of simplified models.

Work experience

2018- CEO of IGNIS - Fire · Design · Consulting (`www.ignis-consulting.eu`)

2006-2008 Structural engineer at kppk, Vienna (`www.kppk.at`)

Additional information

· Scientific committee member for the conference series SiF / Structures in Fire (2014-)

· Scientific committee member for the conference series Wood & Fire Safety (2019-)

· L.J. Markwardt Award (2019)

Affiliations

· Member of the Society of Fire Protection Engineers SFPE

Chapter 10

Motives and views about fire safety for timber buildings

10.1 General

In the framework of conferences and teaching activities, since November 2018 until October 2019, surveys have been conducted on site. In total, nine surveys were led by J. Schmid and reported here. In general, the surveys results were presented in real-time to the audience which allowed for direct contact with the audience and adjust the subsequently presented content of the speeches accordingly. The questionnaire avoided open questions to allow for a simple grouping of the answers. The data collection occurred using the software system Mentimeter. This system allowed the voluntarily participation using the individual's end user devices. All data is anonymised, the privacy rights of the individuals are respected.

The intention of the data specification in the framework of this thesis serves multiple purposes. In general, it shows the view of various target groups comprising architects, structural engineers, academics and practitioners, building owners, industry and authority representatives and non-technicians. In the following Section 10.2, the survey questions are listed, the particular results are given in Section 10.3.

10.2 Survey content

In this Section, the questions including the possible answers are listed. The content of the survey was slightly changed during the duration of 12 months in the years 2018 and 2019. This was done to address participants answers and personal comments at previous events. Some questions allowed for the selection from pre-defined options (type O for pre-defined options or M for a multiple answer possibility) while other questioned asked for the specification of a preference (P) on a scale from 1 to 10 with 10 indicating an major agreement. In the list below, the specification is provided on the number of events, the question was is included in the survey.

1. What is your profession/professional background?[6] (O)

    (a) architect[6]
    (b) authority representative[6]
    (c) designer (structural engineer)[6]
    (d) economics[6]
    (e) forestry[3]
    (f) law[3]
    (g) producer of building products[6]
    (h) student[3]
    (i) other[6]

2. What is the biggest challenge of a regular working day[1] (open question)

3. What building material do you normally deal with?[6] (P)

   (a) concrete[6]

   (b) masonry[6]

   (c) steel[6]

   (d) timber[6]

4. What is the reason that the share of timber buildings is limited?[8](P)

   (a) Durability/robustness reasons[8]

   (b) Fire Safety[8]

   (c) Missing standard solutions[8]

   (d) Costs[8]

   (e) Missing (competent) building contractors[7]

5. What should be the future focus areas for timber buildings?[5] (O, M)

   (a) Carbon-neutral buildings[5]

   (b) Micro-climate buildings[5]

   (c) Multi-family houses[5]

   (d) Cheap buildings[5]

   (e) Big market sector[5]

   (f) Single-family houses[5]

   (g) High-rise buildings or tall buildings[5]

6. Please give us your opinion with respect to Fire Resistance:?[4] (P)

   (a) Small buildings should have lower requirements than large buildings.[1]

   (b) Tall timber buildings should be safer than tall concrete buildings.[1]

   (c) Is it OK that tall buildings collapse after 90 min fire.[1]

   (d) All multi-storey buildings >2 storeys should be sprinkled.[1]

   (e) We should trust the fire brigade to extinguish any fire.[1]

7. How often do you design for fire resistance (P)[1]

10.3   Survey results

10.3.1   Event H

Figure 10.1: Answers of the audience about their background. Event H.

Figure 10.2: Answers of the audience about the building material, typically applied in their business. Event H.

Figure 10.3: Answers of the audience about the answers why the share of timber as building material is limited. Event H.
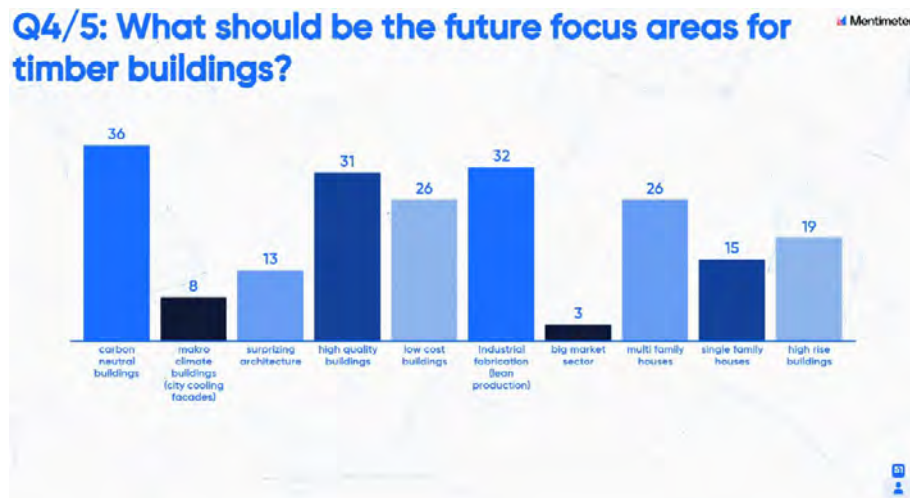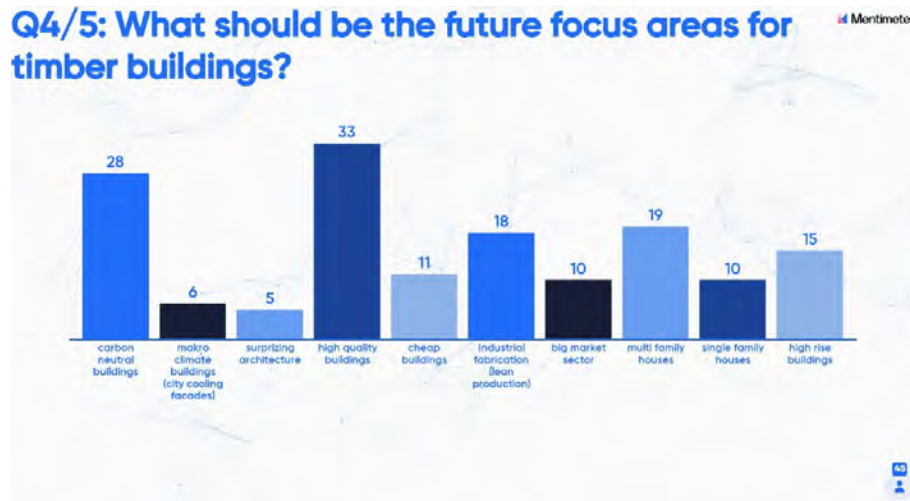

Figure 10.4: Answers of the audience about the building material, typically applied in their business. Event H.

10.3.2 Event L

Figure 10.5: Answers of the audience about fire resistance. Event H.

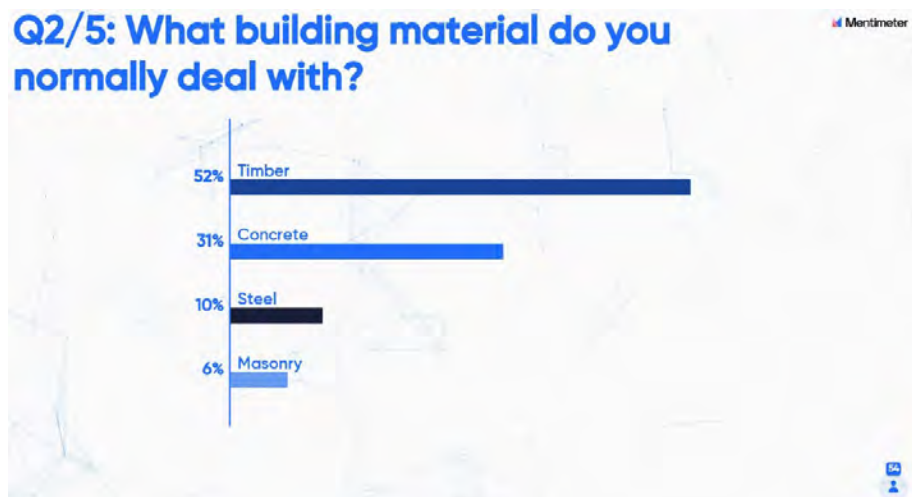Figure 10.6: Answers of the audience about their background. Event L.

Figure 10.7: Answers of the audience about the building material, typically applied in their business. Event L.

Figure 10.8: Answers of the audience about the answers why the share of timber as building material is limited. Event L.

Figure 10.9: Answers of the audience about the building material, typically applied in their business. Event L.
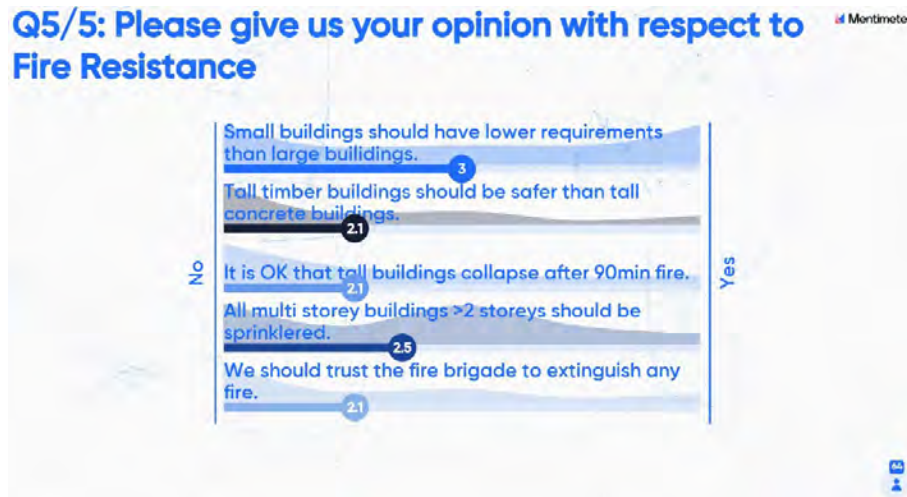
10.3.3 Event O

Figure 10.10: Answers of the audience about fire resistance. Event L.

Figure 10.11: Answers of the audience about their background. Event O.

Figure 10.12: Answers of the audience about the building material, typically applied in their business. Event O.

Figure 10.13: Answers of the audience about the answers why the share of timber as building material is limited. Event O.

10.3.4 Event P

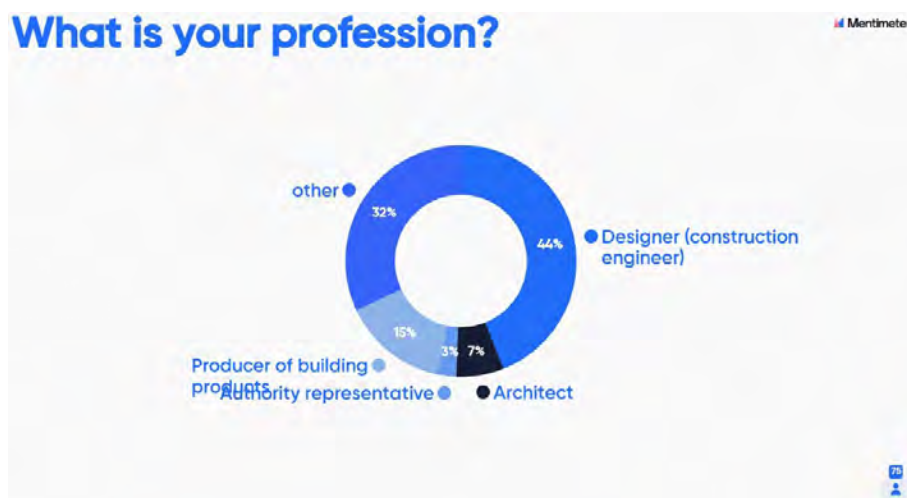Figure 10.14: Answers of the audience about structural fire design. Event O.

Figure 10.15: Answers of the audience about their background. Event P.

Figure 10.16: Answers of the audience about the building material, typically applied in their business. Event P.

Figure 10.17: Answers of the audience about the answers why the share of timber as building material is limited. Event P.

Figure 10.18: Answers of the audience about the building material, typically applied in their business. Event P.

10.3.5 Event T

Figure 10.19: Answers of the audience about fire resistance. Event P.

Figure 10.20: Answers of the audience about their background. Event T.
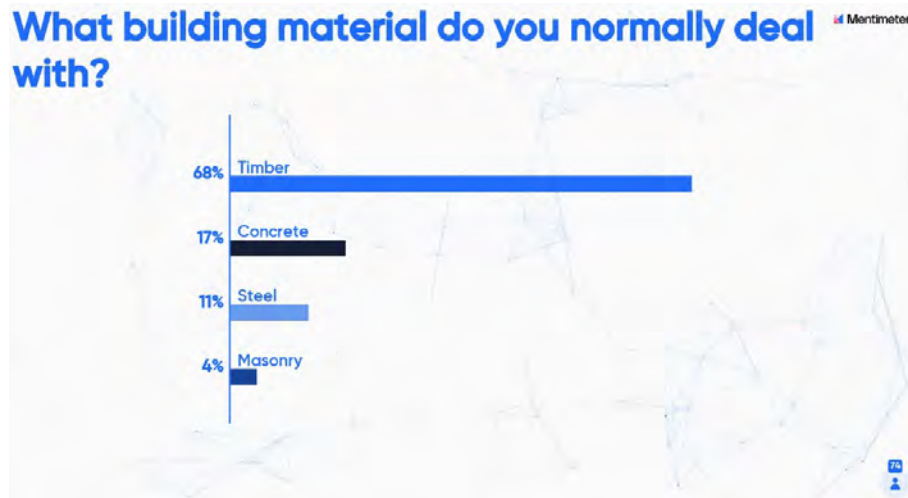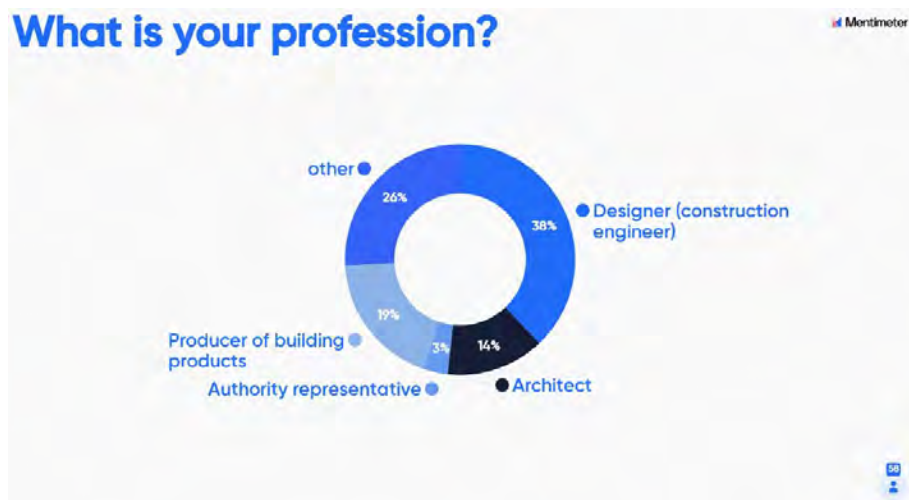
Figure 10.21: Answers of the audience about the building material, typically applied in their business. Event T.

Figure 10.22: Answers of the audience about the answers why the share of timber as building material is limited. Event T.

10.3.6 Event V

Figure 10.23: Answers of the audience about
their biggest challenge. Event T.

Figure 10.24: Answers of the audience about
their background. Event V.

Figure 10.25: Answers of the audience about the building material, typically applied in their business. Event V.

10.3.7 Event Z-L

Figure 10.26: Answers of the audience about the answers why the share of timber as building material is limited. Event V.

Figure 10.27: Answers of the audience about the answers why the share of timber as building material is limited. Event Z-L.
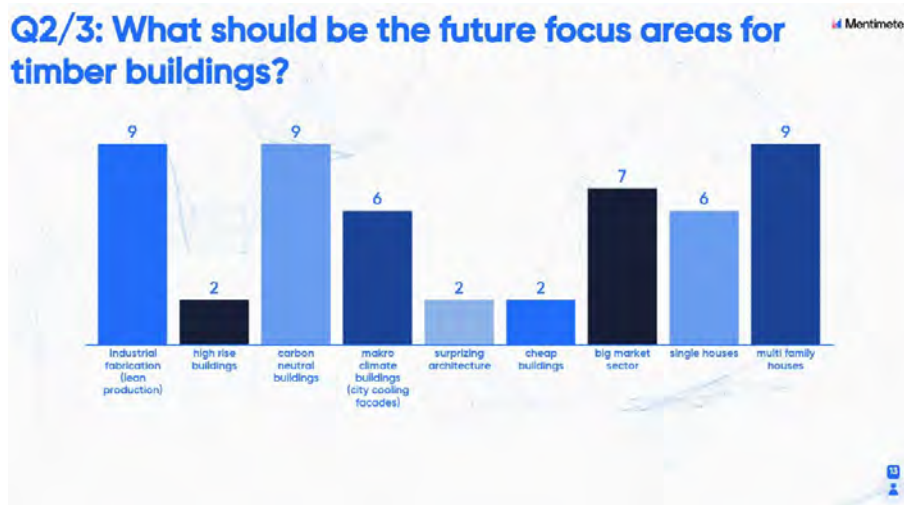

Figure 10.28: Answers of the audience about the building material, typically applied in their business. Event Z-L.

10.3.8 Event Z-S

Figure 10.29: Answers of the audience about
fire resistance. Event Z-L.

Figure 10.30: Answers of the audience about
their background. Event Z-S.

Figure 10.31: Answers of the audience about the building material, typically applied in their business. Event Z-S.

Figure 10.32: Answers of the audience about the answers why the share of timber as building material is limited. Event Z-S.
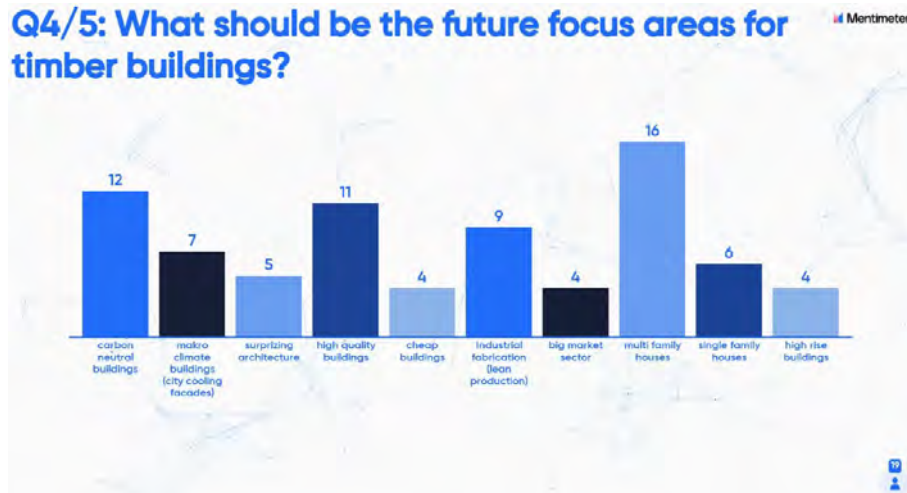
Figure 10.33: Answers of the audience about the building material, typically applied in their business. Event Z-S.

Figure 10.34: Answers of the audience about fire resistance. Event Z-S.

Exposed timber surfaces have become an attractive element for complex buildings. Where structural timber is involved in the fire, the significantly changed fire dynamics should be taken into account and the contribution of the structural timber quantified. Traditionally, the fire resistance framework uses a comparative measure to define the *thermal exposure* of a construction, while for combustible materials the *fire exposure* should be considered. Using the fire exposure definition (radiation and gas temperature, description of the gaseous environment) a new experimental setup was created, the Fire Apparatus for Non-standard Heating and Charring Investigation (FANCI). Using the experimental results from experiments in various scales, the heat balance at the char line and the contribution of structural timber to compartment fires, respectively, was predicted. A framework for the description of the behaviour of structural timber in compartment fires together with the semi-empirical relationships from the experimental campaigns was used to define the Timber Charring and Heat Storage (TiCHS) – model. The model validation was performed by means of existing compartment tests.

ibk

Institut für Baustatik und Konstruktion
Institute of Structural Engineering